WESTERN SYDNEY UNIVERSITY

# Significance of Ubiquitin Conjugating Enzyme 2C in Cell Cycle Exit and Re-entry in Prostate Cancer Cells

By Chanlu (Amber) Xie

A thesis submitted in satisfaction of the requirements for the degree of

Doctor of Philosophy

The School of Science and Health

Western Sydney University

June 2016

**Primary Supervisor: A/Prof Qihan Dong**

**Co-Supervisors: Dr Mu Yao & Dr Paul Sved**

# Original Statement

This thesis is submitted in fulfillment of the requirements of the degree of Doctor of Philosophy in the School of Science and Health at Western Sydney University. The work presented in this thesis is, to the best of my knowledge, original except as acknowledged in the text. I hereby declare that I have not previously submitted this material, either in whole or in part, for a degree or a diploma in any other university.

..... 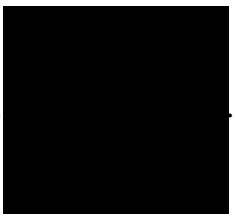 .....

anlu (Amber) Xie
May 2016

# Abstract

Prostate cancer (PCa) is one of the most commonly diagnosed cancers and the second leading causes of cancer deaths in western countries. Nearly one-third of patients with PCa experience cancer recurrence or progression following primary treatment such as surgery or radiation therapy. The presence of quiescent cancer cells has been documented in many types of cancers, including prostate. Quiescent cells are Ki-67 protein-negative and reversibly arrested at the $G_0$ phase. In PCa, the percentage of Ki-67-positive PCa cells is low in low risk disease, but increases in high risk and advanced PCa, suggesting that an increase in transition from $G_0$ state to a proliferating state may contribute to PCa progression. Hence, how to increase the proportion of cancer cells at $G_0$ over those in a proliferating state and/or to prevent the transition from $G_0$ to a proliferating state is pertinent to the prevention of cancer progression and recurrence. However, our understanding of the signals required for maintaining cancer cells at $G_0$ and/or impeding the transition from quiescent to a proliferating state is limited.

In eukaryotes, the ubiquitin proteasome system (UPS) precisely regulates the cell cycle at key checkpoints by targeting cell cycle regulators for proteasome-mediated degradation. The UPS requires the ubiquitin-activating enzyme (E1), the ubiquitin-conjugating enzyme (E2) and ubiquitin ligases (E3) to work in concert to facilitate ubiquitination of target proteins. Ubiquitin conjugating enzyme 2C (UBE2C) is aberrantly overexpressed in a variety of cancers, including PCa. Accumulation of UBE2C stimulates cell proliferation, whereas silencing of UBE2C decreases cell proliferation. The significance of UBE2C in cell cycle exit and re-entry, however, has not been investigated.

The aim of this project was to define the role of UBE2C in the proportion of quiescent over proliferative PCa cells and transition to a proliferating state by quiescent PCa cells. Moreover, the concordance between UBE2C protein/mRNA levels in human PCa tissue and progression of PCa were determined.

To establish the relationship of UBE2C the proportion of $G_0$ cells, PCa cell lines were transfected with UBE2C siRNA or UBE2C expression plasmid. Silencing of UBE2C decreased cell proliferation, whereas overexpression of UBE2C increased cell proliferation, determined by measuring DNA content. Flow cytometric analysis of both DNA and RNA content were subsequently undertaken to investigate if manipulation of UBE2C changed the proportion of $G_0$. Depletion of UBE2C led to accumulation of quiescent cells, while overexpression of UBE2C decreased the proportion of quiescent PCa cells.

To further evaluate the relationship of UBE2C with cell cycle re-entry, we utilised contact inhibition in PC-3 or serum withdrawal in LNCaP and C4-2B cells to induce experimental quiescence. The quiescent state of PCa cells was confirmed by flow analysis. Cell cycle re-entry was rendered by replating the contact-inhibited quiescent cells at low density, or by restoring serum to serum-deprived cells. UBE2C protein levels were decreased during cell cycle exit and increased upon cell cycle re-entry. Overexpression of UBE2C impeded cell cycle exit, and knockdown of UBE2C delayed cell cycle re-entry by quiescent PCa cells.

Next, to determine the molecular mechanism underlying UBE2C action on cell cycle exit and re-entry, $G_0$ regulatory proteins were examined by immunoblot. Knockdown of UBE2C expression increased the protein levels of p27 and decreased protein levels of SKP2 and PIRH2; both are components of E3 ligases responsible for p27 degradation. Additionally, the level of c-MYC was also decreased by UBE2C siRNA. Concomitantly, FBXW7, which

targets c-MYC for degradation, was increased. However, the silencing of UBE2C did not change protein levels of p27 nuclear exporter CRM1.

Lastly, to examine the concordance between UBE2C mRNA levels and progression of PCa, 12 datasets on PCa from ONCOMINE, an online database for genetic variation and mRNA expression in cancer, were analysed. Across these datasets, UBE2C mRNA was highly expressed in the metastasised form of PCa compared with organ-confined primary PCa or benign hyperplastic tissues. At protein levels, the aberrant overexpression of UBE2C was confirmed by immunostaining in PCa tissue specimens (n=70), and was found to be correlated with cancer progression in paired specimens of hormone-sensitive PCa and castration-resistant PCa from the same patient (n=8).

In summary, this study has revealed that UBE2C plays a previously unrecognised vital role in the regulation of the proportion and transition of quiescent PCa cells. These findings suggest: (i) UBE2C blocks cell cycle exit and promotes cell cycle re-entry; (ii) UBE2C can downregulate p27 expression, possibly through augmenting SKP2 and PIRH2 expression; (iii) UBE2C can upregulate c-MYC expression, possibly through reducing FBXW7 expression; and (iv) UBE2C mRNA and/or protein levels are aberrantly increased in the advanced form of PCa, and the increased expression of UBE2C is associated with PCa progression.

# Acknowledgements

I consider myself incredibly lucky to have enrolled in the dissertation research in the School of Science and Health at The University of Western Sydney. I would like to acknowledge a number of people, who gave so much and made my achievements possible.

First and foremost, I would like to express my deepest gratitude to my supervisor, Associate Professor Qihan Dong. His mentorship in scientific knowledge, direct guidance, expert advice, attention, care and support has been endlessly appreciated. I would also like to thank my co-supervisor, Dr Mu Yao for his expert advice over the years and experimental assistance. My supervisors' support and encouragement in the process of my PhD, especially in difficult times of problem solving and method development, will always be remembered.

To those in the School of Science and Health who have gone out of their way to give the support, their contributions have definitely not gone unnoticed or unappreciated. I wish to express my thanks and gratitude to all who have assisted me and guided me along my research and thesis path. I would like to thank Dr Paul Sved, Dr Liza Cubeddu, Dr Amy Nisselle, Dr Jeff Holst and Professor Nick King for assistance in proofing and examining my work. I also thank my lab fellows Dr Johnny Ying Teng and Dr Sheng Hua, and fellow PhD students Su Thae Hnit, Adrian Gimenez and Soma Vignarajan and Honours student Christopher Powell for their great assistance and advice on my work.

Lastly, I would like to thank my Mum and Dad for their continual support in helping me get through my PhD years. Without their support at home, I would not have a chance in today's achievement.

# Table of Contents

# List of Figures

# List of Tables

# Abbreviations

| | |
|---|---|
| **2N** | Diploid |
| **4N** | Tetraploid |
| **AAHPC** | American hereditary prostate cancer study network |
| **ABC** | Avidin-biotin complex kit |
| **ACS** | American cancer scociety |
| **ADPC** | Androgen-dependent prostate cancer |
| **ADT** | Androgen deprivation therapy |
| **AIHW** | Australian institute of health and welfare |
| **AIPC** | Androgen-independent prostate cancer |
| **AJCC** | American joint committee on cancer |
| **AKT** | Protein kinase B |
| **Ala** | Alanine |
| **APC/C** | Anaphase promoting complex or cyclosome |
| **APS** | Ammonium persulfate |
| **AR** | Androgen receptor |
| **Asn** | Asparagine |
| **Asp** | Aspartic acid |
| **ATP** | Adenosine triphosphate |
| **ATRA** | All-trans retinoic acid |
| **BEZ235** | Imidazoquinoline derivative and PI3K inhibitor |
| **BPH** | Benign prostatic hyperplasia |
| **Bub3** | Budding uninhibited by benzimidazoles 3 |
| **BubR** | Bub receptor |
| **C1** | UBE2C siRNA set 1 |
| **C2** | UBE2C siRNA set 2 |
| **C2ORF40** | Chromosome 2 open reading frame 40 |
| **C3** | UBE2C siRNA set 3 |
| **C4-2B** | Bone metastasised subline of LNCaP |

| | |
|---|---|
| **CCI-779** | Cell cycle inhibitor-779 |
| **CDC2/CDC20** | Cell division cycle 2/Cell division cycle 20 |
| **CDH1** | Cadherin-1 |
| **CDK** | Cyclin-dependent kinase |
| **cDNA** | Complementary DNA |
| **CID3** | Contact inhibition 3 days |
| **CIN** | Cancer institute of New South Wales |
| **CKS1** | CDC28 protein kinase regulatory subunit 1 |
| **$CO_2$** | Carbon dioxide |
| **CP1A** | Calpain-1 A |
| **CP1C** | Calpain-1C |
| **c-Rel** | Reticuloendotheliosis oncogene cellular homolog |
| **CRM1** | Chromosome region maintenance 1 |
| **CRPC** | Castration-resistant prostate cancer |
| **$C_T$** | Threshold cycle |
| **C-terminal** | Carboxyl amino acid terminal |
| **CUL1** | Cullin 1 |
| **Cys** | Cysteine |
| **DAB** | 3’ diaminobenzidine tetrachloride |
| **D-box** | Destruction box |
| **DEPC** | Diethylpyrocarbonate |
| **DN** | Dominant negative |
| **DNA** | Deoxyribonucleic acid |
| **dNTP** | Nucleoside triphosphate |
| **DPX** | Di-n-butylphthalate in xylene |
| **DTT** | Dithiothreitol |
| **DUB** | Deubiquitination enzymes |
| **E1** | Ubiquitin-activating enzyme |
| **E2** | Ubiquitin-conjugating enzyme |
| **E2F** | Elongation 2 transcription factor |
| **E3** | Ubiquitin ligases |
| **EDTA** | Ethylenediaminetetraacetic acid |
| **EGF** | Epithelium growth factor |

| | |
|---|---|
| **Empty** | Empty vector |
| **EWS/FLI1** | A transcription factor highly expressed in Ewing's sarcoma and primitive neuroectodermal tumour |
| **FBS** | Fetal bovine serum |
| **FBXW7** | F-Box and WD repeat domain containing 7, E3 ubiquitin protein ligase |
| **FCS** | Fetal calf serum |
| **FoxA1** | Forkhead transcription factor A1 |
| **FOXO1** | Forkhead Box O1 |
| **$G_0$** | Gap 0 phase |
| **$G_1$** | Gap 1 phase of mitosis |
| **$G_2$** | Gap 2 phase of mitosis |
| **GAPDH** | Glyceraldehydes-3-phosphate dehydrogenase |
| **GATA2** | GATA binding protein 2 |
| **GC content** | Guanine and cytosine content in DNA |
| **Gln** | Glutamic acid |
| **Gly** | Glycine |
| **GOI** | Gene of interest |
| **h** | Hour |
| **HCL** | Hydrochloric acid |
| **HETE** | Hydroxyeicosatetraenoic acids |
| **HP** | Hoechst 33258 and Pyronin Y |
| **hPCM** | Human prostate complete media kit |
| **HRP** | Horseradish peroxidase |
| **HSPC** | Hormone sensitive prostate cancer |
| **Ig** | Immunoglobulin |
| **IGF** | Insulin or insulin-like growth factor |
| **Ile** | Isoleucine |
| **JNK** | Jun N-terminal kinases |
| **kDa** | kilo Daltons |
| **KEN-box** | Amino acid sequence $KEN(X)_nP$ |
| **KIP** | Kinase inhibitor protein |
| **KMN** | KNL-1, Mis12 complex (Mis14) and Hec1/Ndc80 network |
| **KMTs** | Kinetochore microtubules |

| | |
|---|---|
| **Leu** | Leucine |
| **LNCaP** | Lymph node metastasis prostate cancer cells |
| **Lys** | Lysine |
| **M** | Mitosis phase |
| **MAD1/ MAD2** | Mitotic arrest deficient-like 1/Mitotic arrest deficient-like 2 |
| **MAX** | MYC-associated factor X |
| **MED1** | Mediator-1 |
| **MEFs** | Mouse embryonic fibroblast |
| **Meis-1** | Myeloid ecotropic viral integration site 1 |
| **Met** | Methionine |
| **min** | Minutes |
| **Mirk** | Minibrain-related kinase |
| **mRNA** | Message RNA |
| **mTOR** | Mammalian target of rapamycin |
| **MTs** | Microtubules |
| **MYC** | Avian myelocytomatosis viral oncogene homolog |
| **MYCL1** | V-Myc avian myelocytomatosis viral oncogene lung carcinoma-derived homolog |
| **MYCN** | V-Myc avian myelocytomatosis viral oncogene neuroblastoma-derived homolog |
| **NaCl** | Sodium chloride |
| **NC** | Negative control |
| **NCI** | National cancer institute |
| **NF-1** | Neurofibromin 1 |
| **NHS** | Normal horse serum |
| **NIH3T3** | Primary mouse embryonic fibroblast |
| **NLS** | Nuclear localisation signal |
| **NOCI** | No contact inhibition |
| **N-terminal** | Amine amino acid terminal |
| **OCPC** | Organ-confined hormone naive prostate cancer |
| **oligo dT** | Short sequence of deoxy-thymine nucleotides |
| **Pax-2** | Paxillin 2 |
| **PBS** | Phosphate-buffered saline |

| | |
|---|---|
| **PC-3** | Bone metastasised prostate cancer cells |
| **PCFA** | Prostate cancer foundation of Australia |
| **PCR** | Polymerase chain reaction |
| **PDB** | Protein data bank |
| **Phe** | Phenylalanine |
| **PI** | Propidium iodide |
| **PI3K** | Phosphatidylinositol 3-kinase |
| **Pim-1** | Proviral integration site mis-1 |
| **PIRH2** | p53-induced RING-H2-type ubiquitin ligase |
| **POL II** | Polymerase II |
| **PrEC** | Prostate epithelial cells |
| **Pro** | Proline |
| **PSA** | Prostate-specific antigen |
| **QNP motif** | Gln4, Asn5 and Pro8 motif |
| **qPCR** | Quantitative PCR |
| **qRT-PCR** | Quantitative real-time reverse transcription PCR |
| **Ras** | Rat sarcoma viral oncogene homolog |
| **Rb** | Retinoblastoma |
| **RING** | Really interesting new gene |
| **RNA** | Ribonucleic acid |
| **RNase OUT** | Recombinant ribonuclease inhibitor |
| **RPD1–3** | Replate at lower density for 1–3 days |
| **RPMI** | Roswell Park Memorial Institute medium |
| **RT** | Reverse transcriptase enzyme |
| **RWD domain** | Domain find in RING finger-WD repeat domain-containing protein |
| **RWPE-1** | HPV18 immortalised human prostate epithelial cells |
| **S** | Synthesis phase of mitosis |
| **SAC** | Spindle assembly checkpoint |
| **SCF** | SKP1-cullin-F-box |
| **SCPC** | Small-cell prostate carcinoma |
| **SDS** | Sodium dodecyl sulphate |
| **Ser** | Serine |
| **siRNA** | Small interference RNA |

| | |
|---|---|
| **siUBE2C** | siRNAs derived specifically against the *UBE2C* gene |
| **SKP2** | S-phase kinase-associated protein 2 |
| **SRD1–7** | Serum replenish day 1–7 |
| **SRF** | Serum response factor |
| **SWD1–7** | Serum withdrawal day 1–7 |
| **TBP** | TATA binding protein |
| **TBST** | Tris-buffered saline containing TWEEN-20 |
| **TEMED** | N, N, N', N'-tetramethylethylenediamine |
| **TGFβ** | Transforming growth factor beta |
| **TGIF** | TGFB-induced factor homeobox 1 |
| **TMAs** | Tissue microarrays |
| **TNM** | Tumour, lymph node, metastasis |
| **TSS** | Transcription start site |
| **TURP** | Transurethral resection of the prostate |
| **Tyr** | Tyrosine |
| **UbcH10** | Human ubiquitin-conjugating enzyme 10 |
| **UBE2C** | Ubiquitin-conjugating enzyme C |
| **UPS** | Ubiquitin proteasome system |
| **USP44** | Ubiquitin-specific peptidase 44 |

# List of Publications

(In the order of authorship)

1. **Xie, C.,** Powell, C., Yao, M., Wu, J., and Dong, Q. (2014). Ubiquitin-conjugating enzyme E2C: A potential cancer biomarker. *Int J Biochem Cell Biol* 47, 113-117.

2. **Xie, C.,** Yao, M., and Dong, Q. (2014). Proliferating cell unclear antigen-associated factor (PAF15): A novel oncogene. *Int J Biochem Cell Biol* 50, 127-1318.

3. Vignarajan, S., **Xie, C.,** Yao, M., Sun, Y., Simanainen, U., Sved, P., Liu, T., and Dong, Q. (2014). Loss of PTEN stabilizes the lipid modifying enzyme cytosolic phospholipase A2α via AKT in prostate cancer cells. *Oncotarget* 5, 6289-6299.

4. Hua, S., **Xie, C.**, Yao, M., and Dong, Q. (2014). Effect of arachidonic acid and its producing enzyme phospholipase A2α on key oncogenic pathways in prostate cancer, in *Arachidonic Acid: Sources, Biosynthesis and Health Effects* (O'Keefe, J. M. ed.), 135-164, Nova Science Publishers, Hauppauge, New York.

5. Hnit, S. S., **Xie, C.,** Yao, M., Holst, J., Bensoussan, A., De Souza, P., Li, Z., and Dong, Q. (2015). p27(Kip1) signaling: Transcriptional and post-translational regulation. *Int J Biochem Cell Biol* 68, 9-14.

6. Yao, M., **Xie, C.**, Kiang, M. Y., Teng, Y., Harman, D., Tiffen, J., and Dong, Q. (2015). Targeting of cytosolic phospholipase A2alpha impedes cell cycle re-entry of quiescent prostate cancer cells. *Oncotarget* 6, 34458-34474.

7. Zheng, Z., He, X., **Xie, C.,** Hua, S., Li, J., Wang, T., Yao, M., Vignarajan, S., Teng, Y., Hejazi, L., Liu, B., and Dong, Q. (2014). Targeting cytosolic phospholipase A2 alpha in

colorectal cancer cells inhibits constitutively activated protein kinase B (AKT) and cell proliferation. *Oncotarget* 5, 12304-12316.

8. Hua, S., Vignarajan, S., Yao, M., **Xie, C**., Sved, P., and Dong, Q. (2015). AKT and cytosolic phospholipase A2alpha form a positive loop in prostate cancer cells. *Curr Cancer Drug Targets* 15, 781-791.
9. Xi, Z., Yao, M., Li, Y., **Xie, C.,** Holst, J., Liu, T., Cai, S., Lao, Y., Tan, H., Xu, H. and Dong, Q. (2016). Guttiferone K impedes cell cycle re-entry of quiescent prostate cancer cells via stabilization of FBXW7 and subsequent c-MYC degradation. *Cell Death and Disease* 7, e2252.
10. Garbutcheon-Singh, K. B., Myers, S., Harper, B. W., Ng, N. S., Dong, Q., **Xie, C.**, and Aldrich-Wright, J. R. (2013). The effects of 56MESS on mitochondrial and cytoskeletal proteins and the cell cycle in MDCK cells. *Metallomics* 5, 1061-1067.

**Conference Abstract:**

1. **Xie, C.**, Powell, C., Yao, M., and Dong, Q. (2014). Ubiquitin conjugating enzyme 2C promotes cell cycle re-entry in quiescent prostate cancer cells. *The Cell Cycle Meeting*, Cold Spring Harbor Laboratory, New York.
2. Hint, S., **Xie, C.**, Yao, M., Chan, C., Youhana, C., and Dong, Q. (2016). The role of Zeste White 10 interactor-1 in cell cycle exit and re-entry in prostate cancer cells. *The Cell Cycle Meeting*, Cold Spring Harbor Laboratory, New York.
3. Teng, Y., Yao, M., Xu, H., Hua, S., **Xie, C.**, Bao, B., and Dong, Q. (2013). Inhibition of cell cycle re-entry of quiescent colon cancer cells by compounds isolated from Garcinia plants. *Advanced Cancer Medical Research (ACMR)*, Singapore.

# Chapter 1

# 1. Introduction

# 1.1. Background

## 1.1.1. Prostate cancer

Prostate cancer (PCa) is the second-most common cause of death in Australia—after cardiovascular diseases (Australian Institute of Health and Welfare (AIHW), 2016). In 2015, there were an estimated 126,800 new cases of cancer diagnosed in Australia (69,790 males and 57,010 females) (AIHW, 2016). The AIHW (2016) reported that, PCa accounted for 24.7% of all new cancer cases in Australian males and 13% of male cancer deaths. The incidence is increasing rapidly as the population of males over the age of 50 grows worldwide (De Marzo *et al.*, 2007). The American Cancer Society (ACS, 2016) claims almost 1 in 7 males will eventually develop PCa during their lifetime, and about 1 in 38 man will die of PCa. Adoption of serum prostate-specific antigen (PSA) screening has led to a dramatic shift towards the diagnosis of low risk PCa (Jemal *et al.*, 2010). In fact, there are more than 2.9 million men in the United States who are living with PCa (ACS, 2016). However, approximately 20–40% of patients treated with radical prostatectomy will have tumour recurrence (Kupelian *et al.*, 2006; Paller and Antonarakis, 2013). Androgen deprivation therapy (ADT) is provided to patients who develop recurrent or metastatic prostate tumours. Unfortunately, 80–90% of patients who received ADT ultimately developed castration resistant PCa (CRPC) 12–33 months after ADT (Lin *et al.*, 2013); with a median overall survival of patients after tumour relapse only 1–2 years (Chuu *et al.*, 2011). There is therefore an acute need to understand the primary risk factors and molecular basis of PCa in order to manage this significant health issue.

## 1.1.2. Risk factors for prostate cancer

Researchers have defined several risk factors for PCa based on clinical, epidemiological and experimental observations. Some risk factors, like diet, can be avoided; others, like age, genetics and hormones, cannot be changed.

### 1.1.2.1. Age

Aging men have a higher risk of PCa. The American Cancer Society (2016) reported PCa is rare in American men younger than 40 with almost 6 in 10 cases of PCa found in men older than 65. The Cancer Institute of New South Wales (CIN, 2010) also stated that the incidence of PCa is relatively low in Australian men aged under 50, it increased sharply for the 50–55 age bracket, and peaked in the 60–69 age bracket, as shown in Figure 1-1**.** Overall, the mortality rate of PCa increased gradually from age 50 to 69 years, increased sharply from 80 years onwards (CIN, 2010). The median age for the diagnosis of PCa was 69, while the median age of death was 80 years (Tracey *et al.*, 2009).

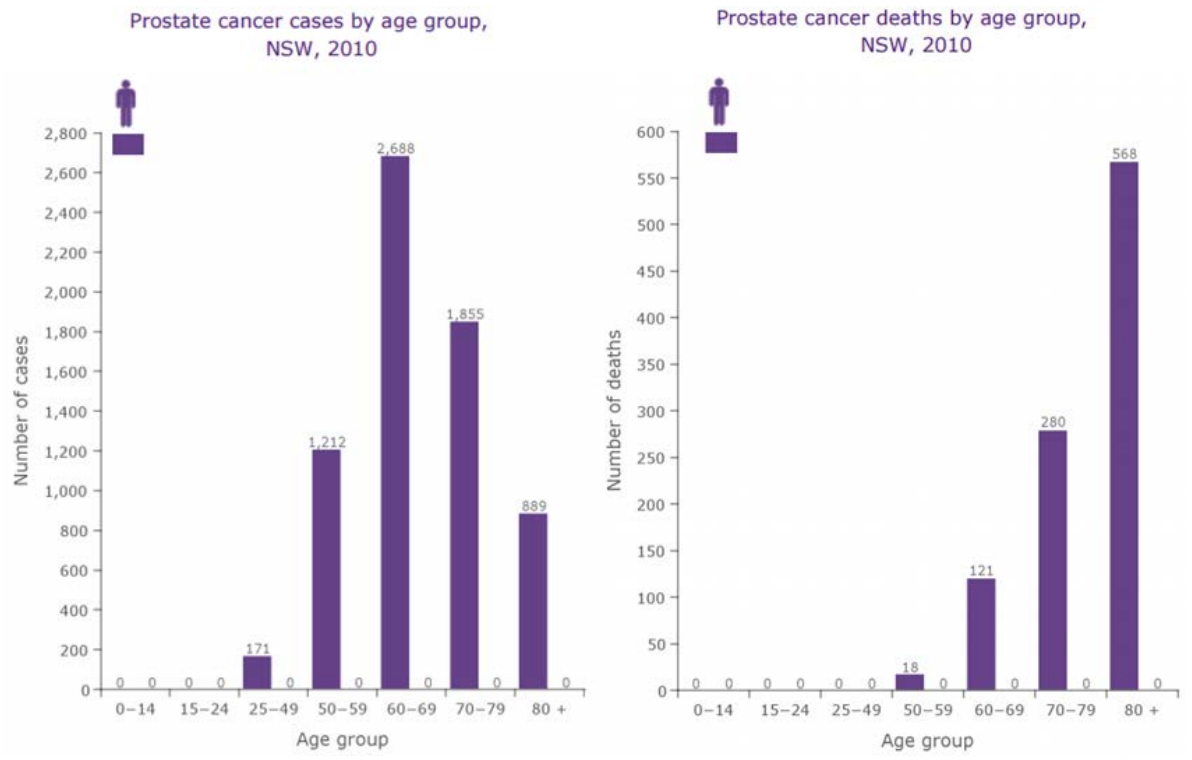


**Figure 1-1. The age specific incidence rates of prostate cancer in New South Wales, 2010.**

The incidence rate rose sharply in men aged 50–55 years and peaked at ages 75–79 years (Left). The mortality of PCa increased gradually for patients between the ages of 40 and 64 years, then sharply increased from 65 years onwards, then decreased after the age of 85 (Right) (CIN, 2010).

## 1.1.2.2. Genetics

Genetics is another possible risk factor for PCa. Men with a family history of more than one relative with PCa – a first-degree relative, such as father, or a family member diagnosed under the age of 60 – are at higher risk (Wigle *et al.*, 2008). Moreover, the incidence of PCa is variable for different races, with some races more susceptible than others. For example, symptomatic carcinoma of the prostate is more common and occurs at an early age in African Americans than in whites, Asians or Hispanics (Lima *et al.*, 2015; Siegel *et al.*, 2014). According to the National Cancer Institute (NCI, 2002), the incidence of PCa is approximately two folds higher in African Americans, along with a three-fold higher

mortality rate. The African American Hereditary Prostate Cancer Study Network (AAHPC) recruited 77 African American extended families, encompassing a total of 418 men with PCa, to participate in the first genome-wide linkage study of PCa in African Americans. The results identified several regions of the human genome at 11q22, 17p11, and Xq21 that are associated with increased susceptibility to PCa (Baffoe-Bonnie *et al.*, 2007). Furthermore, family members with a mutation in the breast cancer susceptibility gene (BRCA1/2) gene, a genetic mutation associated with breast and ovarian cancers, may also increase PCa risk in some men. However, this genetic mutation probably account for only a small percentage of PCa cases (Cavanagh and Rogers, 2015).

#### 1.1.2.3. Hormones

Epidemiologic studies provide inconsistent evidence for the role of endogenous androgen levels in PCa development. However, there is still a possibility that endogenous androgen levels may influence the initiation and promotion of PCa (Wigle *et al.*, 2008). For example, androgen interacts with the androgen receptor (AR) to regulate the transcription of androgen-responsive genes that are essential for prostate growth (Shidaifat, 2009).

#### 1.1.2.4. Diet

Diet appears to be a major determinant in the incidence rate of PCa with particular dietary substances involved still under investigation. Geographical and epidemiological evidence has linked diet to PCa, suggesting its role in the aetiology of the disease (ACS, 2016). The likelihood of the development of PCa may be minimised by eliminating a high consumption of red meat and processed animal polyunsaturated fat (Williams *et al.*, 2010). High blood levels of omega 6, a polyunsaturated fatty acid derived from linoleic acid, was showed to increase the risk of developing advanced PCa by 70% (Wigle *et al.*, 2008). This notion is consistent with results from animal studies, which have shown that an increased dietary

intake of linoleic acid might enhance the risk of developing advanced PCa (Leitzmann *et al.*, 2004). Furthermore, a case-controlled study conducted in Athens demonstrated an increased risk of PCa is associated with the consumption of dairy products and seed oils (Bosetti *et al.*, 2000). In addition, milk, a source of calcium, has also been reported to increase in the risk of PCa (Wigle *et al.*, 2008).

## 1.1.3. Tumour grade and stage

### 1.1.3.1. Diagnosis of prostate cancer

Most patients develop PCa without experiencing any symptoms, it causes a delay in proper diagnosis and treatment, thereby resulting in a high mortality rate(Tracey *et al.*, 2009). An elevated level of PSA may indicate a higher chance of prostate diseases including benign prostatic hyperplasia (BPH) and PCa. However, there are also cases of PCa detected without increased PSA level (Thompson *et al.*, 2004). Therefore, PSA determination in conjunction with digital rectal examination is recommended by a majority of clinical guidelines for the detection of PCa prior to the manifestation of symptoms (Schmid *et al.*, 2004). Biopsy is made for pathological examination if an abnormality is found in PSA levels (PSA $\geq$ 4 ng/mL) and digital rectal examination. The grade and stage of PCa will then be examined.

### 1.1.3.2. Grading

The Gleason score, originally described by Dr Donald Gleason, is specifically used for grading a prostate biopsy (Gleason and Mellinger, 1974). A pathologist determines a Gleason score depending on the glandular pattern of the tissue, as shown in Figure 1-2. The Gleason score is generated as the sum of two scores obtained from both the primary and secondary pattern structure. The primary pattern (>50% of the total cancer cells observed) is a score between 1 and 5 depending on how cancerous the cells look. Then, the next most common

type of cancerous cell type (<50% but >5% of total cells observed) are also graded in the same way. This gives two separate scores out of 5. These scores are then added together to give the overall Gleason score out of 10.

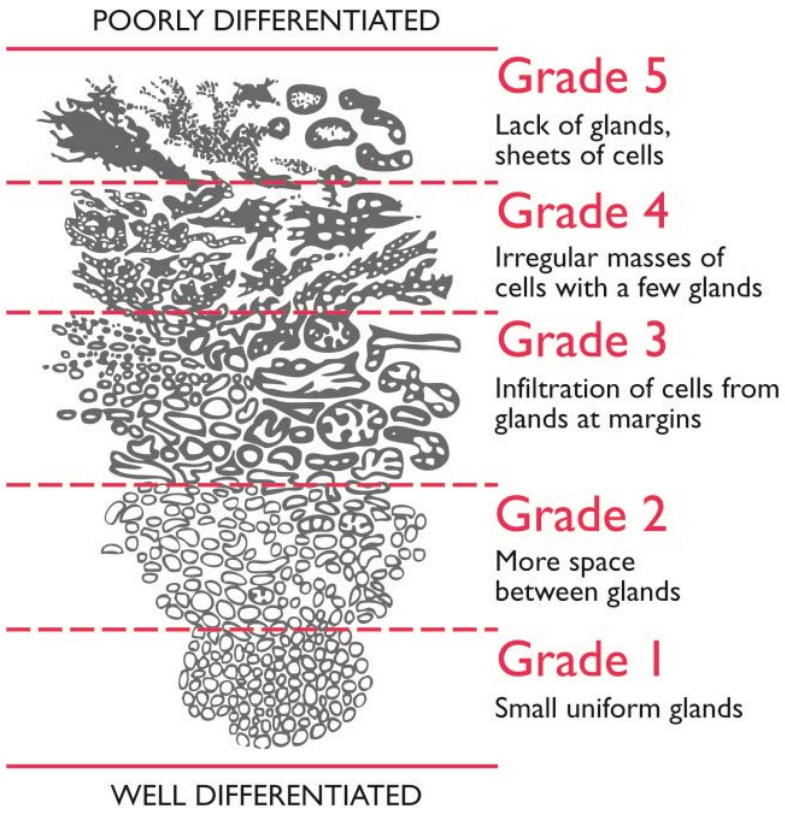


**Figure 1-2. The Gleason score system for histological grading of prostate cancer.**
(Adapted from Orchid Fighting male cancer website: www.Orchid-cancer.org.uk).

The Gleason score is normally associated with the aggressiveness of PCa (Table 1-1). Patients with low grade (Gleason ≤6) tumours have a slow progressing type of PCa. A Gleason score of 7 (3+4 or 4+3) is usually termed a moderate grade while those with a Gleason scores of 8 (3+5, 4+4, 5+3), 9 (4+5, 5+4) and 10 (5+5) have a hazard ratio of lethal cancer 7.4 times higher than those with Gleason score 3+4 (Penney *et al.*, 2011). Additionally, researchers tend to divide a Gleason score of 7 group into two groups: 4+3 and

3+4, as a 3-fold increase of PCa mortality in the setting of 4+3 vs. 3+4 groups was observed (Stark *et al.*, 2009).

**Table 1-1. Gleason scores in categorical order.**

| Gleason score | Risk | |
|---|---|---|
| ⩽6 | Low | Slow-growing and less aggressive cancer |
| 7 | Medium | Faster-growing and moderately aggressive cancer |
| 8–10 | High | Faster-growing and aggressive cancer |

(Adapted from Cancer Council NSW website: www.cancercouncil.com.au).

### 1.1.3.3. Staging

The grade reflects how fast a cancer is growing, whereas the stage of PCa reflects how far the cancer has metastasised (spread). The most widely used staging system for PCa is the American Joint Committee on Cancer (AJCC) TNM system, which stands for Tumour, Node, and Metastasis. The **T** category refers to the extent of the primary tumour, **N** category scores whether the cancer has spread to nearby lymph nodes, an **M** exams whether the cancer has metastasised to other parts of the body (AJCC, 2015). The stages of PCa can be classified by combining the TNM rating, the PSA level in the blood and the Gleason score from a biopsy; these are summarised in Table 1-2.

**Table 1-2. Anatomic stage and prognostic group of prostate cancer.**

| Stage | Tumour | Nodes | Metastasis | PSA (ng/mL) | Gleason Score |
|---|---|---|---|---|---|
| I | T1–2a | N0 | M0 | <10 | ≤6 |
| IIA | T1 | N0 | M0 | <20 | 7 |
| | T1 | N0 | M0 | 10 ≤ PSA <20 | ≤6 |
| | T2a–b | N0 | M0 | <20 | ≤7 |
| IIB | T2c | N0 | M0 | Any | Any |
| | T1–2 | N0 | M0 | <20 | Any |
| | T1–2 | N0 | M0 | Any | ≥8 |
| III | T3a–b | N0 | M0 | Any | Any |
| IV | T4 | N0 | M0 | Any | Any |
| | Any T | N1 | M0 | Any | Any |
| | Any T | Any N | M1 | Any | Any |

Adapted from American cancer society: PCa www.cancer.org/cancer/prostatecancer.

## 1.1.4. Current treatment

Recent treatments for PCa reported by the Prostate Cancer Foundation of Australia ( PCFA, 2016) include: active surveillance, radical prostatectomy, external beam radiotherapy, low/high dose brachytherapy, high intensity focused ultrasound, chemotherapy and androgen ablation therapy (Cooperberg *et al.*, 2011). The choice of treatment depends on many aspects, such as the stage of the PCa, the level of PSA in the blood stream, the age and health condition of the patient as well as the side effects of treatment. Organ-confined PCa (OCPC) is treated by surgery or local irradiation (PCFA, 2013). At the advanced stage when metastases occur, PCa is treated with ADT, as the growth and division of PCa cells is highly dependent on androgen. Gonadotropin-releasing hormone antagonist may also be used to either reduce the level of androgen produced by the body or block the effects of androgen on cancer cells. As a result, it may shrink the size of the tumour, suppress its growth and reduce the level of PSA (ACS, 2016; AIHW, 2016).

However, most PCa eventually becomes androgen-independent and thus resistant to ADT (Lin *et al.*, 2013). One of the approaches used for hormone refractory PCa is chemoprevention, which refers to the administration of synthetic or naturally occurring agents to block, reverse, or delay the process of carcinogenesis (Adhami *et al.*, 2007). However, as both chemotherapy and chemoprevention possess limited efficacy for patients with advanced androgen refractory PCa, these patients generally have a poor prognosis.

The mechanisms of how OCPC develops into CRPC remain to be defined. Therefore, it is important to enhance our understanding of the molecular basis of prostate carcinogenesis to improve future approaches for its treatment or possible prevention.

## 1.2. Quiescent Cancer Cells

Cancer is a consequence of uncontrolled cell division. Quiescent cancer cells, which are Ki-67 negative and arrest at $G_0$, have been found in various cancers including PCa (Coller, 2007; Jackson, 1989). These quiescent cancer cells are in a reversible state of arrest, and have been found to re-entre cell cycle in response to proliferative environmental signals (Desoize and Jardillier, 2000). Recent studies in PCa have shown that the increased proportion of proliferative over quiescent ratio in PCa cells represents an inherent mechanism that at least partially explains recurrence in PCa patients (Almog, 2010; Brackstone *et al.*, 2007; Udagawa, 2008). The Ki-67 protein immunostaining in PCa showed a low positivity in low grade and low volume disease, but increases in high risk and advanced disease, suggesting an accelerated transition from quiescent to a proliferative state during disease progression (Jhavar *et al.*, 2009; Keshari *et al.*, 2011; Khatami *et al.*, 2009; Nagao *et al.*, 2011). However, while the regulation of cell cycle progression is well understood, the signal required for PCa cell to exit and re-enter the cell cycle is still elusive. To understand the role of quiescent

cancer cells in regulation of PCa progression, the basic cell cycle regulation will be summarised below.

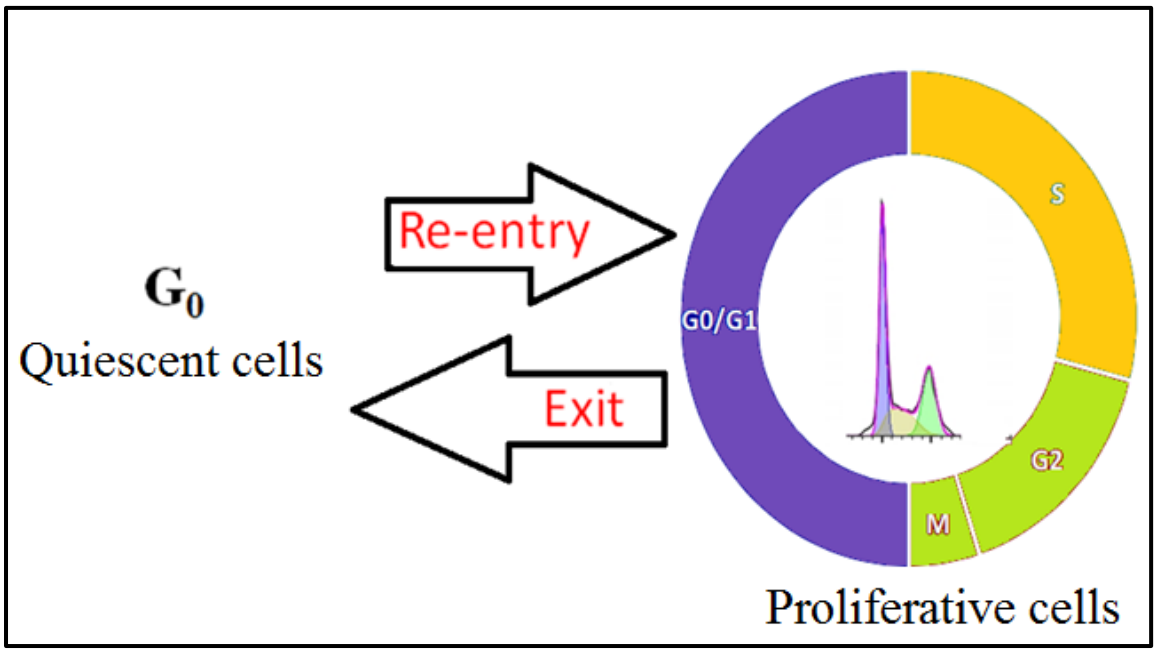


**Figure 1-3. The cell cycle in terms of proliferative versus quiescent cancer cells.**

When cells cease proliferation, they exit the cycle and enter a non-dividing, quiescent state known as $G_0$. These quiescent cancer cells are in a reversible state of arrest. Quiescent cancer cells re-entre cell cycle in response to proliferative environmental signals. Yellow, cells in S phase, DNA replication starts and the amount of DNA increases. Green, cells in $G_2$/M phase, the DNA replication continues until the DNA content reaches a tetraploid (4N) state. Tetraploid cells in the $G_2$ phase start preparing for division and enter the M phase when the cells divide into two identical daughter cells. The daughter cells continue on to another division cycle or enter the $G_0$ phase.

### 1.2.1. Phases of the cell cycle

The basic cell cycle is divided into four sequential phases: gap 1 ($G_1$), synthesis (S), gap 2 ($G_2$) and mitosis (M) (Figure 1-4A). Passage through the cell cycle is strictly controlled by cyclin/cyclin-dependent kinase (CDK) complexes and regulated at three checkpoints, including $G_1$ (restriction) check point, $G_2$/M DNA damage check point and anaphase or the spindle assembly checkpoint (SAC). The timely activation of CDKs by the binding of characteristic partner cyclins and subsequent phosphorylation of specific substrates regulates progression through the different stages of the cell cycle. Each cyclin exhibits a pattern of expression and degradation throughout the progression of the cell cycle (Figure 1-4C). Cyclins D and E, known as $G_1$ cyclins, bind to CDK4/6 and CDK2, respectively, resulting in $G_1$/S transition. Cyclins A and B are mitotic cyclins; cyclin A/CDK2 and cyclin A/ CDK1 complexes are required for S phase progression and the cyclin B/CDK1 complex is required to transition from $G_2$ to M phase. Following their activation, CDKs are inactivated by the degradation of partner cyclins in order for the cell cycle to progress. Checkpoints prevent cells from entering a new phase until they have successfully completed the previous one. Upon DNA damage, checkpoints will be activated to arrest cells for DNA repair or initiation of apoptosis (Takahashi-Yanaga and Sasaguri, 2008; Walczak *et al.*, 2010).

The $G_1$, S and $G_2$ phases are collectively known as interphase. Mitosis can be staged into prophase, prometaphase, metaphase, anaphase and telophase (Figure 1-4A&B). In interphase, individual chromosomes cannot be seen because the chromatin is decondensed in the nucleus. During prophase, chromatin condenses into chromosomes and the chromosomes become highly separated. Nuclear envelope breakdown marks the transition from prophase to prometaphase so that the individual chromosomes are no longer constrained in the nucleus. As shown in Figure 1-4B, during prometaphase, kinetochore-microtubules (KMTs) connect

the spindle microtubules (MTs) and the kinetochores on the chromosomes (Brinkley and Stubblefield, 1966). The chromosome aligns at the spindle equator, which defines metaphase. The MTs emanate from the centrosomes and extend their plus ends towards the cell cortex. Chromosome segregation occurs during anaphase after loss of the sister chromatid cohesion (Perez de Castro *et al.*, 2007). The movement of the chromosomes towards the poles occurs during early anaphase, and the two spindle poles separate during late anaphase. The nuclear envelope begins to reform and the DNA begins to decondense during telophase. Cytokinesis divides the cytoplasm of the cell so that the two daughter nuclei are segregated into individual cells (Walczak *et al.*, 2010).

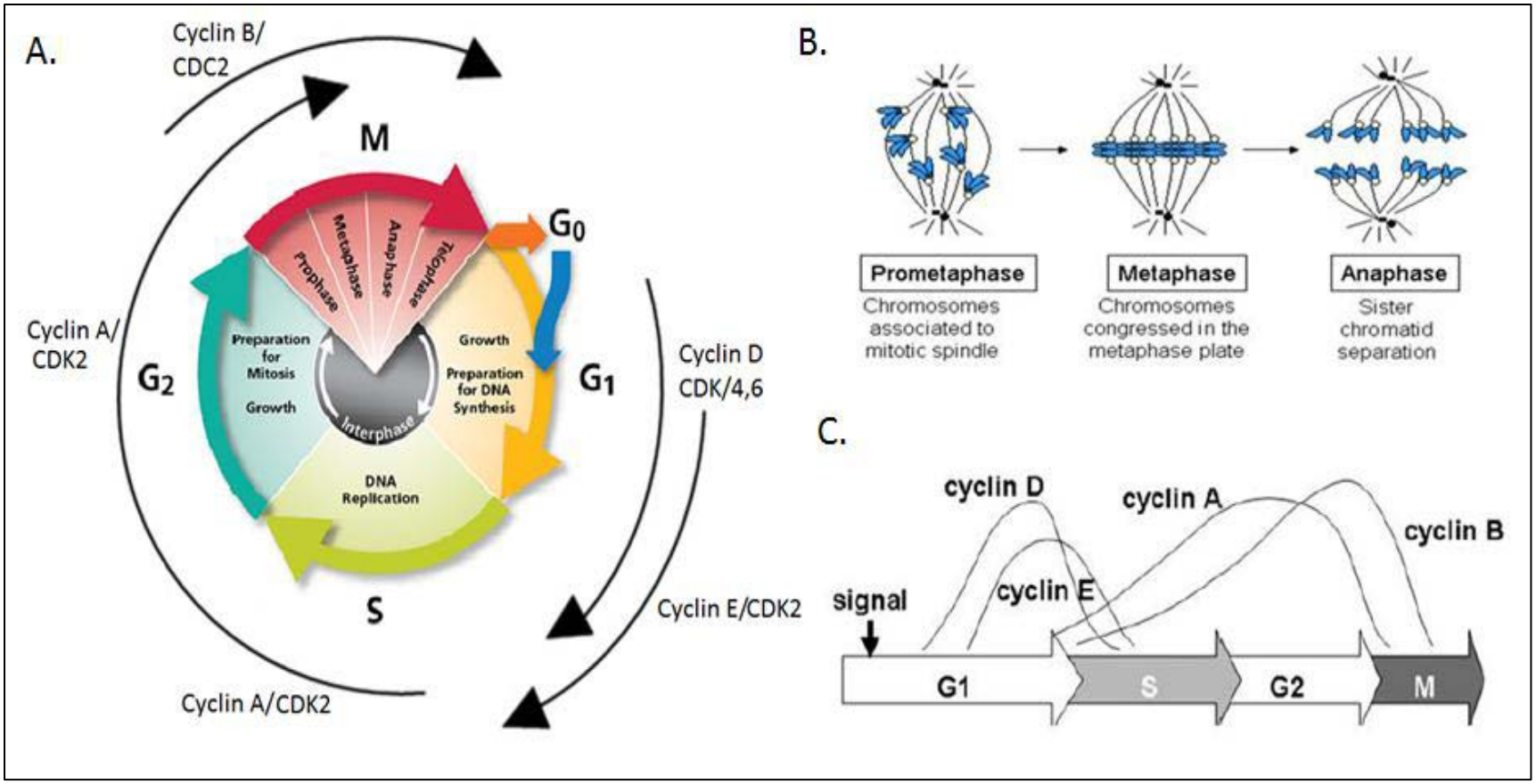


**Figure 1-4. A schematic graph of the cell cycle.**

**A**. Cell cycle phases. **B**. Individual phases of mitosis. **C**. Fluctuating levels of cyclins (Takahashi-Yanaga and Sasaguri, 2008).

## 1.2.2. Known cell cycle regulators

When cells cease proliferation, either due to specific antimitogenic signals or to the absence of proper mitogenic signalling, they exit the cycle and enter a non-dividing, quiescent state known as $G_0$. The $G_0$ regulatory proteins p27 and c-MYC, plays a key role in regulating cell cycle re-entry (Bretones *et al.*, 2015; Chu *et al.*, 2008).

### 1.2.2.1. p27

In 1994, a 27 kDa protein was found to possess a capacity to inhibit the activity of CDK2 following treatment of mink lung epithelial cells with transforming growth factor (TGFβ) (Polyak *et al.*, 1994). This protein was named the CDK inhibitor 1B or p27. As a member of the kinase inhibitor protein (KIP) family, p27 was also named as $p27^{KIP1}$ and thought to control cell cycle progression via binding and inhibiting cyclin-CDK complexes in $G_1$ (Polyak *et al.*, 1994) or even beyond $G_1$ (Grimmler *et al.*, 2007; James *et al.*, 2008; O'Hagan *et al.*, 2000; Sheaff *et al.*, 1997).

The p27 gene is located on chromosome 12p13 (Pietenpol *et al.*, 1995). The CDK-inhibitory domain resides at the N-terminal portion of p27 and is sufficient to arrest cells at $G_0/G_1$. The carboxyl terminal (C-terminal) portion of p27 is less conserved in the KIP family and contains a nuclear localisation signal (NLS) (Russo *et al.*, 1996). p27 regulates $G_0/G_1$ –S progression by inhibiting cyclin/CDK complexes, including cyclin E/A-CDK2 (Aleem *et al.*, 2005; James *et al.*, 2008; Ray *et al.*, 2009; Russo *et al.*, 1996), cyclin D-CDK4/6 (James *et al.*, 2008; Ray *et al.*, 2009) and cyclin B-CDK1 (Aleem *et al.*, 2005).

The protein levels of p27 are tightly regulated, being typically high during $G_0/G_1$ and falling sharply just before cell cycle entry into the S phase (Chu *et al.*, 2008). In $G_0$ phase, p27 is markedly increased in the nucleus of $G_0$-arrested cells (Besson *et al.*, 2006; Rivard *et al.*,

1996). The increase in p27 inhibits CDK/cyclin complexes, blocking the phosphorylation of retinoblastoma (Rb) (Dyson, 1998). Rb physically associates with E2F factors and inhibits E2F-dependent transcription, thereby hindering cell cycle re-entry (Dyson, 1998). Whereas, the protein level of p27 decreased upon cell cycle re-entry, CDKs phosphorylate Rb (p-Rb), releasing E2F to promote transcription of cyclins and thus entering the cell cycle (D'Antonio *et al.*, 2010; Nakayama and Nakayama, 2006) (Figure 1-5).

In addition, in quiescent states, p-Rb also binds to the anaphase promoting complex, or cyclosome-cadherin-1 ($APC/C^{CDH1}$), resulting in the efficient proteolysis of S-phase kinase-associated protein 2 (SKP2) and in the subsequent accumulation of p27 (Santamaria and Pagano, 2007). Cadherin-1 (CDH1), an activator of APC/C, is active in $G_0$ and $G_1$ (Skaar and Pagano, 2008). From late mitosis to mid-$G_1$, dephosphorylated CDH1 binds and activates APC/C, and the major function of $APC/C^{CDH1}$ is to maintain a low CDK activity in $G_0/G_1$ (Santamaria and Pagano, 2007). Thus, the leading keepers of quiescence and differentiation – p-Rb, CDH1, SKP2 and p27 – are tightly linked to each other through proteolytic mechanisms (Santamaria and Pagano, 2007). During cell cycle re-entry, the increased level of proviral integration site mis-1 (Pim-1) stabilises SKP2 by phosphorylation and also inhibits APC/C activity by phosphorylating CDH1, protecting SKP2 from degradation. p27 is then targeted by SKP2 for degradation (Cen *et al.*, 2010). Consistent with notion, SKP2 levels are decreased in $G_0$ and increased in $G_1$ (Krek *et al.*, 2000) (Figure 1-5).

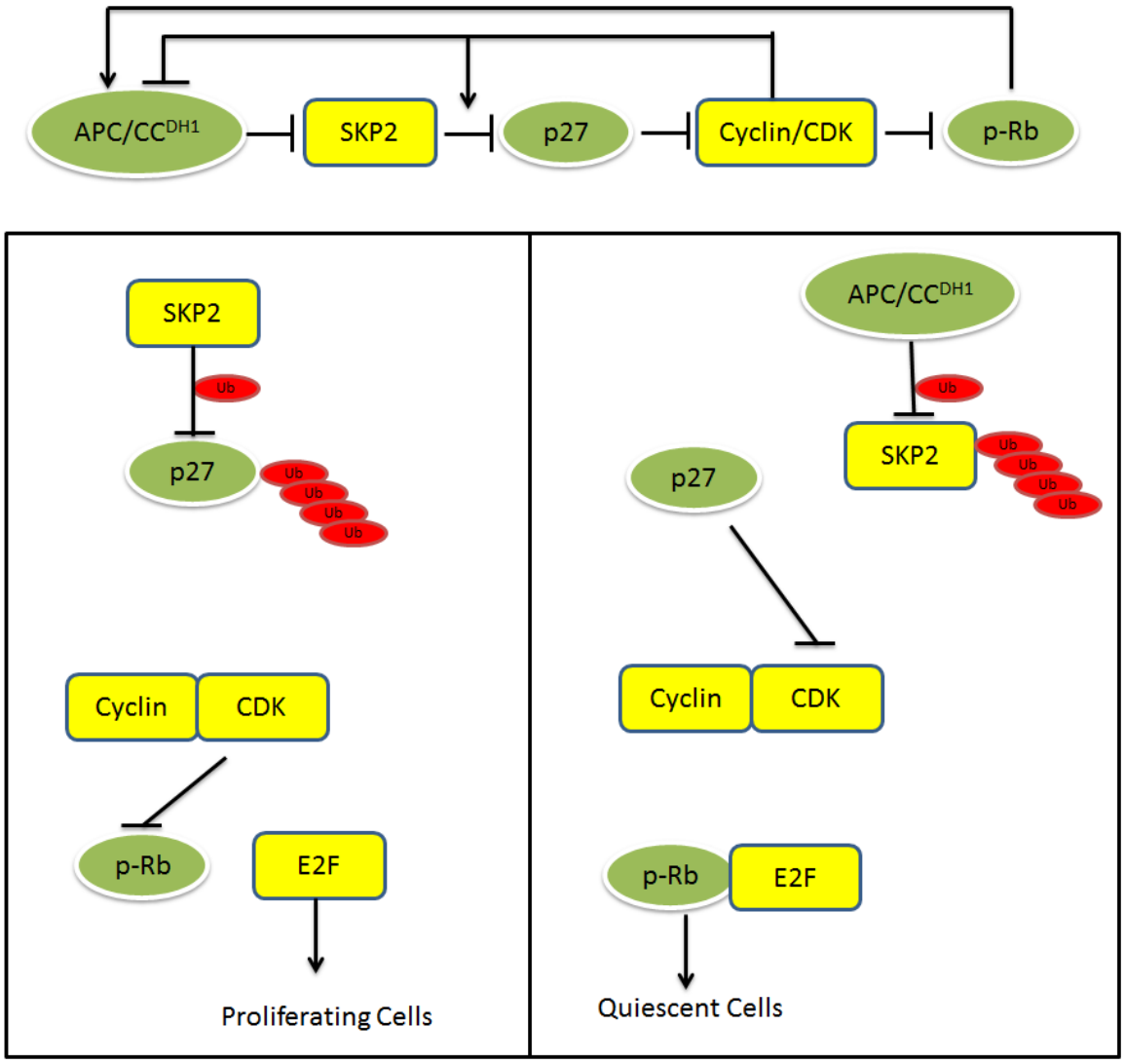


**Figure 1-5. p27 stability and its regulation.**

Proteins in yellow, promoting cell cycle re-entry. Proteins in Green, halting cell cycle re-entry. Proto-oncogenes, keeping tumour suppressors in check. Tumour suppressors, inhibiting proto-oncoproteins (Santamaria and Pagano, 2007).

p27, as a tumour suppressor, is inversely correlated with the prognosis of cancer patients (Sgambato *et al.*, 2000). *p27* is haploinsufficient, with the loss of a single *p27* allele being sufficient to increase tumour incidence (Fero *et al.*, 1998). Decreased levels of p27 protein, in particular nuclear-expressed p27, is implicated in disease progression and poor prognosis in lung, head and neck, colon, breast, ovary and PCa (Chu *et al.*, 2008). p27-null mice show

multiorgan hyperplasia, retinal dysplasia, increased body size and tumour formation (Fero *et al.*, 1996; Kiyokawa *et al.*, 1996), suggesting an indispensable function of p27. Low protein levels or cytoplasmic expression of p27 is associated with cancer aggressiveness and poor clinical prognosis (Chu *et al.*, 2008). The main cause of low p27 expression in cancer is unlikely via mutations or epigenetic silencing, but rather through aberrant p27 degradation, repressed p27 expression, and increased cytoplasmic localisation (Chu *et al.*, 2008). Hence, understanding the regulation of p27 expression via both transcriptional and post-translational mechanisms will provide a potential new target for therapeutic intervention.

### 1.2.2.2. p27 post-translational regulator:SKP2

SKP 2 is an F-box protein that composed of 424 amino acids (Katoh *et al.*, 2013). SKP2 is a component of a E3 ligase called the SKP1-cullin-F-box (SCF) SKP2 complex, that targets several key cell cycle regulators for degradation, such as p27, p21, p57 and cyclin E (Gstaiger *et al.*, 2001; Kitagawa *et al.*, 2009; Marti *et al.*, 1999). Although SKP2 mediates the degradation of both positive and negative cell cycle regulators, its overexpression leads to cell cycle progression via degradation of p27 (Gstaiger *et al.*, 2001). The ubiquitination and subsequent degradation of p27 depends on its phosphorylation at $Thr^{187}$ by cyclin-CDK complexes. SKP2 specifically recognises phosphorylated p27 at $Thr^{187}$ (Carrano *et al.*, 1999).

Therefore, SKP2 is a p27 post translational regulator. Studies in human and experimental tumours have observed the inverse correlation of decreased p27 with elevated SKP2 expression (Cen *et al.*, 2010). Increased protein levels of SKP2 were found to be associated with reduced p27 in a subset of oral epithelial dysplasia and carcinomas when compared with normal epithelial cells/tissue (Gstaiger *et al.*, 2001).

### 1.2.2.3. p27 post-translational regulator: PIRH2

p53-induced RING-H2-type ubiquitin ligase (PIRH2) is a p27-interacting protein. PIRH2 degrades p27 in $G_1$ phase independent of phosphorylation state in both the nucleus and cytoplasm (Hattori *et al.*, 2007). PIRH2 interacts with p27 through the RING finger domain (Hattori *et al.*, 2007). The expression of PIRH2 is low in $G_0$, but is induced in late $G_1$ to S phase in human glioblastoma (T98G) cells (Hattori *et al.*, 2007). Knockdown of PIRH2 thereby prevented the cell cycle re-entry of serum-starved cells following the restoration of serum (Hattori *et al.*, 2007). Hence, PIRH2 is another negative regulator of p27 via ubiquitin-dependent proteasomal degradation (Hnit *et al.*, 2015).

### 1.2.2.4. p27 nuclear exporter: CRM1

As an inhibitor of DNA duplication and cell division, p27 exerts its anti-proliferative action inside the nucleus. Chromosome region maintenance 1 (CRM1) is a carrier protein for nuclear export (Wang *et al.*, 2013), which mediates the cytoplasmic translocation of p27 through binding to its CDK interacting site (Chu *et al.*, 2008). CRM1 activity is low during $G_0$ and increases markedly during the $G_1$–S phase progression. In early $G_1$, phosphorylation of p27 facilitates its binding to CRM1 and subsequent transport from the nucleus to the cytoplasm (Ishida *et al.*, 2002). Interestingly, proteasome inhibition in mid-$G_1$ does not impair nuclear import of p27, but rather leads to accumulation of p27 in the cytoplasm. This suggests that export of p27 precedes its degradation for at least part of the cellular p27 pool, and that active CRM1-mediated export of p27 to the cytoplasm may be linked to cytoplasmic p27 ubiquitination and proteolysis. CRM1-dependent nuclear export of p27 and cytoplasmic degradation therefore permits the incremental activation of cyclin E-CDK2 and thus $G_1$–S phase transition (Connor *et al.*, 2003).In CRM1 siRNA-treated ovarian cancer cells, a reduction of CRM1 protein levels

and coincident accumulation of phosphorylated p27 in the nuclear fraction were observed (Wang *et al.*, 2013). These data suggest that CRM1 plays an essential role in the subcellular localisation of p27 and subsequently in cell cycle regulation. CRM1-positive expression in ovarian cancer was associated with higher tumour grade and lymph node metastases (Hnit *et al.*, 2015; Wang *et al.*, 2013).

### 1.2.2.5. c-MYC

c-MYC is a cellular proto-oncogene associated with a variety of human cancers and is strongly implicated in the control of cell cycle progression, cell metabolism, apoptosis, cell differentiation, tumour expansion and accelerating tumour progression (Whitfield and Soucek, 2012). The human MYC gene family is composed of *MYC, MYCN* and *MYCL1*, and all three *MYC* gene products have similar effects on cell cycle progression (Bretones *et al.*, 2015). The levels of c-MYC expression are crucial for cell cycle re-entry. c-MYC mRNA levels are virtually undetectable in quiescent cells but increase within one to three hours upon mitogen stimulation (Kelly *et al.*, 1983). Forced expression of c-MYC induces cell cycle re-entry of quiescent cells, but the downregulation or inactivation of c-MYC results in the impairment of cell cycle progression (Bretones *et al.*, 2015). Importantly, amplification of c-MYC is found in nearly half of human solid tumours (Beroukhim *et al.*, 2010), including thirty per cent of PCa (Bretones *et al.*, 2015).

In addition, previous studies already show in the absence of c-MYC, the expression of p27 is increased even during the $G_0$/S transition (Mateyak *et al.*, 1999). Transient overexpression of MYC in Jurkat T cells and breast cancer cells increased binding of the MYC homology box II to the *p27* promoter, directly repressing *p27* gene transcription (Bretones *et al.*, 2015; Chandramohan *et al.*, 2008). How c-MYC represses the protein level of p27 is not fully understood but is thought to be, at least in part, through its ability to selectively induce E3

ubiquitin ligase components SKP2, cullin 1 (CUL1) and CDC28 protein kinase regulatory subunit 1 (CKS1), which are all necessary for p27 ubiquitination and degradation (Bretones *et al.*, 2011; Keller *et al.*, 2007; O'Hagan *et al.*, 2000). Other MYC target genes, such as *E2F* (*E2F1*, *E2F2* and *E2F3*) transcription factors, may also play a role in regulating p27, by inducing cyclin E expression (Muller *et al.*, 1997; Pérez-Roger *et al.*, 1997).

### 1.2.2.6. C-MYC post-translational regulator: FBWX7

Regulation of c-MYC protein degradation has attracted attention. The F-box protein of E3 ubiquitin ligase, FBXW7, plays a key role in c-MYC protein degradation in a $Thr^{58}$-dependent manner (Welcker *et al.*, 2004); this residue is often mutated in cancer (Yada *et al.*, 2004). Accordingly, FBXW7 is thought to be a tumour suppressor (Welcker *et al.*, 2004). FBXW7 is one of the few proteins that stimulates c-MYC degradation by ubiquitination (Amati, 2004) and inhibits c-MYC transcriptional activity (Farrell and Sears, 2014). Loss of FBXW7 leads to the accumulation of c-MYC protein and excessive proliferation in the hematopoietic system and the epidermis (Ishikawa *et al.*, 2013; Matsuoka *et al.*, 2008; Thompson *et al.*, 2007). Ablation of FBXW7 leads to the accumulation of c-MYC and promotes tumourigenesis *in vivo* (King *et al.*, 2013). While the turnover of c-MYC is largely dependent on FBXW7, SKP2 is another F-box protein of E3 ligase that participates in degrading c-MYC by binding to the MB2 domain, whereas FBXW7 targets the MB1 domain of c-MYC (Yada *et al.*, 2004).

# 1.3. Ubiquitin Conjugating Enzyme 2C (UBE2C)

## 1.3.1. The ubiquitin proteasome system

In eukaryotes, the ubiquitin proteasome system (UPS) precisely regulates the cell cycle at key checkpoints by targeting cell cycle regulators for proteasome-mediated degradation. The UPS requires the ubiquitin-activating enzyme (E1), the ubiquitin-conjugating enzyme (E2) and ubiquitin ligases (E3) to work in concert to facilitate ubiquitination of target proteins (Figure 1-6). Of the ubiquitin enzymes, E1 is responsible for activating ubiquitin by attaching the molecule to an active site Cys and subsequently transfers the ubiquitin to the E2 active site Cys via a thioester linkage. The E2 then donates the ubiquitin from its Cys to Lys of the target protein through E3-mediated specificity. The E3 enzyme is also responsible for binding to the target protein destined for degradation (Figure 1-6). The human genome contains two genes coding for E1, ~38 genes for E2 and >600 genes for E3 (Ye and Rape, 2009).

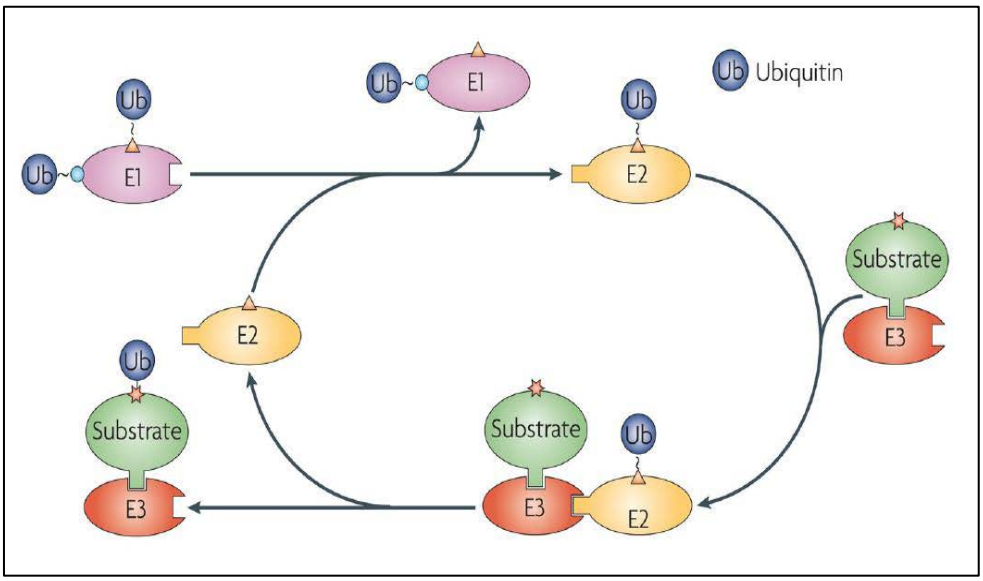


**Figure 1-6. Schematic overview of ubiquitination pathway (Ye and Rape, 2009).**

While monoubiquitination regulates ubiquitin-dependent endocytosis, reorganisation of protein complexes, DNA repair and transcriptional regulation, the labelling of target proteins for degradation requires polyubiquitination (Lin *et al.*, 2002; Ye and Rape, 2009). The assembly of poly-ubiquitin chains is usually initiated by initiating-E2s through the transfer of the first ubiquitin to Lys on a substrate. Subsequently, the E2-E3 pair switches to chain elongation. The decision of whether a Lys residue in the substrate or in the ubiquitin will receive the next ubiquitin is often made by the elongating E2s. However, some initiating E2s extend short ubiquitin chains, before the elongating E2s take over, thereby increasing the rate of ubiquitin chain formation. The covalent addition of a single ubiquitin, referred to as monoubiquitination, can alter protein localisation or its interactions (Mocciaro and Rape, 2012; Mukhopadhyay and Riezman, 2007). At least four ubiquitin molecules have been attached to $Lys^{48}$ and $Lys^{11}$ and are required for targeting proteins for degradation by the 26S proteasome (Hershko *et al.*, 1994; Ye and Rape, 2009). In eukaryotes, most proteins are degraded by the 26S protein, which is a multi-subunit protease that contains a barrel-like 20S proteolytic core particle that houses the active sites and a 19S regulatory particle that governs substrate recognition and entering into the 20S core particle (Mocciaro and Rape, 2012; Thrower *et al.*, 2000).

E3 enzymes are grouped according to their domains. The majority of E3 belong to the RING domain group including the SCF complex and APC/C complex (Meyer and Rape, 2011). E3s have been the focus of many studies due to their deregulation being implicated in cancer. However, the crucial role of E2s in the regulation of cell cycle progression and in particular cancer development and progression has only been suggested recently.

Emerging evidence indicates that the ubiquitin-conjugating enzyme 2C (UBE2C) possesses oncogenic property. The UBE2C is highly conserved and its human homolog (also known as

UbcH10) was cloned in 1997 (Townsley *et al.*, 1997). UBE2C is essential for cell cycle progression, as mutation of the active site ($Cys^{114}Ser$) inhibits destruction of mitotic cyclins (Townsley *et al.*, 1997). Accumulation of UBE2C stimulates cell proliferation and anchorage-independent growth *in vitro* and *in vivo* (Hao *et al.*, 2012). UBE2C mRNA and/or protein levels are aberrantly increased in a wide range of human cancers (van Ree *et al.*, 2010), and high expression of UBE2C is associated with poor clinical outcomes in at least six cancer types (Hao *et al.*, 2012; van Ree *et al.*, 2010). Additionally, a tumour phenotype emerges when UBE2C is overexpressed in transgenic mice (Hao *et al.*, 2012).

## 1.3.2. Structure of UBE2C

E2s are classified into four classes and all share a conserved core domain containing the catalytic Cys residue. Class I consists of the core domain only and requires the presence of an E3 for conjugation of ubiquitin. Class II and III have C- and N-terminal extensions from the core domain, respectively. These extensions may contribute to target protein recognition and regulate the conjugation of ubiquitin to target protein. Class IV contains both C and N-terminal extensions (Wing and Jain, 1995). UBE2C is a class III E2 enzyme.

The human *UBE2C* gene is located at 20q13.12. There are eight transcript variants through alternative splicing. The UBE2C protein referred to in this thesis is the product of splice variant 1 with the longest reading frame. The full length UBE2C contains 179 amino acids with a molecular weight of 19.7 kDa (Lin *et al.*, 2002; Townsley *et al.*, 1997). The first 28 residues comprise an N-terminal extension with various motifs that will be discussed in detail below; the remaining residues form the core domain (Figure 1-7A). The UBE2C protein structure (PDB:1I7K) contains a four-stranded antiparallel β-sheet (B1–4), a conserved $3_{10}$-helix ($3_{10}$) and four α-helices (H1–4; Figure 1-7B). It is intriguing to envisage that a protein with a size of ~20 kDa is able to interact with three to four different proteins, *i.e.*, ubiquitin,

E1, E3 and possibly the target protein (Jiang and Basavappa, 1999). Hence, a unique structural feature of UBE2C must be maintained to allow these interactions.

### 1.3.3. The E2 core domain

The catalytic $Cys^{114}$ responsible for ubiquitin adduct formation is located between B4 and the $3_{10}$. The three-residues-per-turn geometry of the $3_{10}$ places the positively-charged $Lys^{119}$ residue in close proximity to the active site $Cys^{114}$, contributing to ubiquitin adduct formation (Lin *et al.*, 2002). The four β turns (1–4) provide the contact surface for the active site $Cys^{114}$. The residues $Gln^{36}$ (H1), $Leu^{39}$ (H1), $Leu^{59}$ (B2) and $Phe^{60}$ (B2) are predicted to regulate E2 thioester transfer by interacting with the E1 ubiquitin-fold domain (Olsen and Lima, 2013) (Figure 1-7B). UBE2C interacts with the E3 through Loop 1 (89–95), Loop 2 (122–127) and the N-terminal H1. The binding residues for APC/C include $Lys^{33}$, $Met^{43}$, $Met^{44}$ and $Asp^{47}$ in H1, $Phe^{53}$ in B1, $Tyr^{91}$ and $Ala^{124}$ in Loop 1 and 2 (Jin *et al.*, 2008; Lin *et al.*, 2002) (Figure 1-7B). It remains to be determined if UBE2C is recruited by APC2 or APC11 (the core subunits of APC/C) or by the binding site created by APC2 and APC11 complex (Nagy *et al.*, 2012; Summers *et al.*, 2008). The degradation of UBE2C by ubiquitination also requires $Cys^{114}$ and a destruction box (D-box)-like motif involving residues 129–132 ($Arg^{129}$-*X*-*X*-Leu-*X*-*X*-($Leu^{132}$/$Ile^{135}$)-*X*-Asp) (Lin *et al.*, 2002; Rape and Kirschner, 2004). UBE2C also contains a RWD domain, which includes a key $Glu^{38}$ residue in H1 and a $Tyr^{89}Pro^{90}XXXPro^{94}$ motif. The UBE2C RWD domain is thought to be involved in the E2–E3 interaction and in E2 dimer formation (Lin *et al.*, 2002; Nameki *et al.*, 2004).

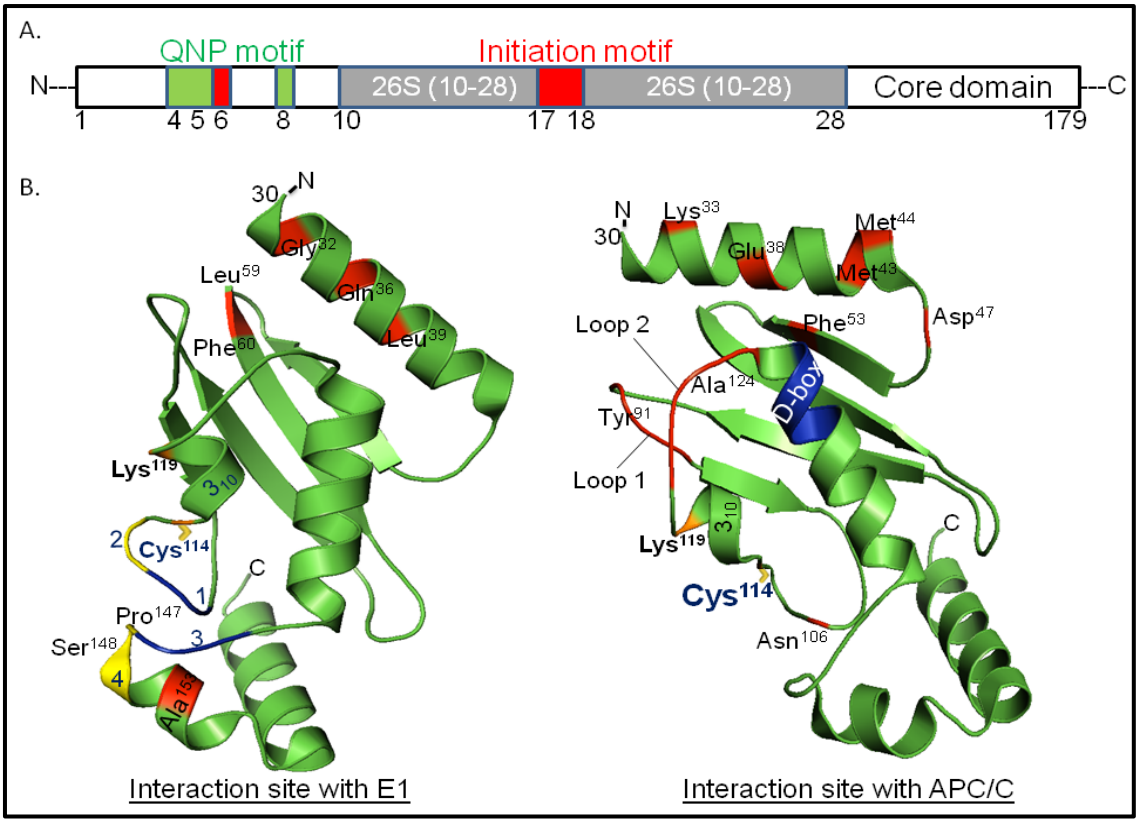


**Figure 1-7. The structure of UBE2C.**

**A**. Predicted functional motifs in UBE2C (1–179). Green, QNP motif (Gln[4], Asn[5] and Pro[8]); Red, initiation motif (Arg[6], Arg[17] and Lys[18]). **B**. Secondary structure in core domain of UBE2C (30–175). Green, α-helices, $3_{10}$-helix and β-sheets. Yellow stick, active site Cys[114]. Orange, Lys[119]. The interaction site of UBE2C to E1 (Left) is shown in red, the four β-turns near the active site are labelled 1–4 and marked as yellow or blue. The loop 1–2 and the interaction sites of UBE2C to APC/C (Right) are shown in red; the D-box like motif is shown in blue. This figure was created with PyMOL (PDB ID: 117).

### 1.3.3.1. The N-terminal extension

The UBE2C N-terminal extension is not essential for ubiquitin-adduct formation but contributes to the regulation of APC/C activity as a part of an inhibitory mechanism (Lin *et al.*, 2002). This is achieved mainly by enhancing the sensitivity of APC/C to its pseudosubstrate inhibitor Emi1 and BubR1, and by conferring D-box-APC/C engagement, which in turn limits the orientation or recruitment of target protein Lys near the E2 active site (Summers *et al.*, 2008). In addition, the interaction between the QNP motif (Gln[4], Asn[5] and Pro[8]) and the APC/C is required for negative regulation of APC/C activity. In the absence of

the QNP motif, the UBE2C core domain strongly promotes APC/C activity. The initiation motif within the N-terminal extension promotes the autoubiquitination of UBE2C (Rape and Kirschner, 2004; Summers *et al.*, 2008; Williamson *et al.*, 2011). Specifically, the candidate residues for initiation motif – $Arg^{6}$, $Arg^{17}$ and $Lys^{18}$ – are required for ubiquitin chain initiation (Williamson *et al.*, 2011). Deletion of the N-terminal residues 1–27 impairs formation of ubiquitin chains (Summers *et al.*, 2008). The N-terminal residues 10–28 are also needed for its own degradation by binding to the 26S proteasome (Zhao *et al.*, 2010) (Figure 1-7B).

## 1.3.4. Biological function of UBE2C

Ubiquitin-conjugating enzyme 2C, as an exclusive partner of APC/C, participates in the degradation of a family of APC/C target proteins by initiating $Lys^{11}$-linked ubiquitin chains (Jin *et al.*, 2008; Meyer and Rape, 2011). The human APC/C is composed of 14 subunits, and the catalytic core consists of a cullin subunit (APC2) and RING domain subunit (APC11). The human APC/C has more than 55 reported target proteins in *Homo sapiens*. Of these, 37 are involved in cell cycle S and M phases (*e.g.*, cyclin A, cyclin B, p21 and securin), 11 are cell-cycle related in general (*e.g.*, E2-C, E2F1, JNK and SKP2), and two are APC/C co-activators (CDC20 and CDH1) (Meyer and Rape, 2011).

### 1.3.4.1. Ubiquitin conjugation

The most common degradation motifs in APC/C target proteins are the D-box and KEN-box. The D-box is recognised by APC/C co-activators CDC20 and CDH1, whereas the KEN-box (with amino acid sequence KEN(X)nP) is recognised by CDH1 only (Meyer and Rape, 2011). Upon recruitment by APC/C, CDC20 and CDH1 serve as D- and KEN-box receptors for various APC/C target proteins. Following binding to target proteins, $APC/C^{CDC20}$ and

APC/C$^{CDH1}$ provide a scaffold for UBE2C to be recruited and oriented, such that the UBE2C facilitates Lys$^{11}$-ubiquitin transfer from UBE2C to target proteins (Figure 1-8). A sequence element named the TEK box (~20 residues downstream of the D- or KEN-box in target proteins) mediates the assembly of Lys$^{11}$-linked ubiquitin chains. The TEK box forms a charged patch around Lys$^{11}$ and exposes the Lys residue in the target protein to the active site of UBE2C, directing Lys$^{11}$ ubiquitin chain transfer (Jin *et al.*, 2008; Meyer and Rape, 2011). By mediating the binding of target proteins to APC/C, the positively-charged initiation motifs in the N-terminus of UBE2C allow APC/C to fine-tune the timing of protein degradation (Jin *et al.*, 2008).

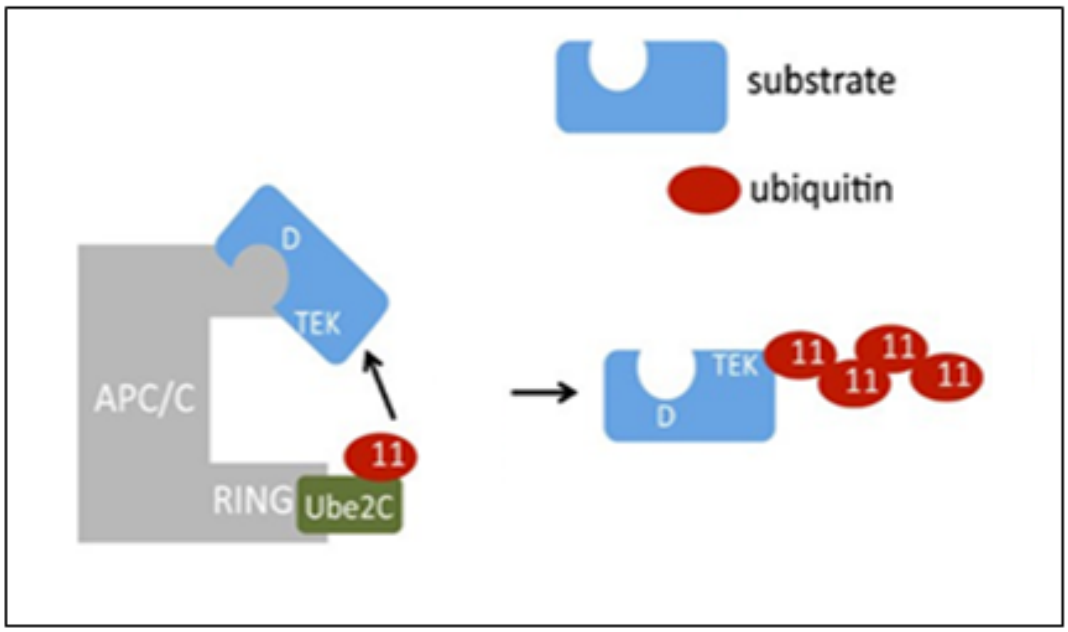


**Figure 1-8. APC/C catalyses the formation of Lys$^{11}$-linked chains.**
APC/C enhances the ubiquitination of substrates by employing UBE2C enzymes.

### 1.3.4.2. Degradation of key proteins regulating cell cycle progression

Ubiquitin-conjugating enzyme 2C is required for destroying mitotic cyclins and other mitosis-related substrates (Aristarkhov *et al.*, 1996; Arvand *et al.*, 1998; Rape and Kirschner,

2004; Rape *et al.*, 2006). During metaphase, UBE2C promotes anaphase progression by degrading securin and cyclin B via APC/$C^{CDC20}$. Separase is a protease that degrades the cohesin rings that link the two sister chromatids together. Typically, securin inactivates separase by forming the securin-separase binding complex. By degrading securin and consequent activation of separase, sister chromatids are separated and thus UBE2C directly promotes anaphase onset (Hao *et al.*, 2012). Cyclin B forms a complex with CDK1 which remains active through the cell cycle until mitosis, where UBE2C-APC/$C^{CDC20}$ induces degradation of cyclin B, rendering CDK1 inactive. CDK1 inactivation is required to keep CDH1 dephosphorylated and thus forming a complex with APC/C by replacing CDC20. This is a prerequisite step for mitotic exit and $G_1$–S progression (Arvand *et al.*, 1998).

### 1.3.4.3. Regulation of the mitotic spindle checkpoint

The metaphase to anaphase transition is tightly controlled by the SAC or mitotic checkpoint (Figure 1-9). SAC proteins include Mitotic arrest deficient-like 2 (MAD2), Budding uninhibited by benzimidazoles 3 (Bub 3) and Bub Receptor 1 (BubR1). The SAC is on to ensure proper kinetochores attachment and correct chromosome segregation. SAC proteins inhibit APC/C activity by sequestering CDC20. Upon proper kinetochore attachment, SAC function is switched off. UBE2C can also switch off SAC by non-degradative ubiquitination of CDC20, causing its dissociation from other SAC proteins. Although this action is APC/C-dependent, UBE2C plays an indispensable role in controlling the molecular switch of the SAC mechanism. Conversely, USP44, a deubiquitinating enzyme, mediates the deubiquitination of CDC20 thus preventing premature anaphase onset (Hao *et al.*, 2012; Reddy *et al.*, 2007; Williamson *et al.*, 2011).

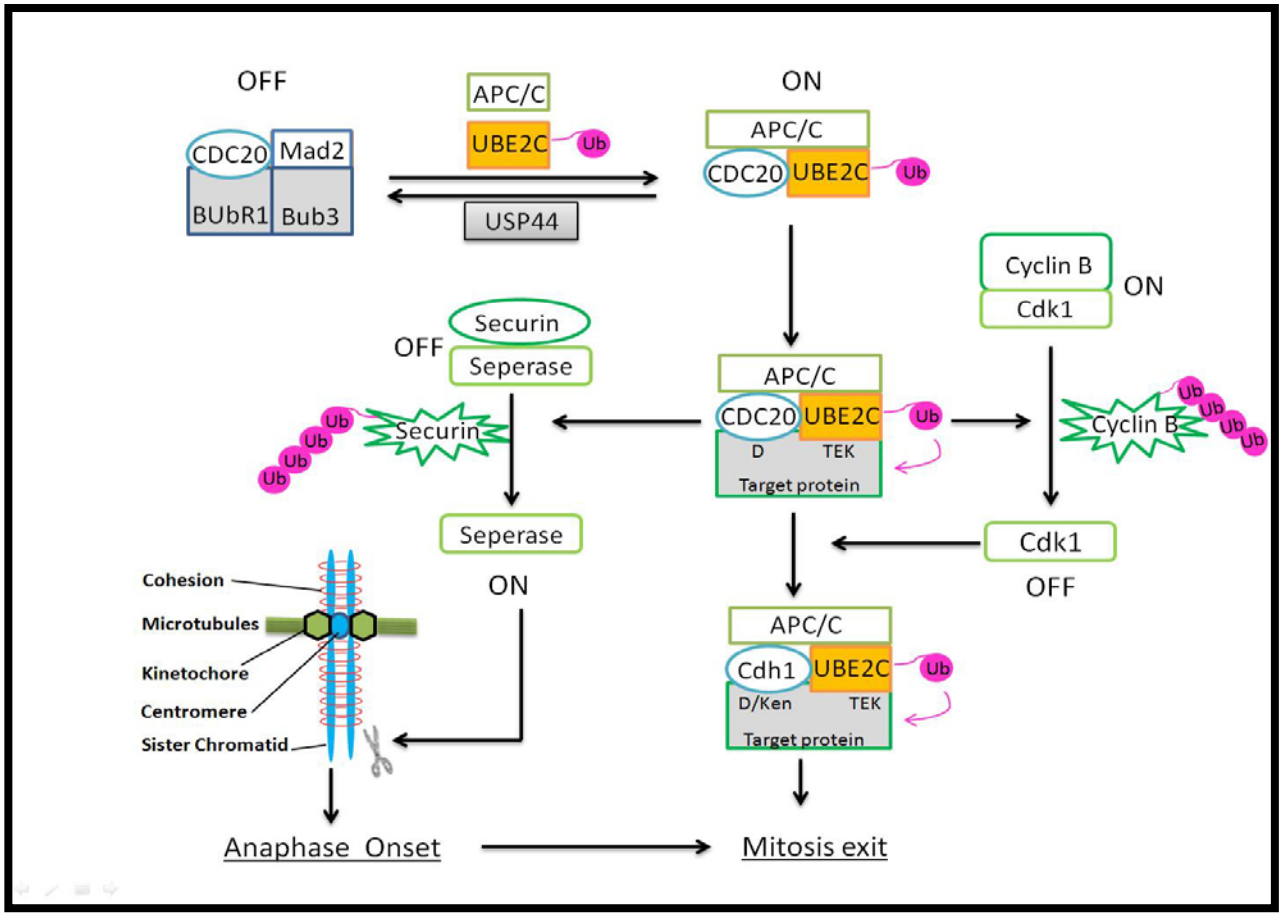


**Figure 1-9. The function of UBE2C.**

CDC20 (a co-activator of APC/C) is inhibited by SAC proteins (MAD2, Bub3 and BubR1). ARP/C and UBE2C facilitate the disassembly of SAC by ubuitination and USP44 antagonises ubiquitination. The freed CDC20 complexes with APC/C and UBE2C, which in turn enhances recruitment of protein for degradation via ubiquitination. Degradation of securing activates seperase, which then degrades the cohesion rings, leading to sister chromatids separating and anaphase onset. Degradation of cyclin B inactivates CDK1, which is required to keep CDH1 active and thus mitotic exit. D, D-box. KEN, Ken-box. TEK; TEK-box.

## 1.3.5. Expression, activation and turnover

### 1.3.5.1. UBE2C expression

Predicted transcription factor binding sites at the *UBE2C* promoter have been identified, including binding sites for c-Rel, Pax-2, Pax-2a, CP1A, CP1C (GeneCard: GC20P044442), NF-1, SRF, TGIF, Meis-1 and c-MYC (Hao *et al.*, 2012). *UBE2C* can be an AR target gene in PCa cells and is responsive to hyperphosphorylated MED1 (Mediator-1, AR co-activator mediator-1) in AR-negative PCa cells (Chen *et al.*, 2011). *UBE2C* expression can also be induced by the oestrogen receptor in breast cancer cells (Wang *et al.*, 2013). UBE2C mRNA and protein levels were also shown to be upregulated when EWS/FLI1 (a transcription factor highly expressed in Ewing's sarcoma and primitive neuroectodermal tumour) was transfected into NIH3T3 cells (Arvand *et al.*, 1998).

UBE2C is localised in the nucleus and the cytoplasm and its levels are cell-cycle regulated: levels of UBE2C are low in $G_1$ (van Ree *et al.*, 2010; Walker *et al.*, 2008) accumulate gradually during S and $G_2$ with a peak at mitosis, and then sharply decrease as cells exit from mitosis (Arvand *et al.*, 1998; Nath *et al.*, 2011; Walker *et al.*, 2008) (Figure 1-10). However, UBE2C levels are not completely undetectable during telophase and early $G_1$ phase (Rape and Kirschner, 2004; van Ree *et al.*, 2010; Walker *et al.*, 2008). Van Ree *et al.* (2010) have also shown that the UBE2C staining is low in $G_1$ and $G_2$ phases in mouse embryonic fibroblasts, and UBE2C transcript levels are low or undetectable in quiescence (Arvand *et al.*, 1998; Yamanaka *et al.*, 2000). In quiescent cells induced by contact inhibition or serum deprivation, UBE2C mRNA and protein levels are low or undetectable (Arvand *et al.*, 1998; Walker *et al.*, 2008). After add-back of 20% fetal calf serum (FCS) for 14 h, UBE2C levels began to rise (2 h before cyclin A, *i.e.*, cells progressed towards S phase). Overall, the

UBE2C level reappears in $G_1$ phase together with or before cyclin A (Walker *et al.*, 2008) (Figure 1-10).

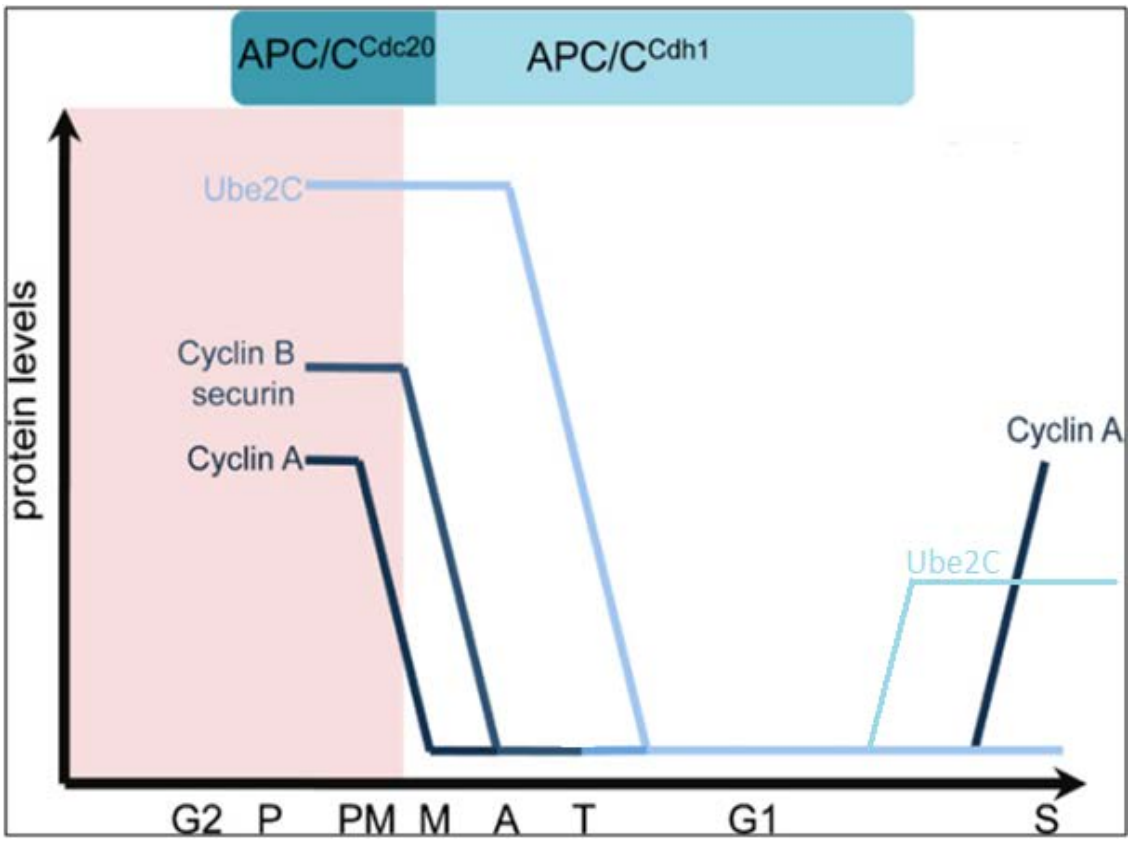


**Figure 1-10. Sequential degradation of APC/C substrates during mitosis.**

P, prophase. PM, prometaphase. M, metaphase. A, anaphase. T, telophase (van Ree *et al.*, 2010; Williamson *et al.*, 2011).

## 1.3.5.2. UBE2C activation

Ubiquitin is activated by E1 in an ATP-dependent manner and then transferred to E2. Hence, when not bound to E3, free E2s are mostly loaded with ubiquitin (at least four $Lys^{11}$-linked ubiquitins are required for 26S proteasome degradation). Free E2s with pre-loaded ubiquitin are available for activation by E3s in order to transfer ubiquitin to a target protein (Ye and Rape, 2009). E3s induce conformational change in E2 in the presence of target proteins, which positions UBE2C $Asn^{106}$ near the active site. This stabilises an oxyanion intermediate in the transition state, causing the full activation of UBE2C.

### 1.3.5.3. UBE2C turnover

Interestingly, UBE2C is degraded in a process described as autoubiquitination, in association with APC/$C^{CDH1}$ but not APC/$C^{CDC20}$ (Grutzmann *et al.*, 2004; Rape and Kirschner, 2004). Throughout mitosis, the APC/C is saturated with targeting proteins, which spares UBE2C degradation as well as APC/C inactivation. After complete target protein destruction, the APC/C ubiquitinates UBE2C (Meyer and Rape, 2011; Rape and Kirschner, 2004). The degradation of UBE2C is a slow process because of deubiquitination enzymes (DUBs), which remove ubiquitin from UBE2C. Most DUBs are activated upon the dissociation of ubiquitin-labelled UBE2C from APC/$C^{CDH1}$ (Rape *et al.*, 2006). The exact DUB responsible for deubiquitination of Lys11-ubiquitin chains is yet to be identified.

## 1.3.6. Medical applications

The role of UBE2C is not limited to promoting cell growth, but also promoting tumour invasion and metastasis. Okamoto *et al.* (2003) examined the expression levels of UBE2C in 24 human cancerous cell lines by using quantitative real time reverse transcription-polymerase chain reaction (RT-qPCR). UBE2C mRNA is barely detectable in the majority of normal tissues (Okamoto *et al.*, 2003). In contrast, *UBE2C* mRNA and/or protein is expressed at high levels in leukemia, lymphoma and melanoma (TCGA data via cBioPortal: UBE2C), and cancers, such as late-stage prostate (Tzelepi *et al.*, 2012; Wang *et al.*, 2009), thyroid (Pallante *et al.*, 2005), esophageal (Lin *et al.*, 2006), breast (Berlingieri *et al.*, 2007), ovarian (Berlingieri *et al.*, 2007), lung, gastric, colon (Li *et al.*, 2014), bladder and uterine (Okamoto *et al.*, 2003; Vasiljevic *et al.*, 2013; Wagner *et al.*, 2004; Xie *et al.*, 2014). An association between the levels of UBE2C and tumour grade/poor prognosis is reported in cancers of the adrenal gland, breast, colon, liver, lung and ovary (Hao *et al.*, 2012; Okamoto *et al.*, 2003; van Ree *et al.*, 2010).

The mechanism of UBE2C upregulation in oncogenic conditions is largely unresolved (Nath *et al.*, 2011). The amplification of the *UBE2C* gene has been reported (Hao *et al.*, 2012; Vasiljevic *et al.*, 2013). Another possible mechanism is the overexpression or hyperactivation of proteins upstream of UBE2C, such as the AR and MED1 in advanced PCa, the oestrogen receptor in breast cancer and c-MYC in other cancer types. Out of 7,949 unique cancer samples, 20 harbour somatic mutations in UBE2C gene (COSMIC: COSG4332). Based on the three-dimensional structure of UBE2C, the $Arg^{129}Ser$ mutation identified in lung squamous cell carcinoma tissue (COSMIC: COSM724441) could be biologically significant, because alterations in the UBE2C putative D-box motif have been shown to stabilise UBE2C against destruction. Conversely, anti-cancer drugs (*e.g.*, tamoxifen, all-trans retinoic acid [ATRA], Icaritin, mTOR inhibitor Everolimus, imidazoquinoline derivatives, PI3K inhibitor [BEZ235] , cell cycle inhibitor-779 [CCI-779]) and expression of a tumour suppressor gene chromosome 2 open reading frame 40 [C2ORF40]) downregulate *UBE2C* mRNA levels, leading to suppression of cancer cell proliferation *in vitro* and *in vivo* (Hao *et al.*, 2012; Kato *et al.*, 2015; Lu *et al.*, 2013; Sun *et al.*, 2015). UBE2C transgenic mice are prone to develop a broad spectrum of spontaneous tumours as well as carcinogen-induced lung tumours with evidence of precocious degradation of cyclin B, extra centrioles, chromosome lagging and aneuploidy (van Ree *et al.*, 2010). In an *in vivo* study, UBE2C silencing decreased the invasiveness of advanced PCa cells (Wang *et al.*, 2011). Together, these results strongly suggest that UBE2C is causally involved in cancer development and progression.

#### 1.3.6.1. UBE2C in prostate cancer

The UBE2C-APC/C pathway has recently been implicated in the progression to AR-mediated CRPC (Tzelepi *et al.*, 2012; Wang *et al.*, 2009). In a study performed by Wang *et al.* (2009), the authors claimed UBE2C is a CRPC-specific AR target gene, which has an essential role in promoting CRPC cell growth by increasing the pool of active APC/C. Recently, two CRPC

cell-specific AR-bound enhancers were found to locate between –32.8 kb and +41.6 kb from the transcription start site (TSS) of the UBE2C gene. The two enhancers interact with UBE2C promoter through chromatin looping in androgen-independent PCa cells (AIPC, LNCaP-abl) but not in androgen-dependent PCa cells (ADPC, LNCaP). The chromatin looping is required for UBE2C gene expression and AIPC cell growth (Wang *et al.*, 2009). Consistent with this notion, silencing of AR co-activator MED1, FoxA1 and AR collaborating factor (GATA2), significantly decreased the activity of AR-bound UBE2C enhancers and promoters, thus decreasing the *UBE2C* gene expression in LNCaP-abl but not in LNCaP cells. In addition, in an *in vivo* study, overexpression of UBE2C increased, whereas silencing UBE2C decreased, invasiveness of LNCaP-abl and bone metastasised subline of LNCaP (C4-2B) but not LNCaP cells (Wang *et al.*, 2011). Collectively, UBE2C is AR-dependent but androgen-independent, which is necessary for the progression of AR-positive CRPC.

However, the molecular mechanisms underlying UBE2C in AR-negative PCa cells have not been fully elucidated. Wang's group (2011) also investigated the UBE2C enhancer activities in PC-3 cells. The mRNA and protein level of UBE2C in PC-3 (AR-negative) cells is significantly greater compared with LNCaP (AR positive) cells. By comparing recruitment of enhancers to UBE2C promoter in PC-3 and LNCaP cells, greater recruitment of FoxA1 and MED1 was found in PC-3 cells. Notably, MED1 is phosphorylated at $Thr^{1032}$ by PI3K/AKT (Wu *et al.*, 2011). Phosphorylated MED1is necessary for UBE2C locus looping by enhancing recruitment of FoxA1, Pol II and TATA binding protein (TBP) to the UBE2C promoter and increase protein-protein interactions on chromatin (Wu *et al.*, 2011). Nevertheless, UBE2C is markedly upregulated in small-cell prostate carcinoma (SCPC), which does not express AR. Collectively, the overexpression of UBE2C in AR-negative PCa cells could derive from

hyperactive UBE2C enhancers and promoter activity (Tzelepi *et al.*, 2012) induced by CDC20 (Nath *et al.*, 2011), p-MED1 and FoxA1 (Chen *et al.*, 2011; Liu *et al.*, 2015).

Overexpression of UBE2C in cancer cells that do not express AR is poorly understood and likely to be complicated. Silencing of UBE2C blocks the cell proliferation of AIPC (abl) and AR-negative CRPC (PC-3) cells but not ADPC-AR positive (LNCaP) cells, providing a potential new target for therapeutic intervention (Chen *et al.*, 2011; Wang *et al.*, 2009).

## 1.4. Hypothesis and Aims

Collectively, previous studies have suggested that UBE2C may play a role in cell cycle regulation and tumourigenesis. The overarching goal of the project is to define the role of UBE2C in regulating the proportion of quiescent over proliferative PCa cells and transition to a proliferating state by quiescent cancer cells. Moreover, the concordance between UBE2C protein/mRNA levels and progression of PCa is determined.

It is hypothesised that UBE2C plays an important role during cell cycle exit of cycling cells and re-entry of quiescent PCa cells. Specifically, exit to $G_0$ phase and cycle re-entry from $G_0$ phase are accomplished via mechanisms involving UBE2C in regulation of p27, SKP2, PIRH2, CRM1, c-MYC and FBXW7.

## 1.4.1. Aims

The specific aims of this project are:

### 1.4.1.1. To define the effect of UBE2C expression on the proportion of $G_0$ cells in prostate cancer cells

To establish the relationship of UBE2C and the proportion of $G_0$ cells, three PCa cell lines LNCaP, C4-2B and PC-3 are transfected with UBE2C siRNA or UBE2C expression plasmid. The proportion of $G_0$ cells are verified by cell cycle analysis with Hoechst 33258 and Pyronin Y double staining.

### 1.4.1.2. To verify the effect of UBE2C expression on cell cycle exit and cell cycle re-entry in prostate cancer cells

We utilise contact inhibition in PC-3 or serum withdrawal in LNCaP and C4-2B cells to induce cell cycle exit, and replate PC-3 cells at low density or replenish serum in LNCaP and C4-2B to render cell cycle re-entry. To evaluate the relationship of UBE2C with cell cycle exit, three PCa cell lines are transfected with UBE2C expression vector during exit. To study the action of UBE2C on cell cycle re-entry, UBE2C is silenced by RNA interference during release from quiescence. The cell cycle distribution and quantification of $G_0$ cells are determined by flow cytometry analysis with Hoechst 33258 and Pyronin Y double staining.

### 1.4.1.3. To determine the mechanism underlying UBE2C action on cell cycle exit and re-entry.

To identify the mechanisms by which UBE2C influences cell cycle exit in PCa cells, we firstly determine the schedule of cell cycle exit (*i.e.*, the time required to synchronise

maximal cells at $G_0$ phases) or re-entry (*i.e.*, the time required to release maximal cells from $G_0$ phases) with UBE2C expression vector or siRNA. We then determine the change in protein levels of $G_0$-regulatory proteins (p27 and c-MYC) and its own regulators through a time course. By comparing with the schedule of cell cycle exit or re-entry, we can determine if the change in $G_0$-regulatory proteins is prior to or after the change in cell cycle status. This is important as it helps to determine if the change in $G_0$-regulatory proteins is the cause or consequence of a change in cell cycle status.

#### 1.4.1.4. To examine the concordance between UBE2C levels and progression of prostate cancer

In order to establish the correlation of UBE2C expression with the PCa progression, the protein levels of UBE2C in human PCa tissues are investigated. The protein levels of UBE2C are determined in non-cancerous prostate tissues and PCa specimens by immunohistochemistry. To further examine whether development of hormone refractory is associated with expression of UBE2C, we compared the immunostaining of UBE2C in paired PCa specimens obtained from the same patient before and after the development of CRPC. To extend the study of UBE2C to mRNA level, differential expression analyses comparing PCa microarray with respective non-cancerous tissues as well as clinicopathology-based cancer subtypes are explored in 12 prostate datasets download from ONCOMINE database.

# Chapter 2

# 2. Materials and Methods

# 2.1. Cell Lines and Cell Culture

## 2.1.1. Prostate cancer cell lines

The bone metastasised PCa cell line, PC-3 (Cat. #: CRL-1435; American Type Culture Collection, USA), and the lymph node metastasised PCa cell line, LNCaP (Cat. #: CRL-1740; American Type Culture Collection, USA) and bone metastasised subline of LNCaP, C4-2B cells (kindly provided by A/Prof Yong Li, St George Hospital, Research and Education Centre, Australia) were grown in RPMI 1640 (Cat. #: A1049101l; Life Technologies, Australia) supplemented with 10% v/v fetal bovine serum (FBS, Life Technologies, Australia), penicillin (100 U/mL; Sigma Aldrich, Australia) and streptomycin (100 µg/mL; Sigma Aldrich, Australia). The prostate epithelial cells (PrEC) were established directly from primary cultures of BPH specimens in our laboratory as described (Yao *et al.*, 2010). PrEC cells were grown in EpiGRO human Prostate Complete Media Kit (hPCM; Millipore, Australia). Nontumourigenic HPV18 immortalised human prostate epithelial cells RWPE-1 (Cat. #: CRL-11609; American Type Culture Collection, USA) were maintained in keratinocyte–serum-free medium (Life Technologies, Australia) supplemented with 5 ng/mL human recombinant epidermal growth factor 1-53 (Life Technologies, Australia) and 50 µg/mL bovine pituitary extract (Life Technologies, Australia). All the cells were cultured at 37 °C in a humid atmosphere containing 95% air and 5% $CO_{2,}$ with media refreshed every 72 h.

## 2.1.2. Passaging of prostate cancer cells

Cells were routinely cultured in Corning® T75 flasks (Cat. #430641) to 70–80% confluence. To subculture cells, the medium was aspirated and cells rinsed with 5 mL of warm phosphate

buffer saline (PBS), followed by 1 mL of TrypLE™ Select (GIBCO®, USA) solution at 37 °C until the cell layer was dispersed. Detached cells were then collected by centrifugation (300x*g* for 6 min) and resuspended in 15 mL fresh cell culture media. Cells were replated at a dilution of 1:3 to 1:6 into new T75 flasks. A hemocytometer and trypan blue (Cat#: 15250061, Thermo Fisher Scientific, Australia) were used to estimate viable cell density prior to seeding. The passage number of cells in this study was 19–36 for LNCaP cells, 25–45 for PC-3 cells, 17-39 for C4-2B cells.

### 2.1.3. Cryopreservation of cell lines

PC-3, LNCaP and C4-2B cells were prepared for cryopreservation by gently trypsinising sub-confluent cells with TrypLE™ Select. After centrifugation, the cell pellet was first resuspended in RPMI containing 20% (v/v) FBS and then added to an equal volume of 10% (v/v) DMSO in cell culture medium. Liquid nitrogen cryotanks were used for long-term storage of cells.

### 2.1.4. Experimental quiescent cell models

Experimental quiescence was elicited by contact inhibition and serum starvation according to a procedure described previously (Yao *et al.*, 2015). PC-3 cells were cultured in 10% FBS to achieve 100% confluence and the confluence maintained for 3 days. LNCaP and C4-2B cells were grown in the presence of 10% FBS until 70% confluence. FBS was then removed from medium for up to 7 days. Quiescent PC-3, LNCaP and C4-2B cells were rendered for cell cycle re-entry by split at a low density and serum restoration, respectively.

# 2.2. Transfection

## 2.2.1. Small interfering RNA transfection

Genetic silence of gene expression was achieved using siRNAs derived specifically against the *UBE2C* gene (siUBE2C). The sequence of siUBE2C is demonstrated in Table 2-1; Scramble Control (NC) with a non-targeting sequence of the same GC content (Stealth Select RNAi™ siRNA, 12935300; Invitrogen, Life Technologies, Australia) was used to disregards potential off-target effects of siRNAs. All siRNAs were purchased from Invitrogen (Life Technologies, Australia).

**Table 2-1. The sequence of Stealth RNAi™ siRNAs against *UBE2C*.**

| siUBE2C | Cat. # | Sequence |
|---|---|---|
| Set 1 | HSS174074 | 5'–CAGUAUAUGAAGACCUGAGGUAUAA–3' |
| | | 5'–UUAUACCUCAGGUCUUCAUAUACUG–3' |
| Set 2 | HSS145952 | 5'–GAACCCAACAUUGAUAGUCCCUUGA–3' |
| | | 5'–UCAAGGGACUAUCAAUGUUGGGUUC–3' |
| Set 3 | HSS145953 | 5'–GAAGGUACCUGCAAGAAACCUACUCA–3' |
| | | 5'–UGAGUAGGUUUCUUGCAGGUACUUC–3' |

Cells were transfected with 20 nM siUBE2Cs using Lipofectamine™ 2000 (Life Technologies, Australia) according to the manufacturer's protocol. Prior to each experiment, Lipofectamine™ 2000 (1:100) and 40 nM siUBE2C were mixed with Opti-MEM medium (GIBCO®, USA) and incubated for 5 min in separate tubes at room temperature. Lipofectamine™ 2000 solution and siRNA solution were combined in a 1:1 ratio and incubated at room temperature for 20 min. The mixture was then mixed with the desired number of cells and plated according to experiment set-up (Table 2-2). The media was

replenished after 8–24 h and cells left to propagate for a maximum of 7 days from exposure to siRNA.

**Table 2-2. The amount of siUBE2Cs and Lipofectamine™ 2000 used for siRNA transfection in experiment set-ups.**

| Transfection reagent | 96-well plate | 6-well plate | T25 flask | T75 flask |
|---|---|---|---|---|
| **siRNA mixture** | | | | |
| NC/siUBE2C (µL) | 0.25 | 2.5 | 5 | 10 |
| Opti-MEM (µL) | 25 | 250 | 500 | 1000 |
| **Lipofectamine™ 2000 mixture** | | | | |
| Lipofectamine™ 2000 (µL) | 0.25 | 2.5 | 5 | 10 |
| Opti-MEM (µL) | 25 | 250 | 500 | 1000 |
| Total per well or flask (µL) | 50 | 500 | 1000 | 2000 |
| Complete medium (µL) | 200 | 2000 | 4000 | 8000 |
| Final concentration (nM) | 20 | 20 | 20 | 20 |

## 2.2.2. Plasmid transfection

pJS55 plasmid-encoding UBE2C-AU1 (Cat. #: 8506; Addgene, Cambridge, MA) and dominant negative (C114S) UBE2C-DN (Cat, #: 8507; Addgene, Cambridge, MA) was kindly provided by Dr. J. V. Ruderman. Competent DH5alpha cells were incubated with DNA plasmid (1 µg) for 30 min on ice. The transformation mix was heated at 37 $^{o}$C for 1 min and then incubated for 2 min on ice. The transformation mix was inoculated on a 10 cm agar plate with ampicillin (100 µg/mL) for overnight selection Individual colonies grown on LB plates were collected and grown overnight in LB medium containing ampicillin (100 µg/mL) at 37 °C with continuous shaking. DNA purification was performed using the QIAprep Spin Midi Kit (Qiagen, USA) according to the manufacturer's instructions.

For overexpression, PC-3 cells were transfected with 1.5 µg UBE2C plasmid, dominant negative (DN) UBE2C plasmid, or control empty vector using Lipofectamine™ RNAiMAX

(Invitrogen, Life Technologies, Australia) according to the manufacturer's protocol. Prior to each experiment, Lipofectamine™ RNAiMAX (7 µL per 1.5 µg plasmid) and vectors were mixed with Opti-MEM medium (GIBCO®, USA) and incubated for 5 min in separate tubes at room temperature. Lipofectamine™ RNAiMAX solution and plasmid solution were combined into a 1:1 ratio and incubated at room temperature for another 20 min. The mixture was then mixed with the desired number of cells in a 50 mL Eppendorf tube for 2 h. The media was replenished after 2 h and cells left to propagate for a maximum of 72 h post-transfection followed by cell cycle analysis or protein extraction.

## 2.3. Cell Cycle Analysis

### 2.3.1. Flow cytometry analysis of the cell cycle using propidium iodide

PC-3 or LNCaP cells seeded in 6-well plates were treated with siUBE2Cs and NC according to above procedures. At the end of treatment, the cells were trypsinised, spun down and re-suspended in 300 µL PBS. The cells were then fixed by adding 700 µL ethanol drop-wise to each sample under a constant vortex and then stored at 4 ºC for at least overnight. Following fixation, cells were washed in PBS and incubated in PBS containing 20 µg/mL propidium iodide (PI) and 100 µg/mL RNase for 1 h. The cells were then washed and resuspended in PBS with 5% (v/v) FBS before being measured by flow cytometry analysis. Positive nuclear stained with PI were gated and cells in each cell cycle phase measured using FlowJo (Version 10; Tree Star Inc., USA).

### 2.3.2. Flow cytometry analysis of the cell cycle using Hoechst 33258 and Pyronin Y

The PCa cells treated in T25 flasks were rinsed by warm PBS, tripsinised and collected for cell counting. Cells were pelleted by centrifugation at 300x*g* for 6 min, and resuspended in 300 µL PBS. To fix cells, 700 µL ethanol was added slowly in to each sample during vortex. The fixed samples were then stored at –20 °C until use. After being washed twice with PBS containing 5% FBS, the cell suspensions were incubated in PBS containing Hoechst 33258 (4 µg/mL; Sigma Aldrich, Australia) at 37 °C for 45 min in the dark, then Pyronin Y (8 µg/mL; Sigma Aldrich, Australia) was directly added to each sample for a further 15 min incubation. The staining solution was removed and cells were resuspended in 500 µL of PBS and subjected to flow analysis with the flow cytometer (FACSCanto II) equipped with BD FACSDiva software (BD Biosciences, Australia) and then analysed using FlowJo software (Version 10; Tree Star Inc., USA).

### 2.3.3. Flow cytometry analysis of the cell cycle using Hoechst 33258, Pyronin Y and p-Rb (p-Ser$^{807/811}$)

For co-staining with p-Rb (p-Ser$^{807/811}$), the cell suspensions were incubated in PBS containing Hoechst 33258 (4 µg/mL; Sigma Aldrich, Australia) and p-Rb (p-Ser$^{807/811}$) with Alexa Fluor® 647 (20 µL/test, BD Biosciences, Australia) at 37 °C for 45 min in the dark, then Pyronin Y (8 µg/mL; Sigma Aldrich, Australia) was directly added to each sample for a further 15 min incubation. The staining solution was removed and cells were resuspended in 500 µL of PBS and subjected to flow analysis.

## 2.4. SYBR Green Assay

The PCa cells were plated in 96-well plates at 6,000 cells per well for PC-3 and C4-2B cells and at 10,000 cells per well for LNCaP cells in 200 µL of medium supplemented with serum. To overexpress or knockdown UBE2C, 50 µL of the Opti-MEM™ medium containing the siUBE2Cs or plasmid was added to each well. The same number of cells was aliquoted as at baseline and stored at –80 °C until use. After each indicated time, the medium was gently aspirated from the plates and rinsed twice with cold PBS. 100 µL of lysis buffer containing SYBR Green (Cat. #: S-7563, Invitrogen, Life Technologies, Australia) at 1:10,000 v/v dilution was added to each well. The lysis buffer was made up of nine portions of buffer A (10 mM Tris-pH 7.5 and 2 M NaCl) and one portion of buffer B (100 mM Tris-pH 7.5, 200 mM disodium EDTA and 10% Triton X-100). The cells were then lysed in the dark for 30 min. The frozen aliquots used as baselines were thawed at room temperature, lysed in the same buffer and transferred to the treatment plate containing the same type of cells. The fluorescence intensity of SYBR Green-stained DNA was measured using a plate reader (FLUOstar Omega; BMG Labtech, Germany) and the change of SYBR Green intensity over the study period was determined by subtracting baseline fluorescence intensity from each treatment.

## 2.5. Immunoblotting

### 2.5.1. Protein extraction

Cells were washed twice with cold PBS (Amresco) and incubated with lysis buffer (RIPA-buffer, containing 65 mM Tris, 50 mM NaCl, 10 M HCl, 5 mM EDTA, 1% NP-40, 0.5%

sodium deoxycholate, 0.1% SDS and 10% glycerol at pH 7.4 (Sigma Aldrich, Australia); 1% (v/v) 5 M sodium fluoride; 1% (v/v) protease inhibitor cocktail (Calbiochem, Millipore, USA) on ice in darkness for 20 min. Cells were then scraped off by rubber policemen (Costor, Mexico) on ice and collected into 1.5 mL Eppendorf tubes; all pipette tips, rubber policemen and Eppendorf tubes were pre-chilled at –20 $^{0}$C to preserve protein in cell lysates. To further avoid protein loss, samples were spun at highest speed for 30 seconds to eliminate air bubbles. Sonication or the 'freeze and thaw method' were performed to further break open cell nuclear membranes, release nuclear contents and thus homogenise proteins from cellular cytoplasm and nuclei. To avoid protein denatured during sonication, samples were sonicated on ice.

## 2.5.2. Protein quantification

The protein concentration was determined using Bio-Rad detergent compatible ($D_c$) protein assay (Bio-Rad Laboratories, CA). For reference purposes, bovine serum albumin (BSA; 10 mg/mL; Sigma Aldrich, Australia) was diluted with RPIA buffer to 7 known concentrations (0, 0.25, 0.5, 1, 2, 3 and 4 mg/mL). A 96-well plate was used and duplicates were performed for each standard and sample. Each well was loaded in sequence with 25 μL of a solution of Reagent A (an alkaline copper tartrate solution), 5 μL of BSA protein standard/sample, and 200 μL of Reagent B (a dilute Folin reagent). The plate was incubated in darkness for 15 min for colour reaction and the absorbance was measured at 690 nm using a spectrophotometer (FLUOstar Omega Microplate Reader; Imgen Technologies, VA). All the absorbance values were subtracted with the mean absorbance of blank wells. Protein concentrations of cell lysates were evaluated using the trend-line equation of a BSA standard curve. A standard curve was prepared each time the assay was performed. The loading volume required for 50

μg of protein was calculated based on the protein concentration of each sample. Samples were then aliquoted and stored in –80 °C until further analysis.

## 2.5.3. Gel preparation

There are two sodium dodecyl sulphate polyacrylamide gels (SDS-PAGEs): the resolving gel and the stacking gel. The sieving properties of SDS-PAGE gels are determined by the percentage of acrylamide and hence the pore size of the gel; for example, on lower percentage polyacrylamide gels, acrylamide forms a loose mash network, so proteins move through the gel at a faster rate. The stacking gel was 4% (low) acrylamide gel, whereas, the percentage of resolving gel (8–12.5%) was chosen according to the molecular weight of the protein of interest (shown in Table 2-3). The lower the molecular weight of the protein, the greater the acrylamide concentration was used and *vice versa* (Figure 2-1).

**Table 2-3. The component of resolving gel and stacking gel.**

| Percentage of gel | 8% | 10% | 12.50% | Percentage of stack | 4% |
|---|---|---|---|---|---|
| 40: 0.8% w/v acrylamide: bisacrylamide | 1 mL | 1.25 mL | 2.35 mL | 40:0.8% w/v acrylamide: bisacrylamide | 500 μL |
| 1.0 M Tris-HCl pH 8.8 | 3 mL | 3 mL | 3 mL | 1 M Tris-Cl pH6.8 | 630 μL |
| 20% SDS | 38 μL | 38 μL | 38 μL | 20% SDS | 25 μL |
| $dH_2O$ | 3.421 mL | 2.921 mL | 2.35mL | $dH_2O$ | 3.655 mL |
| Mix together. Add APS and TEMED just before pouring | | | | | |
| 10% APS | 36 μL | 36 μL | 36 μL | 10% APS | 25 μL |
| TEMED | 7.5 μL | 7.5 μL | 7.5 μL | TEMED | 5 μL |
| Total volume | 7.5 mL | 7.5 mL | 7.5 mL | Total volume | 5 mL |

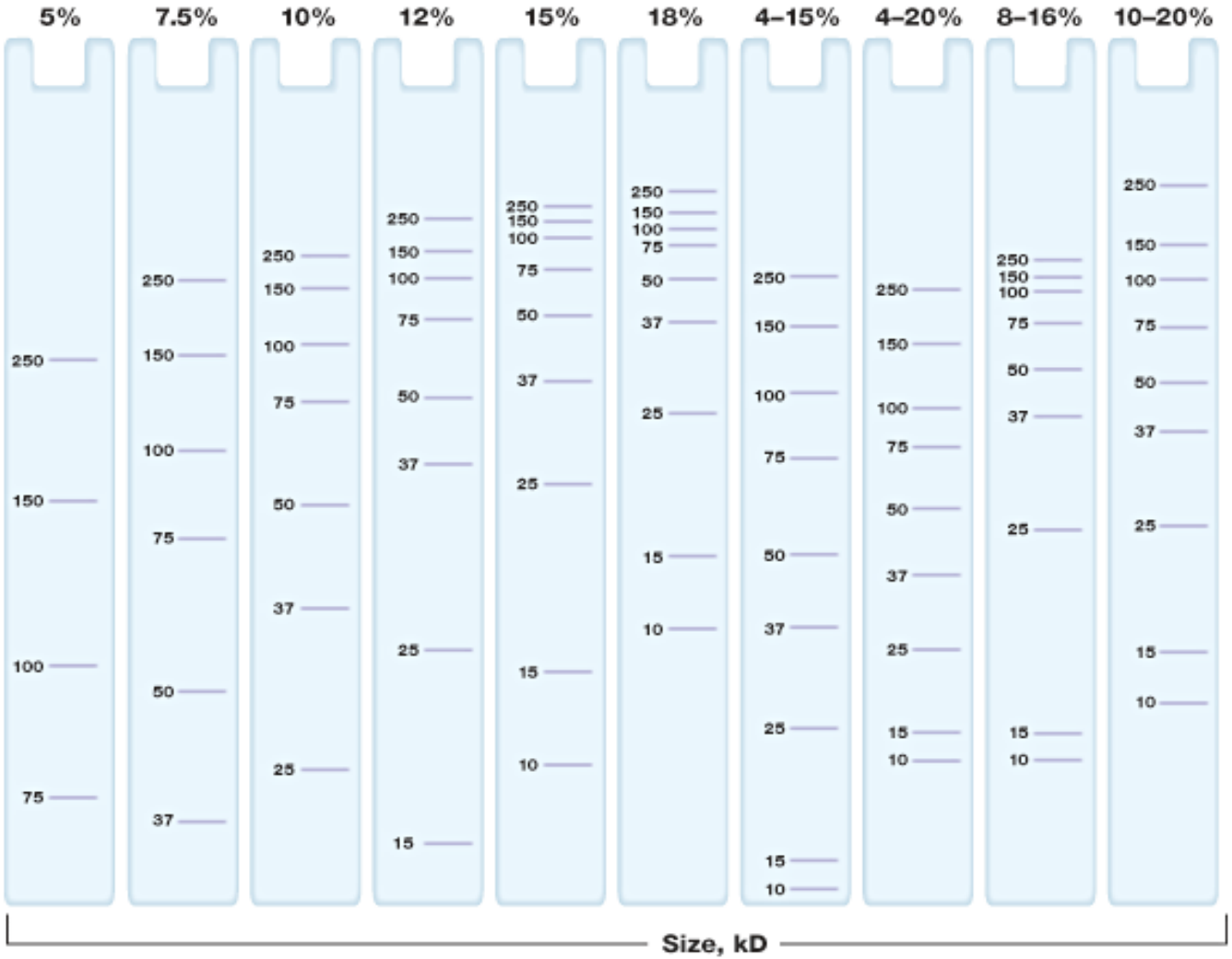


**Figure 2-1. The separation and migration of proteins by SDS-PAGE.**

The distribution of proteins by size (kDa) in different percentages of acrylamide gels (Bio-Rad, Australia).

The Mini-PROTEAN® cell kit from Bio-Rad was used for gel casting. Two glass gel plates (1.5 mm) were assembled and locked into green Bio-Rad frame clips and subsequently into the gel casting stand. To make each gel, the solutions required to resolve the gel monomer are shown in Table 2-3; 10% ammonium persulphate (APS; Sigma-Aldrich, USA) and N, N, N', N'-tetramethylethylenediamine (TEMED; Merck, USA) were added just prior to pouring the gel. The mixture of reagents was promptly poured into assembled gel plates and a small layer of distilled water added on the top to produce a clean, straight top of the resolving gel. The distilled water was poured off after 45 min polymerisation. Similarly, the stacking gel mixture (Table 2-3) was then poured on top of the resolving gel in the assembled glass plates. A 10- or 15-well (1.5 mm) comb was seated and aligned with the top of the short plate to form the loading wells. Following 30 min of polymerisation, the gel casting was wrapped in plastic wrap and stored at 4 °C with running buffer (25 mM Tris, 192 mM glycine, 0.1% SDS).

### 2.5.4. Transferring

After electrophoresis was complete, the power supply was turned off and the electrical leads disconnected. The gel was removed from the gel cassette by carefully separating the two glass gel plates using the releaser. Proteins on the resolving gel were transferred onto a nitrocellulose membrane (Hybond™-C Extra; Amersham Biosciences, USA) for immunoblotting analysis. Prior to transferring, nitrocellulose membranes, filter papers and sponges were soaked in transferring buffer (25 mM Tris, 192 mM glycine with 10-20% methanol). The transfer cassette sandwich (Mini Trans-Blot Cell; Bio-Rad) was assembled in the following order: a) 1 layer of filter sponge, b) 4 layers of filter paper, c) gel, d) nitrocellulose membrane, e) 4 layers of filter paper, and f) 1 layer of filter sponge. Wet-

transfer was then carried out at 100 V for 2–3 h on ice. During transfer, the transfer buffer was stirred to maintain an even ion distribution and temperature in a mini-tank.

## 2.5.5. Blocking and immunodetecting

Following transfer, the nitrocellulose membrane was washed in 1X PBST (10X PBS solution and 0.05 % (v/v) TWEEN®20, pH 7.5) for 5 min to remove SDS in the transferring buffer. To avoid nonspecific antibody binding, membranes were blocked in 1% skim milk in 1X PBST for 30–60 min. Membranes were then washed three times in 1X PBST, changing the buffer every 5 min. All primary antibody hybridisation was performed in PBST with 1% skim milk. The optimal dilution of each primary antibody, which was determined experimentally, is listed in Table 2-4. Membranes were incubated with primary antibody overnight at 4°C. The next day, membranes were washed three times in PBST for 15 min, changing the buffer every 5 min. Then the membranes were incubated with horse radish peroxidase (HRP)-conjugated secondary antibody (anti-mouse A4416 or anti-rabbit A0545; Sigma-Aldrich, Australia) and Precision Strep Tactin-HRP Conjugate (Bio-Rad, Australia) for at least 3 h on ice. All secondary antibodies were diluted 1:10000 in PBST with 1% skim milk. The membranes were rinsed in PBST and incubated with SuperSignal West Pico Chemiluminescent Substrate (Cat #:34078; Thermo Fisher Scientific, Australia) or Clarity™ Western ECL (enhanced chemiluminescence) Blotting Substrate (Cat #:1705060, Bio-Rad, Australia). Immunolabelled protein bands were captured by ChemiDoc™ XRS+ System (Bio-Rad, Australia). Two loading controls, α-TUBULIN and glyceraldehyde 3-phosphate dehydrogenase (GAPDH), were used to avoid overlapping signals from proteins of interest that had a similar molecular weight. Densitometry of the immunoblot results was performed using software Image J (1.38x, National institutes of health, USA) to quantify the ratio of

band intensity between the protein of interest and the housekeeper protein (GAPDH or α-TUBULIN).

**Table 2-4. Primary antibody in western blotting.**

| Antigen | Supplier | Cat. # | Species | Dilution | % Gel | Molecular size (kDa) |
|---|---|---|---|---|---|---|
| p27 | Santa Cruz | sc-528 | Rabbit | 1 in 500 | 10.00% | 27 |
| PIRH2 | Santa Cruz | sc-67033 | Rabbit | 1 in 500 | 10.00% | 36 |
| SKP2 | Santa Cruz | sc-7164 | Rabbit | 1 in 500 | 10.00% | 42 |
| c-MYC | Santa Cruz | sc-70469 | Mouse | 1 in 500 | 10.00% | 60 |
| UBE2C | Boston Biochem | A-650 | Rabbit | 1 in 1000 | 12.50% | 19 |
| FBXW7 | Abcam | ab180472 | Rabbit | 1 in 1000 | 10.00% | 110 |
| CRM1 | Santa Cruz | sc-74454 | Mouse | 1 in 1000 | 10.00% | 110 |
| GAPDH | Santa Cruz | sc-137179 | Mouse | 1 in 20000 | 6.0–12.5% | 37 |
| α-TUBULIN | Santa Cruz | sc-5286 | Mouse | 1 in 10000 | 6.0–12.5% | 50 |

# 2.6. Immunostaining

## 2.6.1. Prostate cell pellet preparation

The expression of UBE2C was determined by immunostaining. The experimental cells in each T75 flask were washed twice by PBS and detached by TriplE™ Select. All cells within the cell culture media, PBS and TriplE™ Select were collected by centrifugation (300x*g* for 6 min) into 1.5 mL Eppendorf tubes. Cell pellets were fixed in 10% formalin at 4 ºC overnight. The formalin was removed by centrifugation and the cells were washed in PBS again, coated and solidified in agarose (2% agarose in PBS), dehydrated and embedded in paraffin blocks. 5 µm sections were cut on a microtome (Finess™, Thermo Fisher Scientific, Australia) and collected onto Superfrost Plus slides (Menxel-Glaser, Germany). Slides were dried at 45 ºC

overnight. In addition, slides were baked at 60 $^{o}$C for 20 min to minimise the possibility that sections may come off the slides prior to immunostaining.

## 2.6.2. Human tissue preparation

The collection of patient specimens for the analysis in this study was approved by the Central Sydney Area health Service (X04-318) and Western Area Health Service Ethics Committee (HREC2000/9/4.18 [1089]). Immediately after surgery with tumour-free resection margins, a sample of prostate tumour tissue was obtained. Specimens were delivered to the pathology lab and macroscopically analysed by pathologists who also selected a small cancer fragment before fixation. Human tissue samples contained adjacent BPH and PCa tissue (n=17), unpaired BPH (n=36) and PCa (n=70), and paired Hormone sensitive PCa (HSPC) and CRPC (n=8). The paired HSPC and CRPC specimens (n=8) were derived from patients who initially underwent transurethral resection of the prostate and were diagnosed with PCa, but after ADT became castration resistant. The 5 µm section of the human tumour tissues sample was provided by Dr Charles Chan and his colleagues as described previously (Tan, 2011). Fractionated tissue sections were then stored at −80 °C till use.

## 2.6.3. Immunostaining analysis

For deparaffinisation, sections were left in xylene for 20 min for cell samples, and overnight for human tissues, and rehydrated in downgrading ethanol (100%, 95%, and 70%) through to distilled water. Heat-induced antigen retrieval was performed to at least partially reverse the formalin-modified tertiary structure of proteins. Tissue sections were heated in 10 mM Tris-EDTA buffer (20.0 mM Tris, 13.4 mM EDTA, 12.4 mM tri-sodium citrate, 0.05% TWEEN®20, pH 8.0) for 20 min. Slides were left in hot buffer, cooled down at room temperature and rinsed with distilled water. Slides were again washed in Tris-buffered saline

containing TWEEN®20 (TBST; 200 mM Tris-HCl, 150 mM NaCl, 10 mM Tris-base, 0.5% TWEEN®20, pH 7.5). To reduce hydrophobic binding of primary antibody to tissue proteins, sections were blocked by incubating slides with 10% v/v normal animal horse serum (NHS; JRH, USA) in TBST for 20 min. 10% NHS was flicked off prior to incubation in the primary antibody. All primary antibody labelling was performed in 10% horse serum in TBST, overnight at 4 ºC. Primary antibody was not added to 10% NHS in TBST in the method control slides. Simultaneously, isotype control was carried out with rabbit or mouse immunoglobulin (DakoCytomation, Denmark) at the same concentration as the primary antibody.

As avidin interacts with biotin with high affinity, peroxidase-conjugated avidin was mixed with biotin to form a large complex prior to secondary antibody incubation. Sequentially, the avidin-free sites in the peroxidase-conjugated complex interacted with the biotin-conjugated secondary antibody; thus, a positive signal was amplified. The next day, biotin-conjugated secondary anti-rabbit or anti-mouse antibody (Vector Laboratories, Australia) and Vectastain Avidin-Biotin complex kit (ABC; Vector Laboratories, Australia), were diluted to 1:1000 in TBST contains 1% NHS. Slides were incubated with secondary antibody and ABC for 30 min and 40 min at room temperature, respectively. Between each of these incubations, sections were rinsed with distilled water and TBST. For peroxide enzymes, 3' diaminobenzidine tetrachloride (DAB) chromogen is used to produce a brown colour in labelled positive cells. Sections were therefore incubated with DAB (Dako, USA) for 6 min or until brown colour was observed. The reaction was stopped by rinsing the slides with distilled water. Haematoxylin counterstain was carried out, followed by quick dips in acidic ethanol and Scott's Blue solution, a cellular nuclear counterstain developed for blue staining. The slides were dehydrated in graded alcohol (75%, 95% and 100%) and mounted in Di-n-butylPhthalate in Xylene (DPX; BDH, England).

# 2.7. Reverse Transcription and Quantitative Real-Time Polymerase Chain Reaction

## 2.7.1. Preparation of total RNA samples

Media was aspirated from the 6-well plates, and then the plates were washed twice with cold PBS before incubation with 350 μL of each lysis buffer (RLT buffer, containing guanidine thiocyanate (Qiagen, USA); and 14.3 M (1% v/v) β-mercaptoethanol (Sigma-Aldrich, Australia) on ice for 10 min. Cells were then lysed, flicked and collected. Sterile, RNase-free pipette tips were used to transfer the cell lysates to Qiagen shredder purple columns to clean up cell pellet debris. The flow through obtained from the columns was collected by centrifugation for 2 min at maximum speed. The flow through were then mixed with an equal amount of 70% RNase-free ethanol prior to transfer to Qiagen mini-pink columns. The Qiagen mini-pink columns were centrifuged for 15 seconds at maximum speed to allow the precipitated RNA to bind to the column matrices. The resulting flow through – containing ethanol, DNA debris and lysis buffer – was discarded. RNA precipitate was first washed by 700 μL of RW1 buffer to remove RNA-bound protein. Flow through – containing protein and ethanol – was collected by centrifugation at maximum speed for 15 seconds, and discarded. To remove any remaining heavy metal, DNA, wash buffer and/or ethanol, the sample was washed twice with second wash buffer (RPE) and centrifuged again at maximum speed for 1 min. The samples within the Qiagen mini-pink columns were transferred to fresh RNase-free tubes. Commercially available RNase-free water (30 μL) was added to dissolve RNA and total RNA was then extracted by centrifugation for 1 min. The quality and quantity of the extracted RNA samples was determined using the NanoDorp ND-1000 Spectrophotometer (Biolab, Australia).

## 2.7.2. Reverse transcription

To enable the PCR analysis of RNA molecules, single strand RNA was transcribed into DNA. A reverse transcriptase (RT) enzyme was utilised alongside an oligonucleotide primer, to create a complementary DNA (cDNA) copy.

Primers were designed to cross exon-intron boundaries, preventing the amplification of genomic DNA. The RT reaction commenced with the addition of 50 ng/mL Random Hexamer, 20 mM dNTP mix and 50 μM Oligo (dT), 2 μg samples having been made up to 20 μL with diethylpyrocarbonate (DEPC)-treated water. Following 5 min at 65 ºC to denature the secondary structure of RNA, samples were cooled down with ice for a minimum of 1 min. 10 μL of Synthesis Mix (10X RT buffer, 25 mM $MgCl_2$, 0.1 M DTT, 40 U/μL RNase OUT and 200 U/μL SuperScript III RT; Invitrogen, USA) was added prior to incubation. Non-RT controls – sample with no SuperScript III – were included to verify the contamination level of cDNA, which may have yielded less than optimal results. Final incubation temperatures varied:

Annealing: 25 ºC for 10 min
cDNA synthesis: 50 ºC for 50 min
Terminate reaction: 85 ºC for 5 min
Store cDNA: hold at 4 ºC
Store samples: hold at –20 ºC until use.

## 2.7.3. Polymerase chain reaction

Each reaction per sample contained master mix (SYBR Green I, diluted 1:400 from stock solution; Invitrogen, USA), qPCR (a ‘ready-to-use’ cocktail containing dNTPs, 3 mM $MgCl_2$

and Platinum Taq Polymerase; Invitrogen, USA), forward and reverse primers and DEPC-treated water) and diluted cDNA template, made up to a 20 μL.

Primers were synthesised by Geneworks (Hindmarsh, Australia). Each primer set (forward and reverse) was designed to exclude genomic DNA from amplification as follows.

UBE2C primer sequence

Forward: 5′–TGGTCTGCCCTGTATGATGT–3'
Reverse: 5′–AAAAGCTGTGGGGTTTTTCC–3'

TBP primer sequence

Forward 5′–GAACCACGGCACTGATTTTC–3'
Reverse: 5′–CCCCACCATGTTCTGAATCT–3'

p27 primer sequence

Forward: 5'–GGCCTCAGAAGACGTCAAAC–3'
Reverse: 5'–ACAGGATGTCCATTCCATGA–3'

c-MYC primer sequence

Forward: 5'–GGATTTTTTTCGGGTAGTGGAA–3'
Reverse: 5'–TTCCTGTTGGTGAAGCTAACGTT–3'

15 μL of the primer with master mix were loaded into each of the sample tubes to ensure accurate distribution between samples. A total of 5 μL of cDNA was diluted by 620 μL water in each template sample so that 5 μL of template (1/625 dilution) was added to the pre-loaded master mix sample tubes. This was performed to ensure accurate distribution of sample cDNA. Triplicates were carried out for each sample to obtain more reliable data.

## 2.7.4. Standard curve

Each run was performed with a standard for the housekeeping or GOI, a non-RT control, and no-template controls (water blank) for each primer set and efficacy of each standard was

compared. Standard samples were prepared using serial 1:5 dilutions of one template cDNA sample, with a starting concentration of 1/625 dilution for a total of five standard points (each dilution run in triplicate). 5 μL of each standard template was again added into separate pre-loaded housekeeping and GOI master mix sample tubes.

Samples were amplified using a Rotor-gene 6.0 RT-PCR machine set to the following conditions:

1st hold temperature: 50 ºC for 2 min
2nd hold temperature: 95 ºC for 10 min
Cycling of three PCR temperatures:
95 ºC for 10 seconds
56 ºC for 15 seconds
72 ºC for 20 seconds
40 repeat cycles
3rd hold temperature: 65 ºC for 90 seconds
Melt curve start temperature: 65 ºC
Raise by 1 ºC each step
Hold 5 seconds on each step afterwards
End temperature: 95 ºC

## 2.7.5. Data analysis

The peak present in the melt curve occurs when there is a rapid increase in the rate of fluctuating florescence. Fluorescence decreases as temperature increases. Non-template control (water) only displays a peak when primer dimers are present.

The threshold cycle parameter ($C_T$) is the calculated fractional cycle number at which the PCR product crosses a threshold of detection (Figure 2-2). The higher the initial amount of template DNA, the more PCR products is accumulated. In addition, a high initial amount of

template DNA also results in the fluorescent intensity reaching the threshold value earlier, *i.e.*, a lower $C_T$ value. The change of the $C_T$ Value was then notmaliazed with TBP and analysed by The Relative Expression Software Tool (REST, version 2009).

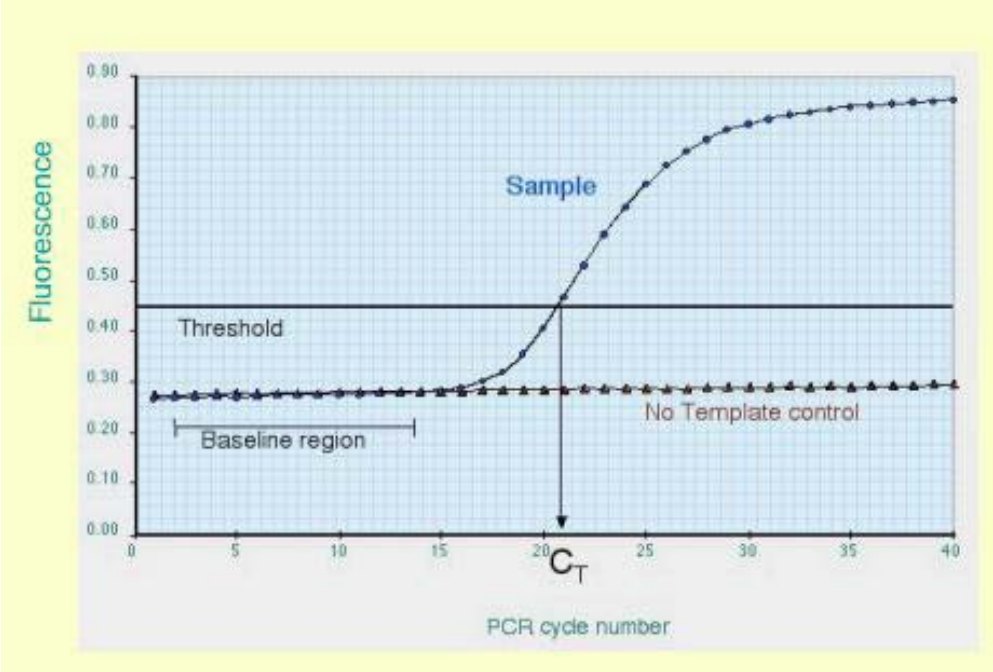


**Figure 2-2. The RT-PCR amplification plot features.**

$C_T$ value is the cycle number at which the set threshold crosses into the exponential phase. The slope of this exponential phase is a measure of efficiency.

# 2.8. Statistical Analysis

Statistical comparison was performed using NCSS/PASS version 12.0 (NCSS Statistical and Power Analysis Software, USA). The scores of UBE2C level in prostate tissue were analysed by paired *t*-test. The processed data was analysed using one-way ANOVA to determine if a significant change had occurred. Fisher's least significant difference multiple-comparison test (significance at $p<0.05$) and Kruskal-Wallis multiple-comparison *z*-value test (significance at *z*-value >1.96) were applied.

# *Chapter 3*

# 3. The Effect of Manipulation of UBE2C Expression on the Proportion of Quiescent Prostate Cancer Cells

# 3.1. Introduction

In a mature mammalian prostate gland, the majority of epithelial cells are in a state of proliferative quiescence (Hartwell *et al.*, 1974; Kriegenburg *et al.*, 2008). Only a select population of cells, referred to as stem cells, proliferate in a controlled manner to replenish lost cells or those damaged after injury (Visvader and Clevers, 2016). Cancer is a consequence of uncontrolled cell proliferation. When cancer cells cease proliferation, either due to specific anti-mitogenic signals or to the absence of proper mitogenic signaling, they exit the cell cycle and enter a quiescent state; these cells also known as quiescent cancer cells (Malumbres and Barbacid, 2001). Quiescent cancer cells, which are Ki-67 protein-negative and arrest in a reversible state of $G_0$, have been found in various cancers including prostate (Coller, 2007; Jackson, 1989). Hence, cancer is made up of both actively proliferative and quiescent cancer cells. Recent studies in PCa have shown that the increased proportion of proliferative over quiescent ratio in PCa cells represents an inherent mechanism that at least partially explains recurrence in PCa patients (Almog, 2010; Brackstone *et al.*, 2007; Udagawa, 2008). Ki-67 protein immunostaining in PCa showed a low positivity in low grade and low volume disease, but increases in high risk and advanced disease, suggesting an accelerated transition from quiescent to a proliferative state during disease progression (Jhavar *et al.*, 2009; Keshari *et al.*, 2011; Khatami *et al.*, 2009; Nagao *et al.*, 2011). These clinical observations propose that a strategy to prevent cancer progression and recurrence is to increase the exit of cycling cancer cells to $G_0$ phase and/or to prevent the transition from $G_0$ to a proliferating state. However, our understanding of the signals required for maintaining cancer cells at $G_0$ and/or impeding the transition from quiescent to proliferating state is limited.

UBE2C is an E2 enzyme that, when associated with an E3 ligase, mediates the proteolysis of a series of key mitotic cell cycle regulators (Xie *et al.*, 2014). *UBE2C* is considered an oncogene associated with a variety of cancers and its overexpression is associated with proliferation of tumour cells (Hao *et al.*, 2012). In PCa cells, overexpression of UBE2C promoted cell proliferation, whereas depletion of UBE2C expression suppresses growth of cells (Wang *et al.*, 2011). Importantly, van Ree *et al.* (2010) showed that overexpression of UBE2C alone in mice is sufficient to induce a broad spectrum of spontaneous tumours as well as carcinogen-induced lung tumours. These data further support the oncogenic role of *UBE2C* in tumour development. However, whether *UBE2C* play a role in the proportion and transition of quiescent cancer cells is unclear.

The aim of studies described in this chapter is to define if *UBE2C* plays a role in influencing the proportion of quiescent PCa cells.

# 3.2. Materials and Methods

## 3.2.1. Prostate cancer cell lines

The PCa cell line LNCaP, PC-3 and C4-2B cells and the noncancerous prostate cells, PrEC and RWPE-1, were cultured as described in **Chapter 2.1.1**.

## 3.2.2. Immunocytochemistry

The sample blocks were prepared as described in **Chapter 2.6.1.** The Expression of UBE2C in cells was determined by immunocytochemical staining as described in **Chapter 2.6.3.**

### 3.2.3. Transfection of prostate cancer cells with siRNA

Prostate cancer cells were transfected with 20 nM siUBE2C or NC and seeded in 6-well plates for immunoblotting or qRT-PCR, in T25 flask for flow cytometry analysis or in 96-well plates for SYBR Green assay as described in **Chapter 2.2.1**.

### 3.2.4. Transfection of prostate cancer cells with plasmid

For overexpression, PCa cells were gown in T75 flasks until semi-confluent, cells were then trypsinised and transfected with plasmid according to **Chapter 2.2.2.** Thereafter, cells were harvested for SYBR Green assay, immunoblotting, qRT-PCR or flow cytometry analysis.

### 3.2.5. SYBR Green assay

The DNA content of PCa cells was determined using SYBR Green assayThe fluorescence intensity of SYBR Green-stained DNA was measured as decribed in **Chapter 2.4**.

### 3.2.6. Immunoblotting

The cells were treated in 6-well plates and cell lysates were prepared with a lysis buffer. Immunoblotting was performed as described under **Chapter 2.5**. The primary antibodies used in this section were listed in Table 2-4**.**

### 3.2.7. Flow cytometry analysis of cells stained with propidium iodide

The cell cycle phase distribution of PCa cells was determined by flow cytometric analysis of cells stained with PI as described in **Chapter 2.3.1**.

## 3.2.8. Flow cytometry analysis of cells stained with DNA and RNA dye

The cell cycle phase distribution of PCa cells was determined by flow cytometric analysis of cellular DNA and RNA content as described in **Chapter 2.3.2**. The triple staining with p-Rb (p-Ser$^{801/811}$) was performed as described in **Chapter 2.3.3**.

## 3.2.9. Statistical analysis

The statistical software NCSS version 12.0 was used for statistical analysis as described in **Chapter 2.8**

# 3.3. Results

## 3.3.1. Knockdown of UBE2C increased the quiescent subpopulation in prostate cancer cells

### 3.3.1.1. Determine UBE2C expression in prostate cell lines by immunocytochemical analysis

To determine the expression of UBE2C in all PCa cell lines used in this study, immuno-cytochemical analysis was performed. Immunostaining of PCa cell lines with anti-UBE2C antibody showed positive staining in LNCaP cells, PC-3 and C4-2B cells (Figure 3-1). Expression of UBE2C was observed at both the membrane and cytoplasm in all PCa cells. There was a negative or low staining in non-cancerous cell lines including PrEC and RWPE-1 cells. No staining was seen in the cells incubated with antibody isotype control.

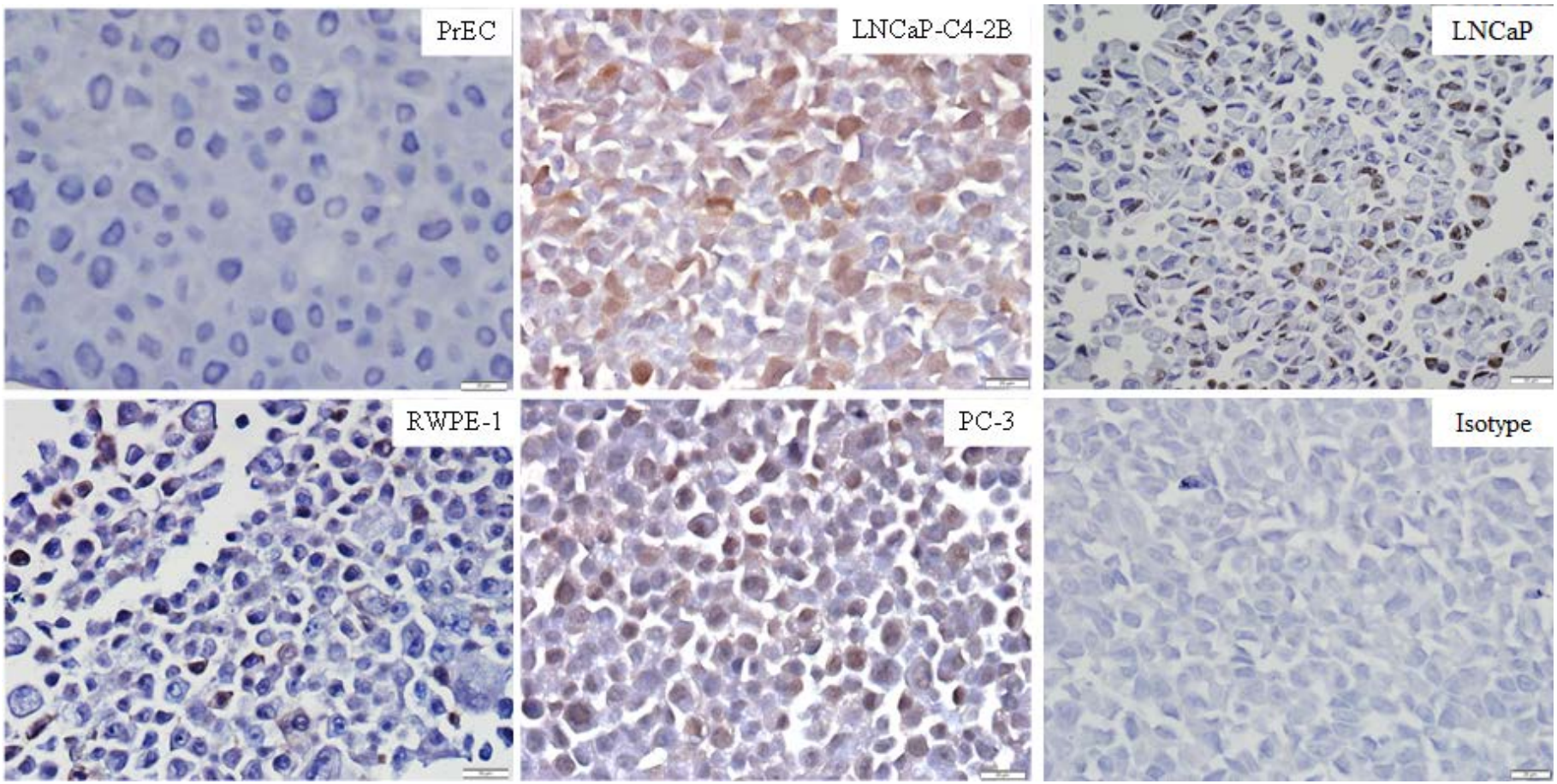


**Figure 3-1. Expression of UBE2C in prostate cell lines.**

Prostate cell lines were maintained in T75 flasks and allowed to reach 70–80% confluence. Cells were then collected and embedded in paraffin, sectioned and stained with anti-UBE2C antibody (A-165, 1:600). Representative images of non-cancerous prostate cells (PrEC and RWPE-1) and PCa cell lines (LNCaP, PC-3 and C4-2B) were taken at 400X magnification. Scale bar=20 μm.

### 3.3.1.2. Effect of UBE2C siRNA on UBE2C expression by immunoblotting

To validate the effect of UBE2C knockdown, we transfected three PCa cell lines (PC-3, LNCaP and C4-2B) with UBE2C siRNAs. PC-3, LNCaP and C4-2B cell lines were treated for 72 h with Opti-MEM, NC or three sets of siUBE2C, and lysates were analysed by immunoblotting. Results showed UBE2C knockdown is more effective in siUBE2C set 1 (C1) and set 3 (C3) compared to set 2 (C2) in all three PCa cell lines (Figure 3-2). Accordingly, C1 and C3 were selected for further study.

### 3.3.1.3. Knockdown of UBE2C decreased cell proliferation in prostate cancer cell lines

The hallmark for cell proliferation is the synthesis of DNA. To monitor the change of cellular DNA content upon UBE2C knockdown, SYBR Green assay was performed on PC-3, LNCaP and C4-2B cell lines. SYBR Green is a dye of double-stranded DNA. DNA content was significantly reduced in PC-3, LNCaP and C4-2B cells following UBE2C knockdown compared with control cells ($p<0.05$). Transfection of LNCaP cells with siUBE2C C1 and C3 reduced SYBR Green intensity by 65% and 33%, respectively within 3 days compared to control cells. An approximate 50% and 90% reduction was observed in PC-3 and C4-2B cells, respectively (Figure 3-3).

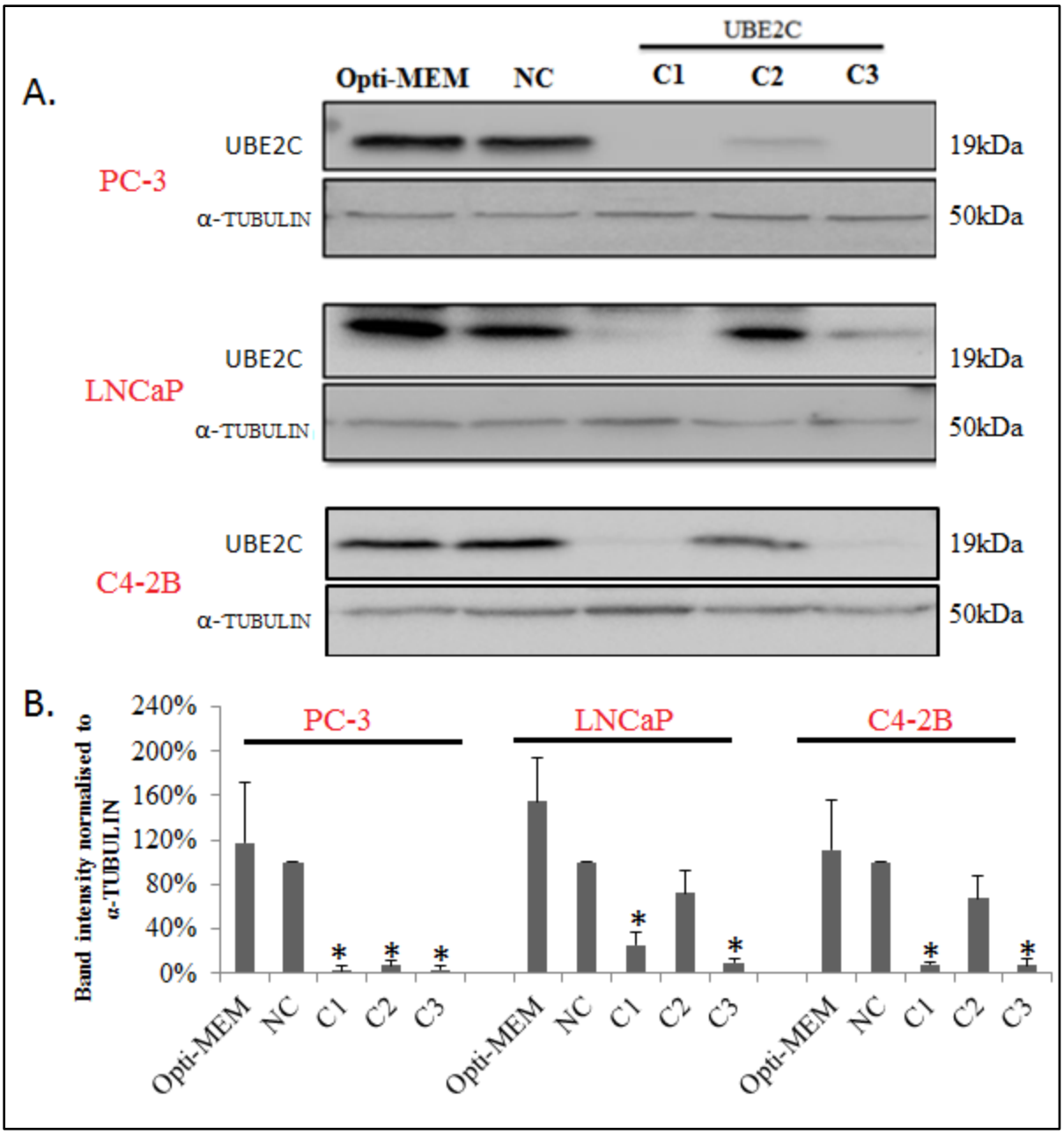


**Figure 3-2. Evaluation of knockdown of UBE2C with siUBE2C.**

PCa cells were seeded in 6-well plates with Opti-MEM, 20 nM NC or siUBE2Cs, including C1, C2 and C3. Cells were lysed 72 h post-transfection. Levels of UBE2C protein in PC-3, LNCaP and C4-2B cells were examined by western blot (anti-UBE2C antibody, A-165, 1:1000). α-TUBULIN expression was determined as a control to assure equal protein loading. A. Representative immunoblotting image in PCa cells. B. Histogram representing densitometric analysis are mean±SD. *, P< 0.05 versus NC in each cell line. The results are representative of three experiments.

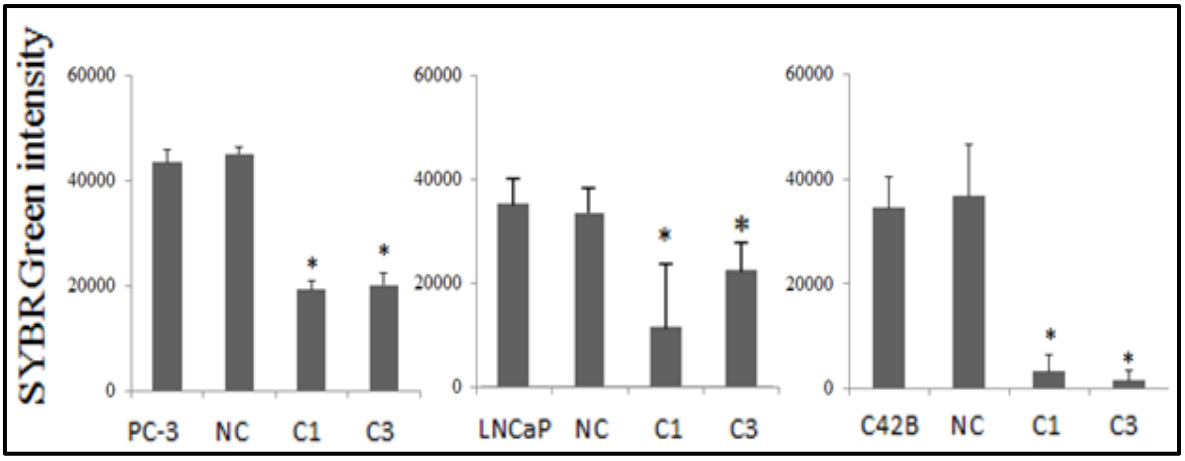


**Figure 3-3. Effect of UBE2C knockdown on DNA content in prostate cancer cells.**

PC-3, LNCaP and C4-2B cells were transfected with 20 nM NC, C1 or C3 in 96-well plates; non-treated cells included as baseline. After 72 h transfection, cells were harvested, stained with SYBR Green and analysed for DNA content. Results are expressed as mean ± SD of three independent experiments. * $p<0.05$ as compared with NC in each cell line.

### 3.3.1.4. Genetic silencing of UBE2C in cell cycle distribution by propidium iodide staining

To delineate the cell cycle status of PCa cells, the cell cycle phase distribution of PCa cells was analysed by measuring the DNA content using flow cytometric analysis of PI-stained cells (Figure 3-4). The doublets were gated out by using PI parameters Area versus Width as shown in Figure 3-4A. The selected singlet cells were then presented in a DNA frequency histogram (Figure 3-4B–D). On the basis of differences in DNA content alone, $G_0/G_1$ cells were identified with low DNA content; $G_2$/M cells with DNA content twice that of $G_0/G_1$ cells; and S phase cells with intermediate DNA content. The DNA content histograms (Figure 3-4B–D) were deconvoluted using FlowJo-V10 Dean-Jett-Fox model algorithms. The average percentage of cells in $G_0/G_1$ phase for human PCa cell lines maintained in log phase growth was 44.1% for PC-3 cells, 33.8% for LNCaP cells and 53.7% for C4-2B cells.

To validate the role of UBE2C in cell cycle phase distribution, we next genetically knocked down UBE2C in PCa cell lines. PCa cells were treated with NC or siUBE2Cs, the protein level of UBE2C was measured after 24, 48 and 72 h treatment by western blot (Figure 3-5). The expression of UBE2C protein was reduced in both C1 and C3-treated PC-3 and C4-2B cells 24 h after siUBE2Cs transfection. Notably, 48–72 h was required for both sets of siUBE2C to diminish UBE2C protein levels in LNCaP cells, suggesting a cell line-dependent difference in response to siUBE2C in the three PCa cell lines.

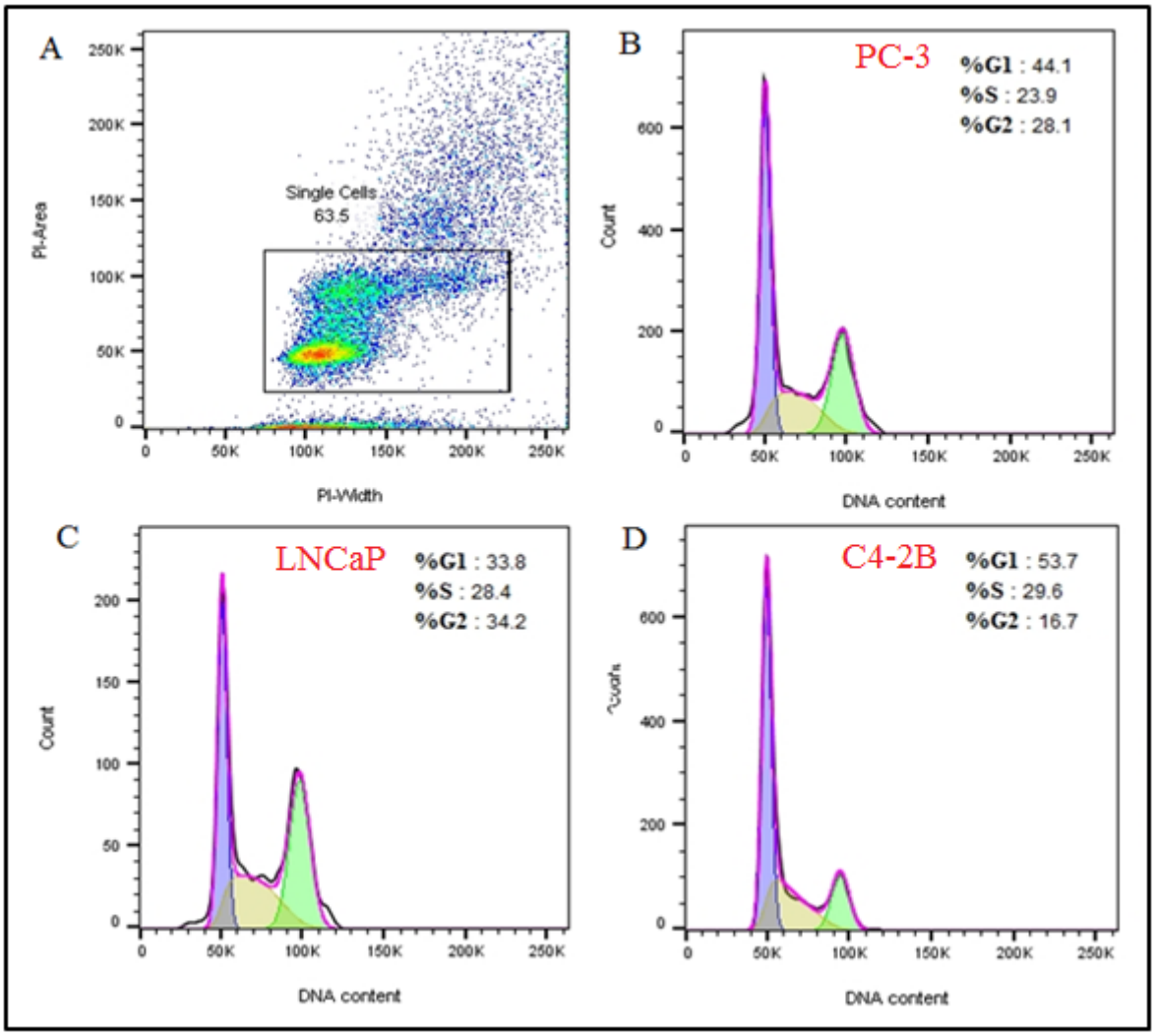


**Figure 3-4. DNA content histogram of prostate cancer cell lines using single parameter flow cytometer (PI staining).**

Prostate cell lines were maintained in T25 flasks and allowed to reach 70–80% confluence. Cells were then collected and fixed in 70% ethanol at 4 ºC. The cells were then stained by PI and subjected to flow cytometric analysis. **A.** The single cells were gated out by using PI parameters Area versus Width. **B.** DNA content histogram of PC-3 cells. **C.** DNA content histogram of LNCaP cells. **D.** DNA content histogram of C4-2B cells. This figure was created with FlowJo Dean-Jett-Fox model. The Dean-Jett-Fox model fitted the 2N population with a purple Gaussian distribution, the 4N population with a green Gaussian distribution, and the S population with a yellow polynomial.

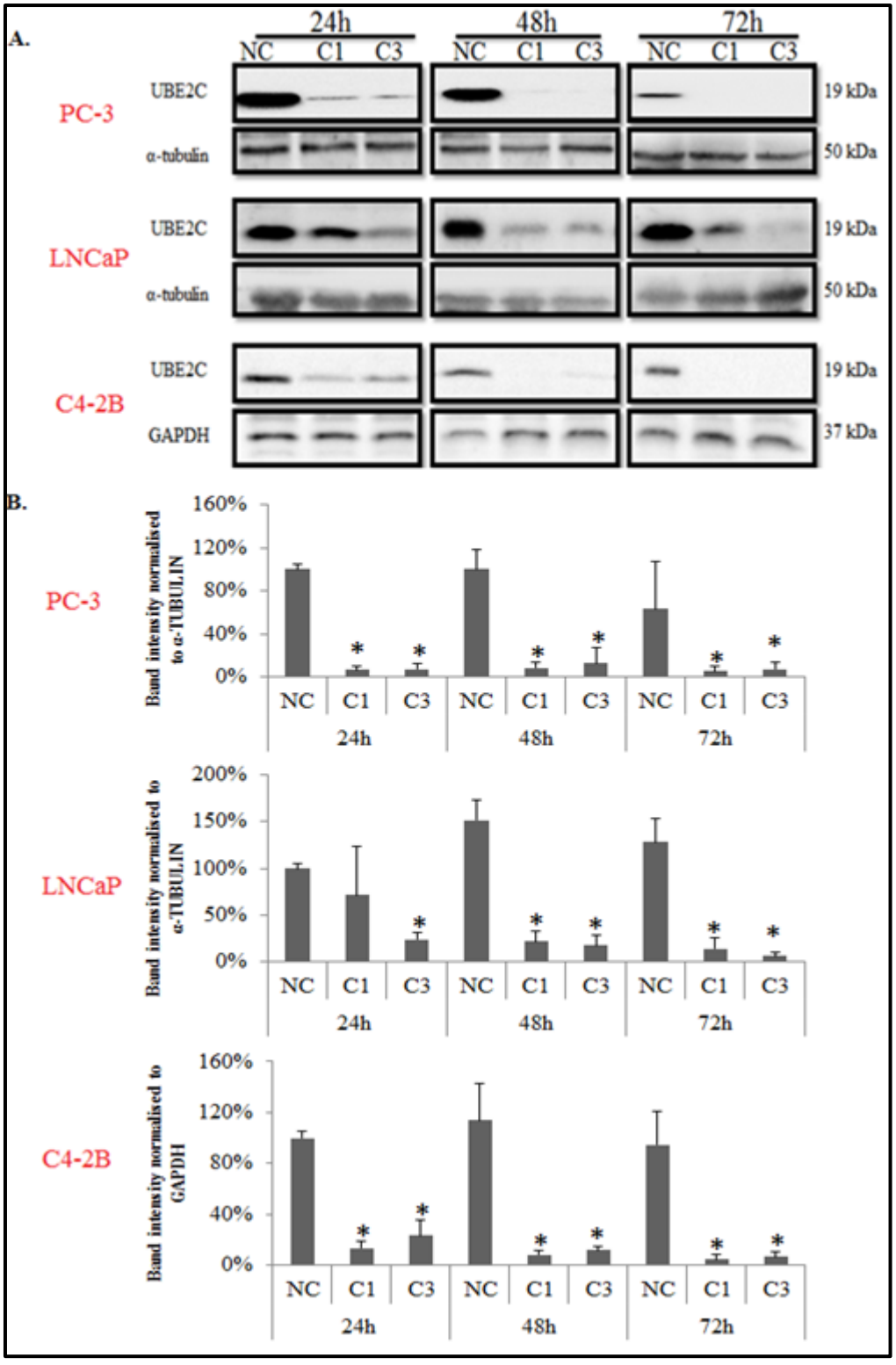


**Figure 3-5. Expression of UBE2C in siUBE2C-transfected prostate cancer cells.**

PC-3, LNCaP and C4-2B cells were transfected with 20 nM NC, C1 or C3 in 6-well plates with a time course experiment. The cells were harvested 24, 48 and 72 h following transfection. Levels of UBE2C protein in PC-3, LNCaP and C4-2B cells were examined by western blot analysis. **A.** Representative immunoblotting image in PCa cells. **B.** Histogram representing densitometric analysis are mean± SD. *, P< 0.05 versus NC in each cell line. The results are representative of three experiments.

Next, we examined the effects of siUBE2Cs on cell cycle progression by PI staining. In PC-3 and C4-2B cells, reducing UBE2C protein levels caused an increase in the proportion of cells in $G_2$/M phase, compared to the cells treated with NC. Furthermore, the PC-3 cells in $G_0/G_1$ phase were decreased upon siUBE2C transfection, whereas no change was observed in C4-2B cells. However, loss of UBE2C in LNCaP cells increased the fraction of cells in $G_0/G_1$ but no significant change in the fraction of cells in S and $G_2$/M phase. The average percentage of each phase of the cell cycle in three different PCa cell lines after knockdown UBE2C over 3 days are summarised in Table 3-1.

**Table 3-1. The effect of siUBE2C on cell cycle distribution analysed by PI flow (Mean±SD).**

| | | Phase | | |
|---|---|---|---|---|
| | | $G_0/G_1$ (%) | S (%) | $G_2/M$ (%) |
| **PC-3 cells** | | | | |
| 24h | NC | 46.0 ± 3.4 | 24.6 ± 0.3 | 27.3 ± 3.7 |
| | C1 | 44.2 ± 1.8 | 29.1 ± 3.3 | 24.6 ± 0.6 |
| | C3 | 42.2 ± 0.2 | 30.9 ± 0.2* | 24.2 ± 1.4 |
| 48h | NC | 47.3 ± 1.6 | 27.7 ± 1.6 | 22.5 ± 1.6 |
| | C1 | 36.9 ± 1.3* | 25.9 ± 0.1 | 34.9 ± 1.0 |
| | C3 | 51.3 ± 5.6 | 26.2 ± 1.3 | 20.0 ± 1.0 |
| 72h | NC | 48.9 ± 0.1 | 27.3 ± 0.4 | 20.6 ± 0.5 |
| | C1 | 45.2 ± 0.6 | 26.7 ± 3.8 | 25.9 ± 4.0* |
| | C3 | 38.6 ± 0.9* | 24.5 ± 0.1 | 38.6 ± 0.6* |
| **LNCaP cells** | | | | |
| 24h | NC | 65.4 ± 0.9 | 17.9 ± 2.4 | 14.2 ± 0.4 |
| | C1 | 63.3 ± 1.6 | 21.1 ± 0.8 | 14.0 ± 0.7 |
| | C3 | 65.0 ± 0.2 | 20.9 ± 1.1 | 13.2 ± 0.4 |
| 48h | NC | 62.2 ± 1.8 | 17.7 ± 0.4 | 13.5 ± 3.7 |
| | C1 | 63.3 ± 5.9 | 22.6 ± 3.7 | 11.2 ± 1.0 |
| | C3 | 63.3 ± 3.3 | 21.8 ± 1.1 | 13.8 ± 2.8 |
| 72h | NC | 60.8 ± 1.6 | 15.1 ± 0.6 | 15.4 ± 2.3 |
| | C1 | 60.6 ± 3.6 | 18.5 ± 1.3 | 10.3 ± 1.4 |
| | C3 | 68.4 ± 0.8* | 17.7 ± 1.1 | 11.4 ± 0.8 |
| **C4-2B cells** | | | | |
| 24h | NC | 45.2 ± 1.0 | 38.5 ± 0.7 | 13.8 ± 1.4 |
| | C1 | 43.9 ± 1.0 | 42.4 ± 1.8 | 12.0 ± 1.2 |
| | C3 | 40.8 ± 0.7 | 40.7 ± 0.0 | 13.7 ± 0.6 |
| 48h | NC | 61.4 ± 2.5 | 21.1 ± 1.9 | 15.0 ± 1.1 |
| | C1 | 63.4 ± 1.5 | 23.7 ± 3.8 | 11.2 ± 1.6 |
| | C3 | 65.0 ± 0.6 | 23.8 ± 1.1 | 10.6 ± 0.0 |
| 72h | NC | 67.1 ± 3.7 | 25.5 ± 1.1 | 5.7 ± 0.5 |
| | C1 | 64.6 ± 1.4 | 25.4 ± 2.0 | 7.4 ± 0.9* |
| | C3 | 66.1 ± 0.8 | 25.4 ± 0.8 | 7.2 ± 0.0* |

For PI-cell cycle analysis, the cells were fixed in 70% ethanol and kept at –20 ºC until PI staining followed by flow cytometry. Representative quantification data of three independent double staining experiments. * $p<0.05$ vs. NC.

### 3.3.1.5. Depletion of UBE2C decreased Ki-67 staining in PC-3 cells

Since the effects of silencing of UBE2C on the proportion of cells in $G_0/G_1$ phase varies between different cell lines, we employed immunocytochemical staining of Ki-67 to further elucidate the role of UBE2C on the proportion of quiescent and proliferating cells. PC-3 cells were used to determine the expression of Ki-67. Ki-67 staining demonstrated a marked decrease in the percentage of Ki-67-positive cells in both sets of siUBE2C-treated PC-3 cells compared to NC-treated control cells (Figure 3-6). Collectively, knockdown of UBE2C is expected to increase the proportion of $G_0$ cells in PC-3 cells.

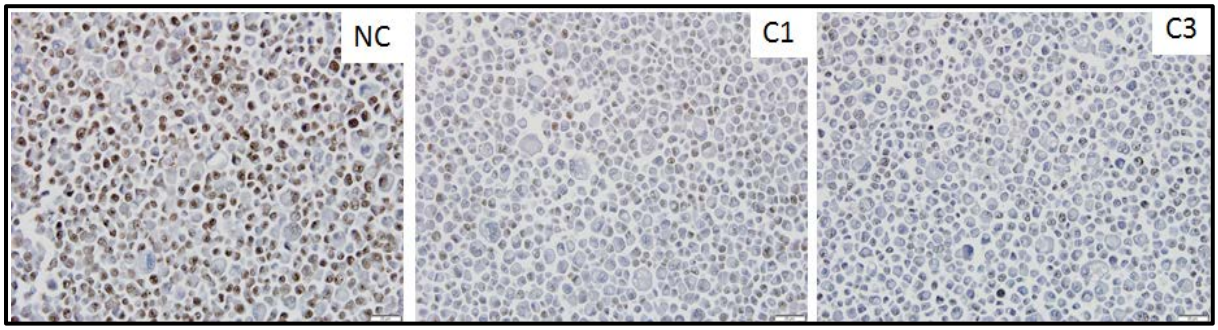


**Figure 3-6. Ki-67 staining in siUBE2C-treated PC-3 cells.**

PC-3 cells were transfected with 20 nM NC, C1 or C3 in T75 flasks for 72 h. Prostate cell lines were maintained in T75 flasks and allowed to reach 70–80% confluence. Cells were then collected and embedded in paraffin, sectioned and stained with anti-Ki-67 antibody (1:2000). Representative image (200X magnification) of PC-3 cells with Ki-67 staining was taken at 200X magnification. Scale bar=50 µm.

### 3.3.1.6. Validation of flow cytometric analysis of HP double staining by quiescent prostate cancer cells

The decreased Ki-67-positive PC-3 cells together with decreased $G_0/G_1$ phase in the same cell line raised an interesting possibility: although the fraction of cells in $G_0$ and $G_1$ phase decreased, the proportion of $G_0$ over proliferating $G_1$ cells could be altered. We employed HP double staining to further elucidate this possibility. The HP double staining method provides an *in vitro* measurement to distinguish cells in $G_0$ from $G_1$ phase. To verify the method, the

PCa cells were synchronised at $G_0$ and then measured by flow cytometric analysis using HP double staining. By using both Ki-67 immunostaining and PI staining, our laboratory previously demonstrated that to achieve quiescence in PC-3 and LNCaP cells requires 3 days contact inhibition (CID3) and 7 days serum withdrawal (SWD7), respectively (Yao *et al.*, 2015). Consistent with our published previous PI staining result, cell stains with HP double staining also showed about 80% of PC-3 cells and 90% of LNCaP cells were synchronised into $G_0/G_1$ phase (Figure 3-7 and Figure 3-8).

To further validate the method, we performed a time course experiment to synchronise PC-3, LNCaP and C4-2B cells at indicated time intervals (Figure 3-7, Figure 3-8, Figure 3-9). By simultaneously determining DNA and RNA content, $G_0$ cells were gated out by their low Pyronin Y staining (low total RNA content) and 2N DNA content (Figure 3-7). Flow cytometric analysis revealed a significant increase in $G_0$ cells in synchronised PC-3 (Figure 3-7), LNCaP (Figure 3-8) and C4-2B cells (Figure 3-9) in a time-dependent manner, compared to non-synchronised PCa cells ($p<0.05$). The percentage of cells in $G_0$ phase was 28% in non-contact inhibited (NOCI) cells, but approximately 70% after synchronisation in CID3 samples (Figure 3-7). In addition, our observations were consistent with the notion that although the total percentage of cells in $G_0/G_1$ remained around 85% during 3 days' contact inhibition, there was a significant increase in the $G_0$ population but a decrease in the $G_1$ population.

Similar results were observed in LNCaP and C4-2B cells. The proportion of cells in $G_0$ phase increased from 14.6% to 76.7% in LNCaP cells after 7 days' serum withdrawal (Figure 3-8), while C4-2B cells rose from 11.5% to 84.8% upon synchronisation (Figure 3-9).

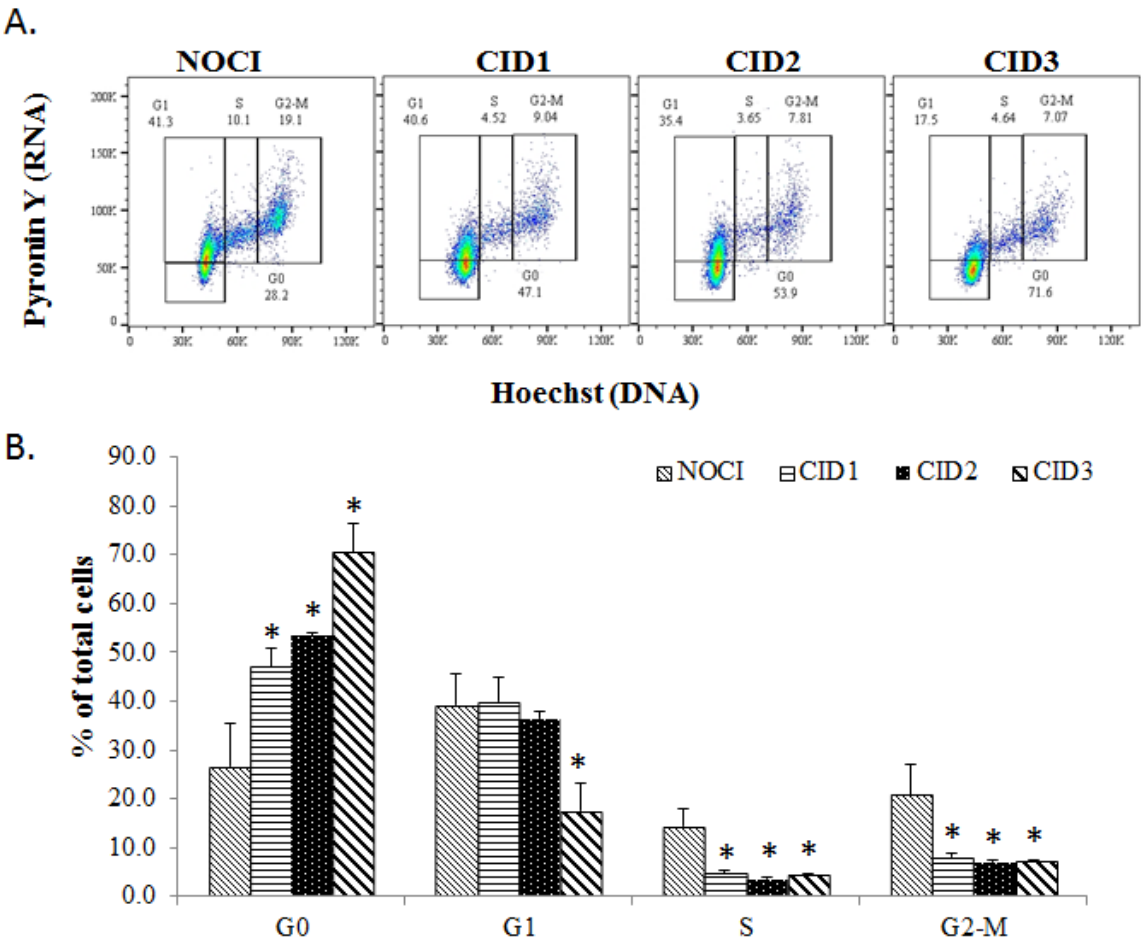


**Figure 3-7. Validation of HP double-staining in PC-3 cells.**

NOCI, PC-3 cells were cultured in 10% FCS with no contact inhibition. Cells were analysed for cell cycle distribution by HP double staining by simultaneously labelling the cells with both DNA and RNA. Boxes outline cells in $G_0$, $G_1$, S and $G_2$/M. $G_0$ and $G_1$ both have 2N DNA content so the $G_1$ box is directly over the $G_0$ box, with the $G_0$ cells having less total RNA. CID1–CID3, PC-3 cells were maintained in a confluent state in T25 flasks for up to 3 days. Thereafter, cells were collected for cell cycle analysis by using the same gating. **A.** Representative flow image in PC-3 cells. **B.** Histogram illustrates the cell cycle distribution during cell cycle exit. * $p$<0.05 vs. NOCI.

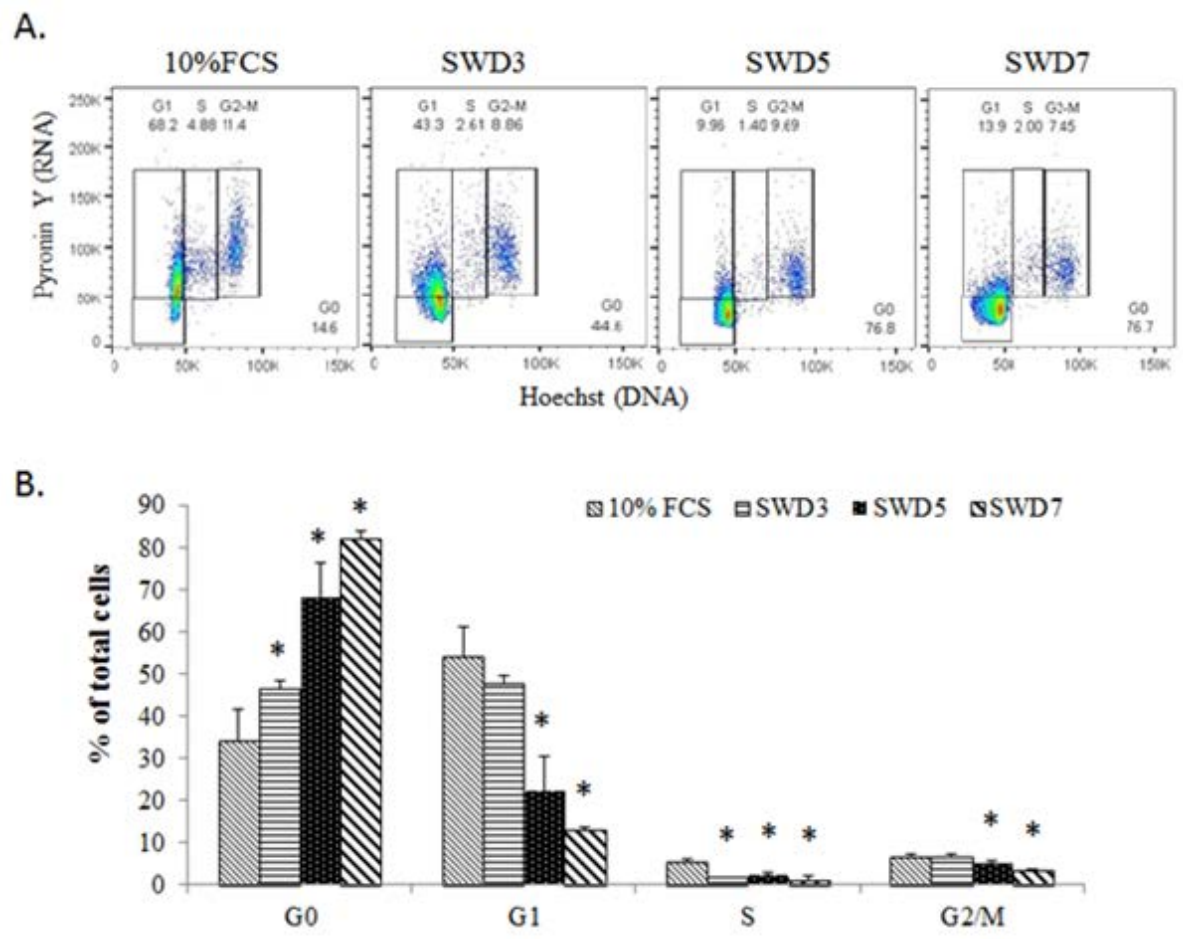


**Figure 3-8. Validation of HP double staining in LNCaP cells.**

10% FCS, LNCaP cells were grown in 10% FCS medium in T25 flasks. Cells were analysed for cell cycle distribution by HP double staining by simultaneously labelling the cells with both DNA and RNA. Boxes outline cells in $G_0$, $G_1$, S and $G_2$/M. SWD3-D5; LNCaP cells were serum-deprived in T25 flasks for up to 7 days. Thereafter, cells were collected for cell cycle analysis by using the same gating. **A.** Representative flow image in LNCaP cells. **B.** Histogram illustrates the cell cycle distribution during cell cycle exit. * $p<0.05$ vs. 10% FCS.

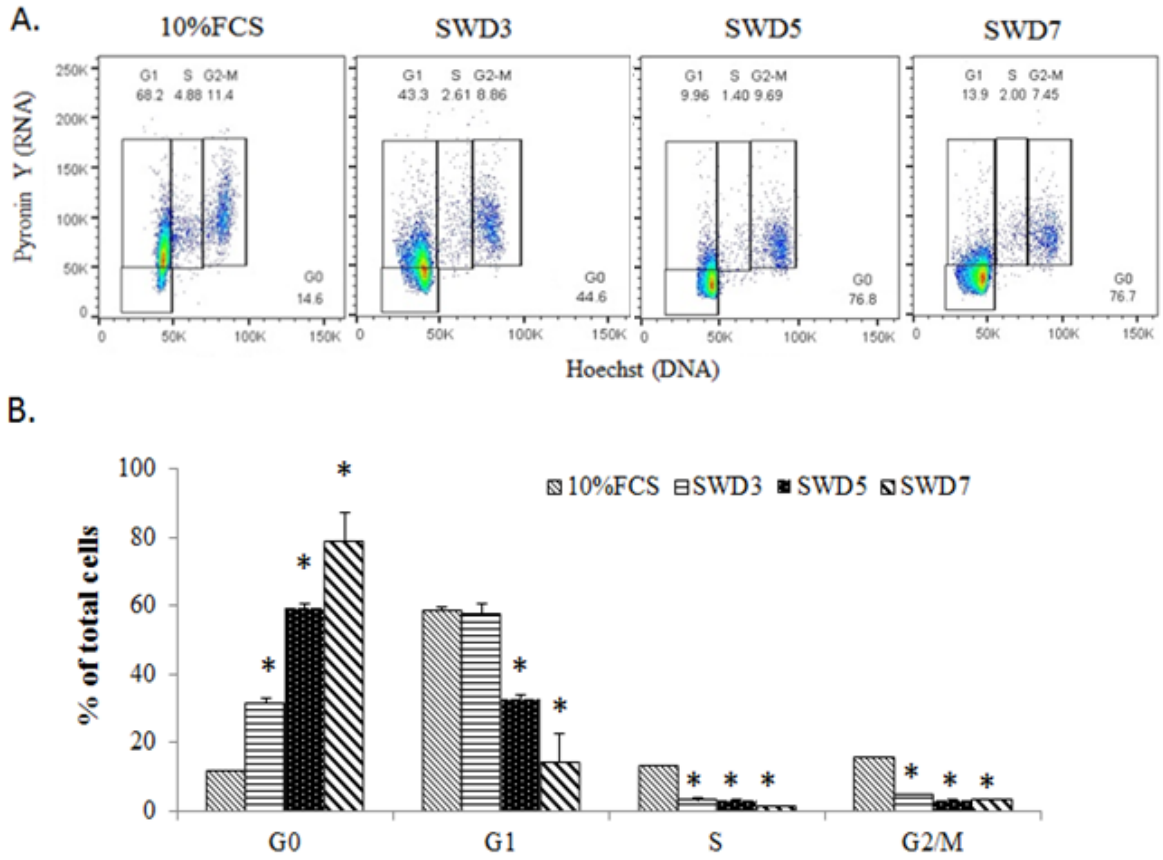


**Figure 3-9. Validation of HP double staining in C4-2B cells.**

10% FCS, C4-2B cells were grown in 10% FCS medium in T25 flasks. Cells were analysed for cell cycle distribution by HP double staining by simultaneously labelling the cells with both DNA and RNA. Boxes outline cells in $G_0$, $G_1$, S and $G_2$/M. SWD3-D5; C4-2B cells were serum-deprived in T25 flasks for up to 7 days. Thereafter, cells were collected for cell cycle analysis by using the same gating. **A.** Representative flow image in C4-2B cells. **B.** Histogram illustrates the cell cycle distribution during cell cycle exit. * $p$<0.05 vs. 10% FCS.

### 3.3.1.7. Validation of flow cytometric analysis of HP double staining by p-Rb (Ser$^{807/811}$)

It is well established that Rb is hypophosphorylated at Ser$^{807/811}$ in quiescent cells, resulting in an inhibition of cell cycle progression (Serrano *et al.*, 1993; Sherr and Roberts, 1995). To further validate the HP double staining method, PCa cells were co-stained with HP double stain and anti-p-Rb (Ser$^{807/811}$) with Alexa Fluor® 647antibody. Simultaneous incubation with anti-p-Rb (Ser$^{807/811}$) antibody demonstrated an equivalent staining pattern as Pyronin Y when compared to Hoechst staining, as shown in Figure 3-10. The low RNA content cells were indeed hypophosphorylated at Ser$^{807/811}$. Morover, the staining patterns for p-Rb (Ser$^{807/811}$) and Pyronin Y were highly correlated in all three PCa cells, further demonstrating the capability of HP double staining to accurately distinguish $G_0$ cells from $G_1$ cells (Figure 3-11).

Therefore, HP double staining was employed in subsequent studies to determine the cell cycle distribution, including quiescent cells. Additionally, 3 day contact inhibition and 7 day serum withdrawal were used to render quiescence in PCa cells for the following studies.

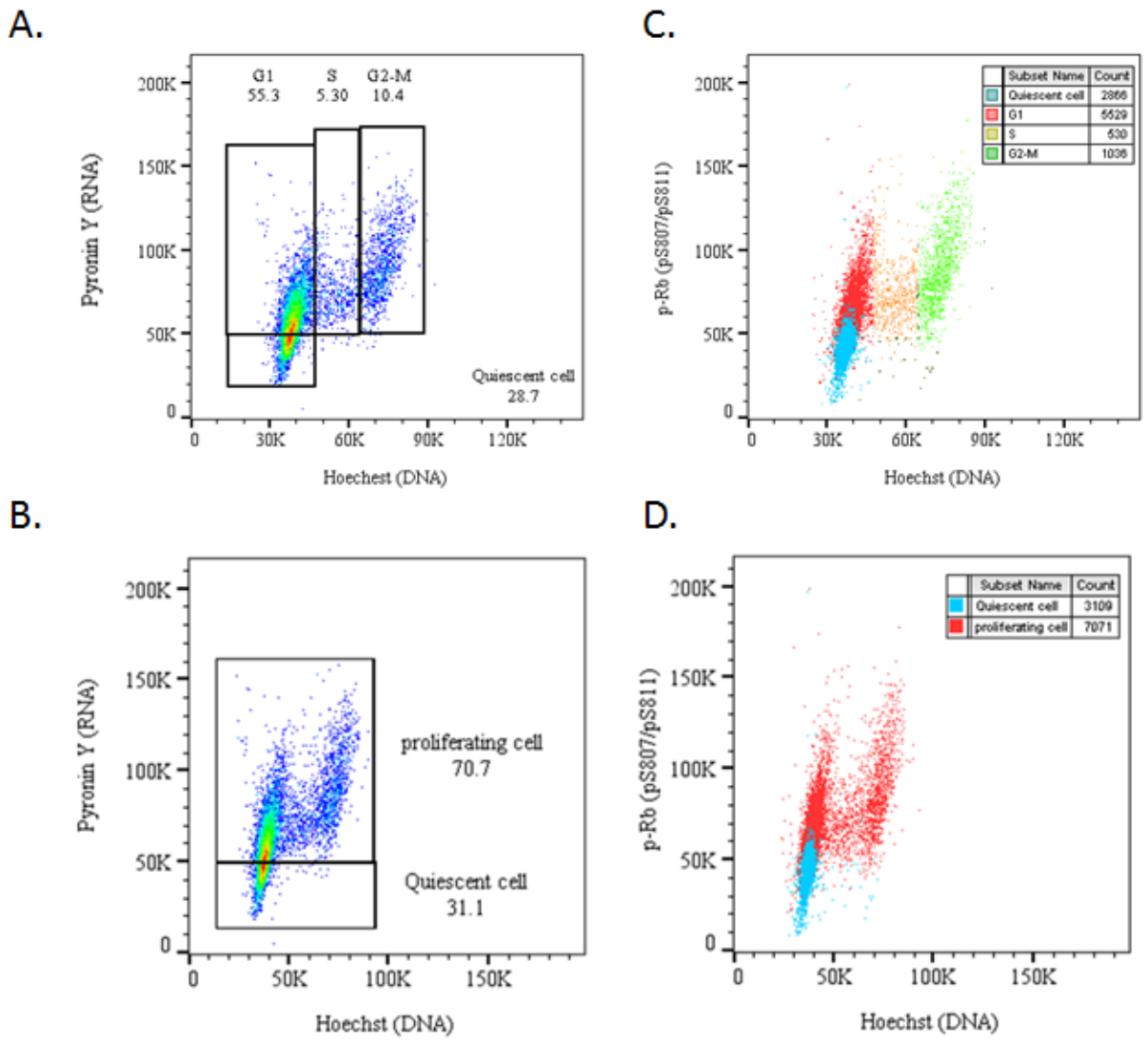


**Figure 3-10. Distribution of cell cycle in PC-3 cells.**

PC-3 cells were cultured in 10% FCS with no contact inhibition; cells were collected and fixed in 70% ethanol and kept at –20 ºC until Hoechst, Pyronin Y and p-Rb (p-Ser$^{807/811}$) with Alexa Fluor® 647 triple staining and subsequent flow cytometry. **A** and **B.** The bivariate dot pot of DNA and RNA. **A.** Boxes outline quiescent cells, and cells in $G_1$, S and $G_2$/M phases. **B.** Boxes outline proliferative cells and quiescent cells. **C** and **D.** The bivariate distribution of DNA and p-Rb **(**p-Ser$^{807/811}$). This figure was created with FlowJo. The cells gated in **A** and **B** was converted to **C** and **D** by change Pyronin Y parameter to p-Rb parameter. **C.** Cells in blue correspond to quiescent cells gated in Figure A, Red refers to $G_1$ cells, yellow refers to S phase cells and green refers to $G_2$/M cells. **D.** Cells in blue correspond to quiescent cells, whereas red refers to proliferative cells gated in Figure B.

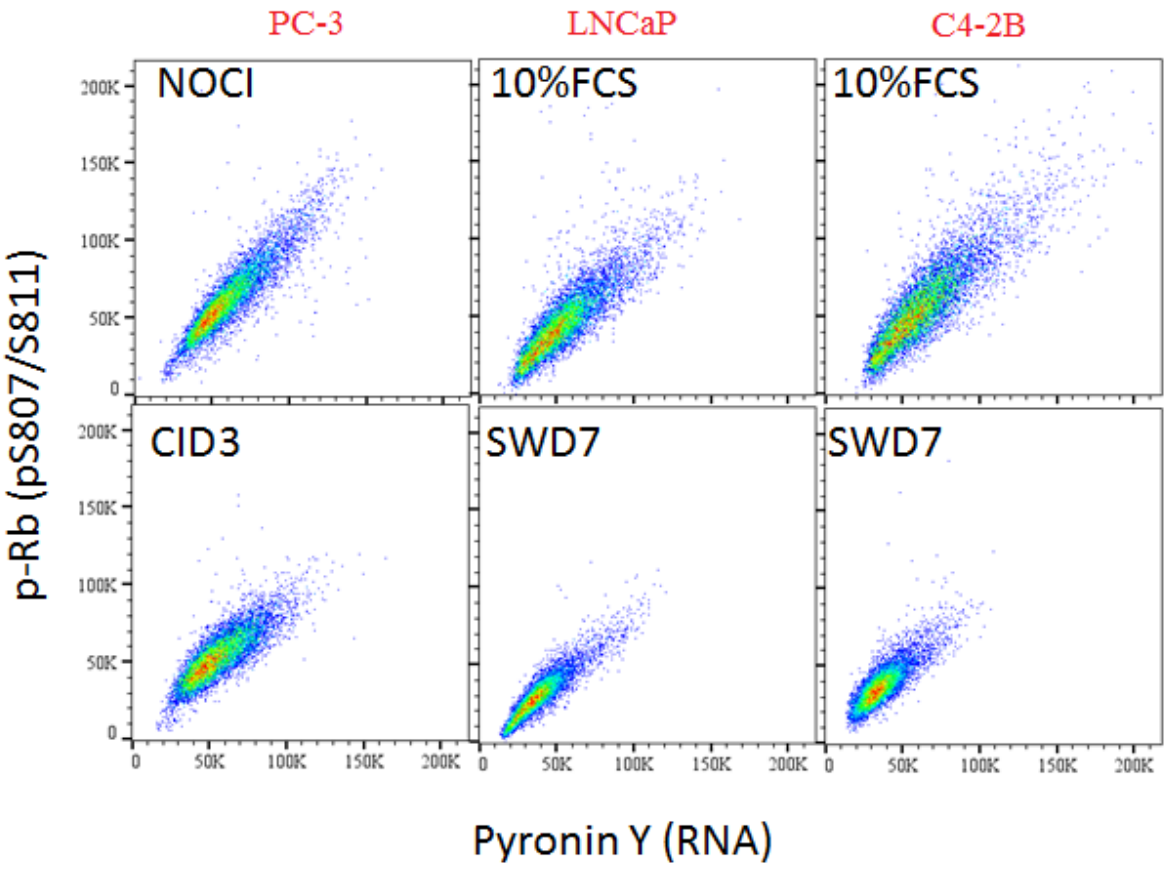


**Figure 3-11. The correlation of p-Rb (p-Ser$^{807/811}$) and Pyronin Y in prostate cancer cell lines.**

Non-synchronised and synchronised PCa cells were collected and fixed in 70% ethanol and kept at –20 ºC until Hoechst, Pyronin Y and p-Rb (p-Ser$^{807/811}$) with Alexa Fluor® 647 triple staining and subsequent flow cytometry. The image is **a** representative bivariate dot plot of p-Rb (p-Ser$^{807/811}$) and RNA in PCa cells. FCS, baseline cells with 10% FCS. SWD7, serum withdrawal for 7 days. NOCI, no contact inhibition. CID3, contact inhibition 3 days.

### 3.3.1.8. Knockdown of UBE2C increased the $G_0$ subpopulation in PC-3 cells

To determine the effect of UBE2C on PC-3 cell cycle status including the $G_0$ subpopulation, PC-3 cells were transfected with 20 nM NC or siUBE2Cs for up to 3 days and subjected to HP double staining. Upon 48 h UBE2C knocking down, the escalation in the level of quiescence became significant compared to NC ($p$<0.01). The percentage of cells in $G_0$ phase was 23% in control cells, but 36–40% after being treated siUBE2Cs (Figure 3-12). Consistently, there was a significant decrease in $G_1$ population following 24 h siUBE2Cs treatment compared to the NC ($p$<0.01). At 48 and 72 h, both the decrease in $G_0$ and increase in $G_1$ fractions reached significance compared to the NC ($p$<0.01). Depletion of UBE2C also led to $G_2$/M arrest following 3 days siUBE2C transfection ($p$<0.01). However, silencing of UBE2C did not significantly change the subpopulation of S phase cells in PC-3 cells ($p$=0.3). These results provide evidence that UBE2C-knockdown arrested PC-3 cells at $G_0$ phase of the cell cycle.

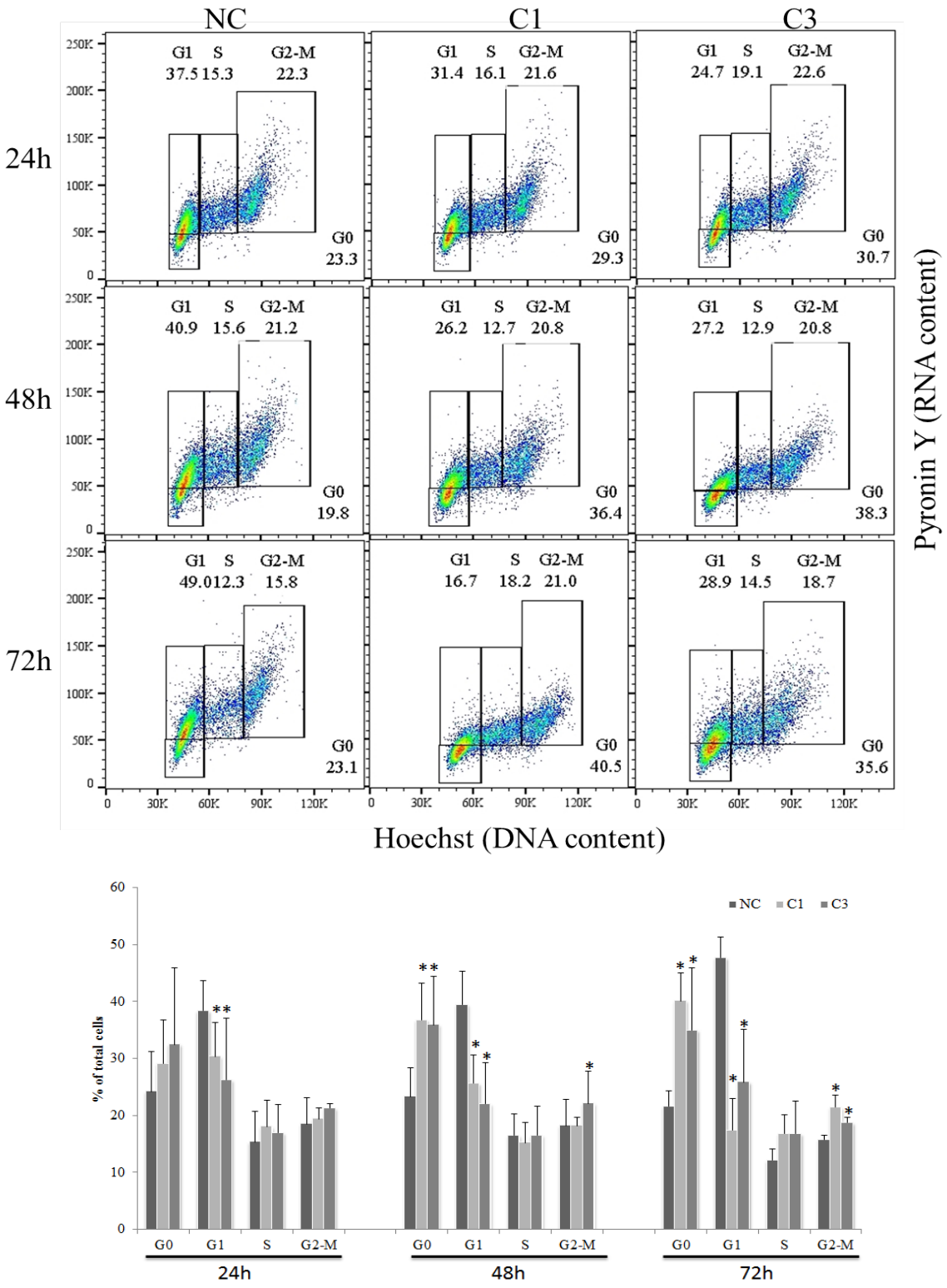


**Figure 3-12. Knockdown of UBE2C induced cell cycle exit in PC-3 cells.**

PC-3 cells were transfected with 20 nM NC, C1 or C3 in 6-well plates with a time course experiment. The cells were harvested 24, 48 and 72 h following transfection. Cells were analysed for cell cycle distribution by HP double staining by simultaneously labelling the cells with both DNA and RNA. Boxes outline cells in $G_0$, $G_1$, S and $G_2$/M. Representative flow image and quantification data of three experimental repeats. * $p$<0.05 vs. NC for each time point. This figure was created with FlowJo-V10.

### 3.3.1.9. Knockdown of UBE2C increased the $G_0$ subpopulation in LNCaP cells

To investigate the effect of UBE2C in LNCaP, cells were transfected with control or siUBE2Cs and cell cycle distribution was analysed by HP double staining. LNCaP cells displayed a significant accumulation of cells in $G_0$ at 72 h post-transfection of siUBE2Cs compared to NC ($p$<0.01). The percentage of cells in $G_0$ phase was 23% in control cells, but 43% after treatment with C1 and 48% in C3-treated cells (Figure 3-13). A significant decrease in $G_1$ population was found following 3 days siUBE2Cs treatment compared to the NC ($p$<0.01). Knockdown of UBE2C also led to a significant arrest in the $G_2$/M phase of the cell cycle after 48 and 72 h transfection. We found no effect of UBE2C knockdown on the S phase in LNCaP cells ($p$=0.7). These results indicate the loss of UBE2C led to accumulation of $G_0$ phase of the cell cycle in LNCaP cells.

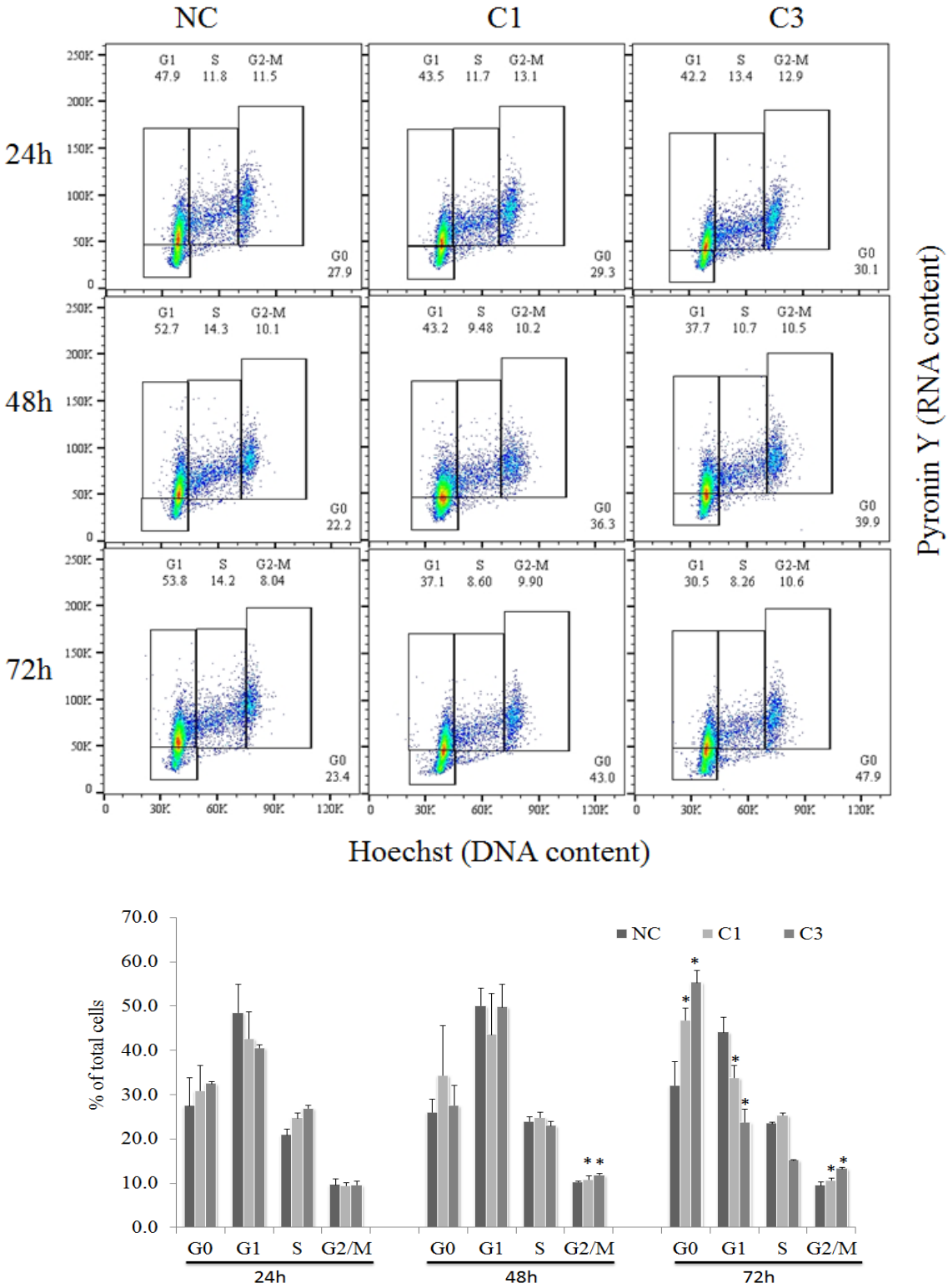


**Figure 3-13. Knockdown of UBE2C induced cell cycle exit in LNCaP cells.**

LNCaP cells were transfected with 20 nM NC, C1 or C3 in 6-well plates with a time course experiment**.** The cells were harvested 24, 48 and 72 h following transfection**.** Cells were analysed for cell cycle distribution by HP double staining by simultaneously labelling the cells with both DNA and RNA. Boxes outline cells in $G_0$, $G_1$, S and $G_2$/M. Representative flow image and quantification data of three experimental repeats. * $p$<0.05 vs. NC for each time point. This figure was created with FlowJo-V10.

### 3.3.1.10. Knockdown of UBE2C increased the $G_0$ subpopulation in C4-2B cells

To further investigate the effect of UBE2C in cell quiescence, C4-2B cells were transfected with either NC or siUBE2Cs and the distribution of $G_0$ cells was monitored by HP double staining (Figure 3-14). There was a 73% increase in population of quiescent cells upon UBE2C knockdown for 48 h compared to control cells, and the fraction of $G_0$ cells was observed to reach the maximum at 72 h (227% of control; $p<0.01$). The decrease in population of cells in $G_1$ and S phases become significant 48 h after siUBE2Cs transfection compared to control cells. In addition, knocking down UBE2C increased $G_2$/M-phase cells following 3 days siUBE2Cs treatment compared to the NC ($p<0.01$). These results indicate decrease of UBE2C promoted the accumulation of $G_0$ cells in C4-2B cells.

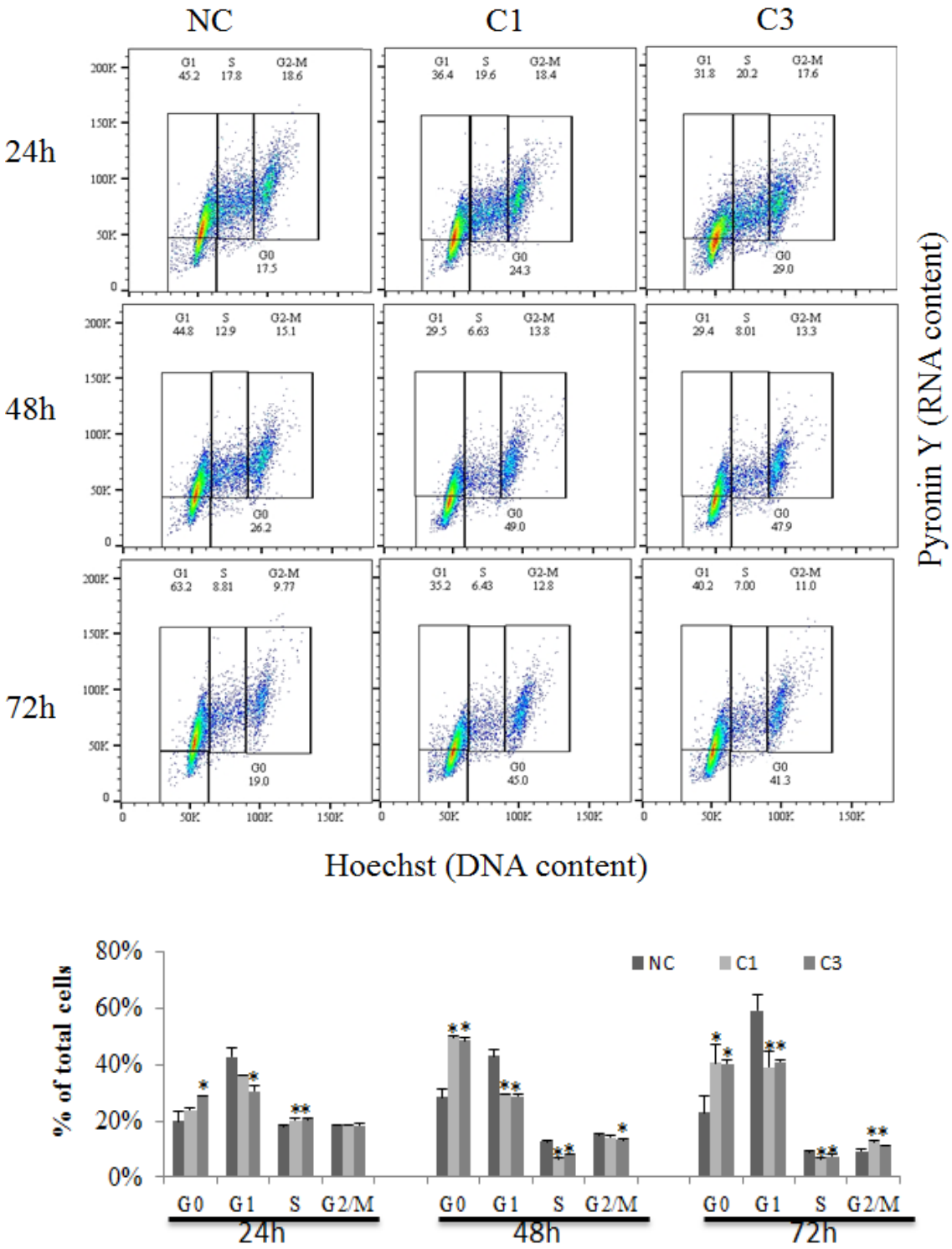


**Figure 3-14. Knockdown of UBE2C induced cell cycle exit in C4-2B cells.**

C4-2B cells were transfected with 20 nM NC, C1 or C3 in 6-well plates with a time course experiment. Cells were analysed for cell cycle distribution by HP double staining by simultaneously labelling the cells with both DNA and RNA. Boxes outline cells in $G_0$, $G_1$, S and $G_2$/M. Representative flow image and quantification data of three experimental repeats. * $p$<0.05 vs. NC for each time point. This figure was created with FlowJo-V10.

In summary, the population of quiescent $G_0$ cells was elevated by downregulation of UBE2C protein levels in all three PCa cells lines. A time line illustrating the change of UBE2C protein and the cell cycle distribution is summarised in Table 3-2.

**Table 3-2. The summary schedule for the change of UBE2C protein level relative to cell cycle distribution in LNCaP, PC-3 and C4-2B cells after siUBE2C treatment.**

| UBE2C | 24h | 48h | 72h | $G_0$ | 24h | 48h | 72h | $G_1$ | 24h | 48h | 72h | S | 24h | 48h | 72h | $G_2$/M | 24h | 48h | 72h |
|---|---|---|---|---|---|---|---|---|---|---|---|---|---|---|---|---|---|---|---|
| LNCaP | | ✓ | ✓ | | | | ✓ | | | | ✓ | | | | | | | ✓ | ✓ |
| PC-3 | ✓ | ✓ | ✓ | | | ✓ | ✓ | | ✓ | ✓ | ✓ | | | | | | | ✓ | ✓ |
| C4-2B | ✓ | ✓ | ✓ | | | ✓ | ✓ | | | ✓ | ✓ | | ✓ | ✓ | ✓ | | | ✓ | ✓ |

✓, indicates a significant change compared to NC, $p<0.05$.

## 3.3.2. Overexpression of UBE2C decreased the quiescent subpopulation in prostate cancer cells

We have shown that knockdown UBE2C increased quiescent cells. To further confirm the functional role of UBE2C in cell cycle status, UBE2C was overexpressed in PCa cells, the cell proliferation was determined by SYBR Green assay, and the cell cycle distribution was analysed by HP double staining.

### 3.3.2.1. Overexpression of UBE2C confirmed by immunoblotting

To validate the role of UBE2C overexpression on PCa cells, we first measured the level of exogenous UBE2C expression in three PCa cell lines by western blotting. The pJS55 plasmid containing UBE2C-AU1 (UBE2C) or DN UBE2C-AU1 was kindly provided by Dr JV Ruderman (Harvard Medical School, Boston, MA) (Townsley *et al.*, 1997). The UBE2C and UBE2C-DN differ by a cysteine-to-serine conversion at residue 114, which is part of the UBE2C active site. The PC-3, LNCaP C4-2B cells treated with empty vector were included as another negative control. UBE2C protein levels were increased within the first 24 h post-

transfection and reached the maximum at 48 h in PC-3 and C4-2B cells, whereas an effective increase in UBE2C protein levels was only shown 48 h post-transfection in LNCaP cells (Figure 3-15).

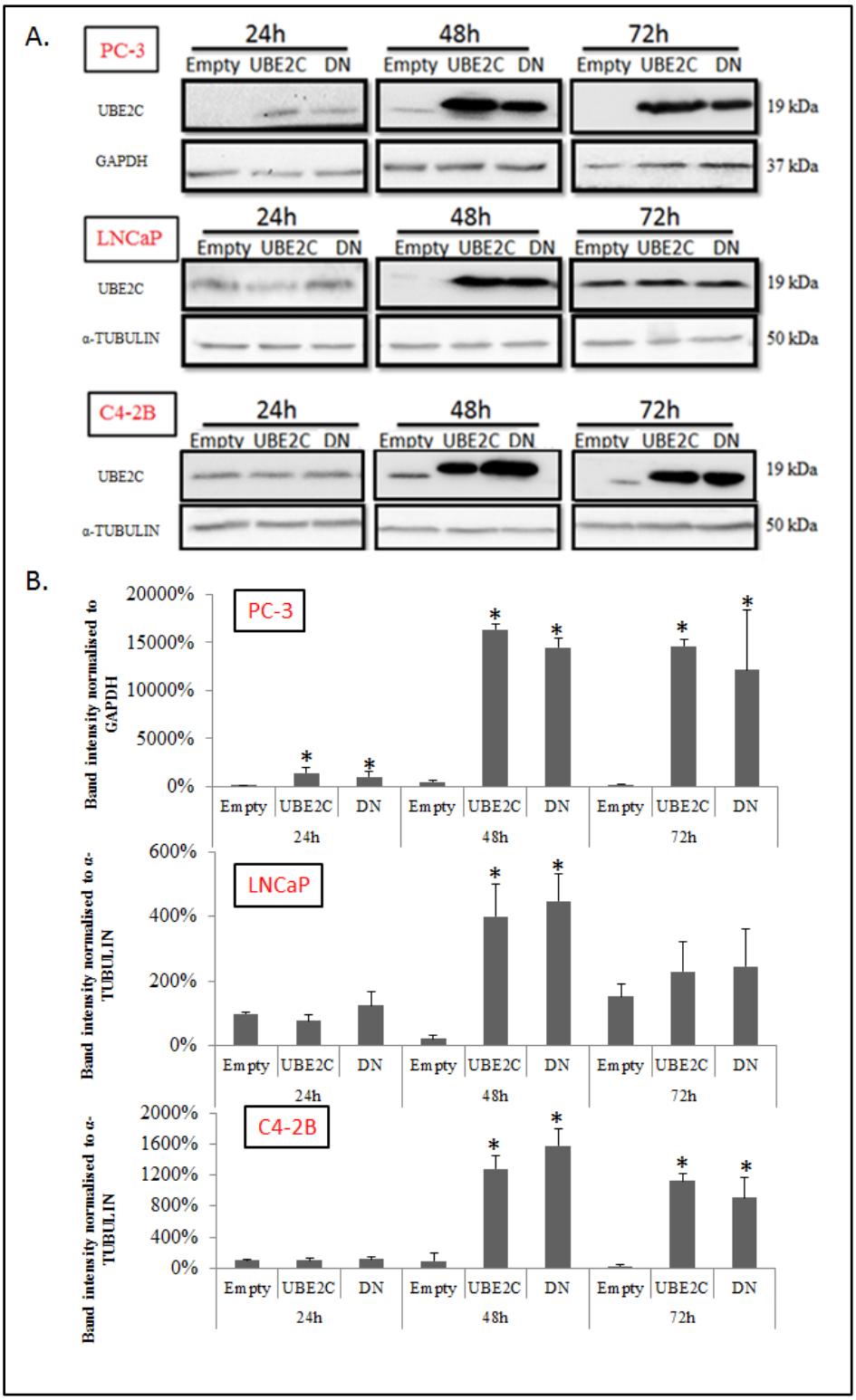


**Figure 3-15. Expression of UBE2C in prostate cancer cells by western blotting.**

Expression vector containing empty vector (Empty), UBE2C or UBE2C-DN was transfected into PCa cells. The cell culture media were replenished after 2 h following induction; cells were harvested 24, 48 and 72 h following transfection. Cells were then lysed and analysed by immunoblotting. **A.** Representative immunoblotting image in PCa cells. **B**. Histogram representing densitometric analysis are mean± SD. *, P< 0.05 versus Empty vector in each cell line. The results are representative of three experiments.

### 3.3.2.2. Upregulation of UBE2C expression promoted cell proliferation by SYBR Green assay

To determine the effect of an increase in UBE2C levels on cell proliferation, PC-3, LNCaP and C4-2B cells were transfected with empty vector, or vector containing UBE2C or UBE2C-DN, and subjected to SYBR Green assay. All three PCa cells showed a significant increase in DNA content 48 h after transfection with UBE2C vector compared with empty vector ($p$<0.05; Figure 3-16). UBE2C-DN was also included to determine if UBE2C activity is required for cell proliferation. There was no difference observed in cells cultured with plasmids containing UBE2C-DN compared to empty vector control (Figure 3-16). These observations suggest that the UBE2C active site is involved in UBE2C-mediated cell growth promotion.

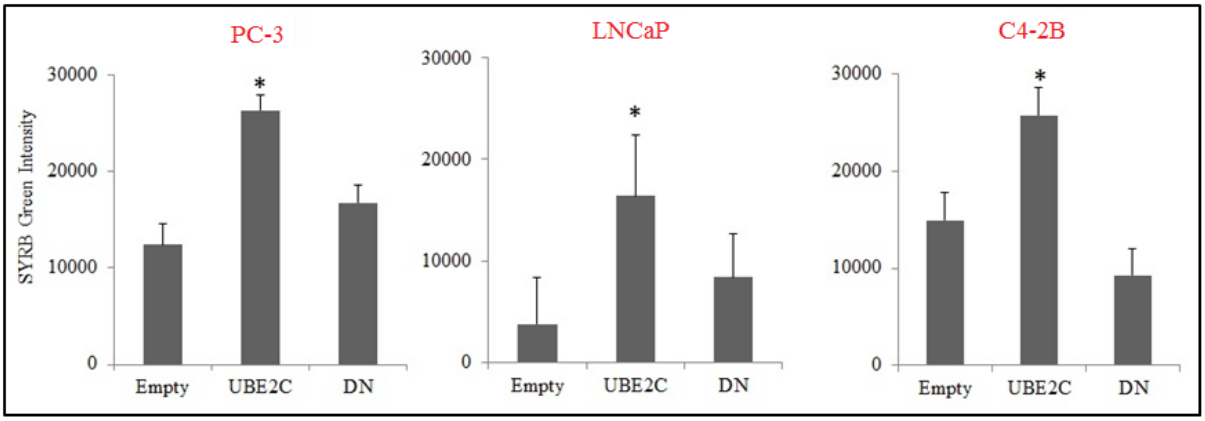


**Figure 3-16. The overexpression of UBE2C increased cell proliferation in prostate cancer cells by SYBR Green assay.**

Expression vector containing empty vector (Empty), UBE2C or UBE2C-DN was transfected into PC-3 and LNCaP cells. The cell culture media were replenished after 2 h following induction; cells were harvested 48 h following transfection. * $p$<0.05 vs. empty vector.

### 3.3.2.3. Upregulation of UBE2C expression reduced $G_0$ cell distribution in PC-3 cells by HP double staining

To measure the cell cycle progression, in particular the percentage of cells in $G_0$ phase, PC-3 cells were transfected with either empty vector, or vector containing UBE2C or UBE2C-DN, then cell cycle distribution was analysed by HP double staining (Figure 3-17). Comparing the percentage of cells in $G_0$ phase revealed overexpression of UBE2C reduced $G_0$ cells by 35–46% after 24, 48 and 72 h transfection compared to empty vector-treated cells ($p<0.05$). In addition, the $G_1$ population following UBE2C transfection was significantly raised compared to the cells cultured in the presence of empty vector ($p<0.05$). We found excess UBE2C-DN expression had no impact on the distribution of the cell cycle in PC-3 cells (Figure 3-17). Together, our observation indicates the upregulation of wild type UBE2C expression promotes cell cycle progression in PC-3 cells.

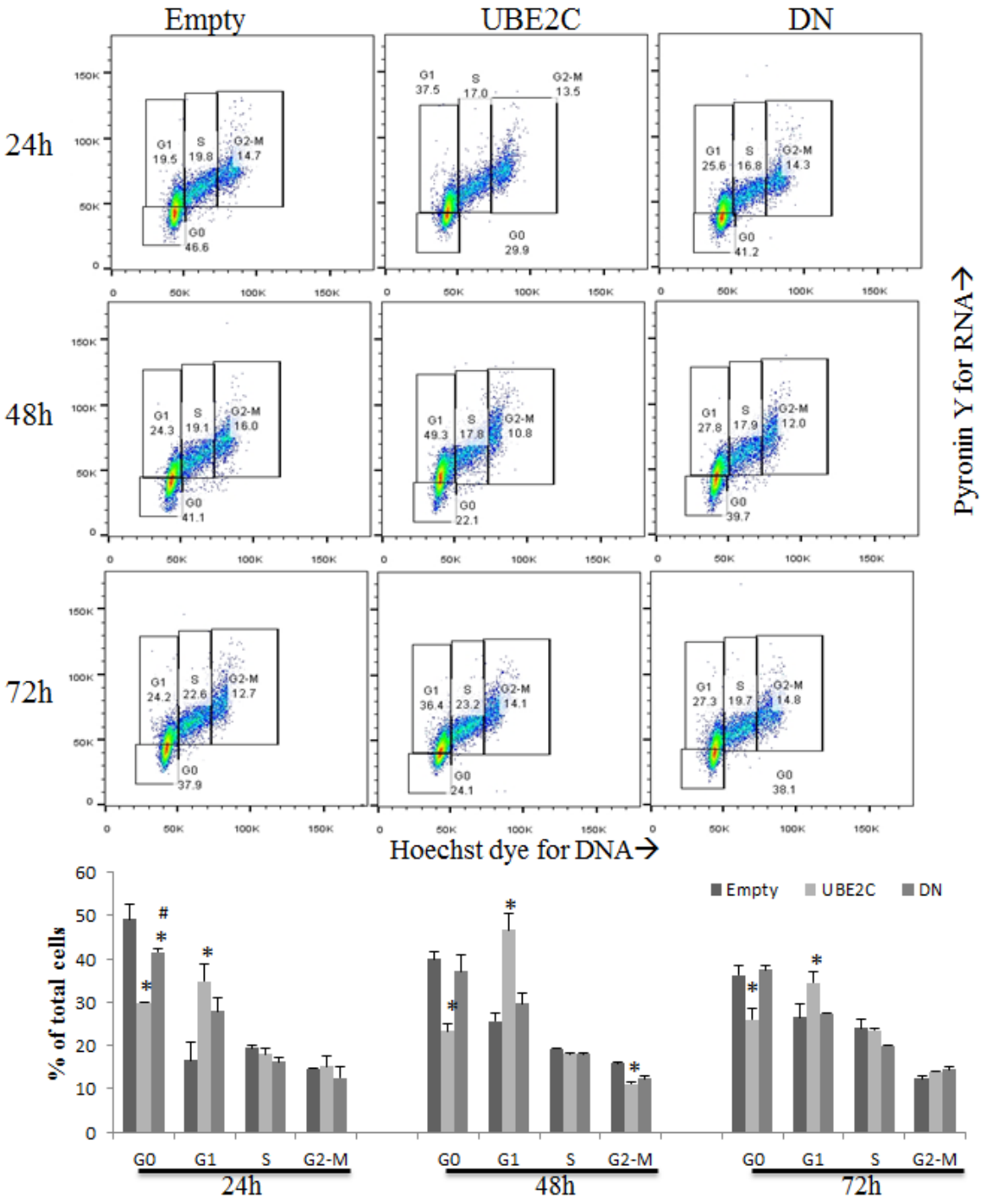


**Figure 3-17. The effect of overexpressing UBE2C on cell cycle distribution in PC-3 cells.**

Expression vector containing empty vector (Empty), UBE2C or UBE2C-DN was transfected into PC-3 cells. The cell culture media were replenished after 2 h following induction, cells were harvested 24, 48 and 72 h following transfection. For cell cycle analysis, cells were fixed in 70% ethanol and kept at –20 ºC until Hoechst and Pyronin Y staining and subsequent flow cytometry. Quantification data of three independent experiments in PC-3. * $p<0.05$ vs. empty vector. # $p<0.05$ vs. wild type UBE2C transfected sample.

### 3.3.2.4. Upregulation of UBE2C reduced $G_0$ cell distribution in LNCaP cells by HP double staining

To examine whether the overexpression of UBE2C regulated $G_0$ cell distribution, LNCaP cells were co-stained with HP and subjected to flow analysis. Similar to PC-3 cells, overexpression of UBE2C in LNCaP cells decreased the subpopulation of $G_0$ cells compared to the cells treated with empty vector ($p<0.01$; Figure 3-18). Moreover, LNCaP showed a higher fraction of $G_1$ and S phase cells after 48 h transfection. We found excess UBE2C-DN expression had no impact on the distribution of the cell cycle in LNCaP cells. However, the percentage of cells in $G_2$/M phase was slightly escalated with excess expression of UBE2C and UBE2C-DN ($p<0.05$). Collectively, these results suggesting that the amplification of wild type UBE2C promoted cell cycle progression in LNCaP cells.

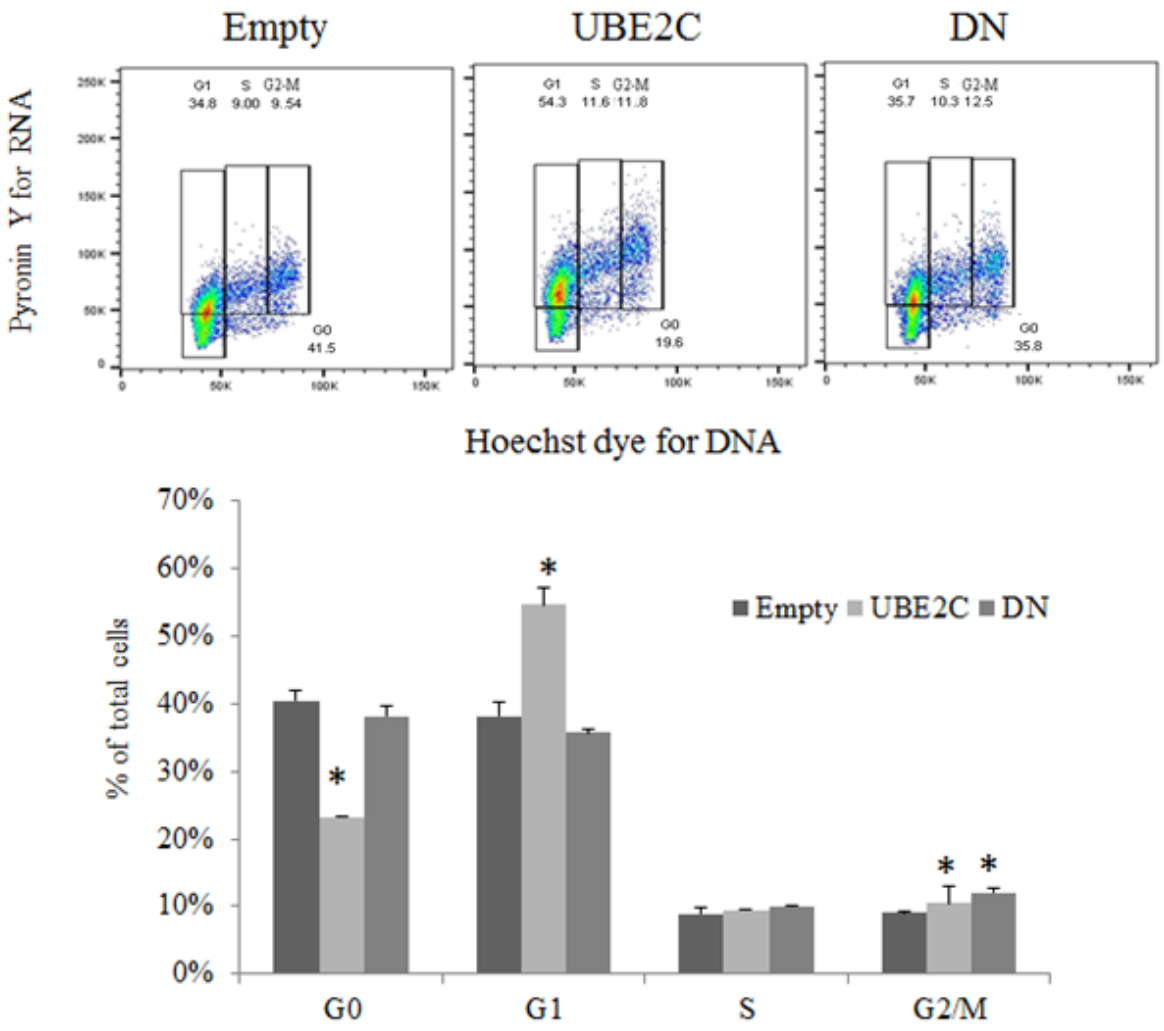


**Figure 3-18. The effect of UBE2C vector on the proportion of cells in $G_0$ in LNCaP cells.**

Expression vector was transfected into LNCaP cells. The cell culture media were replenished after 2 h following induction; cells were harvested 48 h following transfection. For cell cycle analysis, cells were fixed in 70% ethanol and kept at –20 ºC until HP staining and subsequent flow cytometry. Representative flow image and quantification data of three independent experiments in LNCaP cells. * $p$<0.05 vs. empty vector. Empty, empty vector. DN, vector containing UBE2C-DN.

### 3.3.2.5. High expression of UBE2C reduced $G_0$ cell distribution in C4-2B cells by HP double staining

To determine whether the upregulation of UBE2C regulated $G_0$ cell distribution in PCa cells, C4-2B cells were co-stained with HP and analysed by cell cycle analysis. Comparing the percentage of cells in $G_0$ phase revealed overexpressing UBE2C in C4-2B cells reduced $G_0$ cells by approximately 20–30% after 48 and 72 h transfection compared to empty vector-treated cells ($p<0.05$; Figure 3-19). Furthermore, C4-2B cells showed a higher fraction of $G_1$ after 48 h transfection. We found UBE2C-DN expression had no significant impact on the distribution of the cell cycle in C4-2B cells. Collectively, these results suggesting that the amplification of wild type UBE2C promoted cell cycle progression in C4-2B cells.

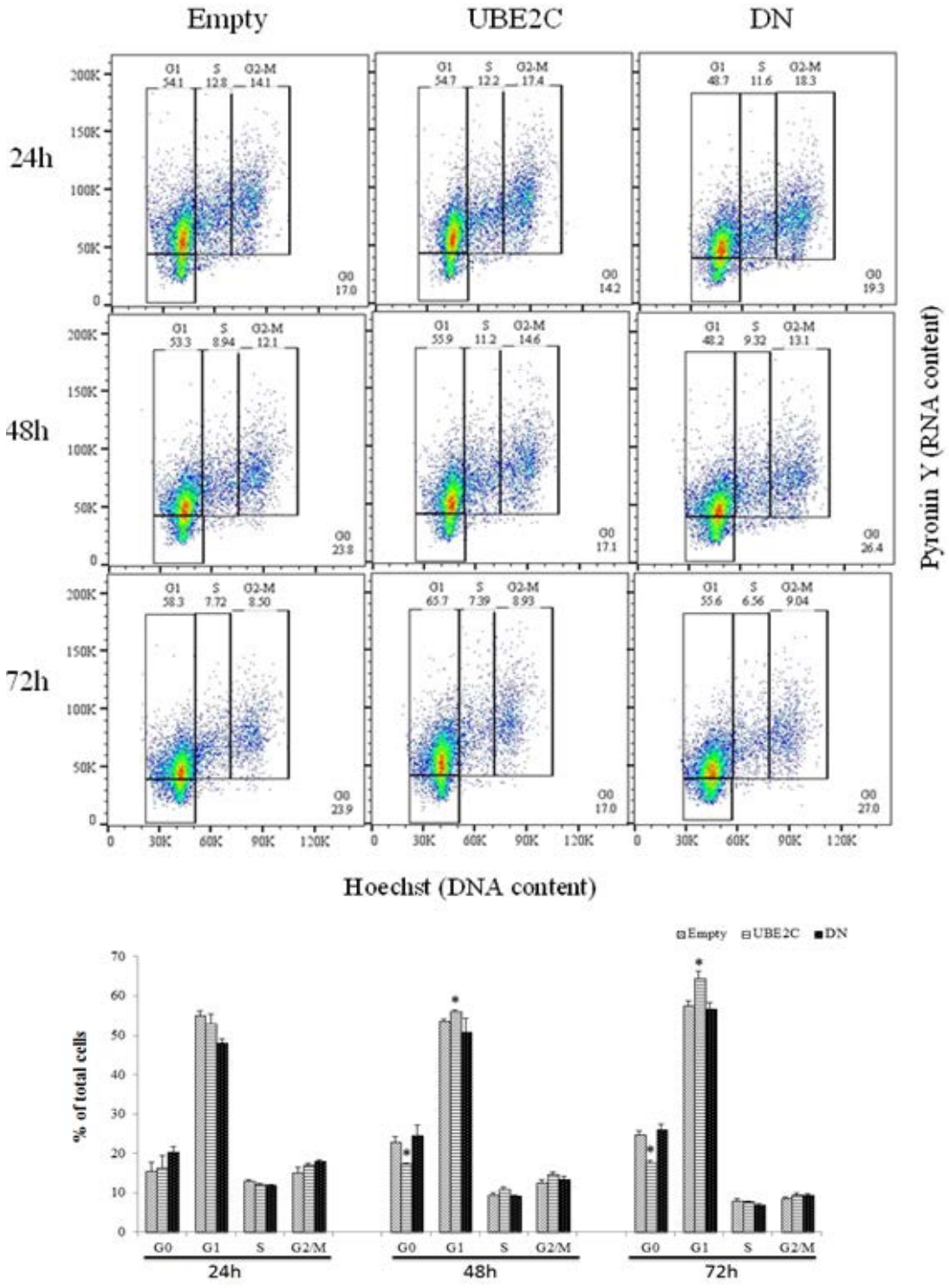


**Figure 3-19. The effect of overexpressing UBE2C on cell cycle distribution in C4-2B cells.**

Expression vector containing empty vector (Empty), UBE2C or UBE2C-DN was transfected into C4-2B cells. The cell culture media were replenished after 2 h following induction, cells were harvested 24, 48 and 72 h following transfection. For cell cycle analysis, cells were fixed in 70% ethanol and kept at –20 ºC until Hoechst and Pyronin Y staining and subsequent flow cytometry. Quantification data of three independent experiments in PC-3. * $p<0.05$ vs. empty vector. # $p<0.05$ vs. wild type UBE2C transfected sample.

## 3.3.3. Overexpression of UBE2C impeded cell cycle exit in prostate cancer cells

### 3.3.3.1. UBE2C protein levels are reduced during cell cycle exit

As noted above, the expression of UBE2C appears to be correlated to the proportion of quiescent and proliferating cells in PCa cells. To verify the presence of this correlation between UBE2C expression and in-cell cycle progression, we then examined the UBE2C level in PCa cells during cell cycle exit. The experimental quiescence of three PCa cell lines was achieved and verified in Figure 3-7-Figure 3-9. The decline of UBE2C protein was started at day 1 after contact inhibition or serum withdrawal for each of the cell lines. Further decrease of UBE2C was found in a time-dependent manner. To diminish UBE2C into an undetectable level in LNCaP and C4-2B cells required 5 days serum deprivation, whereas 3 days contact inhibition was not able to reduce UBE2C level completely in PC-3 (Figure 3-20). The timeframe required to enrich quiescent cells and the corresponding UBE2C level during cell cycle exit in PCa cells is summarised in Table 3-3.

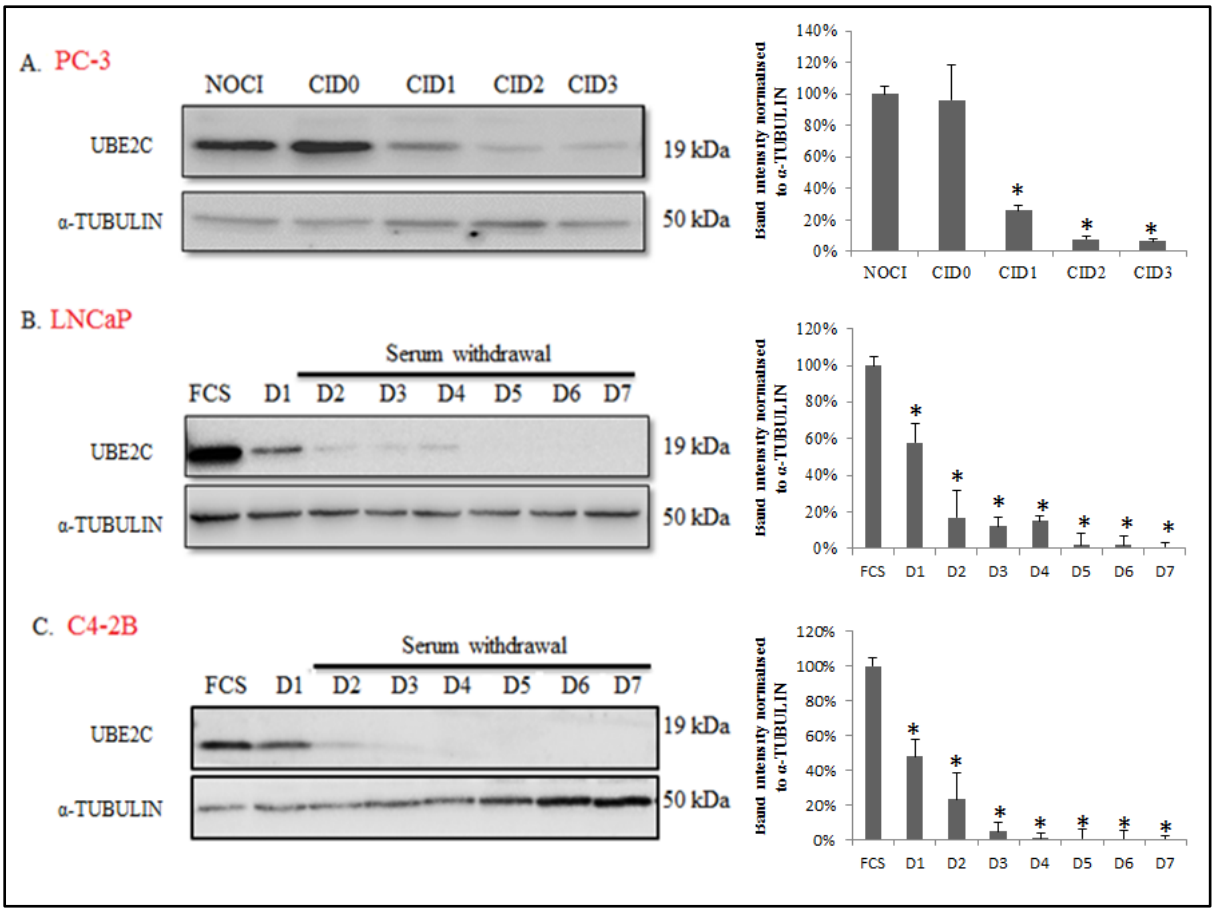


**Figure 3-20. The expression of UBE2C protein during cell cycle exit.**

**A**. PC-3 cells were rendered to quiescent status by 3 day contact inhibition. **B**. LNCaP and **C**. C4-2B cells were made quiescent by 7 day serum withdrawal. Levels of UBE2C protein in PC-3, LNCaP and C4-2B cells were examined by western blot analysis. α-TUBULIN expression was determined as a control to assure equal protein loading. NOCI, no contact inhibition. CID3, contact inhibition 3 days. FCS, baseline cells with 10% FCS. D1–7, day 1–7 with serum withdrawal. The results are representative of three experiments. **Left**. Representative immunoblotting image in PCa cells. **Right.** Histogram representing densitometric analysis are mean± SD. *, P< 0.05 versus NOCI or FCS in each cell line. The results are representative of three experiments.

**Table 3-3. The timeframe required for enriching quiescent cells and the corresponding UBE2C level during cell cycle exit in prostate cancer cells.**

| **Re-entry** | UBE2C level by Western blot | **D1** | **D2** | **D3** | **D5** | **D7** | Change in $G_0$ fraction by flow cytometry | **D1** | **D2** | **D3** | **D5** | **D7** |
|---|---|---|---|---|---|---|---|---|---|---|---|---|
| PC-3 | | ↓ | ↓↓ | ↓↓↓ | | | | ↑ | ↑↑ | ↑↑↑ | | |
| LNCaP | | ↓ | ↓↓ | ↓↓ | ↓↓↓ | ↓↓↓ | | | | ↑ | ↑↑ | ↑↑ |
| C4-2B | | ↓ | ↓↓ | ↓↓ | ↓↓↓ | ↓↓↓ | | | | ↑ | ↑↑ | ↑↑↑ |

↓, a decrease occurred. ↑, an increase occurred. The number of arrows indicates the level of change. D1–7, time following contact inhibition or serum starvation.

### 3.3.3.2. Overexpression of UBE2C impeded cell cycle exit in PC-3 cells

Based on the study described above, the UBE2C level is decreased during cell cycle exit. However, whether the decreased UBE2C protein level is a cause or a merely a reflection of cell cycle status was unknown. To investigate the effects of UBE2C on cell cycle progression, we first transfected PC-3 cells with either empty, UBE2C or UBE2C-DN vector. Next, these transfected PC-3 cells were induced to quiescence by maintaining 100% confluency for indicated time intervals (Figure 3-21). Cells were then subjected to HP double staining and subsequent flow cytometric analysis. Upon contact inhibition, the fraction of $G_0$ cells was increased in a time-dependent manner in all cells. But, the increase in the fraction of $G_0$ in UBE2C-transfected cells was less than that in empty and UBE2C-DN treated PC-3cells, suggesting the high expression of UBE2C significantly delayed cell cycle exit of PC-3 cells. It is interesting to note that there was a significant increase in the percentage of cells in $G_2$/M in UBE2C-DN transfected cells compared with empty or UBE2C-treated cells.

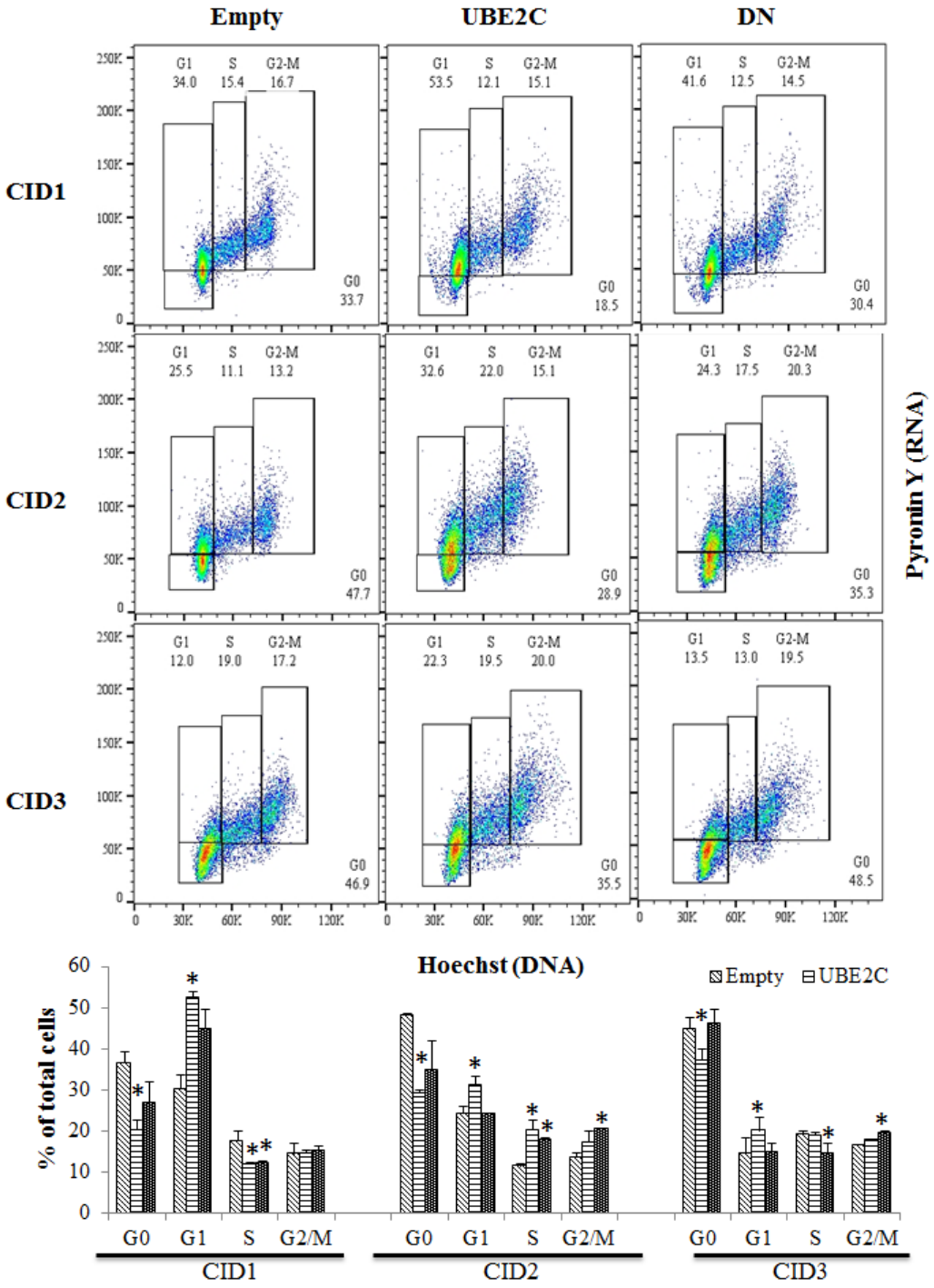


**Figure 3-21. Distribution of cell cycles in UBE2C-overexpressing PC-3 cells during cell cycle exit.**

PC-3 cells were first transfected with expression vectors. The cell culture media were replenished after 2 h following induction and seeded into T25 flasks for another 22 h to allow attachment and contact inhibition. Thereafter, cells synchronised by contact inhibition for times indicated. Cells were then harvested, fixed in 70% ethanol and kept at –20 ºC until HP double staining and subsequent flow cytometry. Representative flow image and quantification data of three independent experiments in PC-3 cells. * $p<0.05$ vs. empty vector. Empty, empty vector. DN, vector containing UBE2C-DN. CID1–3, contact inhibition 1–3 days.

#### 3.3.3.3. Overexpression of UBE2C impeded cell cycle exit in LNCaP cells

To confirm the effects of UBE2C on cell cycle progression in another PCa cell line, the relationship of UBE2C and cell cycle exit was also tested in LNCaP cells. LNCaP cells were first transfected with expression vector; serum was removed 24 h post-transfection. Due to the limitation of the sensitivity of LNCaP to expression vector, LNCaP cells were induced to quiescence by serum starvation for only 1 day. The UBE2C overexpressed LNCaP cells showed less cells in quiescence compared with the cells transfected with empty vector and UBE2C-DN (Figure 3-22). The percentage of cells in $G_0$ phase was 8% in UBE2C overexpressed LNCaP cells, whereas 20% in both empty vector and UBE2C-DN treated cells.

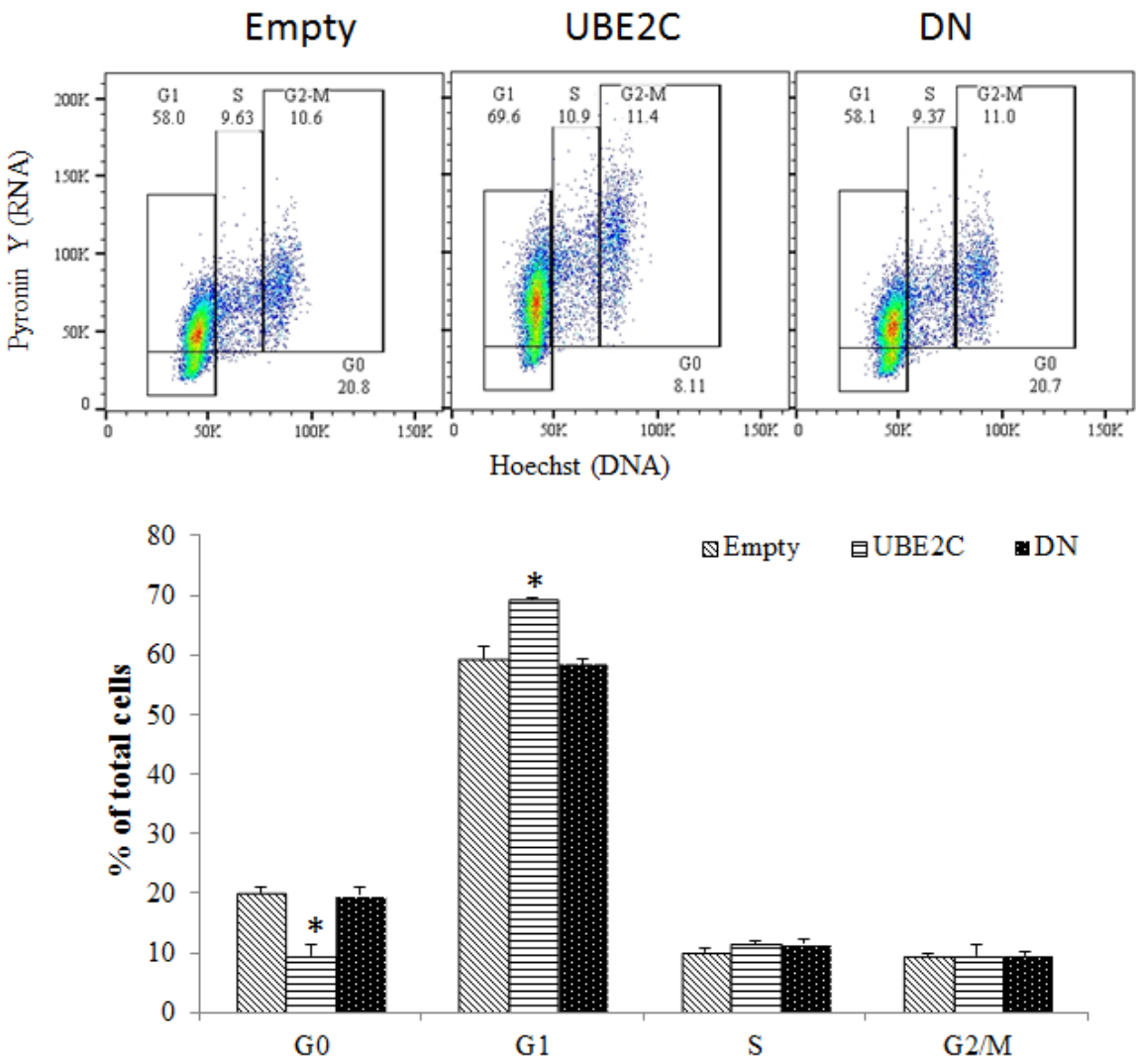


**Figure 3-22. Distribution of cell cycles in serum-starved LNCaP cells with UBE2C overexpression.**

LNCaP cells were first transfected with expression vectors. The cell culture media were replenished after 2 h following induction and seeded into T25 flasks for another 22 h to allow attachment. Thereafter, cells were serum-deprived for another 24 h. Cells were then harvested, fixed in 70% ethanol and kept at –20 ºC until HP staining and subsequent flow cytometry. Representative flow image and quantification data of three independent experiments in LNCaP cells. * $p$<0.05 vs. empty vector. Empty, empty vector. DN, vector containing UBE2C-DN.

### 3.3.3.4. Overexpression of UBE2C impeded cell cycle exit in C4-2B cells

To confirm the cellular effects of UBE2C on cell cycle exit, cell cycle distribution of UBE2C overexpressed C4-2B cells were also tested. C4-2B cells were first transfected with expression plasmid; and then serum was removed 24 h post-transfection. Thereafter, C4-2B cells were induced to quiescence by serum withdrawal for up to 3 days (Figure 3-23). Cells were then subjected to HP double staining and subsequent flow cytometric analysis. During cell cycle exit, the fraction of $G_0$ cells was increased in a time-dependent manner. However, the increase in the fraction of $G_0$ in UBE2C-transfected cells was less than that in empty and UBE2C-DN treated C4-2B cells. After 3 days serum starvation, the proportion of quiescent cells increased to 80% in empty vector or UBE2C-DN transfected control cells, whereas only 67% in UBE2C-overexpressing C4-2B cells, suggesting the high expression of UBE2C significantly postponed cell cycle exit of C4-2B cells. Therefore, overexpression of UBE2C delayed cell cycle exit in PCa cells.

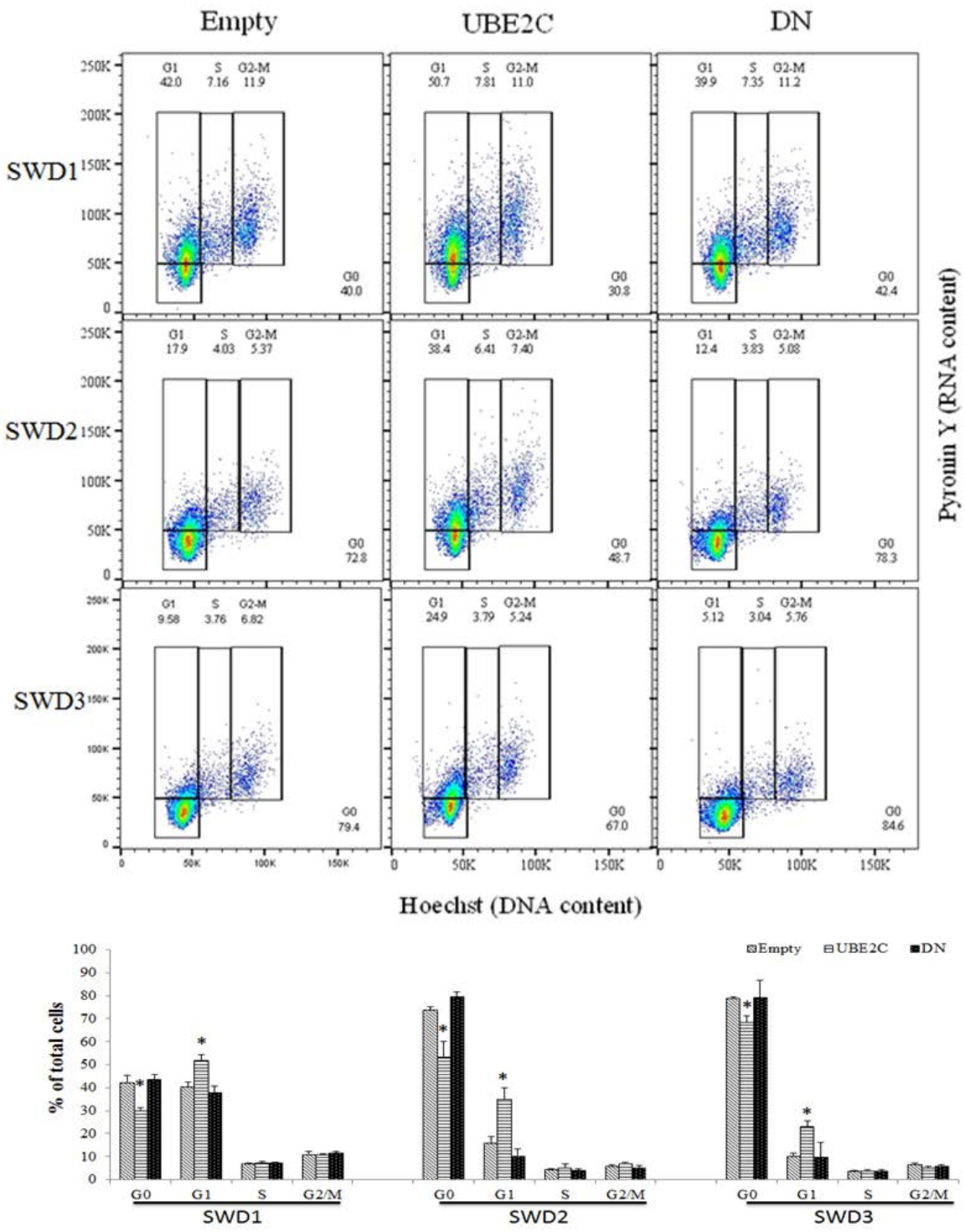


**Figure 3-23. Distribution of cell cycles in UBE2C-overexpressing C4-2B cells during cell cycle exit.**

C4-2B cells were first transfected with expression vectors. The cell culture media were replenished after 2 h following induction and seeded into T25 flasks for another 22 h to allow attachment and then serum withdrawal for up to 3 days. Cells were then harvested, fixed in 70% ethanol and kept at –20 ºC until HP double staining and subsequent flow cytometry. Representative flow image and quantification data of three independent experiments in C4-2B cells. * $p<0.05$ vs. empty vector. Empty, empty vector. DN, UBE2C-DN. SRD1–3, serum replenished (SR) 1–3 days.

## 3.3.4. Knockdown of UBE2C impeded cell cycle re-entry

Following the revelation that overexpression of UBE2C delayed cell cycle exit in PCa cells, we next addressed the question of whether knockdown of UBE2C can delay the cell cycle re-entry. PCa cells were induced to quiescence and then transfected with siUBE2Cs at the time when the cells were released from the quiescence. The cell cycle distributions of PCa cells were determined by HP double staining. Moreover, the concordance between UBE2C protein levels and cell cycle progression were also determined.

### 3.3.4.1. Validation of cell cycle re-entry by HP double staining

To validate if the quiescent cells re-enter the cell cycle, PC-3, LNCaP and C4-2B cells were first induced to experimental quiescence. The $G_0$ arrested PC-3 cells were re-plated at lower density for 3 days to achieve cell cycle re-entry (RPD1–3). During the period of cell cycle re-entry, the percentage of quiescent cells decreased by 55% in RPD3 PC-3 cells compared with CID3 samples (Figure 3-24). In LNCaP and C4-2B cells, cell cycle re-entry was rendered by restoration of serum to serum-deprived cells for a period of 7 days (SRD1–7). Upon release from quiescence, quiescent LNCaP and C4-2B cells re-entered the cell cycle, as a significant decrease of $G_0$ cells was observed for both LNCaP cells (76.5% to 27.6%) and C4-2B cells (87.8% to 19.4%; Figure 3-25 & Figure 3-26).

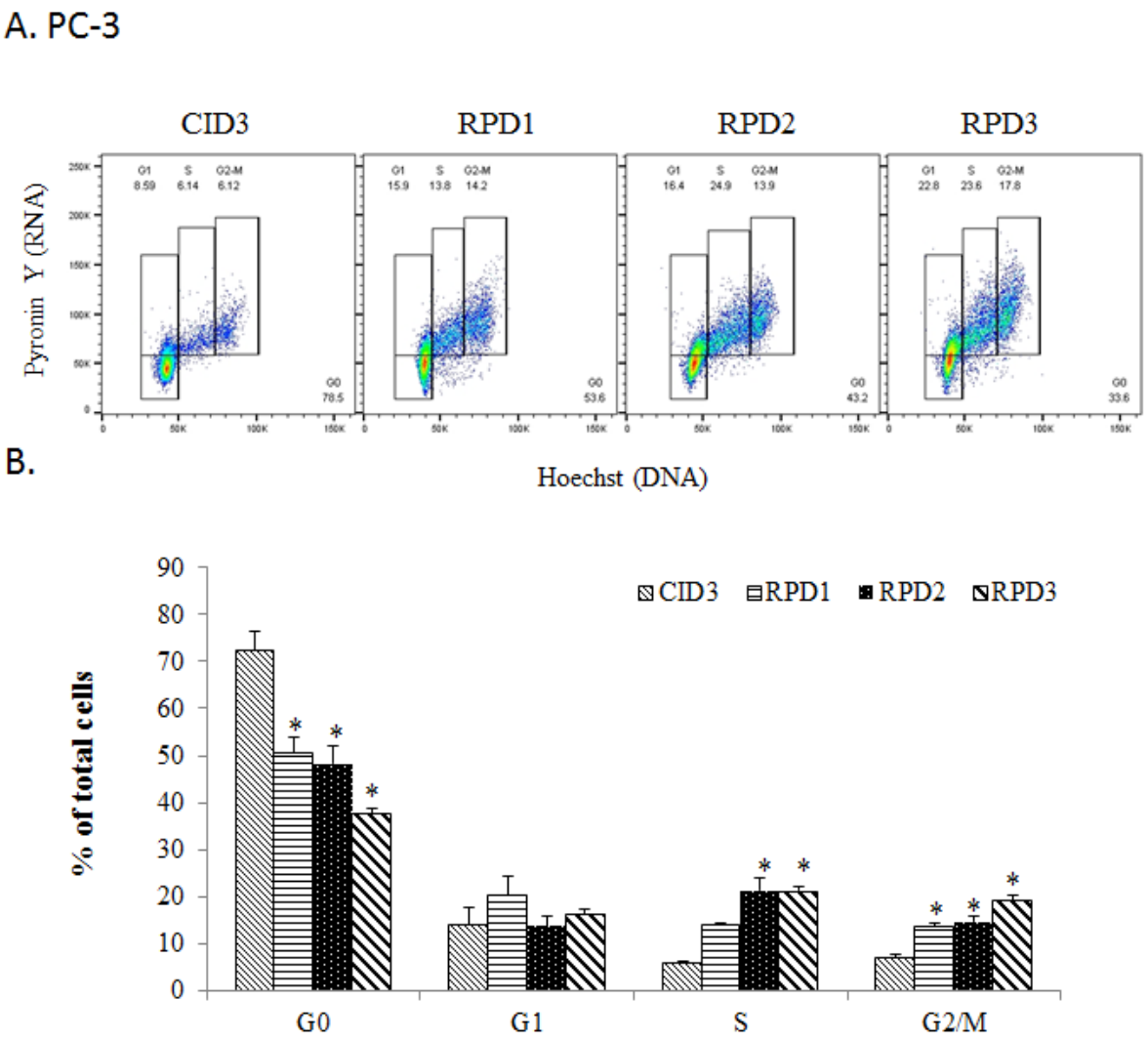


**Figure 3-24. Distribution of cell cycles in PC-3 cells during cell cycle re-entry.**

CID3: PC-3 cells were synchronised to $G_0$ by contact inhibition in T25 flasks for 3 days. Thereafter, cells were collected for cell cycle analysis using HP double staining. Boxes outline cells in $G_0$, $G_1$, S and $G_2$/M. RPD1–3; quiescent PC-3 cells were re-plated at lower density to allow cell re-entry to the cell cycle. The cell cycle distribution was analysed using the same gating. **A.** Representative flow image in PC-3 cells. **B.** Histogram illustrates the cell cycle distribution during cell cycle re-entry. * $p$<0.05 vs. CID3.

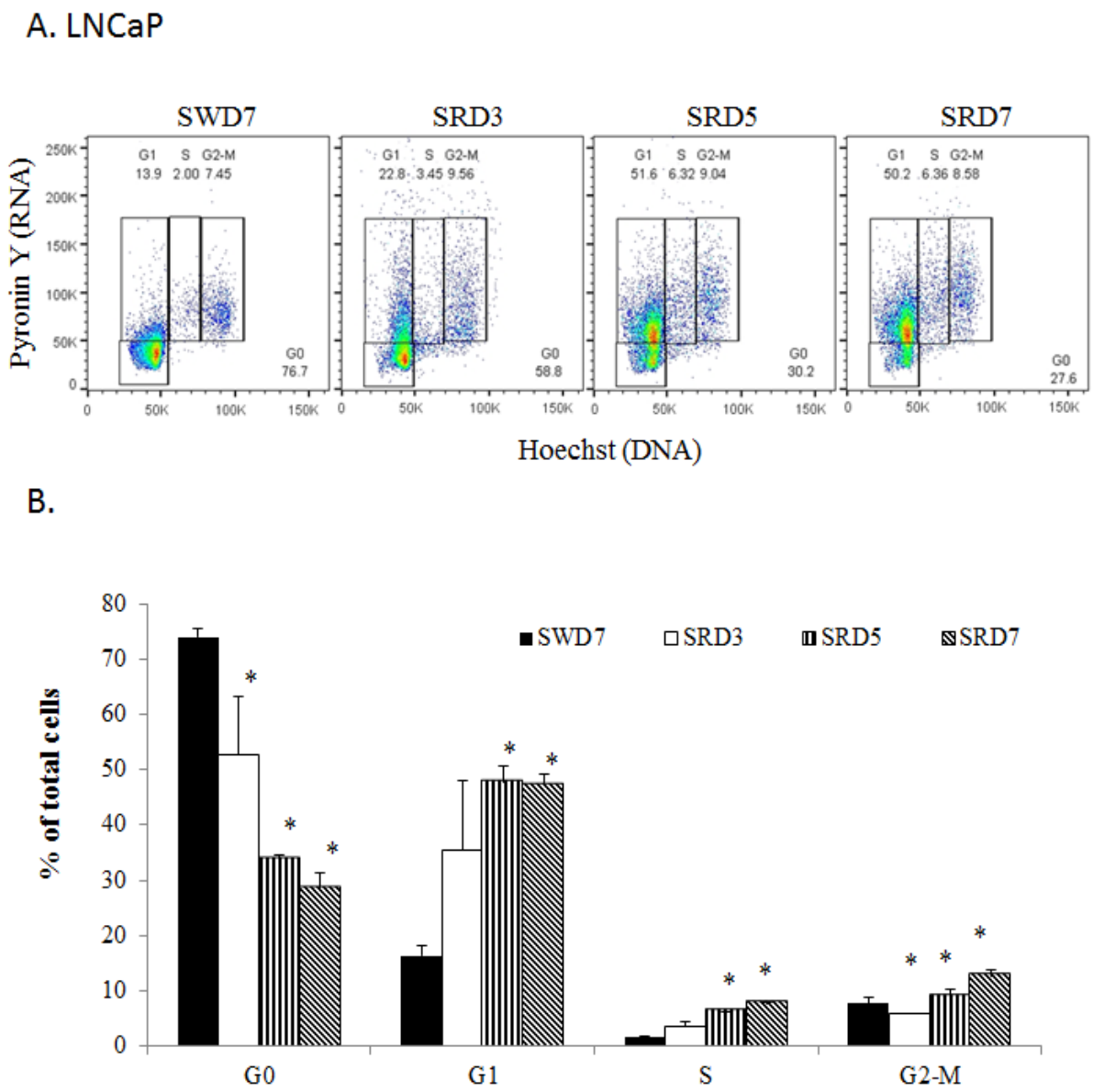


**Figure 3-25. Distribution of cell cycles in LNCaP cells during cell cycle re-entry.**

SWD7: LNCaP cells were synchronised to $G_0$ by serum deprivation in T25 flasks for 7 days. Thereafter, cells were collected for cell cycle analysis using HP double staining. SRD3-D7, cell cycle re-entry was rendered by restoration of serum to serum-deprived cells for up to 7 days. The cell cycle distribution was analysed using the same gating.
**A.** Representative flow image in LNCaP cells. **B.** Histogram illustrates the cell cycle distribution during cell cycle re-entry. * $p<0.05$ vs. SWD7.

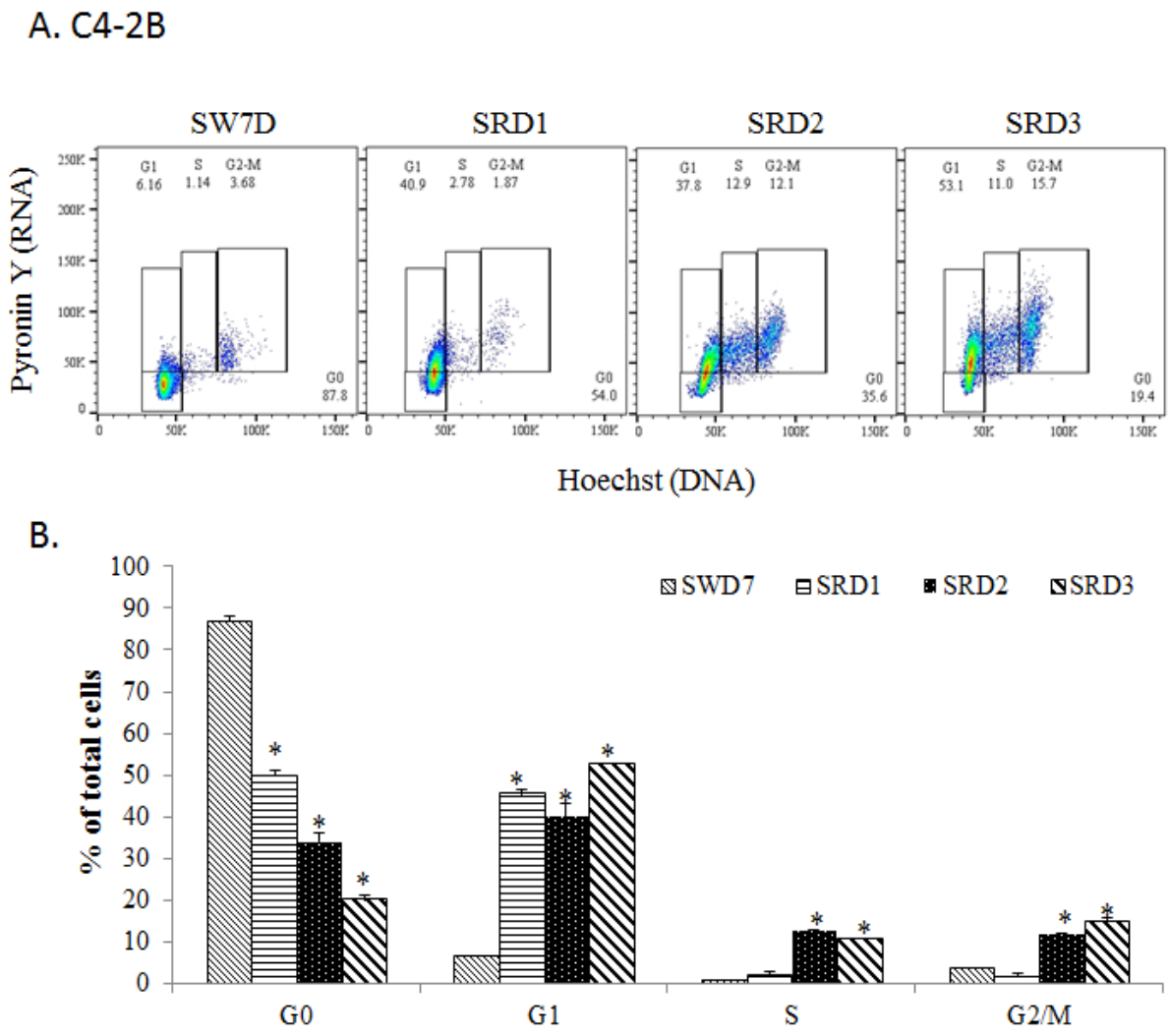


**Figure 3-26 Distribution of cell cycles in C4-2B cells during cell cycle re-entry.**

SWD7: C4-2B cells were synchronised to $G_0$ by serum deprivation in T25 flasks for 7 days. Thereafter, cells were collected for cell cycle analysis using HP double staining. SRD3-D7, cell cycle re-entry was rendered by restoration of serum to serum-deprived cells for up to 7 days. The cell cycle distribution was analysed using the same gating. **A.** Representative flow image in C4-2B cells. **B.** Histogram illustrates the cell cycle distribution during cell cycle re-entry. * $p<0.05$ vs. SWD7.

### 3.3.4.2. UBE2C protein levels are increased during cell cycle re-entry

To determine the correlation of UBE2C protein level and cell cycle status, immunoblotting was performed to detect the change of UBE2C during cell cycle re-entry. Upon cell cycle re-entry, a marked increase of UBE2C protein levels was detected during cell cycle re-entry in PC-3, LNCaP and C4-2B cells (Figure 3-27). Consistent with our flow results shown above, which showed that the cells re-enter the cell cycle progressively after release, UBE2C protein levels increased gradually during cell cycle re-entry in a time-dependent manner. Thus, the UBE2C protein level is suggested to be positively correlated to the transition of quiescent to proliferating cells in PCa cells. The timeframe required for a PCa cell to re-enter the cell cycle and its corresponding UBE2C protein level is summarised in Table 3-4.

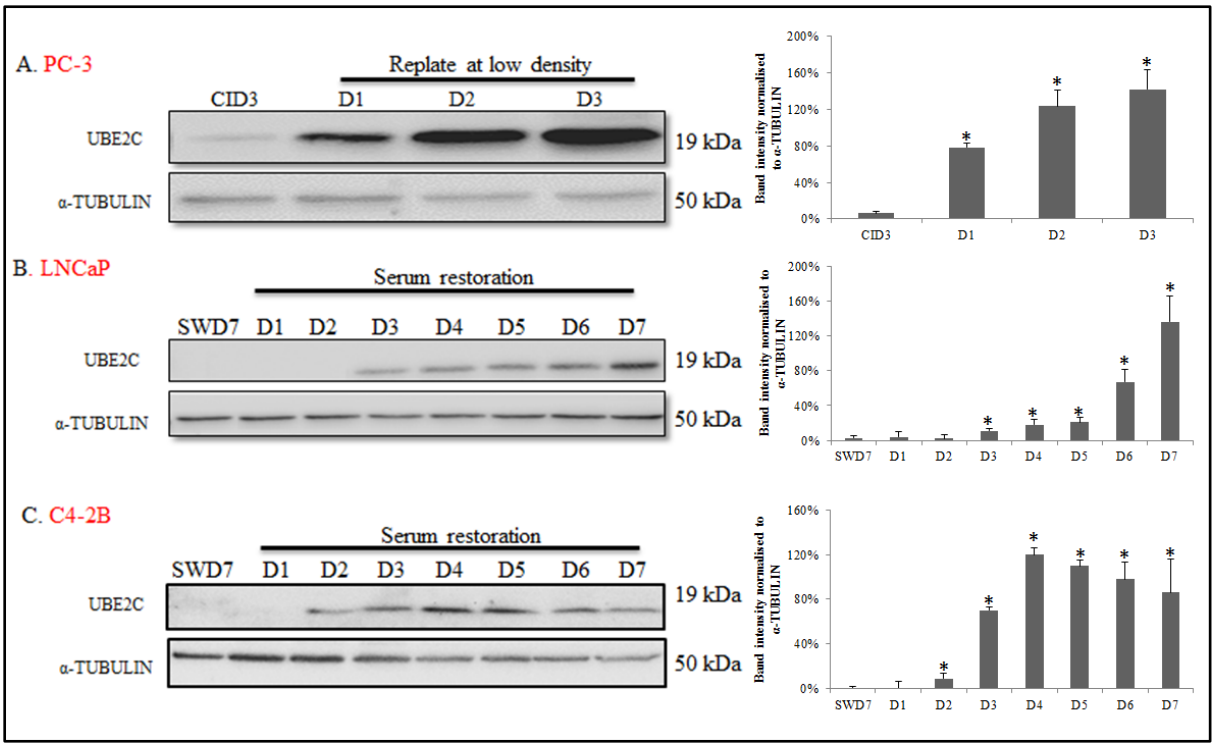


**Figure 3-27. Expression of UBE2C protein in prostate cancer cells during cell cycle re-entry.**

Quiescent PCa cells were induced to quiescence by 3 day contact inhibition or 7 day serum withdrawal. The cell cycle re-entry was achieved by re-plating cells at lower density for 3 days or serum restoration for 7 days. Levels of UBE2C protein in PC-3, LNCaP and C4-2B cells were examined by western blot analysis. α-TUBULIN expression was determined as a control to assure equal protein loading. CID3, contact inhibition for 3 days. RPD1–3 quiescent PC-3 cells were re-plated at lower density to allow cell re-entry to the cell cycle. SWD7, serum withdrawal for 7 days. SRD1–3, serum replenished for 1–3 days. **Left.** Representative immunoblotting image in PCa cells. **Right.** Histogram representing densitometric analysis are mean±SD. *, P< 0.05 versus CID3 or SWD7 in each cell line. The results are representative of three experiments.

**Table 3-4. The timeframe required for enriching cell re-entry and the corresponding UBE2C level during cell cycle re-entry in prostate cancer cells.**

| **Re-entry** | UBE2C level by western blot | **D1** | **D2** | **D3** | **D5** | **D7** | Change in $G_0$ fraction by flow cytometry | **D1** | **D2** | **D3** | **D5** | **D7** |
|---|---|---|---|---|---|---|---|---|---|---|---|---|
| PC-3 | | ↑ | ↑↑ | ↑↑↑ | | | | ↓ | ↓ | ↓↓ | | |
| LNCaP | | | ↑ | ↑ | ↑↑ | ↑↑↑ | | | | ↓ | ↓↓ | ↓↓ |
| C4-2B | | ↑↑ | ↑↑↑ | ↑↑↑ | ↑↑↑ | ↑↑↑ | | ↓ | ↓↓ | ↓↓↓ | | |

↓, a decrease occurred. ↑, an increase occurred. The number of arrows indicates the level of change. D1–7, time following release from quiescence.

### 3.3.4.3. Knockdown of UBE2C impeded cell cycle re-entry in PC-3 cells

To determine the role of UBE2C in regulating cell cycle re-entry, we employed contact inhibition in PC-3 to synchronise cells to quiescence. PC-3 cells were then transfected with either NC or siUBE2Cs at the time when the cells were induced to cell cycle re-entry. The knockdown of UBE2C during cell cycle re-entry was confirmed by immunoblotting. The effect of siUBE2C on the proportion of cells in $G_0$ phase during cell cycle re-entry was determined in a time course experiment. By comparing the percentage of $G_0$ cells before and after the induction of cell cycle re-entry, depletion of UBE2C retained 15–25% more $G_0$ cells than NC treated PC-3cells (Figure 3-28). As expected, there was a significant decrease in $G_1$ population following 24 h treatment with siUBE2Cs compared to the NC after release from quiescence ($p<0.01$). Knockdown of UBE2C also led to $G_2$/M arrest following 3 day release from quiescence ($p<0.01$). The percentage of S-phase cells remained unchanged or decreased only in C3-treated PC-3 cells 24 h after cell cycle re-entry ($p<0.05$). The results provide evidence that knockdown of UBE2C delays cell cycle re-entry by quiescent PC-3 cells.

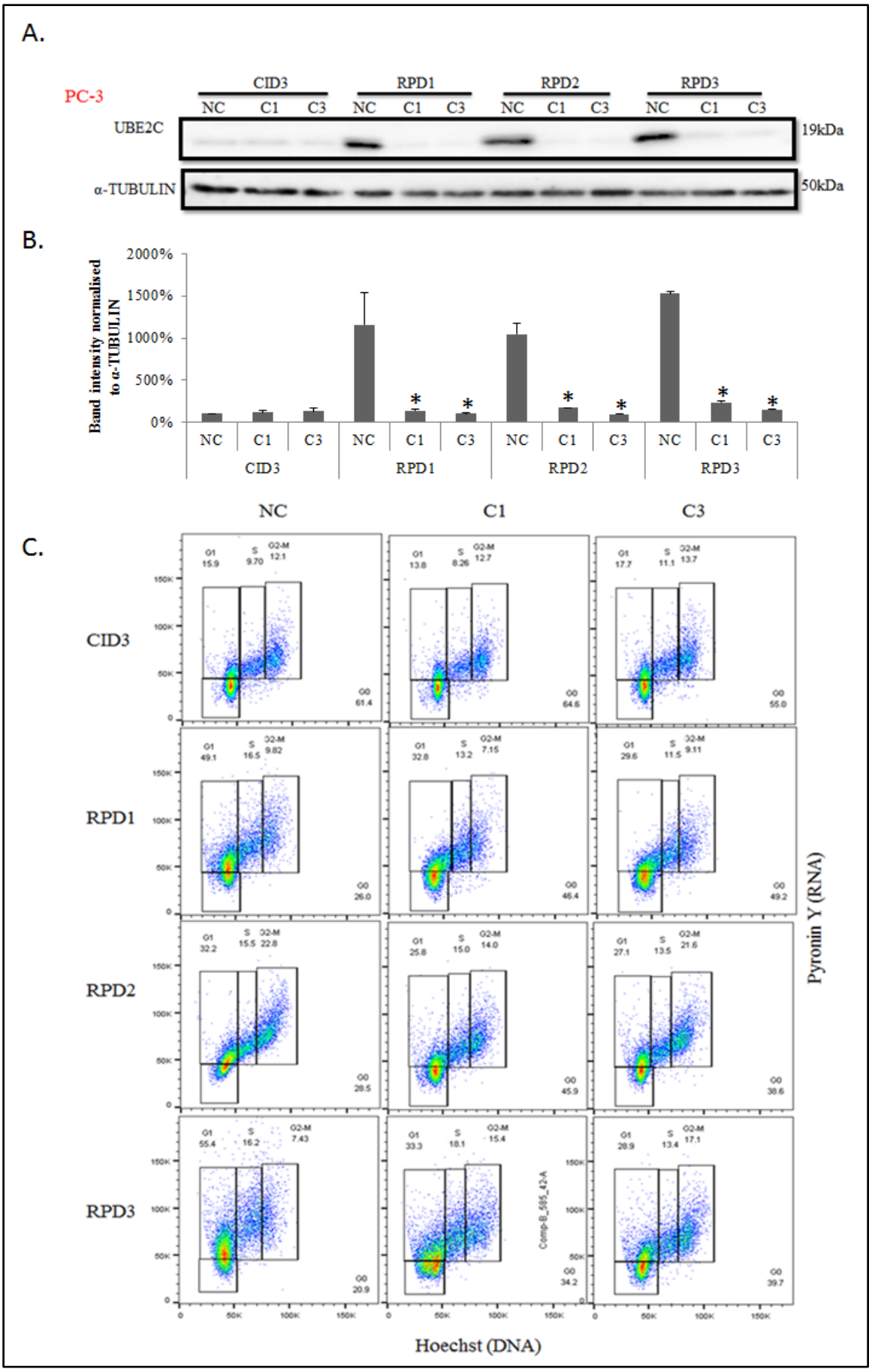
A.
PC-3
CID3
RPD1
RPD2
RPD3
NC C1 C3 NC C1 C3 NC C1 C3 NC C1 C3
UBE2C
19kDa
α-TUBULIN
50kDa
B.
Band intensity normalised to α-TUBULIN
2000%
1500%
1000%
500%
0%
NC C1 C3 NC C1 C3 NC C1 C3 NC C1 C3
CID3 RPD1 RPD2 RPD3
C.
NC
C1
C3
CID3
RPD1
RPD2
RPD3
Pyronin Y (RNA)
Hoechst (DNA)

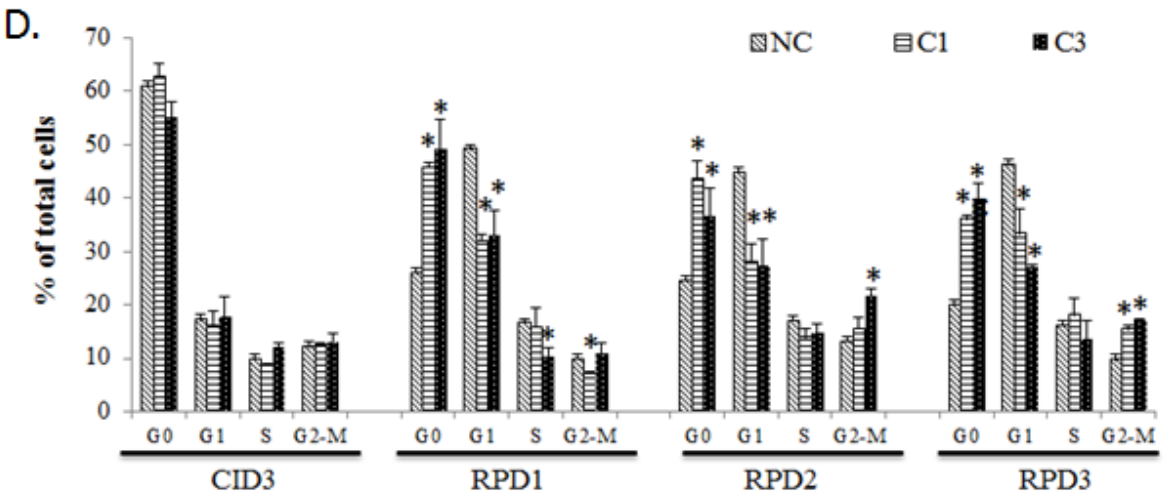


**Figure 3-28. The effect of siUBE2C on the distribution of cell cycles in PC-3 cells during cell cycle re-entry.**

CID3: PC-3 cells were synchronised to $G_0$ by contact inhibition in T25 flasks for 3 days. PC-3 cells were then transfected with NC, C1 or C3 at the time when the cells were induced to cell cycle re-entry. RPD1–3, the quiescent PC-3 cells were re-plated at lower density to allow cell re-entry to the cell cycle. **A.** Representative immunoblotting image in PC-3 cells. **B**. Histogram representing densitometric analysis are mean± SD (n=3). *, P< 0.05 vs. NC at each time point. The effect of siUBE2C on the proportion of cells in $G_0$ phase during cell cycle re-entry was determined by using HP double staining. The cell cycle distribution was analysed using the same gating. **C.** Representative flow image in PC-3 cells. **D.** Histogram illustrates the cell cycle distribution during cell cycle re-entry. * $p$<0.05 vs. NC at each time point.

### 3.3.4.4. Knockdown of UBE2C impeded cell cycle re-entry in LNCaP cells

To verify the results obtained from PC-3 cells that UBE2C siRNA impeded cycle re-entry, we synchronised LNCaP cells using serum withdrawal method. LNCaP cells were then transfected with 20 nM either NC or siUBE2Cs at the time when the cells were released from quiescence. By comparing the percentage of $G_0$ cells with or without UBE2C depletion, the percentage of $G_0$ cells decreased after cell cycle release. The effect of siUBE2C was observed 48 h after release by serum restoration, which was 40% higher in siUBE2C-treated cells compared to NC-treated cells (Figure 3-29). Moreover, depletion of UBE2C retained 110% more $G_0$ cells than NC-treated LNCaP cells after release for 3 days.

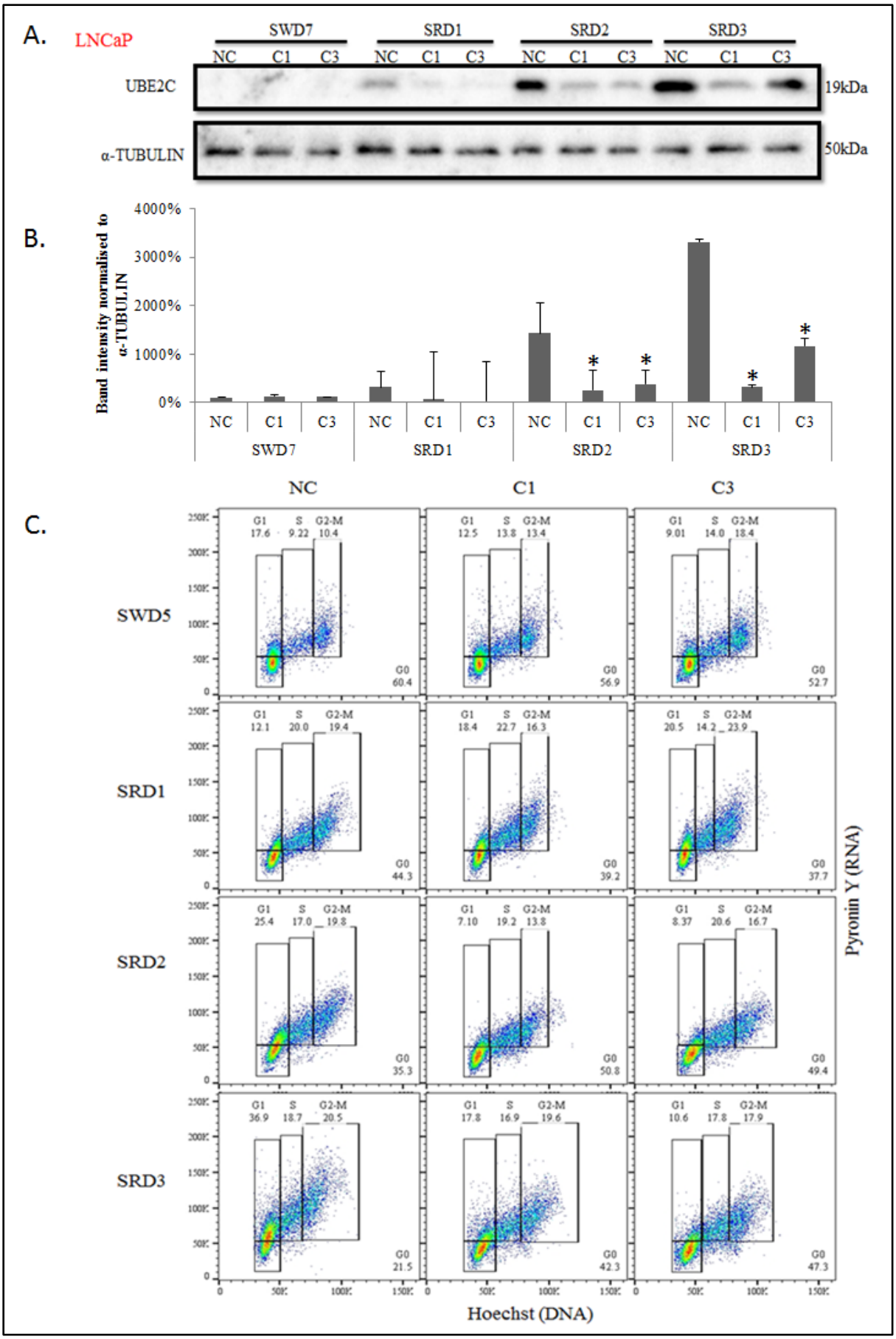
A.
LNCaP
SWD7
SRD1
SRD2
SRD3
NC C1 C3 NC C1 C3 NC C1 C3 NC C1 C3
UBE2C
19kDa
α-TUBULIN
50kDa
B.
Band intensity normalised to α-TUBULIN
4000%
3000%
2000%
1000%
0%
NC C1 C3 NC C1 C3 NC C1 C3 NC C1 C3
SWD7 SRD1 SRD2 SRD3
C.
NC
C1
C3
SWD5
SRD1
SRD2
SRD3
G1 S G2-M
17.6 9.22 10.4
12.5 13.8 13.4
9.01 14.0 18.4
12.1 20.0 19.4
18.4 22.7 16.3
20.5 14.2 23.9
25.4 17.0 19.8
7.10 19.2 13.8
8.37 20.6 16.7
36.9 18.7 20.5
17.8 16.9 19.6
10.6 17.8 17.9
G0
60.4
56.9
52.7
44.3
39.2
37.7
35.3
50.8
49.4
21.5
42.3
47.3
Pyronin Y (RNA)
Hoechst (DNA)

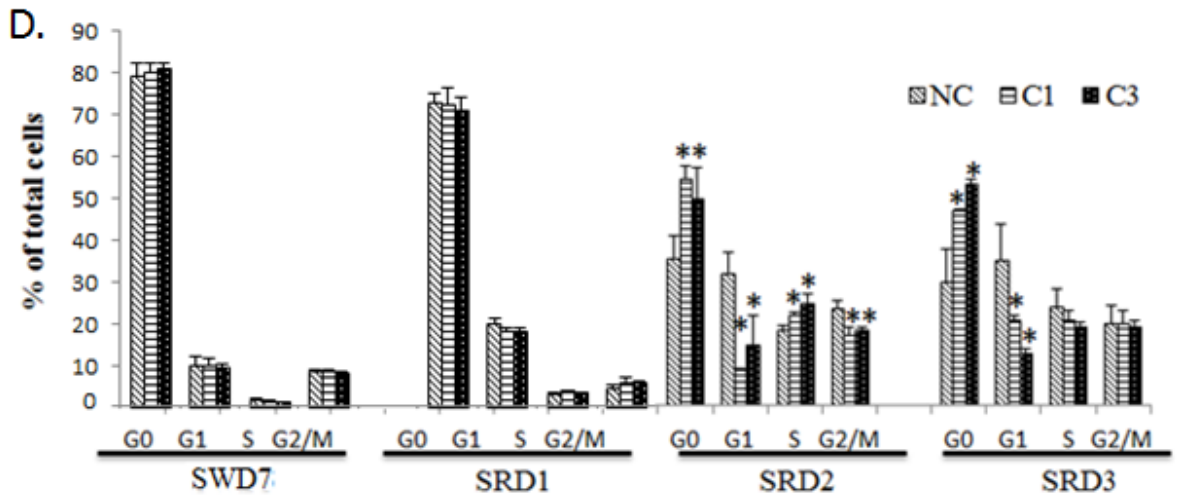


**Figure 3-29. The effect of siUBE2C on the distribution of cell cycles in LNCaP cells during cell cycle re-entry.**

SWD7: LNCaP cells were synchronised to $G_0$ by serum deprivation in T25 flasks for 7 days. LNCaP cells were then transfected with NC, C1 or C3 at the time when the cells were induced to cell cycle re-entry. SRD1–3, cell cycle re-entry was rendered by restoration of serum to serum-deprived cells for up to 7 days. **A.** Representative immunoblotting image in LNCaP cells. **B**. Histogram representing densitometric analysis are mean± SD (n=3). *, P< 0.05 vs. NC at each time point. The effect of siUBE2C on the proportion of cells in $G_0$ phase during cell cycle re-entry was determined by using HP double staining. The cell cycle distribution was analysed using the same gating. **C.** Representative flow image in LNCaP cells. **D.** Histogram illustrates the cell cycle distribution during cell cycle re-entry. * $p$<0.05 vs. NC at each time point.

The results further support the notion that knockdown of UBE2C retains cells in quiescent state. Notably, there was no impact of siUBE2C in the quiescence of LNCaP cells at first day of release by serum restoration. This observation may be explained by comparing the protein level of UBE2C in NC-treated cells, although the protein level of UBE2C in SRD1 was increased compared with SWD7, it remained relatively low compared with SRD2 or SRD3. In addition, approximately 70% of LNCaP cells were arrested at $G_0$ phase after SRD1, compared to 80% of cells in SWD7 samples, suggesting the majority of LNCaP cells remained quiescent after 24 h serum restoration. The quiescent LNCaP cells required more than 24 h to re-enter the cell cycle. Therefore, siUBE2C impeded cell cycle re-entry in SRD2.

### 3.3.4.5. Knockdown of UBE2C impeded cell cycle re-entry in C4-2B cells

To further extend the above described study to anther cell line, the same experiment was repeated in C4-2B cells. The cell cycle re-entry was hindered in C4-2B cells treated with siUBE2C after 2–3 day serum restoration in comparison with control conditions. Following 3 day serum restoration, the fraction of quiescent cells decreased dramatically from 77.6% to 26.3% of the population in NC-treated cells. However, the decreased fraction of $G_0$ cells was less in C4-2B cells treated with siUBE2C, from approximately 80% to 55% of the total population (Figure 3-30). Furthermore, the percentage of proliferative cells was lower in UBE2C-knockdown cells compared with NC-treated cells following release from quiescence. Taken together, these data suggest that knockdown UBE2C is capable of impeding cell cycle re-entry by quiescent PCa cells.

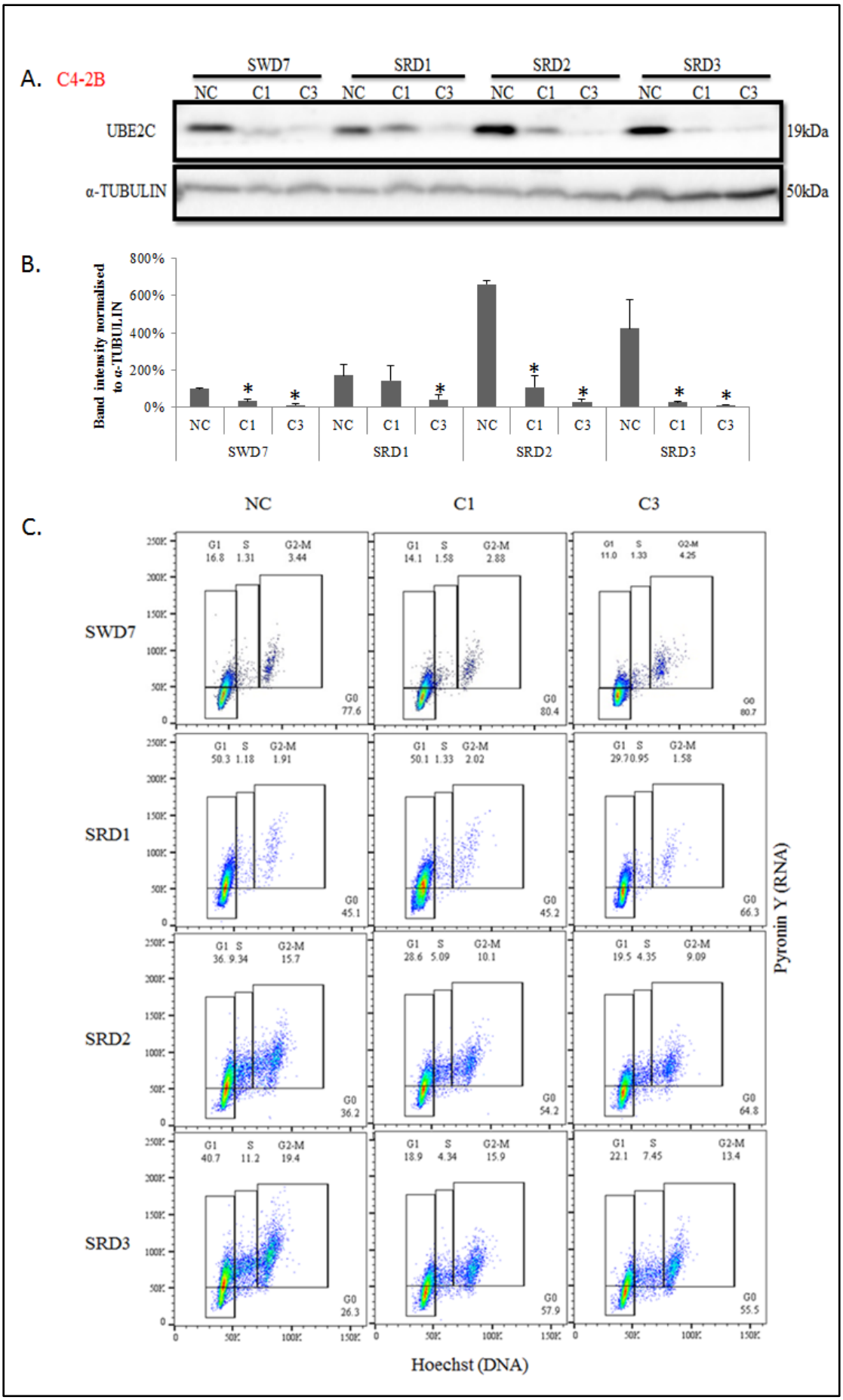
A. C4-2B
SWD7
SRD1
SRD2
SRD3
NC C1 C3 NC C1 C3 NC C1 C3 NC C1 C3
UBE2C
19kDa
α-TUBULIN
50kDa
B.
Band intensity normalised to α-TUBULIN
800%
600%
400%
200%
0%
NC C1 C3 NC C1 C3 NC C1 C3 NC C1 C3
SWD7 SRD1 SRD2 SRD3
C.
NC
C1
C3
SWD7
SRD1
SRD2
SRD3
Pyronin Y (RNA)
Hoechst (DNA)

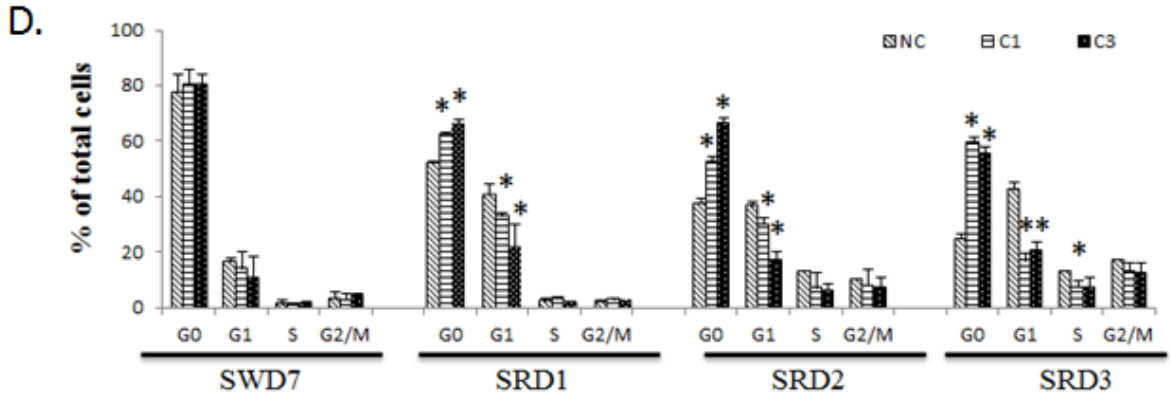


**Figure 3-30. The effect of siUBE2C on the distribution of cell cycles in C4-2B cells during cell cycle re-entry.**

SWD7: C4-2B cells were synchronised to $G_0$ by serum deprivation in T25 flasks for 7 days. C4-2B cells were then transfected with NC, C1 or C3 at the time when the cells were induced to cell cycle re-entry. SRD1–3, cell cycle re-entry was rendered by restoration of serum to serum-deprived cells for up to 7 days. **A.** Representative immunoblotting image in C4-2B cells. **B**. Histogram representing densitometric analysis are mean±SD (n=3). *, P< 0.05 vs. NC at each time point. The effect of siUBE2C on the proportion of cells in $G_0$ phase during cell cycle re-entry was determined by using HP double staining. The cell cycle distribution was analysed using the same gating. **C.** Representative flow image in C4-2B cells. **D.** Histogram illustrates the cell cycle distribution during cell cycle re-entry. * $p$<0.05 vs. NC at each time point.

# 3.4. Discussion

In normal circumstances, most cells are arrested at a quiescent state (Hartwell *et al.*, 1974; Kriegenburg *et al.*, 2008). The transition from quiescence to proliferation is an important self-repair mechanism utilised to replace cell loss (Cooper, 2003; Pardee, 1974). However, disruption of the regulation of the cell cycle is a recurrent theme in carcinogenesis (Kastan and Bartek, 2004). The objective of this study was to determine the effect of UBE2C on cell cycle control in PCa cells. The choice of three cell lines – PC-3, LNCaP and C4-2B – was based on the fact that PCa is either HSPC or CRPC. LNCaP (AR positive) is a cell model of HSPC; PC-3 (AR negative) is a model of CRPC cells, while C4-2B was chosen as it is an AR positive CRPC cell line (Chen *et al.*, 2011; Thalmann *et al.*, 2000; Wang *et al.*, 2009). In this

study, we investigated the relationship of UBE2C in regulating the proportion of quiescent cancer cells using two genetic approaches, *i.e.*, gene silencing with siRNA and overexpression with expression vectors. We also verified the HP double staining method to quantify the proportion of $G_0$ cells in a population of PCa cells, as well as during transition from quiescence to proliferation. Our observations clearly demonstrated there is a correlation between UBE2C protein levels and cell cycle exit and re-entry. More importantly, our data indicated that UBE2C plays a causal role in cell cycle exit and re-entry. As UBE2C effect on cell cycle regulation is consistent overall in all three PCa cell lines, it is most likely that the UBE2C action is AR independent.

### 3.4.1. Expression level of UBE2C in cancerous and non-cancerous prostate cell lines

UBE2C mRNA and protein have been shown to be overexpressed in PCa (Tzelepi *et al.*, 2012; Wang *et al.*, 2009). In this study, we determined the expression of UBE2C in five prostate cell lines. We found that the expression of UBE2C is high in all three cancerous PCa cell lines compared to the two non-cancerous prostate cell lines (Figure 3-1). Our findings suggest that the cell lines used in our study are consistent with the reported role of UBE2C in promoting tumour grade and progression (Chen *et al.*, 2010; Cunha *et al.*, 2010; Loussouarn *et al.*, 2009).

### 3.4.2. Expression of UBE2C correlated with cellular proliferation

In PCa cells, overexpression of UBE2C increases, whereas silencing of UBE2C decreases, cell proliferation and invasiveness (Wang *et al.*, 2011). Our observation of cell proliferation

assays showed a similar pattern. That is, a positive correlation between UBE2C levels and cell proliferation in PCa cells. Silencing of UBE2C decreased cell proliferation, whereas overexpression of UBE2C increased, when measured by DNA content (Figure 3-3 & Figure 3-16).

## 3.4.3. Validation of HP double staining

UBE2C is a mitotic cyclin-specific E2 ubiquitin-conjugating enzyme; we speculated that, the cell cycle might be distorted and might arrest in $G_2$/M phase after UBE2C is downregulated(Reddy *et al.*, 2007). The knockdown of UBE2C by siRNA increases cells in $G_2$/M phase in PC-3 cells and C4-2B cells but not in LNCaP cells (Chen *et al.*, 2011; Walker *et al.*, 2008; Wang *et al.*, 2011; Wang *et al.*, 2009). However, in this study, the fraction of cells in $G_0$/$G_1$ phase remained unchanged or decreased following UBE2C knockdown in PCa cell lines (Table 3-1). Our immunostaining of Ki-67 protein in PC-3 cells showed a decrease in positivity, suggested the proportion of quiescent cells could be increased (Figure 3-6). The conventional method of DNA content analysis was unable to distinguish $G_0$ from $G_1$, as both $G_1$ and $G_0$ cells are diploid (2N). However, ribosomes were degraded in quiescent $G_0$ cells. Shapiro (1981) first proposed a method to differentiate staining of cellular RNA and DNA by HP double staining (Shapiro, 1981). Hoechst 33258 is an exclusive DNA dye while Pyronin Y reacts with both DNA and RNA. However, in the presence of Hoechst 33258, the staining of Pyronin Y for DNA content is blocked, and Pyronin Y stains RNA only (Zbigniew Darzynkiewicz *et al.*, 2004). Hence, the $G_0$ cells could be distinguished as diploid and as having low RNA content by using multi-parameter flow cytometry based on simultaneously labelling the cell nuclear DNA and RNA.

In this study, flow cytometric analysis with HP double staining was validated by using synchronised PCa cells. The experimental model of quiescent PCa cells was induced by 3

days contact inhibition or 7 days serum withdrawal. Flow analysis of cells with HP double staining showed a time-dependent increase in the proportion of quiescent cells during synchronisation (Figure 3-7–Figure 3-9). The HP double staining was further validated by co-staining with p-Rb ($Ser^{807/811}$). Cells with 2N DNA and low RNA content were low in Rb at p-$Ser^{807/811}$ **(**Figure 3-10 & Figure 3-11), which is hypo-phosphorylated in quiescent cells (Serrano *et al.*, 1993; Sherr and Roberts, 1995). Hence, flow cytometric analysis with HP double staining was an effective method to identify quiescence in PCa cells.

### 3.4.4. UBE2C expression is associated with the proportion of quiescent prostate cancer cells

The HP double staining method was subsequently applied to determine if manipulating UBE2C changes the proportion of cells in $G_0$ phase. PCa cell lines were transfected with UBE2C siRNA or UBE2C expression plasmid. Depletion of UBE2C led to accumulation of quiescent cells (Figure 3-12–Figure 3-14), while overexpression of UBE2C decreased the proportion of quiescent PCa cells (Figure 3-17-Figure 3-19).

In our studies, the UBE2C protein levels were depleted prior to the change occurring in accumulation of $G_0$ cells in each cell line (Table 3-2). The UBE2C was knocked down 24 h after induction of siUBE2C in PC-3 and C4-2B cells, whereas the accumulation of quiescent cells became significant at 48 h. Similarly, the significant increase of $G_0$ cells in LNCaP cells occurred 24 h after successful UBE2C depletion. These observations suggest a causal role of UBE2C in cellular quiescence.

To assess whether or not this observation was associated with UBE2C catalytic activity, PCa cells were transfected with UBE2C or UBE2C-DN plasmid to render gene overexpression.

Overexpressed UBE2C in PCa cells decreased the proportion of cells in $G_0$ phase, whereas no change was observed in UBE2C-DN induced cells (Figure 3-17-Figure 3-19).

UBE2C-DN is created by changing the catalytic Cysteine to Serine, which blocks UBE2C-mediated protein ubiquitination and destruction (Townsley *et al.*, 1997). Our result suggests that the catalytic $Cys^{114}$ of UBE2C could be important for UBE2C-mediated cell cycle progression. It is worth noting that, although transfecting UBE2C-DN has no impact in $G_0$ cells, it increased the proportion of cells in $G_2$/M phase in LNCaP cells. Similar results have also been reported by Townsley (1997). More recent studies suggest the mitosis arrest caused by induction of UBE2C-DN is due to its capacity to compete with endogenous UBE2C to bind to its E3 ligands, thus inhibiting degradation of mitotic cyclins and subsequently mitotic arrest (Bose *et al.*, 2012; Townsley *et al.*, 1997).

### 3.4.5. Cellular mechanism of UBE2C regulating cell cycle exit and re-entry

To further evaluate the relationship of UBE2C with cell cycle exit and re-entry, we utilised contact inhibition in PC-3 or serum withdrawal in LNCaP and C4-2B cells to induce experimental quiescence, as previously published in our laboratory (Yao *et al.*, 2015). The quiescent state of PCa cells were confirmed by flow cytometric analysis with HP double staining (Figure 3-7–Figure 3-9). Cell cycle re-entry was rendered by replating the quiescent cells at low density, or by restoration of serum to serum-deprived cells (Figure 3-24–Figure 3-26). The protein level of UBE2C protein was decreased during cell cycle exit and increased upon cell cycle re-entry in PCa cells (Table 3-3 & Table 3-4). In line with this observation, UBE2C levels have been shown to be cell cycle-regulated (Okamoto *et al.*, 2003).

We then determined the effect of UBE2C expression in regulating cell cycle re-entry in quiescent PCa cells by two independent genetic approaches. Firstly, PCa cells were transfected with UBE2C overexpression vector, and then induced to quiescence by contact inhibition or serum withdrawal. Synchronisation of PCa cells was slowed down by overexpression of UBE2C compared with control cells, whereas no impact was found in UBE2C-DN expressed cells (Figure 3-21–Figure 3-23). These results suggest overexpression of UBE2C delayed cell cycle exit. It was noted that the C4-2B cells transfected with empty vector had a higher proportion of cells at $G_0$ phase compared with the non-transfected cells following synchronisation at $G_0$. In PC-3 cells, a decrease in the proportion of cells at $G_0$ phase was noted following synchronisation in the empty vector transfected cells in comparison to the non-transfected cells. This phenomenon reminds us the importance to use empty vector-transfected cells as contrl, but not non-transfected cells. Moreover, this discrepancy should not affect the validity of the results, as the comparison in the study is always between wildtype-UBE2C and empty vector/DN-transfected cells.

In addition, PCa cells were induced to quiescence, and cells were treated with siUBE2C during cell cycle re-entry by replating the quiescent cells at low density or by restoring serum to serum-deprived cells. The proportion of $G_0$ cells was higher in PCa cells with UBE2C-knockdown compared with control cells (Figure 3-28-Figure 3-30). Therefore, loss of UBE2C delayed cell cycle re-entry by quiescent PCa cells. These observations further support the regulatory role of UBE2C in the transition of quiescent cells to proliferative cells.

In summary, we have established three novel observations:

i. UBE2C protein levels were decreased during cell cycle exit and increased upon cell cycle re-entry in three PCa cell lines.

ii. Depletion of UBE2C led to accumulation of quiescent cells, while overexpression of UBE2C decreased quiescent cells in PCa cell lines.

iii. Overexpression of UBE2C impeded cell cycle exit and its knockdown delayed cell cycle re-entry by quiescent PCa cells.

Further studies are needed to investigate the mechanism underlying UBE2C action on cell cycle exit and re-entry.

# *Chapter 4*

# 4. Molecular Mechanism of UBE2C in Regulating the Proportion of Quiescent Prostate Cancer Cells

# 4.1. Introduction

Ubiquitin-activating enzyme (E1), the ubiquitin-conjugating enzyme (E2) and ubiquitin ligases (E3) are three enzymes required for UPS to work in concert to facilitate ubiquitination of target protein substrates (Rape, 2010). UBE2C is an E2 enzyme, which is an exclusive partner of APC/C. By orchestrating the sequential degradation of a large number of cell cycle regulators, UBE2C together with APC/C is essential for cell cycle control (Song and Rape, 2011). The human APC/C has more than 55 reported target proteins. Of these, 37 are involved in cell cycle S and M phases (*e.g.*, cyclin A/B, p21 and securin), 11 are cell-cycle related in general (*e.g.*, E2-C, E2F1, JNK and SKP2), and two are APC/C co-activators (CDC20 and CDH1) (Meyer and Rape, 2011).

Unlike the ample information gathered regarding the E3 APC/C, the E2s participating in the cell cycle have not been fully understood. UBE2C regulates the mitotic SAC by targeting securin for degradation, which in turn activates separase to degrade cohesin rings, leading to separation of sister chromatids and anaphase onset (Hao *et al.*, 2012; Reddy *et al.*, 2007; Williamson *et al.*, 2011). Overexpression of UBE2C leads to uncontrolled APC/C activity and genomic instability, including chromosome mis-segregation, chromosomal lagging during mitosis and aneuploidy (Hao *et al.*, 2012). UBE2C also participates in the destruction of mitotic cyclins, including cyclin B. Degradation of cyclin B inactivates CDK1, which leads to unphosphorylation and activation of CDH1. $APC/C^{CDH1}$ and low activity of CDK1 are prerequisite steps for mitotic exit and $G_1$ and S progression (Aristarkhov *et al.*, 1996; Arvand *et al.*, 1998; Rape and Kirschner, 2004; Rape *et al.*, 2006). Accumulation of UBE2C stimulates cell proliferation, whereas silencing of UBE2C decreases cell proliferation (Chen *et al.*, 2011; Wang *et al.*, 2009). Expression of UBE2C-DN arrests cells in mitosis (Townsley

*et al.*, 1997). Knockdown of PC-3 cells delays cell cycle progression from $G_2$/M to $G_1$ phase, highlighting the role of UBE2C in regulating mitotic exit (Chen *et al.*, 2011).

Observations outlined in Chapter 3 indicated that UBE2C is a vital cell cycle regulation factor involved in regulating the proportion of quiescent over proliferative PCa cells and transition to proliferating state by quiescent cancer cells. A key question is how UBE2C influences cell quiescence in PCa cells. Understanding how UBE2C regulates the transition of quiescent cells to proliferating cells is limited. To address this question, we examined a range of cell cycle regulators that had previously been associated with cell quiescence: $G_0$-regulatory proteins, including p27 and its regulators, c-MYC and FBXW7. Moreover, the mechanism of how UBE2C influences these proteins was investigated.

# 4.2. Materials and Methods

## 4.2.1. Prostate cancer cell lines

The PCa cell lines LNCaP, PC-3 and C4-2B cells were cultured as described in **Chapter 2.1.1**.

## 4.2.2. Transfection of prostate cancer cells with siRNA

Prostate cancer cells were transfected with 20 nM NC, C1 or C3. The cells were incubated for the indicated time and the media was replenished. The cells were left to propagate for the time indicated. Thereafter, cells were harvested for SYBR Green assay, immunoblotting, RT-PCR or flow cytometry analysis.

### 4.2.3. Transfection of prostate cancer cells with plasmid

For overexpression, PCa cells were gown in T75 flasks until semi-confluent, then trypsinised and transfected with plasmid according to **Chapter 2.2.2.**

### 4.2.4. Immunoblotting

The cells were treated in 6-well plates and cell lysates prepared with a lysis buffer. Immunoblotting was performed as described in **Chapter 2.5**. The primary antibodies used are listed in Table 2-4.

### 4.2.5. RT-PCR

RT-PCR was performed as described in **Chapter 2.7**. All the primer sequences used for RT-PCR in this study are listed in **Chapter 2.7.3**.

### 4.2.6. Statistical analysis

The statistical software NCSS version 12.0 was used for statistical analysis as described in **Chapter 2.8**

# 4.3. Results

## 4.3.1. Knockdown of UBE2C increased p27 protein expression in prostate cancer cells

The $G_0$-maintenance protein p27 is a CDK/cyclin inhibitor, which is found in quiescent cells and its elevated level is required for blocking cell cycle re-entry and the maintenance of quiescent state (Chu *et al.*, 2007; Rivard *et al.*, 1996). To verify whether the mode of UBE2C involves the $G_0$-maintenance protein p27, we determined the effect of siUBE2C on p27 protein levels in three PCa cell lines (PC-3, LNCaP and C4-2B cells; Figure 4-1). In PC-3 cells, the protein level of p27 was clearly increased by knockdown UBE2C at 24 h after exposure to siUBE2C. Accumulation of p27 protein was also observed in LNCaP and C4-2B cells 48 h post-transfection of siUBE2Cs.

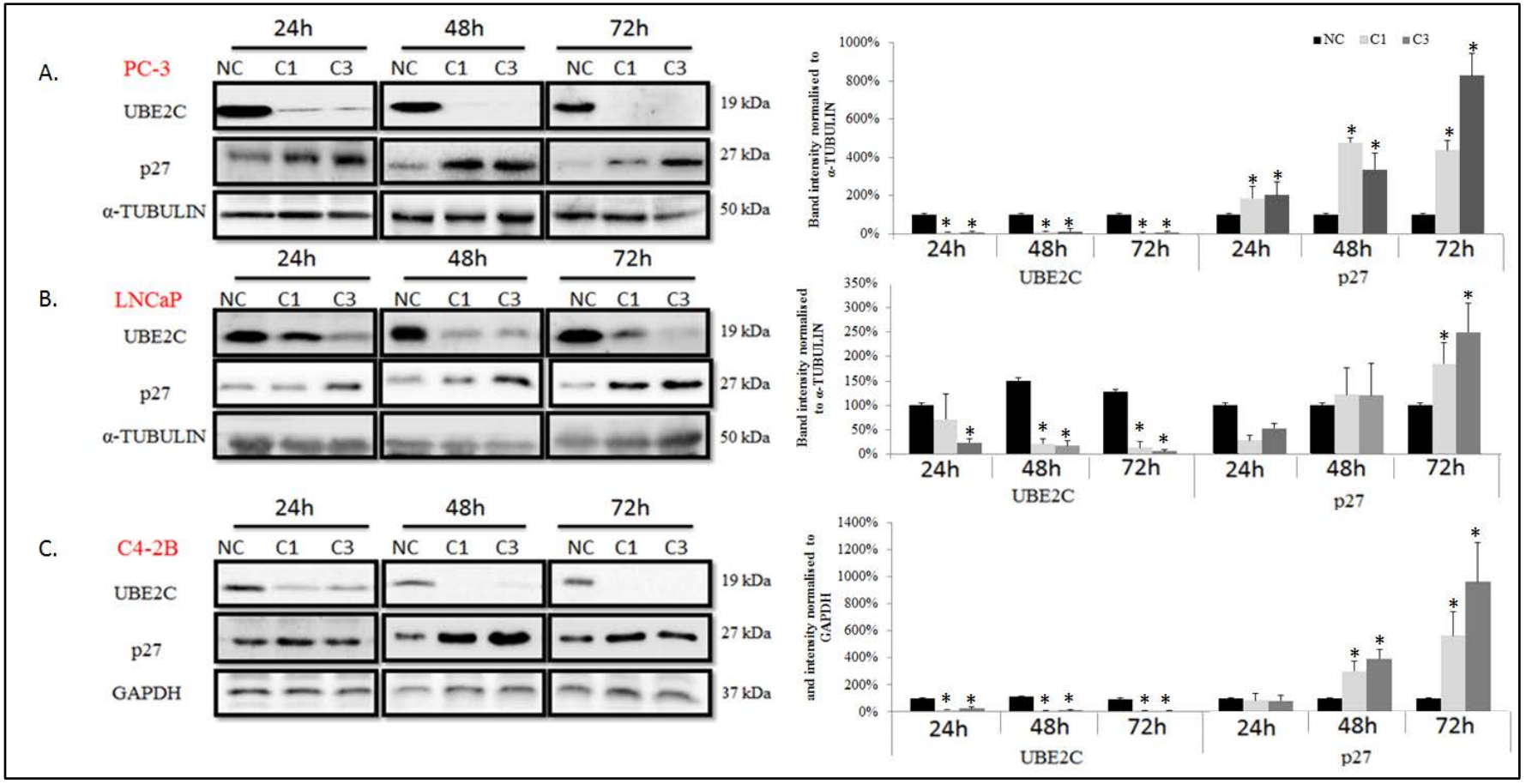


**Figure 4-1. Effect of siUBE2C on p27 protein levels in PC-3, LNCaP and C4-2B cells by immunoblotting.**

**A**. PC-3, **B.** LNCaP and **C.** C4-2B cells were transfected with 20 nM NC, C1 or C3. The cell culture medium was replenished 24 h following transfection. The cells were harvested 24, 48 and 72 h following transfection. Cell lysate protein (50 μg/lane) was analysed by immunoblotting. GAPDH and α-TUBULIN: loading control. **Left.** Representative immunoblotting image in PCa cells. **Right**. Histogram representing densitometric analysis are mean±SD (n=3). *, P< 0.05 vs. NC at each time point.

### 4.3.2. Knockdown of UBE2C by siRNA decreased p27 negative regulators in prostate cancer cells

To further elucidate the mechanistic basis and action of UBE2C on $G_0$-maintenance protein p27, immunoblot analysis was conducted to examine the expression of p27 regulators (SKP2, PIRH2 and CRM1). SKP2 and PIRH2 are components of E3 ligases responsible for p27 proteolysis by proteasome, while CRM1 is a carrier protein for p27 nuclear export. These three proteins can influence p27 protein levels via regulation of p27 protein stability and subcellular localisation.

#### 4.3.2.1. Knockdown of UBE2C decreased SKP2 and PIRH2 in PC-3 cells

To investigate whether p27 protein regulators were affected by UBE2C in PC-3 cells, immunoblotting analysis of CRM1, SKP2 and PIRH2 was performed. While CRM1 levels were not largely affected by siUBE2C, a reduction of UBE2C protein levels and coincident reduction of SKP2 and PIRH 2 and accumulation of p27 were observed 24 h post-transfection (Figure 4-2).

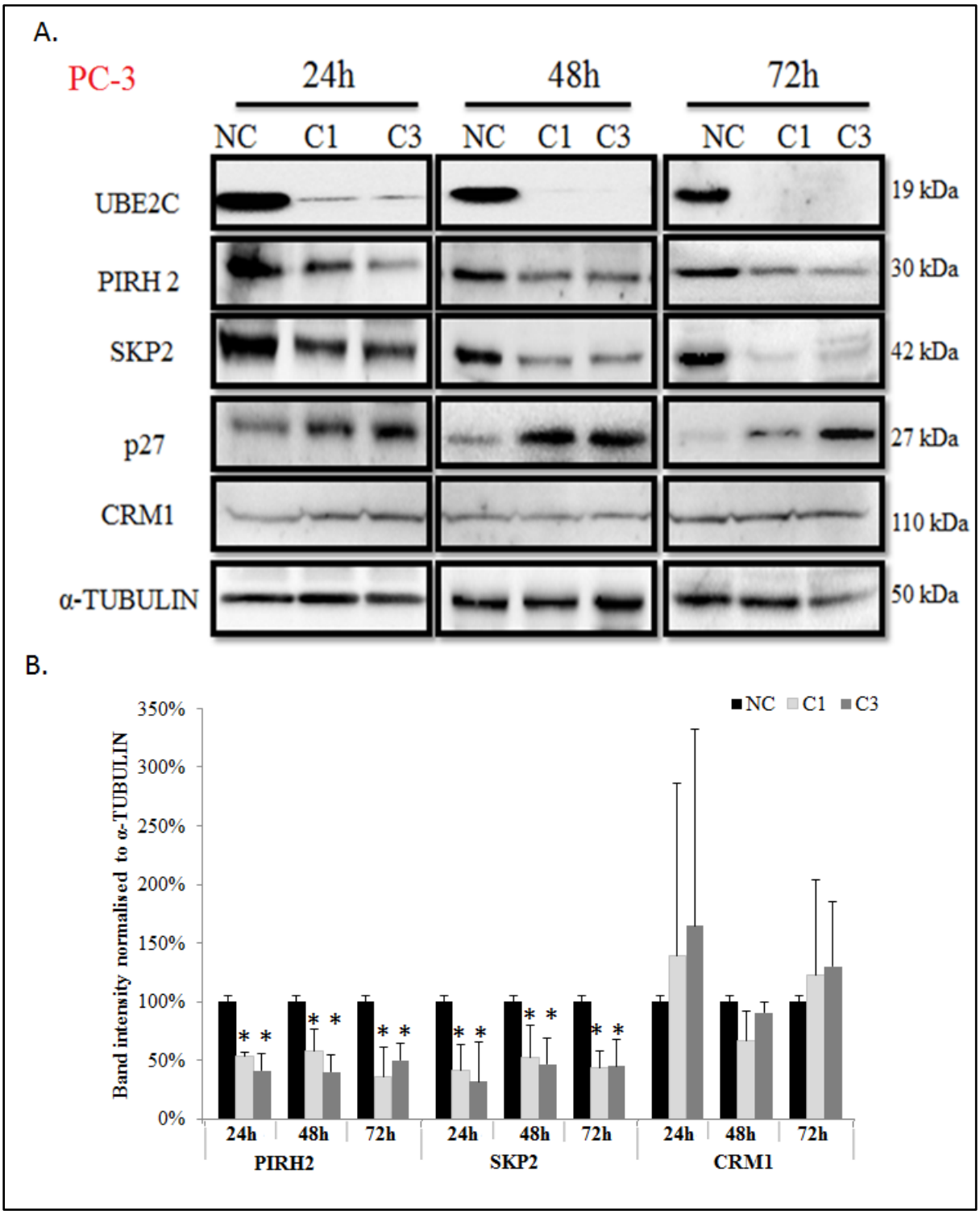


**Figure 4-2. Effect of siUBE2C on p27 protein levels in PC-3 cells by immunoblotting.**

PC-3 cells were transfected with 20 nM NC, C1 or C3. The cell culture medium was replenished 24 h following transfection. The cells were harvested 24, 48 and 72 h following transfection. Cell lysate protein (50 μg/lane) was analysed by immunoblotting. α-TUBULIN: loading control. **A.** Representative immunoblotting image in PC-3 cells. **B.** Histogram representing densitometric analysis are mean±SD (n=3). *, P< 0.05 vs. NC at each time point.

#### 4.3.2.2. Downregulation of UBE2C led to a reduction of SKP2 and PIRH2 followed by a decrease in c-MYC levels in PC-3 cells

Since the key cell cycle regulators were all changed 24 h post-transfection, we then determined the effect of siRNA in a shorter time course to determine the sequence of the change in these key proteins. PC-3 cells were treated with siUBE2Cs or NC for 4, 8, 12, 16, 20 and 24 h. The UBE2C level was verified by immunoblotting at indicated times with or without siUBE2C treatment. siUBE2C treatment for 8 h was sufficient for UBE2C knockdown (Figure 4-3). The protein levels of PIRH2 and SKP2 were reduced by UBE2C knockdown at 16 h post-transfection. The increase of $G_0$-maintenance protein p27 was observed 8 h after the reduction of SKP2 and PIRH2 occurred (Figure 4-3). The change of SKP2 and PIRH2 were 8 h ahead of the increased p27 protein, suggesting regulation of UBE2C on p27 is through downregulating SKP2- and PIRH2-mediated p27 degradation.

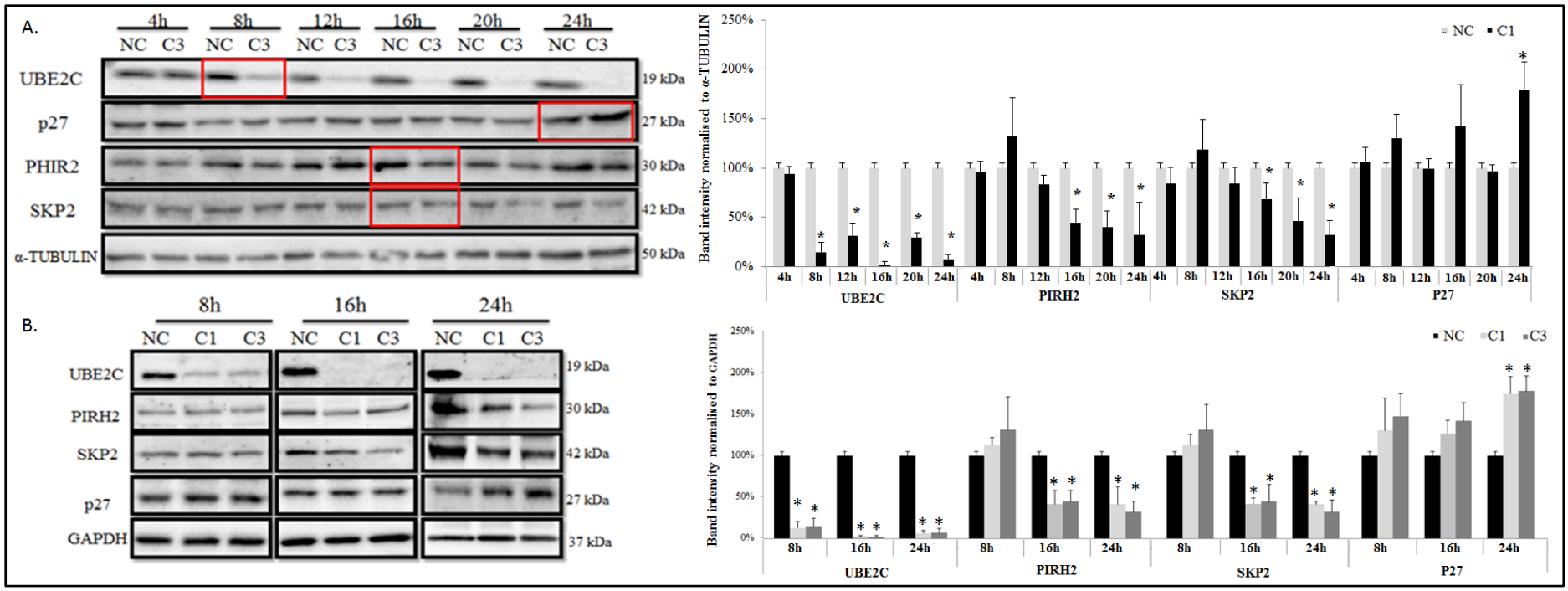


**Figure 4-3. Effect of siUBE2C on p27 protein levels in PC-3 cells by immunoblotting with short time points.**

PC-3 cells were transfected with 20 nM NC, C1 or C3. The cells were harvested every 4 h following transfection till 24 h. Cell lysate protein (50 µg/lane) was analysed by immunoblotting. α-TUBULIN: loading control. **Left.** Representative immunoblotting image in PC-3 cells. **Right**. Histogram representing densitometric analysis are mean±SD (n=3). *, P< 0.05 vs. NC at each time point.

#### 4.3.2.3. Knockdown of UBE2C decreased SKP2 and PIRH2 in LNCaP cells

To extend the observation to another cell line, the protein level of p27 regulators was also examined in LNCaP cells. A reduction of UBE2C protein levels and concordant reduction of SKP2 and PIRH 2 and accumulation of p27 were observed over 3 days following siUBE2C treatment (Figure 4-4). We found that the transfection of siUBE2C in LNCaP was effective 48 h post-transfection (Figure 3-5); whereas the reduction of SKP2 and PIRH2 occurred 48–72 h following transfection of siUBE2C. However, the protein level of CRM1 remained unchanged after UBE2C knockdown in LNCaP cells.

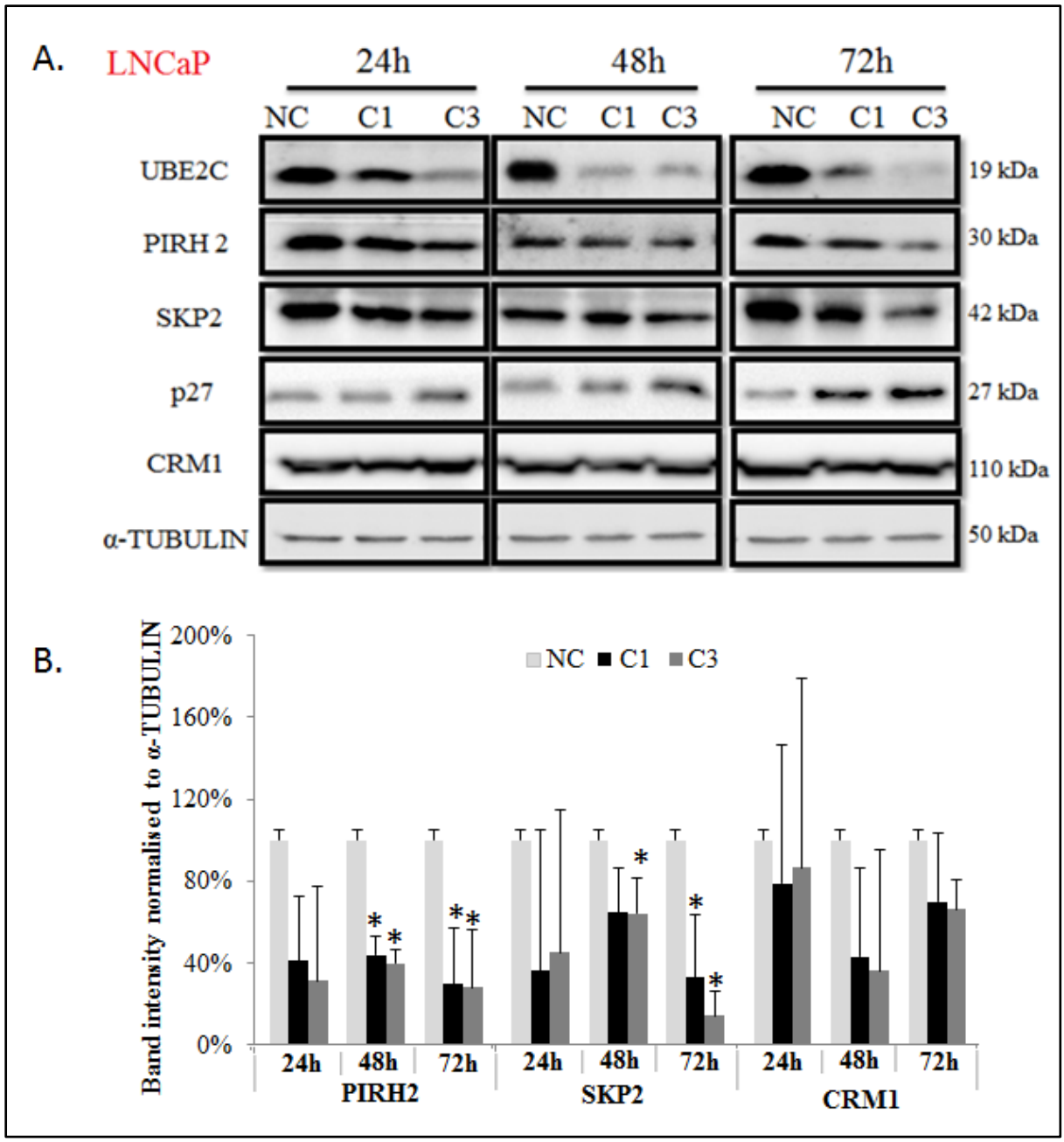


**Figure 4-4. Effect of siUBE2C on p27 protein levels in LNCaP cells by immunoblotting.**

LNCaP cells were transfected with 20 nM NC, C1 or C3. The cell culture medium was replenished 24 h following transfection. The cells were harvested 24, 48 and 72 h following transfection. Cell lysate protein (50 µg/lane) was analysed by immunoblotting. α-TUBULIN: loading control. **A.** Representative immunoblotting image in LNCaP cells. **B**. Histogram representing densitometric analysis are mean± SD (n=3). *, P< 0.05 vs. NC at each time point.

#### 4.3.2.4. Knockdown of UBE2C decreased SKP2 and PIRH2 in C4-2B cells

To further determine the effect of UBE2C on the expression of p27 and its regulators, we evaluated CRM1, SKP2 and PIRH2 using immunoblotting in another PCa cell line. C4-2B cells were exposed to siUBE2Cs for up to 72 h (Figure 4-5). Both sets of siUBE2Cs were effective in repressing the expression of UBE2C, showing an accumulation of p27 and a decrease of PIRH2 and SKP2 protein levels within the first 24 h after exposure to siUBE2C. However, there was no impact on protein level of CRM1 after transfection over a period of 72 h in comparison to control (Figure 4-5).

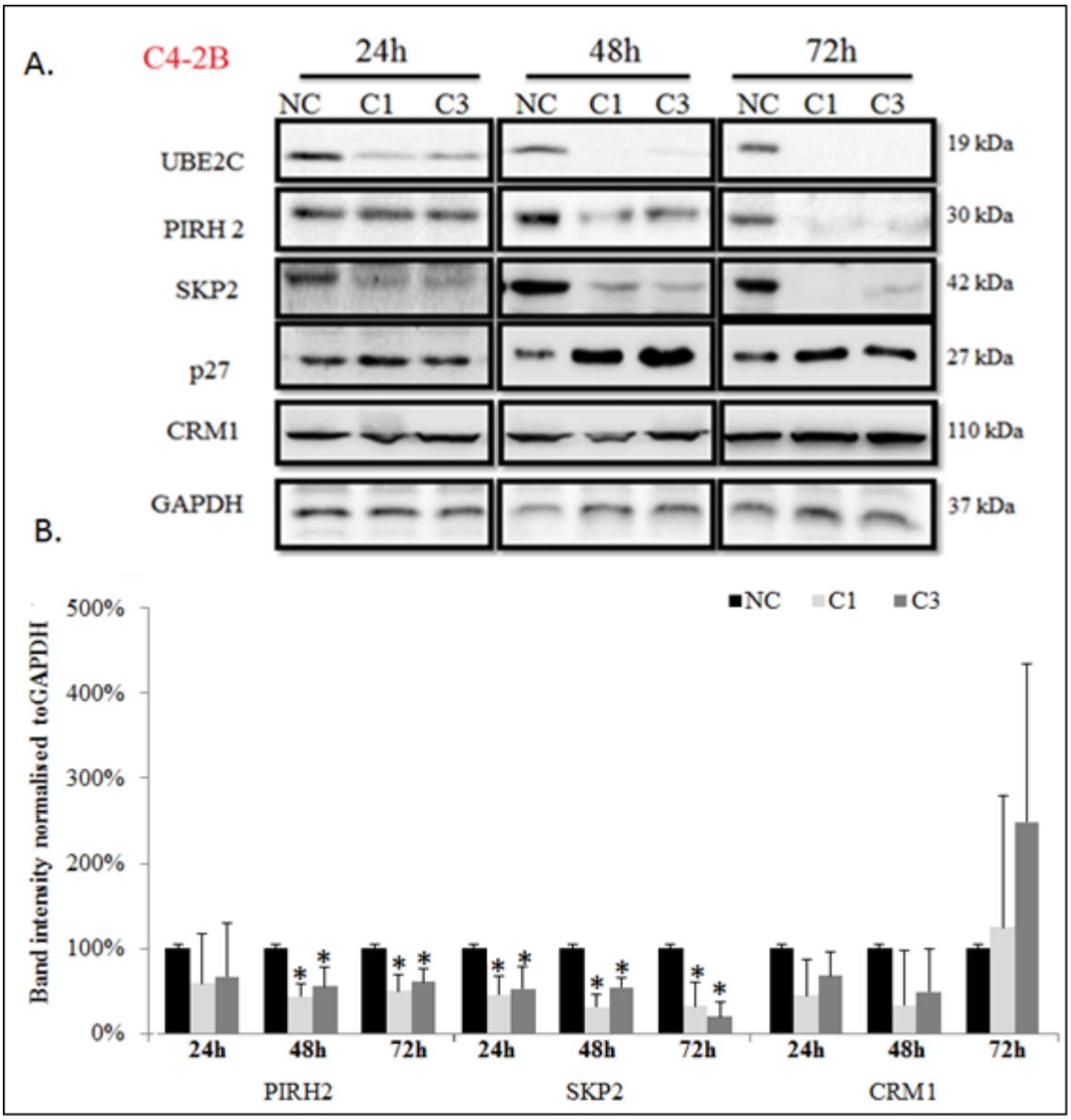


**Figure 4-5. Effect of siUBE2C on p27 protein levels in C4-2B cells by immunoblotting.**

C4-2B cells were transfected with 20 nM NC, C1 or C3. The cell culture medium was replenished 24 h following transfection. The cells were harvested 24, 48 and 72 h following transfection. Cell lysate protein (50 µg/lane) was analysed by immunoblotting. GAPDH: loading control. **A.** Representative immunoblotting image in C4-2B cells. **B**. Histogram representing densitometric analysis are mean±SD (n=3). *, P< 0.05 vs. NC at each time point.

Overall, it is interesting to note that the change in SKP2 and PIRH2 occurred prior to the change in p27 in PCa cells. Comparing with the timeframe of protein scheduled to change could provide evidence to prove that the effect of UBE2C on p27 is possibly due to the decrease of its E3 ligase-mediated degradation.

#### 4.3.2.5. Downregulation of UBE2C led to an accumulation of FBWX7 and a decrease in c-MYC levels in prostate cancer cells

c-MYC is a positive regulator of UBE2C (Zhao *et al.*, 2012) and a transcriptional repressor of p27. FBXW7 plays a key role in c-MYC protein degradation (Amati, 2004; Farrell and Sears, 2014). The effect of siUBE2C on c-MYC and FBXW7 protein levels was tested in PC-3, LNCaP and C4-2B cells. Silencing of UBE2C reduced c-MYC levels, suggesting a possible positive feedback loop between UBE2C and c-MYC (Figure 4-6). We then determined FBXW7 protein levels after 3 days of siUBE2C treatment. In all three PCa cells, suppression of UBE2C led to an elevated protein level of FBXW7 (Figure 4-6). Overall, these experiments show that the repression of UBE2C led to a downregulation of c-MYC and an upregulation of FBXW7.

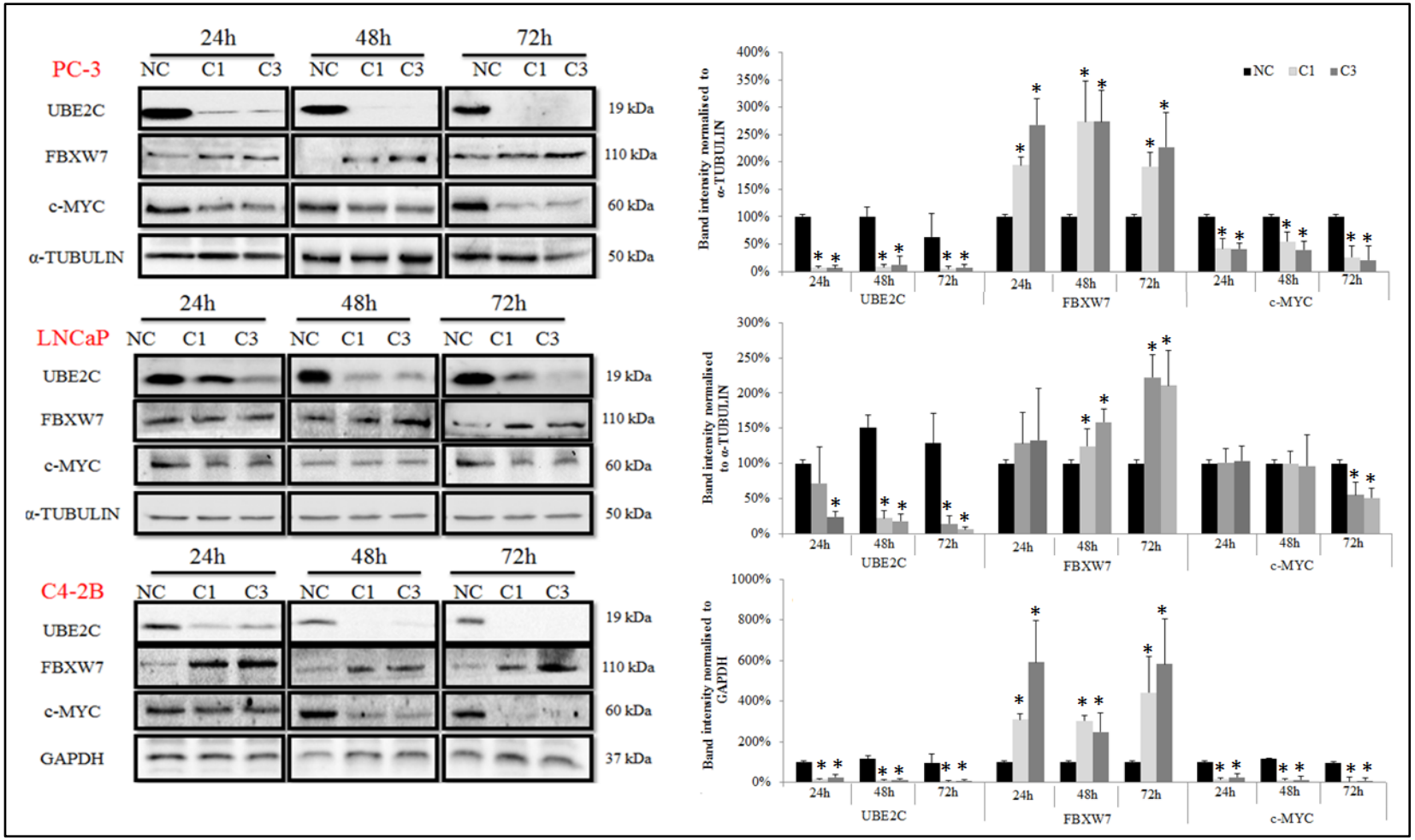


**Figure 4-6. Effect of siUBE2C on c-MYC and FBXW7 protein levels in prostate cancer cell lines.**

**A**. PC-3, **B.** LNCaP and **C.** C4-2B cells were transfected with 20 nM NC, C1 or C3. The cell culture medium was replenished 24 h following transfection. The cells were harvested 24, 48 and 72 h following transfection. Cell lysate protein (50 µg/lane) was analysed by immunoblotting. α-TUBULIN: loading control. **Left.** Representative immunoblotting image in PCa cells. **Right**. Histogram representing densitometric analysis are mean± SD (n=3). *, P< 0.05 vs. NC at each time point.

#### 4.3.2.6. Downregulation of UBE2C led to an accumulation of FBWX7 followed by a decrease in c-MYC levels in PC-3 cells

Since the protein level of UBE2C was knocked down by siUBE2C 8 h post-transfection, the sequence of the change in UBE2C, c-MYC and FBXW7 was determined. PC-3 cells were treated with siUBE2Cs or NC for 4, 8, 12, 16 and 20 h. The UBE2C level was verified by immunoblotting at indicated times with or without siUBE2C treatment. The increase of FBXW7 protein level occurred 16 h followed by UBE2C knockdown, and prior to the decrease of c-MYC protein levels in PC-3 cells (Figure 4-6 & Figure 4-7). Comparing with the timeframe of protein scheduled to change could provide some evidence to prove that the effect of UBE2C on c-MYC is possibly due to the increase of its E3 ligase-mediated degradation.

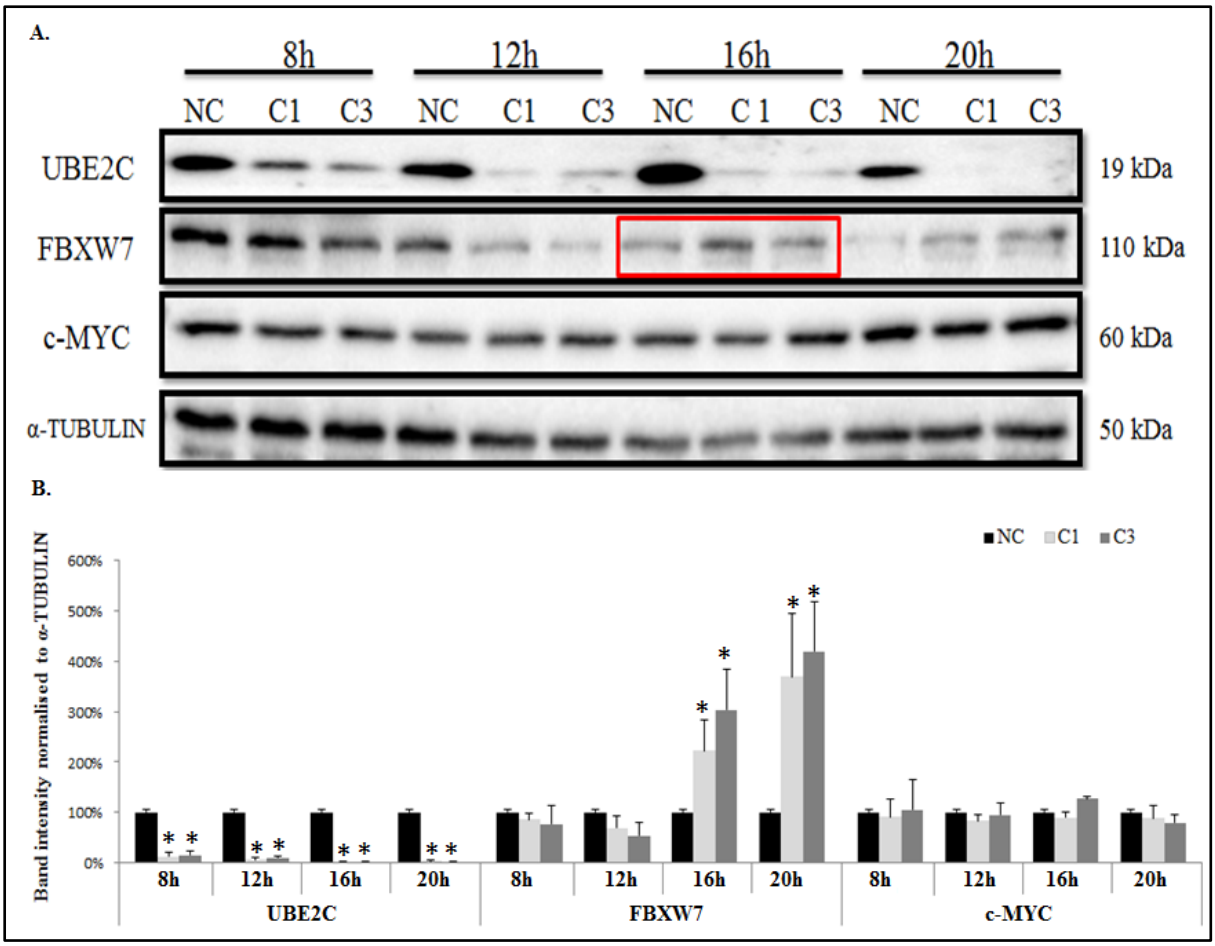


**Figure 4-7. Effect of siUBE2C on c-MYC protein levels and its regulator FBXW7 in PC-3 cells by immunoblotting with short time points.**

PC-3 cells were transfected with 20 nM NC, C1 or C3. The cells were harvested every 4 h following transfection till 20 h. Cell lysate protein (50 µg/lane) was analysed by immunoblotting. α-TUBULIN: loading control. The results are representative of three experiments. **A.** Representative immunoblotting image in PC-3 cells. **B**. Histogram representing densitometric analysis are mean±SD (n=3). *, P< 0.05 vs. NC at each time point.

### 4.3.2.7. Knockdown of UBE2C had no effect on mRNA of p27 and c-MYC in PC-3 cells

The accumulation of p27 following siUBE2C could be a result of a decrease in p27 proteasomal degradation, as supported by the reduction of SKP2 and PIRH2, or an increase in p27 gene transcription. Similarly, the siUBE2C-induced reduction of c-MYC could be a result of an increase in c-MYC proteasomal degradation, as suggested by the elevation of

FBXW7, or a decrease in c-MYC gene transcription. Hence, mRNA levels of UBE2C, p27and c-MYC after 24 h siUBE2C treatment were determined by RT-PCR. The mRNA level of UBE2C was significantly reduced ($p<0.05$), while there was no change in p27 or c-MYC mRNA levels (Figure 4-8).

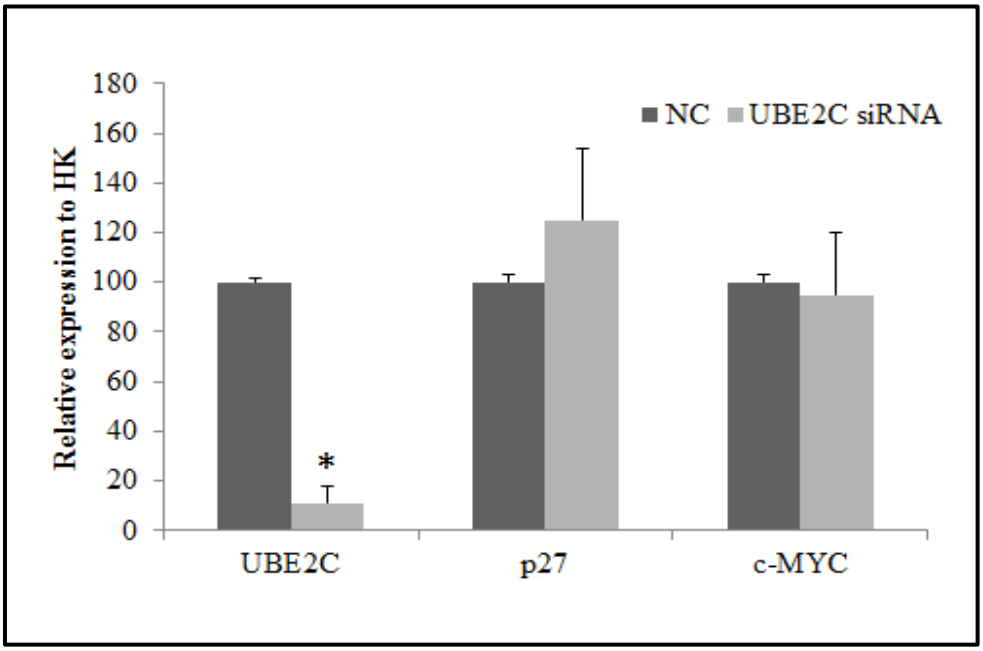


**Figure 4-8. Effect of siUBE2C on p27 and c-MYC mRNA levels in PC-3 cells by RT-PCR.**
PC-3 cells were transfected with 20 nM NC or UBE2C siRNA. The cells were harvested 24 h following transfection. Samples was analysed by RT-PCR. HK, housekeeping protein TBP was used as loading control. The results are representative of three experiments. ***** $p<0.05$ vs. NC.

Although there was some difference between the cell lines in their response to siUBE2C, the increase in p27 and decrease in c-MYC protein level in LNCaP and C4-2B cells needed longer time than for PC-3 cells (Table 4-1). The effect of UBE2C on p27 was likely via the regulation of the SKP2 and PIRH2-mediated post-translational degradation. This is because the knockdown of UBE2C reduced SKP2 and PIRH2 levels, which occurred prior to the change of p27 protein, whereas the mRNA level of p27 remained unchanged. Also, the reduction of c-MYC was mostly likely through FBXW7 mediated post-translational destruction, because the siUBE2C led to increase of FBXW7 followed by a decrease in c-

MYC protein level, while no change was found in c-MYC mRNA level. Although SKP2 can also contribute to c-MYC protein degradation, that was unlikely to have happened, because SKP2 levels were decreased after UBE2C knockdown.

**Table 4-1. The summary of the timeframe required for siUBE2C to affect the levels of key proteins in LNCaP, PC-3 and C4-2B cells compared to NC.**

| | $G_0$ increase | p27 | SKP2 | PIRH2 | c-MYC | FBXW7 | UBE2C |
|---|---|---|---|---|---|---|---|
| PC-3 | 48h | 24h | 16h | 16h | 24h | 16h | 8h |
| LNCaP | 72h | 48-72h | 48-72h | 48h | 72h | 48h | 48h |
| C4-2B | 48h | 48h | 24h | 24-48h | 24-48h | 24h | 24h |

*$G_0$ increase refers to the proportion of cells at $G_0$ phase that were significantly increased at the indicated time.

## 4.4. Discussion

In our experiment, the expression of UBE2C in PCa played a vital role in cell cycle regulation, involved in regulating the transition between quiescent and proliferative cells. The objective of this study was to identify the underlying mechanism of UBE2C in regulation of cell quiescence. We first defined a role of UBE2C on p27 and its regulators, including SKP2 and PIRH2. In addition, we showed the level of c-MYC also decreased, whereas FBXW7, which targets c-MYC for proteolysis, was increased by siUBE2C.

### 4.4.1. UBE2C influenced cell quiescence via mechanisms involving p27

In our study, we screened several key cell cycle regulators for their ability to regulate cell quiescence, including $G_0$-maintained protein p27. p27, a tumour suppressor, overexpression

of p27 is sufficient to arrest cells in quiescent state (Chu *et al.*, 2008). Downregulation of UBE2C expression by siUBE2C increased p27 protein level. Knockdown of UBE2C decreased the protein levels of SKP2 and PIRH2, which are components of E3 ligases responsible for p27 proteolysis. However, depleting UBE2C did not result in changed p27 mRNA levels. Therefore, the effect of UBE2C on p27 was likely via regulation of the SKP2- and PIRH2-mediated post-translational degradation.

Further investigation on the sequential change of UBE2C, p27 and its regulators, confirmed that the change in levels of p27 occurred after SKP2 and PIRH2 were reduced (Table 4-1). Although there was some difference between the cell lines in their response to siUBE2C – the increase in p27 and decrease in c-MYC protein level in LNCaP and C4-2B cells took longer than that required in PC-3 cells – the accumulation of quiescent PCa cells occurred after the accumulation of p27 in all three PCa cell lines. Collectively, under siRNA treatment of UBE2C, at least in part, p27 functioned as a $G_0$-maintenance protein to retain cells in a quiescent state. The control mechanism of UBE2C was likely via SKP2 and PIRH2, rather than a more direct relationship with p27.

In addition, it is generally believed that the degradation of p27 requires its cytoplasmic relocalisation (Rodier *et al.*, 2001). Low cytoplasmic levels of p27 are associated with cancer aggressiveness and poor clinical prognosis (Chu *et al.*, 2008). CRM1, a p27 nuclear exporter, remained unchanged by siUBE2C. Therefore, downregulation of UBE2C had no impact in CRM1-mediated p27 cytoplasm translocation, suggesting the mechanism behind UBE2C in regulating cell cycle is irrelevant to the regulation of p27 subcellular location.

### 4.4.2. UBE2C influenced cell quiescence via mechanisms involving c-MYC

In addition, c-MYC is a cellular proto-oncogene. The expression of c-MYC is low in quiescent cells and increase upon cell cycle re-entry (Kelly *et al.*, 1983). Amplification of c-MYC is found in nearly half of all human solid tumours (Beroukhim *et al.*, 2010), including thirty percent of PCa (Bretones *et al.*, 2015). Suppression of UBE2C decreased c-MYC protein levels together with an increase of FBXW7 level. FBXW7 is one of the few proteins targeting c-MYC for degradation and inhibiting c-MYC transcriptional activity (Amati, 2004; Farrell and Sears, 2014). Although SKP2 is another component of E3 ligases responsible for c-MYC proteolysis, SKP2 is decreased in UBE2C knockdown cells and is therefore unlikely to be involved in c-MYC degradation. Additionally, UBE2C knockdown led to a decrease in c-MYC protein level, while no impact was found in c-MYC mRNA level. Thus, our results indicated that the reduction of UBE2C mediated c-MYC was more likely post-translational and FBXW7-dependent. Our observation suggested that knockdown of UBE2C increased FBXW7 level, resulting in the sequential degradation of c-MYC protein levels and subsequent $G_0$ accumulation (Table 4-1). Therefore, the effect of UBE2C on the proportion of quiescent cancer cells was via a pathway involving c-MYC.

In addition, early studies showed the regulation of c-MYC on `cell quiescence, at least in part through its ability to directly repress *p27* gene transcription (Bretones *et al.*, 2015; Chandramohan *et al.*, 2008). However, the change in c-MYC and p27 occurred at a similar time, so it is unlikely the increase of p27 was due to the decrease of c-MYC. Further study is required to determine whether c-MYC plays a role in regulating p27 in PCa cells with UBE2C knockdown.

It is unclear whether the regulation of E3 ligases by UBE2C, including SKP2, PIRH2 and FBXW7, is direct or indirect. Further study is needed to determine the mechanism of how UBE2C controls p27 and c-MYC through its post-translational regulation. There are three possible steps of overexpression of UBE2C in regulating cell proliferation: (1) increase the pool of active APC/C; (2) inactivate the mitotic checkpoint; and (3) enhance cell cycle progression from $G_2$/M to $G_1$ phase (Chen *et al.*, 2011; Reddy *et al.*, 2007; Wang *et al.*, 2011; Wang *et al.*, 2009). However, the current understanding of the catalytic role of UBE2C in UPS is unable to explain our observations of p27 protein levels. SKP2 is one of 55 targets of APC/C; we speculated that knockdown of UBE2C would increase APC/C target proteins, and thus decrease p27. Unexpectedly, downregulation of UBE2C decreased SKP2 protein levels. Although c-MYC is also reported to induce the expression of *SKP2* (Bretones *et al.*, 2011; Keller *et al.*, 2007; O'Hagan *et al.*, 2000); a decrease in c-MYC by UBE2C can explain the decrease in SKP2. However, the SKP2 protein level was decreased before the decrease of c-MYC. Also, we found no change in SKP2 mRNA following UBE2C siRNA treatment (data not shown). Hence, c-MYC is unlikely to be the cause of the reduction of SKP2 protein level. Further study is required to identify the role of UBE2C in SKP2 regulation.

In summary, we have established two novel observations:

i. UBE2C can downregulate p27 expression, possibly through augmenting SKP2 and PIRH 2 expression.

ii. UBE2C can upregulate c-MYC, possibly through reducing FBXW7 expression.

The possible pathway of UBE2C in regulating cell quiescence is proposed in Figure 4-9.

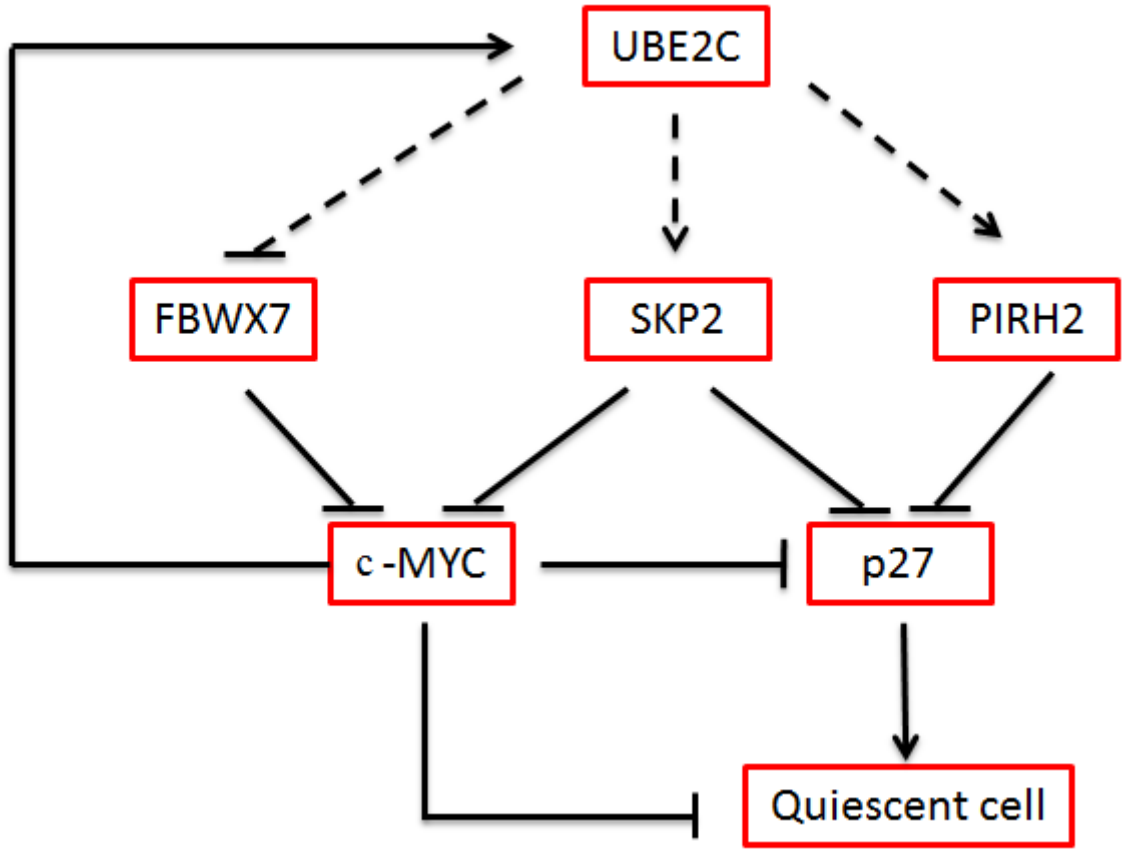


**Figure 4-9. The proposed mechanism of UBE2C in regulating cell quiescence.**

# Chapter 5

# 5. Concordance Between UBE2C Expression Levels and Progression of Prostate Cancer

# 5.1. Introduction

Worldwide, one patient dies from PCa every 4 minutes (Assinder *et al.*, 2015). This significant mortality is a result of limited treatment options available (Assinder *et al.*, 2015). Active surveillance is a viable management option for men with low-grade, clinically localised PCa. However, approximately 30–40% of men on active surveillance will progress to high-grade disease over 5 years, which mandates surgery or radiation (Singh *et al.*, 2010). At the advanced stage, when metastases occur, PCa is treated with ADT but development of CRPC becomes inevitable in a majority of cases when ADT fails. Patients with CRPC have an average survival time of 16–18 months after recurrence (Liu *et al.*, 2015). Recently treatment of PCa entered the era of personalised therapy. Treatment on a personal basis now involves a simultaneous case-specific analysis of clinical and pathological characteristics and distinguishes at diagnosis men who have a potentially lethal, indolent course of disease. Analysis of a patient's genetic and tumour biomarker profiles enables selection of suitable individualised treatment for PCa. Therefore, there is an acute need to discover predictive prognostic biomarkers.

The *UBE2C* gene has been associated with malignant transformation and aggressiveness of many solid tumours. *UBE2C* mRNA is barely detectable in the majority of normal tissues (Okamoto *et al.*, 2003). In contrast, *UBE2C* mRNA and/or protein is expressed at high levels in leukaemia, lymphoma and melanoma, and various cancers – thyroid, oesophageal, breast, ovarian, lung, gastric, colon, bladder and uterine (Okamoto *et al.*, 2003; Vasiljevic *et al.*, 2013; Wagner *et al.*, 2004; Xie *et al.*, 2014). An association between the levels of UBE2C protein and tumour grade/poor prognosis is reported in cancers of the adrenal gland, breast, colon, liver, lung and ovary (Okamoto *et al.*, 2003; van Ree *et al.*, 2010; Zhao *et al.*, 2012).

In PCa, UBE2C level is undetectable in normal prostate tissue (Okamoto *et al.*, 2003), low in HSPC and high in CRPC (Tzelepi *et al.*, 2012; Wang *et al.*, 2009).

To date, only one report exits with regard to the protein level of UBE2C in PCa progression, describing evidence for an overexpression of UBE2C in CRPC (n=230) compared to HSPC (n=98) and BPH (n=44) (Wang *et al.*, 2009). Although this previous study was based on large numbers of patients with PCa, the association between UBE2C expression and clinical prognosis of PCa patients has not been fully defined. Hence, in this chapter, we aimed to determine whether UBE2C expression was associated with PCa stage and grade. The expression of UBE2C in PCa and non-cancerous prostate tissues was detected by immunohistochemical analysis. The association between UBE2C expression and clinicopathological characteristics of PCa patients was also evaluated in public gene expression datasets to test the hypothesis that UBE2C is a potential prognostic biomarker and therapeutic target for PCa.

# 5.2. Materials and Methods

## 5.2.1. Human tissue preparation

The collection of patient specimens for the analysis in this study was approved under the Central Sydney Area Health Service (X04-318) and Western Area Health Service Ethics Committee [HREC2000/9/4.18 (1089)]. Human tissue samples were prepared as described in **Chapter 2.6.2**.

### 5.2.2. Immunohistochemistry

Expression of UBE2C in the human PCa sample was determined by immunohistochemical staining. The staining was performed as described in **Chapter 2.6.3.** The staining intensity was graded by a pathologist.

### 5.2.3. Gene expression analysis of human prostate cancer dataset

The mRNA correlation analysis on *UBE2C* was performed across ONCOMINE datasets corresponding to metastatic PCa. All data were log-transformed provided by ONCOMINE. Pairwise signature comparisons were performed using a student *t-test* or one-way ANOVA. $p<0.01$ was considered significant. The description of datasets is summarised in Table 5-1.

**Table 5-1. Summary of prostate datasets downloaded from ONCOMINE.**

| Dataset | BPH | Primary | Metastasis | Total (n) | *p* value | Year | Source | Platform |
|---|---|---|---|---|---|---|---|---|
| Arredouani | 8 | 13 | - | 21 | 8.20E-03 | 2009 | *Clin Cancer Res* | Human Gene U133 Plus 2.0 array |
| Chandran | - | 10 | 21 | 31 | *p*<0.0001 | 2007 | *BMC* | CodeLink UniSet Human 20K I Bioarray |
| Grasso | 28 | 59 | 34 | 122 | *p*<0.0001 | 2012 | *Nature* | Agilent Human Genome 44K |
| laTulippe | - | 23 | 9 | 32 | *p*<0.0001 | 2002 | *Cancer Res* | Human Genome U95A-Av2 Array |
| Lapointe | 41 | 62 | 9 | 112 | *p*<0.0001 | 2004 | *Proc Natl Acad Sci USA* | not defined |
| Luo | 9 | 16 | - | 25 | 3.00E-04 | 2001 | *Cancer Res* | not defined |
| Magee | 4 | 8 | 3 | 15 | 1.10E-03 | 2001 | *Cancer Res* | Human GeneFL Array |
| Taylor | 29 | 131 | 19 | 179 | *p*<0.0001 | 2010 | *Cancer cell* | RefSeq Genes |
| Varambally | 5 | 7 | 6 | 18 | *p*<0.0001 | 2005 | *Cancer cell* | Human Gene U133 Plus 2.0 array |
| Yu | 23 | 64 | 24 | 111 | *p*<0.0001 | 2004 | *J Clin Oncol* | Human Genome U95A-Av2 Array |
| | Grade 2 | Grade 3 | Grade 4 | | | | | |
| Bittner | 23 | 32 | 3 | 58 | 1.00E-04 | 2005 | not published | Human Gene U133 Plus 2.0 array |
| Gleason Grade | 6 / 3+4 | 4+4 / 8 | 9 / 10 | | | | | |
| Setlur | 110 / 98 | 55 / 41 | 54 / 5 | 363 | *p*<0.0001 | 2008 | *J Natl Cancer Inst* | Illumina DASL Transcriptionally Informative Gene Panel |

*p* value indicates statistical significance vs. BPH in Arredouani, Grasso, Taylor, Varambally, Magee, Lapointe, Luo and Yu dataset.
*p* value indicates statistical significance vs. primary PCa in Chandran and LaTulippe dataset.
*p* value indicates statistical significance vs. Grade 2 in Bittner dataset.
*p* value indicates statistical significance vs. Gleason grade 6 in Setlur dataset.

### 5.2.4. Statistical analysis

The statistical software NCSS version 12.0 was used for statistical analysis as described in **Chapter 2.8**. ONCOMINE analysis used the student *t*-test or one-way ANOVA in GraphPad Prism v.6. Data are expressed as mean±SD.

## 5.3. Results

### 5.3.1. Protein level of UBE2C in human prostate cancer tissue

#### 5.3.1.1. Expression of UBE2C was higher in prostate cancer tissues compared with unpaired BPH

To determine the expression of UBE2C in human prostate tissue, immunohistochemistry staining against UBE2C was performed. Negative UBE2C staining was observed in 95% of unpaired BPH samples (n=36; Figure 5-1A, left). Weak staining of UBE2C was exhibited in 2 out of 36 (5.5%) BPH patients. In contrast, positive staining of UBE2C protein was found in 52 of 70 (74.3%) PCa cases treated with radical prostatectomy and transurethral resection of prostate specimens (Figure 5-1A right). Analysis of the UBE2C positivity of cells with low or high intensity staining between BPH and cancer specimens was significantly different ($p$=0.001; Figure 5-1B). The staining was localised in both nucleus and cytoplasmic staining (Figure 5-1A).

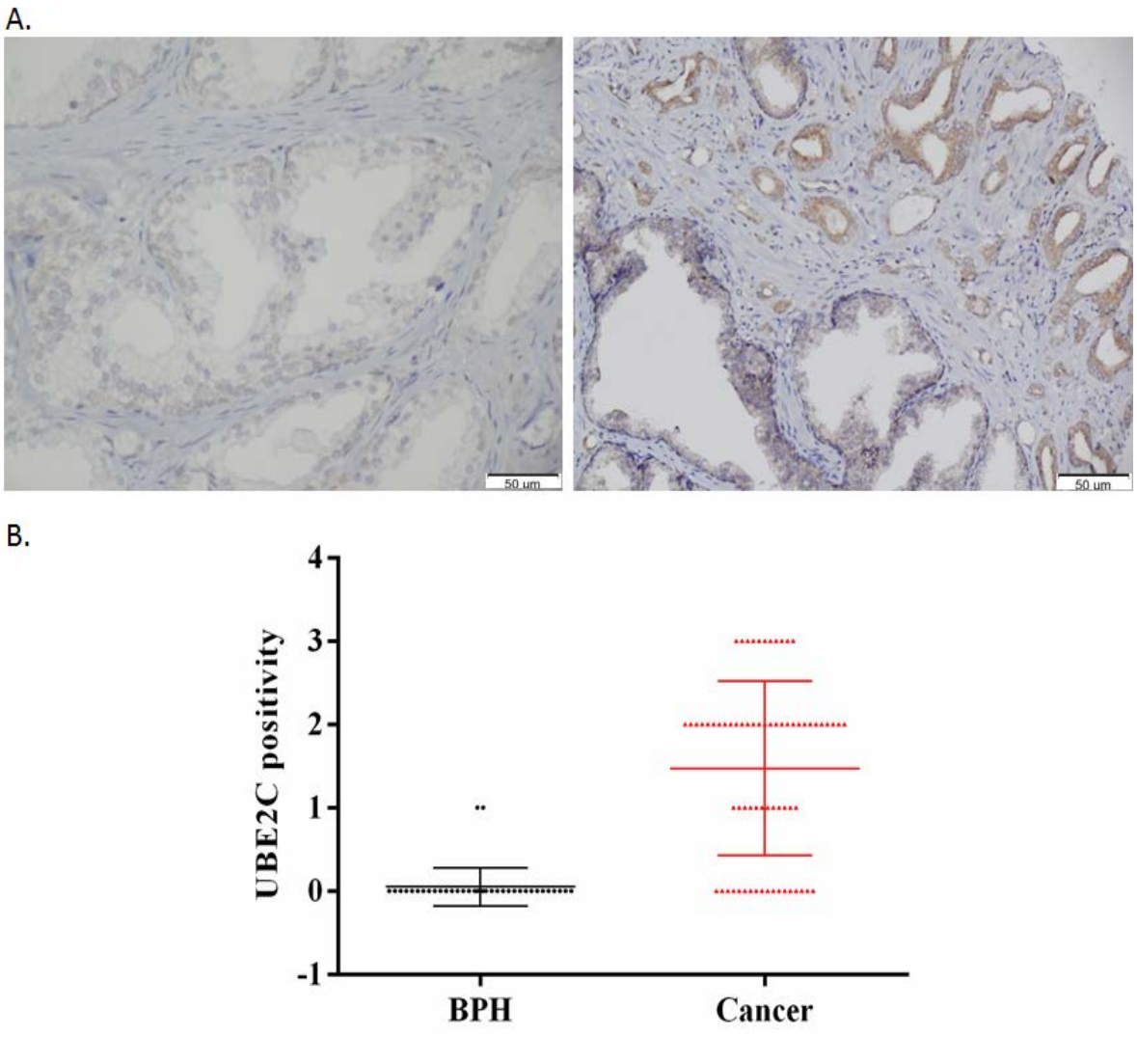


**Figure 5-1. Expression of UBE2C in prostate tissues by immunohistochemical staining of UBE2C.**

UBE2C was immunostained in human prostate tissue containing unpaired BPH (n=36) and PCa (n=70). **A.** Representative tissue stained with antibody against UBE2C (magnification X200). BPH tissue (Left) and PCa tissue (Right). **B.** $p$=0.001 between unpaired BPH and cancer by unpaired $t$-test. IHC staining for UBE2C in tissues was scored by pathologist: 0, negative; 1, weak staining; 2, intermediate; and 3, strong.

#### 5.3.1.1 Expression of UBE2C was higher in prostate cancer compared with adjacent non-malignant tissue

To further verify the expression of UBE2C in human prostate tissue, we compared the immunostaining of UBE2C in PCa areas with adjacent non-malignant tissue (n=17). The staining of UBE2C was significantly higher in PCa tissue compared with non-malignant prostate epithelia by immunohistochemical analysis ($p<0.01$; Figure 5-2A). In 13 out of 17 (76.5%) paired samples, there was a clear increase in UBE2C staining in the PCa disease status ($p=0.001$; Figure 5-2B). The remaining 4 pair samples were negative for UBE2C staining in both non-malignant prostate and PCa tissues.

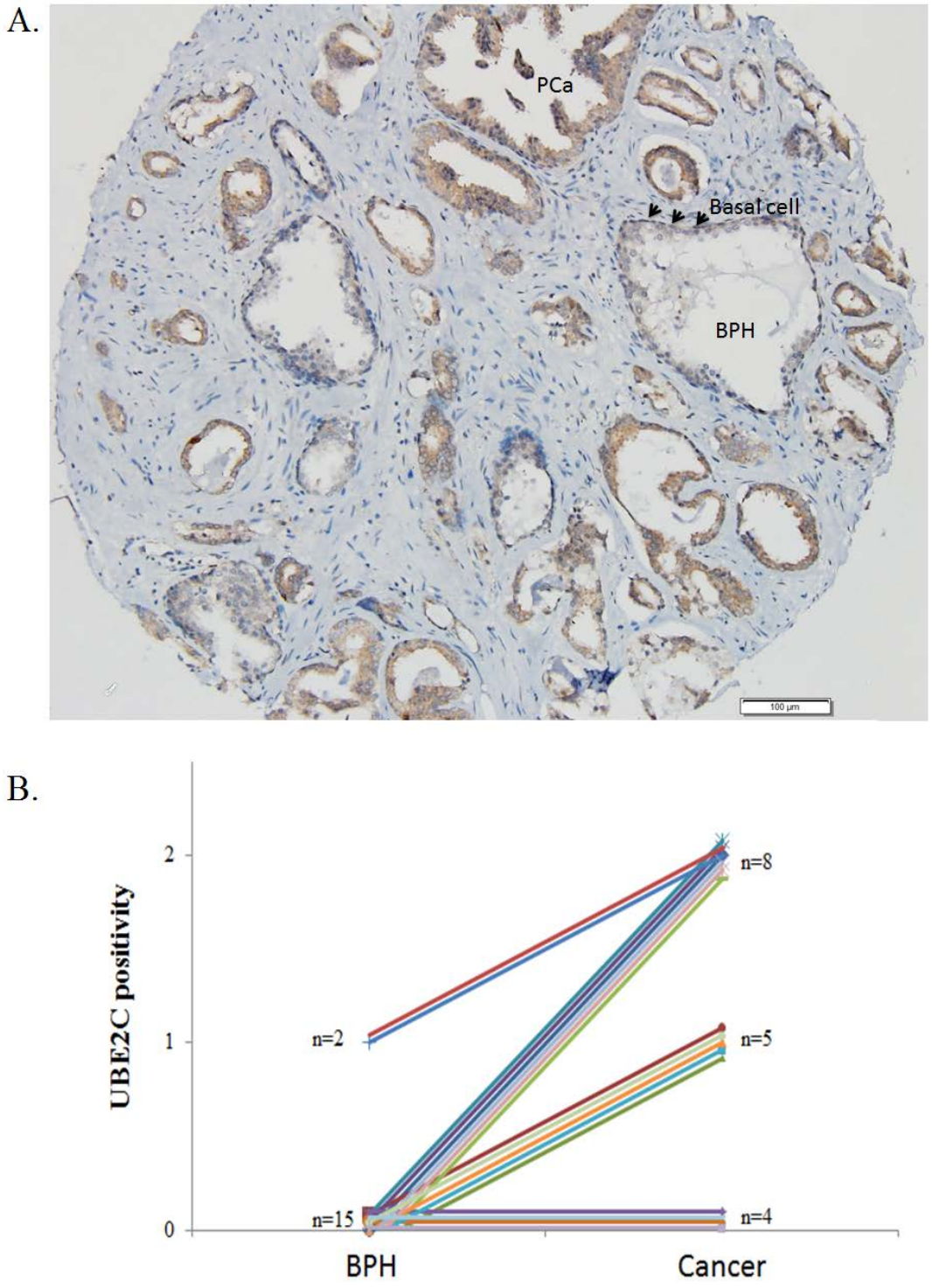


**Figure 5-2. Expression of UBE2C in paired non-malignant and malignant prostate tissues by immunohistochemical staining of UBE2C.**

UBE2C was immunostained in tissues containing adjacent BPH and PCa tissue (n=17). **A.** Representative tissue stained with anti-UBE2C antibody (magnification X100). **B.** $p$=0.001 between paired BPH and PCa by paired $t$-test. IHC staining for UBE2C was scored by pathologist: 0, negative; 1, weak staining; 2, intermediate; and 3, strong.

#### 5.3.1.2 Expression of UBE2C was higher in castration-resistant prostate cancer (CRPC) compared with patient-matched hormone sensitive prostate cancer (HSPC)

To further investigate whether development of hormone refractory PCa is associated with changes in UBE2C, we compared the immunostaining of UBE2C in HSPC obtained by transurethral resection of prostate (n=8; Figure 5-3A, left) with the same patient samples once the patient had reached castration-resistant status and required a repeat transurethral resection of the prostate (Figure 5-3A, right). The protein levels of UBE2C were found to increase in CRPC tissue compared with that in HSPC tissue in six out of eight (75.0%) paired samples ($p$ =0.003; Figure 5-3B). While the other two sets were stained with UBE2C with intermediate intensity in both HSPC and CRPC tissues, the staining intensity did not change appreciably with disease progression.

Collectively, high-grade PCa showed intense, uniform staining for UBE2C that was significantly different from that in adjacent BPH or HSPC, both of which showed only focal or weak UBE2C staining. Further, UBE2C was associated with high-grade histological tumours in individual cases.

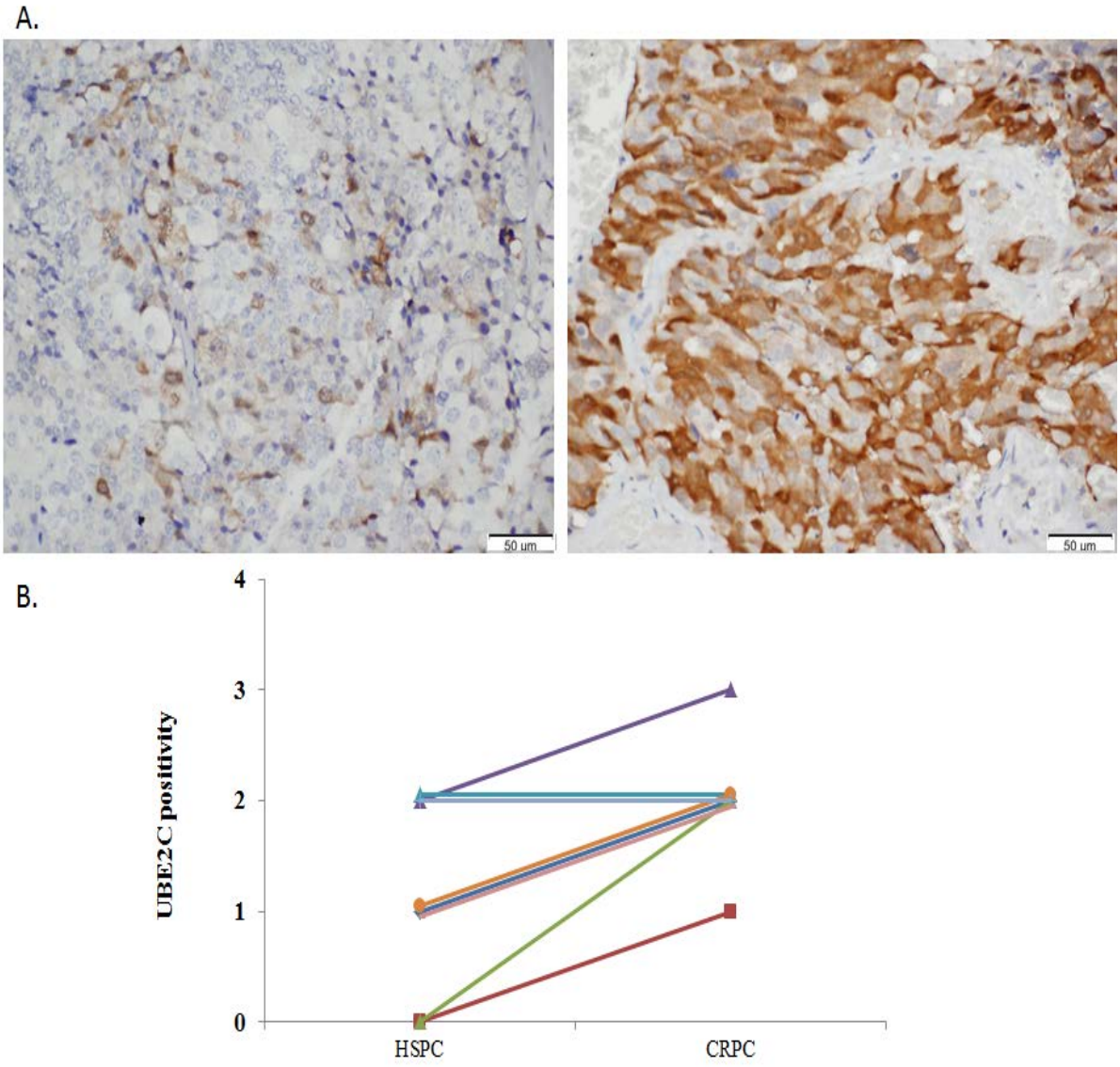


**Figure 5-3. Expression of UBE2C in paired HSPC and CRPC tissues by immunohistochemical staining.**

UBE2C was immunostained in TMA containing paired hormone sensitive (HSPC) and castration resistant PCa (CRPC; n=8). **A.** Representative tissue stained with antibody against UBE2C (magnification X200). HSPC tissue (Left) and CRPC tissue (Right). **B.** $p$=0.003 between paired HSPC and CRPC by paired $t$-test. The IHC staining for UBE2C in tissues was scored by pathologist: 0, negative; 1, weak staining; 2, intermediate; and 3, strong.

### 5.3.2 mRNA of UBE2C in human prostate cancer tissues

UBE2C was found to be aberrantly overexpressed in CRPC when compared to HSPC, offering a rationale to investigate UBE2CmRNA in primary, advanced by tumour grade, and metastatic PCa. Twelve datasets was downloaded from the ONCOMINE database (www.oncomine.org), which is a web-based database of a curated collection of cancer microarrays. The studies used Affymetrix, the spotted cDNA or oligonucleotide microarray platforms for gene expression analysis (Table 5-1), except the Lapointe and Luo prostate datasets, for which the microarray platforms were not specified in ONCOMINE.

#### 5.3.2.1 Overexpression of UBE2C in prostate cancer tissues

To determine whether PCa is associated with UBE2C expression, *UBE2C* mRNA expression was examined in the Arredouani and Luo prostate datasets. Arredouani (n=21) and Luo (n=25) prostate datasets contain microarray results of BPH and primary PCa samples. Examining the mRNA level of *UBE2C* in the two independent datasets revealed a positive correlation of PCa and UBE2C expression ($p<0.01$; Figure 5-4A&B).

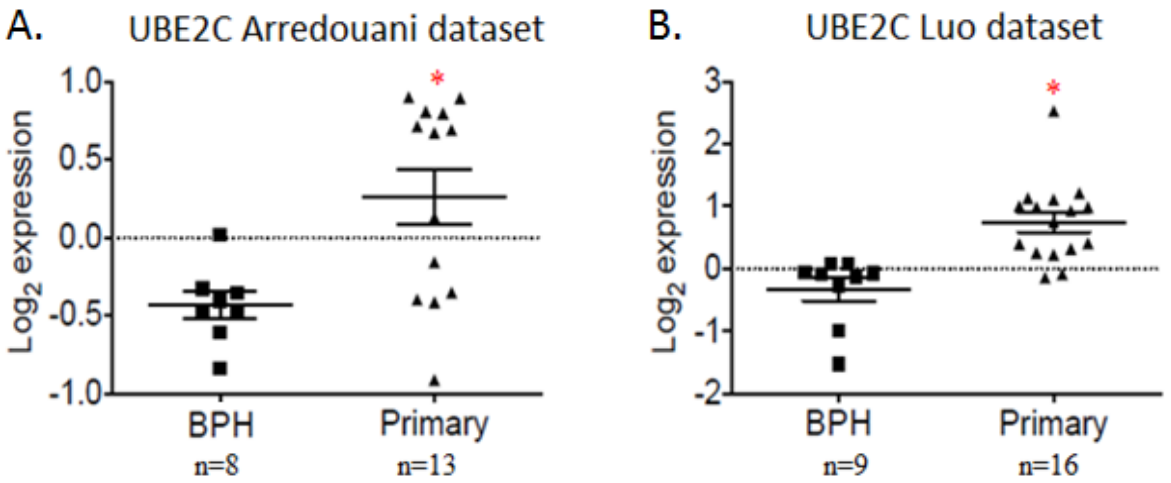


**Figure 5-4. UBE2C mRNA level in BPH and prostate cancer tissues.**

The UBE2C mRNA levels in BPH and primary cancer tissue are plotted in **A.** Arredouani dataset (n=21) and **B.** Luo dataset (n=25). Data are mean±SD. * $p<0.01$ compared to BPH by unpaired *t*-test.

### 5.3.2.2 Overexpression of UBE2C in high grade prostate cancer tissues

To determine whether UBE2C expression is associated with tumour grade, the *UBE2C* mRNA expression was examined in the Bittner prostate dataset. The expression of UBE2C showed a significant correlation with increased tumour grade (Figure 5-5A). In addition, PCa patients were sorted by Gleason grade in the Setlur prostate dataset. There were significant differences in expression of UBE2C in tumours with Gleason grades of 8/9 (n=95) versus Gleason grades of 6 (n=110; $p<0.01$; Figure 5-5B). Nevertheless, there was no statistical difference in UBE2C expression between tumours with Gleason 7 (n=153) and Gleason 6 (n=110).

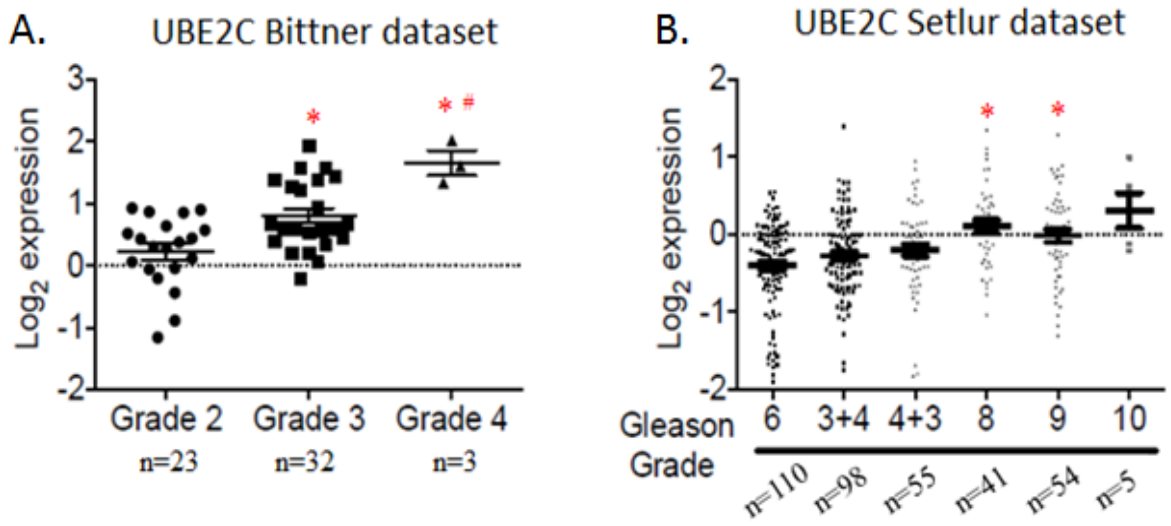


**Figure 5-5. Association of UBE2C mRNA level and tumour grade in prostate cancer tissues.**

**A.** UBE2C expression in tissues with different Gleason scores (n=58) * $p<0.01$ compared to Grade 2 by unpaired *t*-test, # $p<0.01$ compared to Grade 3 PCa by unpaired *t*-test.
**B.** UBE2C expression in tissues with different Gleason score (n=363). Data are mean±SD. * $p<0.01$ compared to Gleason Grade 6 by unpaired *t*-test.

### 5.3.2.3 High expression of UBE2C in metastatic prostate cancer tissues

To compare the microarray signature of PCa with or without metastasis studies, eight datasets were analysed (Figure 5-6). The mRNA level of UBE2C was investigated in six prostate datasets (Grasso, Lapointe, Magee, Taylor, Varambally and Yu), containing BPH, primary and metastatic PCa samples. In six independent prostate datasets, enriched UBE2C expression was found in metastatic PCa versus primary PCa and BPH samples ($p<0.01$; Figure 5-6A–F). Additionally, in the Chandran and LaTulippe datasets, there was a significant increase in UBE2C expression in the presence of PCa metastatic samples compared to primary PCa ($p<0.01$; Figure 5-6G–H). Furthermore, analysis of the Taylor prostate dataset also revealed significant increases in UBE2C expression in primary PCa compared with BPH ($p<0.01$; Figure 5-6B).

Taken together, enhanced UBE2C expression was positively correlated to tumour stage and grade, suggesting UBE2C is a prognostic biomarker as well as a potential therapeutic target in PCa.

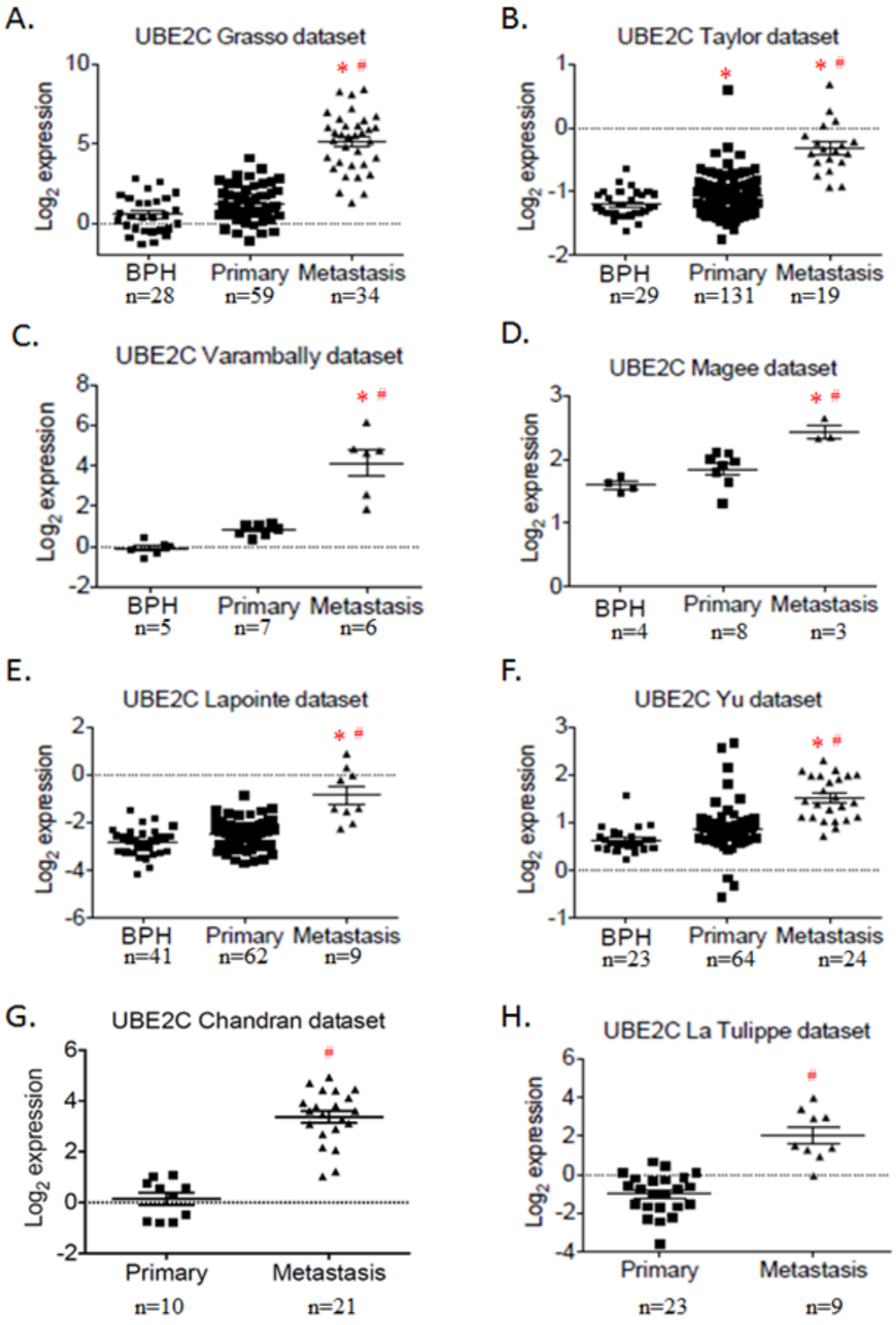


**Figure 5-6. Association of UBE2C mRNA level and pathological features in prostate cancer tissues.**

**A–F.** UBE2C relative expression in BPH, primary and metastasised PCa samples in **A**, Grasso dataset (n=122); **B**, Taylor dataset (n=179); **C**, Varambally dataset (n=18); **D**, Magee dataset (n=15); **E**, Lapointe dataset (n=112); and **F**, Yu dataset (n=111). UBE2C mRNA expression in primary and metastasised PCa tissues in **G**, Chandran dataset (n=31) and **H**, La Tulippe dataset (n=32). Data are mean±SD. * $p<0.01$ compared to BPH by unpaired *t*-test, # $p<0.01$ compared to primary PCa by unpaired *t*-test.

## 5.4 Discussion

UBE2C is highly expressed in PCa (Tzelepi *et al.*, 2012; Wang *et al.*, 2009), whereas it is undetectable in normal prostate tissue (Okamoto *et al.*, 2003). UBE2C has been associated with malignant progression and aggressive invasion of tumours, and is predictive of poor survival and a high risk of relapse in wide range of solid tumours (Ma *et al.*, 2016; Xie *et al.*, 2014). Since UBE2C is a prominent proto-oncogene, which is causally involved in tumour development, the association of UBE2C to PCa progression has attracted attention (van Ree *et al.*, 2010). The objective of this study was to determine whether UBE2C expression is a potential prognostic biomarker and therapeutic target for PCa. The expression of UBE2C in PCa and non-cancerous prostate tissues was detected by immunohistochemical analysis. The paired HSPC and CRPC samples from the same patients were also included to verify the correlation of UBE2C expression to disease progression, so that individual variation could be avoided. We also used a public gene expression dataset to determine the association between UBE2C mRNA expression and clinicopathological characteristics.

### 5.4.1 UBE2C protein level in human prostate cancer tissue

The present study evaluated the expression levels of UBE2C in 70 human PCa tissues and 36 non-cancerous prostate tissue specimens. We have shown that UBE2C is present in PCa tissue, but absent in the majority (95%) of non-cancerous prostate tissues. The expression levels of UBE2C in PCa tissues were significantly higher compared to BPH by immunohistochemistry analysis. In 17 patient-matched pairs, 76% of patients with PCa showed higher UBE2C staining compared to their corresponding matched BPH. This result was consistent with previous data published by Okamoto *et al.* (2003).

Furthermore, the immunohistochemical analysis of paired specimens indicated that UBE2C protein expression was increased in CRPC compared with HSPC, suggesting the relation of UBE2C with disease progression ($p<0.01$; Figure 5-3). Although this study was small in numbers, the expression of UBE2C was determined in PCa tissue before disease progressed, and the tissues from the same men were examined when they reached castration resistant status; thus, each man acted as his own control.

Our results were consistent with previous studies, which have revealed the association of UBE2Cwith the malignant transformation and tumour progression of PCa tissues (LaTulippe *et al.*, 2002). *UBE2C* gene expression has also been reported to increase with advancing pathological stages in nasopharyngeal carcinoma, thyroid cancer, esophageal squamous cell carcinoma, colorectal cancer and glioma (Ma *et al.*, 2016; Wang *et al.*, 2009; Xie *et al.*, 2014). Additionally, an overexpression of UBE2C stimulated cell proliferation and invasion in PCa cells (Shuliang *et al.*, 2013; Wang *et al.*, 2009). Collectively, the immunohistochemical analysis shows that UBE2C may be vital in the aggressive progression of PCa.

### 5.4.2 UBE2C mRNA level in human prostate cancer tissue

The association between UBE2C expression and the clinical prognosis of PCa patients has not been fully assessed. ONCOMINE datasets on PCa have shown an upregulation of *UBE2C* gene expression. We incorporated the expression of UBE2C for primary-localised, metastasised and advanced tumour grade PCa. A higher UBE2C expression was associated with a significantly increased tumour stage and tumour grade. There is limited prior work examining *UBE2C* gene expression compared with both disease stage and grade. Setlur *et al.* (2008) and his colleagues yielded a list of about 100 pathways that were significantly dysregulated by comparing the program of gene expression in a model of the progression of

HSPC to CRPC. The ubiquitin proteasome pathway is one of the few identified pathways that are dysregulated during PCa aggressive invasion. By comparing the program of gene expression of *UBE2C* in a model of the progression of HSPC to CRPC and protein expression from actual CRPC cases, we found that the expression of UBE2C – an E2 enzyme in the ubiquitin proteasome pathway – was involved in PCa disease progression. This is consistent with Penney (2011), who found expression of UBE2C predicted tumour grade in PCa by measuring the mRNA expression in the Swedish Watchful Waiting cohort (n=358) and Physician's Health Study (n=109). The *UBE2C* mRNA signature to PCa Gleason grade was comparing in individuals with tumours of Gleason scores ≤6 to those ≥ 8, and Gleason of 7 was applied to differentiate lethal cases (Penney *et al.*, 2011). More recently, similar results were reported in Kuner's group which found maternal embryonic Leucine zipper kinase (MELK) – which was highly associated with UBE2C expression – also correlated with PCa tumour grade (Gleason grade ≥4+3 vs. ≤3+4) (Kuner *et al.*, 2013). These clinical findings were replicated *in vitro*, with overexpression of UBE2C found to increase PCa cell proliferation and invasion by MTT assay, colony formation and matrigel invasive assay (Shuliang *et al.*, 2013).

In summary, it has been suggested that UBE2C represents a promising cancer biomarker. Therefore, UBE2C overexpression may be used as a predictor of poor prognosis in patients with PCa. We hope our finding will facilitate further research, ultimately leading to the improved understanding of cancer and the development of novel diagnostic and therapeutic strategies.

# Chapter 6

# 6. Final Discussion

# 6.1 Discussion

UBE2C is an E2 enzyme that facilitates UPS-mediated precise destruction of key cell cycle regulators during cell division (Rape, 2010; Reddy *et al.*, 2007). Aberrantly expressed UBE2C has been reported in a variety of cancers including PCa (Hao *et al.*, 2012; Xie *et al.*, 2014). Earlier studies showed that accumulation of UBE2C stimulates cell proliferation, whereas silencing UBE2C decreases cell proliferation in PCa cells (Chen *et al.*, 2011; Wang *et al.*, 2011; Wang *et al.*, 2009). However, the effect of UBE2C on cell quiescence has not been examined.

In this PhD project, I found that UBE2C may play a causal role in cell cycle exit and re-entry in PCa cell lines. Inhibition of UBE2C by genetic silencing led to accumulation of quiescent cells, while increase in UBE2C expression by expression vector decreased the proportion of quiescent PCa cells. Overexpression of UBE2C impeded cell cycle exit to $G_0$, and knockdown of UBE2C delayed cell cycle re-entry by quiescent PCa cells. Therefore, UBE2C may regulate the proportion of cells at quiescence through two possible cellular mechanisms: UBE2C inhibits cell exit to $G_0$ and promotes cell re-entry by quiescent cells.

The molecular mechanism of UBE2C action on the regulation of cell quiescence is likely via $G_0$ regulatory proteins including p27 and c-MYC. The RT-PCR results suggested the regulation of UBE2C on p27 and c-MYC expression was post-translational, as no significant change in mRNA levels of p27 and c-MYC was detected. The immunoblotting results also suggested that UBE2C may have played a regulatory role in E3 ligases responsible for p27 (*i.e.*, SKP2 and PIRH2) and c-MYC (*i.e.*, FBXW7) degradation. The effect of UBE2C on p27 did not involve p27 nuclear exporter CRM1, because silencing of UBE2C had no impact on the protein level of CRM1.

### 6.1.1 UBE2C expression influenced the proportion of quiescent prostate cancer cells

In this project, the association of UBE2C and cell quiescence was verified by carefully designed experiments. Important considerations for these experimental designs included the choice of cell lines, methods to induce quiescence and to quantify the fraction of $G_0$ cells, and the genetic approach to intervene UBE2C expression.

First, three PCa cell lines with moderate UBE2C expression were chosen in this experiment. LNCaP (AR positive) was a cell model of HSPC; PC-3 (AR negative) was a model of CRPC cells, while C4-2B was chosen as it is an AR positive CRPC cell line (Chen *et al.*, 2011; Thalmann *et al.*, 2000; Wang *et al.*, 2009). AR has been found to play a crucial role in the development of CRPC, at least in part, through a mechanism of enhanced expression of UBE2C (Kato *et al.*, 2015; Wang *et al.*, 2009). Although our study did not examine the effect of manipulating androgen or AR on UBE2C expression, the UBE2C action on quiescence was similar in all three cell lines in the presence or absence of AR. Hence, it suggested that the regulation of cell cycle exit and re-entry by UBE2C may be AR-independent.

Second, experimental quiescence was induced by two complementary methods. Instead of using drugs to synchronise cells, serum removal and contact inhibition are believed to induce relatively less perturbations to the cells (Schorl and Sedivy, 2007). Our synchronising condition, which induced the maximum percentage of cells in $G_0/G_1$ phase, caused minimal impact to cell viability in PCa cell lines. Culture for 7 days of serum-deprived LNCaP cells or 3 days of contact inhibited PC-3 cells can enrich $G_0/G_1$ cells by 80–90%, as shown by our group recently (Yao *et al.*, 2015). It is worth noting that by including both serum-deprived

LNCaP cells and contact inhibited PC-3 cells, any bias due to choice of synchronisation method can be avoided.

Third, to investigate the effect of UBE2C on cell quiescence, we established a method to directly quantify $G_0$ cells. PI staining is a useful technique that allows analysis of DNA content and cell cycle distribution. However, as noted previously, it is impossible to distinguish $G_0$ from $G_1$, as both $G_1$ and $G_0$ cells are diploid. Based on the fact quiescent cells degrade their polyribosomes leading to low RNA content (Darzynkiewicz *et al.*, 1975), the $G_0$ cell distribution can be determined by simultaneously labelling DNA and RNA with HP double staining and then analysing by two-parameter flow cytometry (Shapiro, 1981). Indeed, contact inhibition and serum starvation enriched the $G_0$ phase cells in this study by approximately 70–90%, determined by HP double staining. This double staining method was further validated by co-staining with p-Rb ($Ser^{807/811}$), because quiescent cells should be hypophosphorylated (Serrano *et al.*, 1993; Sherr and Roberts, 1995). The cells with low RNA content were also found to be low in Rb at p-$Ser^{807/811}$. Hence, flow cytometric analysis with HP double staining was an effective method to identify quiescence in PCa cells.

Finally, to ensure the most accurate assessment of the true experimental outcome, two genetic approaches were employed for this study. Depletion of UBE2C was achieved by using two siRNAs targeting different sequences for specific knockdown of *UBE2C*. There was no significantly different outcome between the two siUBE2Cs. In addition, overexpression of UBE2C was induced by expression vector, and a UBE2C-DN control. Overexpressed UBE2C in PCa cells decreased the proportion of cells in $G_0$ phase, compared with no change observed in UBE2C-DN-induced cells. Collectively, there was no pharmacological inhibitor of UBE2C present. Using two genetic approaches provided strong and clear evidence to support a relation between UBE2C protein levels and cell cycle exit and re-entry.

### 6.1.2 UBE2C regulated the proportion of quiescent prostate cancer cells probably via p27

High levels of p27 have been found in quiescent cells and maintain cells in a quiescent state (Arvand *et al.*, 1998; Chu *et al.*, 2007). Downregulation of p27 is observed when cells are recruited to the cell cycle (Carrano *et al.*, 1999; Fukuda *et al.*, 1997; Hattori *et al.*, 2007; Sgambato *et al.*, 2000). Moreover, p27 is a tumour suppressor. Overexpression of p27 alone is sufficient to arrest cells in the quiescent state and low levels of p27 are associated with poor clinical prognosis (Chu *et al.*, 2008; Deng *et al.*, 2009; Sgambato *et al.*, 2000; Yao *et al.*, 2015). The post-translational regulation of p27 is mediated by several key regulators including SKP2, PIRH2 and CRM1. This study showed knockdown of UBE2C lead to a decrease in protein levels of SKP2 and PIRH2. Importantly, the decrease in these protein levels occurred before the increase in p27 protein levels. Together with no change of p27 mRNA levels, we propose that UBE2C controlled the turnover of p27 through SKP2 and PIRH2. Notably, high levels of SKP2 and PIRH2 have been found to link with low levels of p27 and poor prognosis in several malignancies (Carrano *et al.*, 1999; Huang *et al.*, 2011; Shimada *et al.*, 2009; Wu *et al.*, 2013; Yao *et al.*, 2015).

### 6.1.3 UBE2C regulated the proportion of quiescent prostate cancer cells probably via c-MYC

c-MYC is another important regulator of $G_0$ cells that was implicated as one of the first identified oncogenes (Wasylishen and Penn, 2010). Amplification of c-MYC has been reported to accelerate the $G_1$–S transition, immortalise cells, promote cell proliferation and lead to genomic instability (Luoto *et al.*, 2010; Wasylishen and Penn, 2010; Yin *et al.*, 1999). Excess expression of c-MYC is found in nearly half of human solid tumours (Beroukhim *et*

*al.*, 2010), including thirty percent of PCa (Bretones *et al.*, 2015). FBXW7 is one of the few proteins that targets c-MYC for degradation and inhibits c-MYC transcriptional activity (Amati, 2004; Farrell and Sears, 2014). Previously, our lab found that silencing FBXW7 by siRNA led to an accumulation of c-MYC in LNCaP and PC-3 cells (paper in press).

In this study, siUBE2C led to a decrease in c-MYC protein level, while no impact was found on c-MYC mRNA level. Additionally, silencing of UBE2C increased FBXW7 levels, prior to the decrease of c-MYC. Thus, our results indicate that the reduction of UBE2C mediated a change in c-MYC, which was most likely post-translational and FBXW7-dependent. SKP2 is another component of E3 ligases responsible for c-MYC proteolysis, as SKP2 is decreased in UBE2C knockdown cells, and is therefore unlikely to be involved in c-MYC degradation (Bretones *et al.*, 2011). Therefore, the effect of UBE2C on the proportion of quiescent cancer cells was possibly via c-MYC and FBXW7.

### 6.1.4 Concordance between UBE2C expression and prostate cancer progression

Previous studies have shown an aberrant overexpression of UBE2C mRNA and protein in PCa tissue (Hao *et al.*, 2012; LaTulippe *et al.*, 2002; Stanbrough *et al.*, 2006; Wang *et al.*, 2009). However, we have shown for the first time change in UBE2C protein levels in paired specimens of HSPC and CRPC from same patient. Although there were only eight patients in this study (as it is very rare to be able to collect TURP specimens twice from same patient), the increase in UBE2C levels in CRPC compared with HSPC were significant ($p$=0.003). Together with confirmation by immunostaining of our collected human PCa tissue specimens (n=70), and analysis of UBE2C mRNA levels across 12 prostate datasets using ONCOMINE, it was clear that UBE2C mRNA and protein were highly expressed in an advanced

metastasised form of PCa compared with organ-confined primary PCa or BPH. Hence, developing new treatment strategies by targeting UBE2C may be warranted.

## 6.2 Future Directions

UBE2C is an E2 enzyme, which is an exclusive partner of APC/C. Silencing UBE2C may reduce the destruction of APC/C target proteins and therefore APC/C target proteins are expected to increase as a result of knockdown of UBE2C. However, SKP2, one of 55 targets of APC/C, was significantly decreased when UBE2C was downregulated in this study. This unexpected observation suggested that the action of UBE2C on cell quiescence can be APC/C independent (Chen *et al.*, 2011; Reddy *et al.*, 2007; Wang *et al.*, 2011; Wang *et al.*, 2009). Although c-MYC was also reported to induce the expression of the *SKP2* gene (Bretones *et al.*, 2011; Keller *et al.*, 2007; O'Hagan *et al.*, 2000), the SKP2 protein level is decreased before the decrease of c-MYC. Also, we found no change in SKP2 mRNA following UBE2C siRNA treatment (data not shown). Hence, c-MYC was unlikely to be the cause of the reduction of SKP2 protein levels. Further study is therefore required to identify the role of UBE2C in SKP2 regulation.

Interestingly, there was a clear difference between wild type and UBE2C-DN in regulating the proportion of quiescent PCa cells. Forced expression of UBE2C in PCa cells decreased the proportion of cells in $G_0$ phase, whereas no change was observed in UBE2C-DN-induced cells, suggesting the catalytic $Cys^{114}$ of UBE2C could be important for UBE2C-mediated cell cycle progression. It is worth noting that, although transfection of UBE2C-DN had no impact on $G_0$ cells, it increased the proportion of cells in $G_2$/M phase in LNCaP cells. Similar results have also been reported by Townsley (1997). Other recent studies suggested the mitosis arrest caused by induction of UBE2C–DN was due to its capacity to compete with endogenous

UBE2C to bind to its E3 ligands, thus inhibiting the degradation of mitotic cyclins and causing subsequent mitotic arrest (Bose *et al.*, 2012; Townsley *et al.*, 1997). Further study is needed to verify the underlining mechanism of how the UBE2C catalytic site is involved in regulating the proportion of quiescent cells. This could be achieved by overexpressing UBE2C and UBE2C-DN and pulling down the physical partner by immunoprecipitation of UBE2C. Mass spectrometry could then be used to identify the possible difference in partner proteins of UBE2C and UBE2C-DN.

## 6.3 Conclusion

This project has revealed that UBE2C plays a previously unrecognised role in regulating the proportion of quiescent PCa cells and their transition to a proliferating state. Our findings suggest:

i. UBE2C impedes cell cycle exit and promotes cell cycle re-entry.

ii. UBE2C can upregulate SKP2 and PIRH2, which possibly promote p27 turnover.

iii. UBE2C can inhibit FBXW7 expression, which may prevent c-MYC from degrading.

iv. UBE2C mRNA and/or protein levels are aberrantly increased in the advanced form of prostate cancers, and the increased expression of UBE2C is associated with PCa progression.

To induce PCa cells arrested at quiescence is an interesting and important strategy and may lead to prevention of PCa progression and recurrence. UBE2C can be one of the therapeutic targets to achieve exactly that.

# References

ACS. (2016). *Prostate Cancer*. Georgia: American Cancer Society. [Accessed March 2016].

Adhami, V. M., Malik, A., Zaman, N., Sarfaraz, S., Siddiqui, I. A., Syed, D. N., Afaq, F., Pasha, F. S., Saleem, M., and Mukhtar, H. (2007). Combined inhibitory effects of green tea polyphenols and selective cyclooxygenase-2 inhibitors on the growth of human prostate cancer cells both *in vitro* and *in vivo*. *Clin Cancer Res*, 13, 1611-1619.

AIHW. (2016). *Australian Cancer Incidence and Mortality (ACIM) books: prostate cancer*. Canberra: Australian Institute of Health and Welfare. [Accessed January 2016].

AJCC. (2015). *American Joint Committee on Cancer* Chicago, IL: American Joint committee on Cancer. [Accessed November 2015].

Aleem, E., Kiyokawa, H., and Kaldis, P. (2005). Cdc2-cyclin E complexes regulate the G1/S phase transition. *Nat Cell Biol*, 7, 831-836.

Almog, N. (2010). Molecular mechanisms underlying tumor dormancy. *Cancer lett*, 294, 139-146.

Amati, B. (2004). Myc degradation: dancing with ubiquitin ligases. *Proc Natl Acad Sci U S A*, 101, 8843-8844.

Aristarkhov, A., Eytan, E., Moghe, A., Admon, A., Hershko, A., and Ruderman, J. V. (1996). E2-C, a cyclin-selective ubiquitin carrier protein required for the destruction of mitotic cyclins. *Proc Natl Acad Sci U S A*, 93, 4294-4299.

Arvand, A., Bastians, H., Welford, S. M., Thompson, A. D., Ruderman, J. V., and Denny, C. T. (1998). EWS/FLI1 up regulates mE2-C, a cyclin-selective ubiquitin conjugating enzyme involved in cyclin B destruction. *Oncogene*, 17, 2039-2045.

Assinder, S. J., Beniamen, D., and Lovicu, F. J. (2015). Cosuppression of Sprouty and Sprouty-related negative regulators of FGF signalling in prostate cancer: a working hypothesis. *Biomed Res Int*, 2015, 827462.

Baffoe-Bonnie, A. B., Kittles, R. A., Gillanders, E., Ou, L., George, A., Robbins, C., Ahaghotu, C., Bennett, J., Boykin, W., Hoke, G., Mason, T., Pettaway, C., Vijayakumar, S., Weinrich, S., Jones, M. P., Gildea, D., Riedesel, E., Albertus, J., Moses, T., Lockwood, E., Klaric, M., Faruque, M., Royal, C., Trent, J. M., Berg, K., Collins, F. S., Furbert-Harris, P. M., Bailey-Wilson, J. E., Dunston, G. M., Powell, I., and Carpten, J. D. (2007). Genome-wide linkage of 77 families from the African American Hereditary Prostate Cancer study (AAHPC). *Prostate*, 67, 22-31.

Berlingieri, M. T., Pallante, P., Guida, M., Nappi, C., Masciullo, V., Scambia, G., Ferraro, A., Leone, V., Sboner, A., Barbareschi, M., Ferro, A., Troncone, G., and Fusco, A. (2007). UbcH10 expression may be a useful tool in the prognosis of ovarian carcinomas. *Oncogene*, 26, 2136-2140.

Beroukhim, R., Mermel, C. H., Porter, D., Wei, G., Raychaudhuri, S., Donovan, J., Barretina, J., Boehm, J. S., Dobson, J., Urashima, M., Mc Henry, K. T., Pinchback, R. M., Ligon, A. H., Cho, Y. J., Haery, L., Greulich, H., Reich, M., Winckler, W., Lawrence, M. S., Weir, B. A., Tanaka, K. E., Chiang, D. Y., Bass, A. J., Loo, A., Hoffman, C., Prensner, J., Liefeld, T., Gao, Q., Yecies, D., Signoretti, S., Maher, E., Kaye, F. J., Sasaki, H., Tepper, J. E., Fletcher, J. A., Tabernero, J., Baselga, J., Tsao, M. S., Demichelis, F., Rubin, M. A., Janne, P. A., Daly, M. J., Nucera, C., Levine, R. L., Ebert, B. L., Gabriel, S., Rustgi, A. K., Antonescu, C. R., Ladanyi, M., Letai, A., Garraway, L. A., Loda, M., Beer, D. G., True, L. D., Okamoto, A., Pomeroy, S. L., Singer, S., Golub, T. R., Lander, E. S., Getz, G., Sellers, W. R., and Meyerson, M. (2010). The landscape of somatic copy-number alteration across human cancers. *Nature*, 463, 899-905.

Besson, A., Gurian-West, M., Chen, X., Kelly-Spratt, K. S., Kemp, C. J., and Roberts, J. M. (2006). A pathway in quiescent cells that controls p27Kip1 stability, subcellular localization, and tumor suppression. *Genes Dev*, 20, 47-64.

Bose, M. V., Gopisetty, G., Selvaluxmy, G., and Rajkumar, T. (2012). Dominant negative Ubiquitin-conjugating enzyme E2C sensitizes cervical cancer cells to radiation. *Int J Radiat Biol*, 88, 629-634.

Bosetti, C., Tzonou, A., Lagiou, P., Negri, E., Trichopoulos, D., and Hsieh, C. C. (2000). Fraction of prostate cancer incidence attributed to diet in Athens, Greece. *Eur J Cancer Prev*, 9, 119-123.

Brackstone, M., Townson, J. L., and Chambers, A. F. (2007). Tumour dormancy in breast cancer: an update. *Breast Cancer Res*, 9, 208.

Bretones, G., Acosta, J. C., Caraballo, J. M., Ferrandiz, N., Gomez-Casares, M. T., Albajar, M., Blanco, R., Ruiz, P., Hung, W. C., Albero, M. P., Perez-Roger, I., and Leon, J. (2011). SKP2 oncogene is a direct MYC target gene and MYC down-regulates p27(KIP1) through SKP2 in human leukemia cells. *J Biol Chem*, 286, 9815-9825.

Bretones, G., Delgado, M. D., and Leon, J. (2015). Myc and cell cycle control. *Biochim Biophys Acta*, 1849, 506-516.

Brinkley, B. R., and Stubblefield, E. (1966). The fine structure of the kinetochore of a mammalian cell *in vitro*. *Chromosoma*, 19, 28-43.

Carrano, A. C., Eytan, E., Hershko, A., and Pagano, M. (1999). SKP2 is required for ubiquitin-mediated degradation of the CDK inhibitor p27. *Nat Cell Biol*, 1, 193-199.

Cavanagh, H., and Rogers, K. M. (2015). The role of BRCA1 and BRCA2 mutations in prostate, pancreatic and stomach cancers. *Hered Cancer Clin Pract*, 13, 16.

Cen, B., Mahajan, S., Zemskova, M., Beharry, Z., Lin, Y. W., Cramer, S. D., Lilly, M. B., and Kraft, A. S. (2010). Regulation of Skp2 levels by the Pim-1 protein kinase. *J Biol Chem*, 285, 29128-29137.

Chandramohan, V., Mineva, N. D., Burke, B., Jeay, S., Wu, M., Shen, J., Yang, W., Hann, S. R., and Sonenshein, G. E. (2008). c‐Myc represses FOXO3a‐mediated transcription of the gene encoding the p27Kip1 cyclin dependent kinase inhibitor. *J Cell Biochem*, 104, 2091-2106.

Chen, S., Chen, Y., Hu, C., Jing, H., Cao, Y., and Liu, X. (2010). Association of clinicopathological features with UbcH10 expression in colorectal cancer. *J Cancer Res Clin Oncol*, 136, 419-426.

Chen, Z., Zhang, C., Wu, D., Chen, H., Rorick, A., Zhang, X., and Wang, Q. (2011). Phospho-MED1-enhanced UBE2C locus looping drives castration-resistant prostate cancer growth. *EMBO J*, 30, 2405-2419.

Chu, I., Sun, J., Arnaout, A., Kahn, H., Hanna, W., Narod, S., Sun, P., Tan, C. K., Hengst, L., and Slingerland, J. (2007). p27 phosphorylation by Src regulates inhibition of cyclin E-Cdk2. *Cell*, 128, 281-294.

Chu, I. M., Hengst, L., and Slingerland, J. M. (2008). The Cdk inhibitor p27 in human cancer: prognostic potential and relevance to anticancer therapy. *Nat Rev. Cancer*, 8, 253-267.

Chuu, C. P., Kokontis, J. M., Hiipakka, R. A., Fukuchi, J., Lin, H. P., Lin, C. Y., Huo, C., and Su, L. C. (2011). Androgens as therapy for androgen receptor-positive castration-resistant prostate cancer. *J biomed sci*, 18, 63.

CIN. (2010). *Cancer Incidence and Mortality Report*. NSW: Cancer Institue of New South Wales. [Accessed October 2015].

Coller, H. A. (2007). What's taking so long? S-phase entry from quiescence versus proliferation. *Nature reviews. Mol cell biol*, 8, 667-670.

Connor, M. K., Kotchetkov, R., Cariou, S., Resch, A., Lupetti, R., Beniston, R. G., Melchior, F., Hengst, L., and Slingerland, J. M. (2003). CRM1/Ran-mediated nuclear export of p27(Kip1) involves a nuclear export signal and links p27 export and proteolysis. *Mol Biol Cell*, 14, 201-213.

Cooper, S. (2003). Reappraisal of serum starvation, the restriction point, G0, and G1 phase arrest points. *FASEB J*, 17, 333-340.

Cooperberg, M. R., Carroll, P. R., and Klotz, L. (2011). Active surveillance for prostate cancer: progress and promise. *J Clin Oncol*, 29, 3669-3676.

Cunha, I. W., Carvalho, K. C., Martins, W. K., Marques, S. M., Muto, N. H., Falzoni, R., Rocha, R. M., Aguiar, S., Simoes, A. C., Fahham, L., Neves, E. J., Soares, F. A., and Reis, L. F. (2010). Identification of genes associated with local aggressiveness and metastatic behavior in soft tissue tumors. *Transl Oncol*, 3, 23-32.

D'Antonio, K. B., Schultz, L., Albadine, R., Mondul, A. M., Platz, E. A., Netto, G. J., and Getzenberg, R. H. (2010). Decreased expression of Cyr61 is associated with prostate cancer recurrence after surgical treatment. *Clin Cancer Res*, 16, 5908-5913.

Darzynkiewicz, Z., Traganos, F., Sharpless, T., and Melamed, M. R. (1975). Conformation of RNA *in situ* as studied by acridine orange staining and automated cytofluorometry. *Exp Cell Res*, 95, 143-153.

De Marzo, A. M., Platz, E. A., Sutcliffe, S., Xu, J., Gronberg, H., Drake, C. G., Nakai, Y., Isaacs, W. B., and Nelson, W. G. (2007). Inflammation in prostate carcinogenesis. *Nat Rev Cancer*, 7, 256-269.

Deng, X., Ewton, D. Z., and Friedman, E. (2009). Mirk/Dyrk1B maintains the viability of quiescent pancreatic cancer cells by reducing levels of reactive oxygen species. *Cancer Res*, 69, 3317-3324.

Desoize, B., and Jardillier, J. (2000). Multicellular resistance: a paradigm for clinical resistance? *CROH*, 36, 193-207.

Farrell, A. S., and Sears, R. C. (2014). MYC degradation. *Cold Spring Harb Perspect Med*, 4.

Fero, M. L., Randel, E., Gurley, K. E., Roberts, J. M., and Kemp, C. J. (1998). The murine gene p27Kip1 is haplo-insufficient for tumour suppression. *Nature*, 396, 177-180.

Fero, M. L., Rivkin, M., Tasch, M., Porter, P., Carow, C. E., Firpo, E., Polyak, K., Tsai, L. H., Broudy, V., Perlmutter, R. M., Kaushansky, K., and Roberts, J. M. (1996). A syndrome of multiorgan hyperplasia with features of gigantism, tumorigenesis, and female sterility in p27(Kip1)-deficient mice. *Cell*, 85, 733-744.

Fukuda, M., Asano, S., Nakamura, T., Adachi, M., Yoshida, M., Yanagida, M., and Nishida, E. (1997). CRM1 is responsible for intracellular transport mediated by the nuclear export signal. *Nature*, 390, 308-311.

Gleason, D. F., and Mellinger, G. T. (1974). Prediction of prognosis for prostatic adenocarcinoma by combined histological grading and clinical staging. *J Urol*, 111, 58-64.

Grimmler, M., Wang, Y., Mund, T., Cilensek, Z., Keidel, E. M., Waddell, M. B., Jakel, H., Kullmann, M., Kriwacki, R. W., and Hengst, L. (2007). Cdk-inhibitory activity and stability of p27Kip1 are directly regulated by oncogenic tyrosine kinases. *Cell*, 128, 269-280.

Grutzmann, R., Pilarsky, C., Ammerpohl, O., Luttges, J., Bohme, A., Sipos, B., Foerder, M., Alldinger, I., Jahnke, B., Schackert, H. K., Kalthoff, H., Kremer, B., Kloppel, G., and Saeger, H. D. (2004). Gene expression profiling of microdissected pancreatic ductal carcinomas using high-density DNA microarrays. *Neoplasia (New York)*, 6, 611-622.

Gstaiger, M., Jordan, R., Lim, M., Catzavelos, C., Mestan, J., Slingerland, J., and Krek, W. (2001). Skp2 is oncogenic and overexpressed in human cancers. *Proc Natl Acad Sci U S A*, 98, 5043-5048.

Hao, Z., Zhang, H., and Cowell, J. (2012). Ubiquitin-conjugating enzyme UBE2C: molecular biology, role in tumorigenesis, and potential as a biomarker. *Tumour Biol*, 33, 723-730.

Hartwell, L. H., Culotti, J., Pringle, J. R., and Reid, B. J. (1974). Genetic control of the cell division cycle in yeast. *Science*, 183, 46-51.

Hattori, T., Isobe, T., Abe, K., Kikuchi, H., Kitagawa, K., Oda, T., Uchida, C., and Kitagawa, M. (2007). Pirh2 promotes ubiquitin-dependent degradation of the cyclin-dependent kinase inhibitor p27Kip1. *Cancer Res*, 67, 10789-10795.

Hershko, A., Ganoth, D., Sudakin, V., Dahan, A., Cohen, L. H., Luca, F. C., Ruderman, J. V., and Eytan, E. (1994). Components of a system that ligates cyclin to ubiquitin and their regulation by the protein kinase cdc2. *J Biol Chem*, 269, 4940-4946.

Hnit, S. S., Xie, C., Yao, M., Holst, J., Bensoussan, A., De Souza, P., Li, Z., and Dong, Q. (2015). p27(Kip1) signaling: Transcriptional and post-translational regulation. *Int J Biochem Cell Biol*, 68, 9-14.

Huang, X., Qian, X., Cheng, C., He, S., Sun, L., Ke, Q., Zhang, L., Pan, X., He, F., Wang, Q., Meng, J., Ni, R., and Shen, A. (2011). Expression of Pirh2, a p27(Kip1) ubiquitin ligase, in hepatocellular carcinoma: correlation with p27(Kip1) and cell proliferation. *Hum Pathol*, 42, 507-515.

Ishida, N., Hara, T., Kamura, T., Yoshida, M., Nakayama, K., and Nakayama, K. I. (2002). Phosphorylation of p27Kip1 on serine 10 is required for its binding to CRM1 and nuclear export. *J Biol Chem*, 277, 14355-14358.

Ishikawa, Y., Hosogane, M., Okuyama, R., Aoyama, S., Onoyama, I., Nakayama, K. I., and Nakayama, K. (2013). Opposing functions of Fbxw7 in keratinocyte growth, differentiation and skin tumorigenesis mediated through negative regulation of c-Myc and Notch. *Oncogene*, 32, 1921-1932.

Jackson, R. C. (1989). The problem of the quiescent cancer cell. *Advances in Enzyme Regulation*, 29, 27-46.

James, M. K., Ray, A., Leznova, D., and Blain, S. W. (2008). Differential modification of p27Kip1 controls its cyclin D-cdk4 inhibitory activity. *Mol Cell Biol*, 28, 498-510.

Jemal, A., Center, M. M., DeSantis, C., and Ward, E. M. (2010). Global patterns of cancer incidence and mortality rates and trends. *Cancer Epidemiol Biomarkers Prev*, 19, 1893-1907.

Jhavar, S., Bartlett, J., Kovacs, G., Corbishley, C., Dearnaley, D., Eeles, R., Khoo, V., Huddart, R., Horwich, A., Thompson, A., Norman, A., Brewer, D., Cooper, C. S., and Parker, C. (2009). Biopsy tissue microarray study of Ki-67 expression in untreated, localized prostate cancer managed by active surveillance. *Prostate Cancer Prostatic Dis*, 12, 143-147.

Jiang, F., and Basavappa, R. (1999). Crystal structure of the cyclin-specific ubiquitin-conjugating enzyme from clam, E2-C, at 2.0 A resolution. *Biochemistry*, 38, 6471-6478.

Jin, L., Williamson, A., Banerjee, S., Philipp, I., and Rape, M. (2008). Mechanism of ubiquitin-chain formation by the human anaphase-promoting complex. *Cell*, 133, 653-665.

Kastan, M. B., and Bartek, J. (2004). Cell-cycle checkpoints and cancer. *Nature*, 432, 316-323.

Kato, M., Banuelos, C. A., Imamura, Y., Leung, J. K., Caley, D. P., Wang, J., Mawji, N. R., and Sadar, M. D. (2015). Co-targeting Androgen Receptor Splice Variants and mTOR signaling pathway for the Treatment of Castration-Resistant Prostate Cancer. *Clin Cancer Res*, 22, 2744-54

Katoh, M., Igarashi, M., Fukuda, H., Nakagama, H., and Katoh, M. (2013). Cancer genetics and genomics of human FOX family genes. *Cancer lett*, 328, 198-206.

Keller, U. B., Old, J. B., Dorsey, F. C., Nilsson, J. A., Nilsson, L., MacLean, K. H., Chung, L., Yang, C., Spruck, C., Boyd, K., Reed, S. I., and Cleveland, J. L. (2007). Myc targets Cks1 to provoke the suppression of p27Kip1, proliferation and lymphomagenesis. *EMBO J*, 26, 2562-2574.

Kelly, K., Cochran, B. H., Stiles, C. D., and Leder, P. (1983). Cell-specific regulation of the c-myc gene by lymphocyte mitogens and platelet-derived growth factor. *Cell*, 35, 603-610.

Keshari, K. R., Tsachres, H., Iman, R., Delos Santos, L., Tabatabai, Z. L., Shinohara, K., Vigneron, D. B., and Kurhanewicz, J. (2011). Correlation of phospholipid metabolites with prostate cancer pathologic grade, proliferative status and surgical stage - impact of tissue environment. *NMR in Biomedicine*, 24, 691-699.

Khatami, A., Hugosson, J., Wang, W., Damber, J. E., Khatami, A., Hugosson, J., Wang, W., and Damber, J.-E. (2009). Ki-67 in screen-detected, low-grade, low-stage prostate cancer, relation to prostate-specific antigen doubling time, Gleason score and prostate-specific antigen relapse after radical prostatectomy. *Scand J Urol Nephrol*, 43, 12-18.

King, B., Trimarchi, T., Reavie, L., Xu, L., Mullenders, J., Ntziachristos, P., Aranda-Orgilles, B., Perez-Garcia, A., Shi, J., Vakoc, C., Sandy, P., Shen, S. S., Ferrando, A., and Aifantis, I. (2013). The ubiquitin ligase FBXW7 modulates leukemia-initiating cell activity by regulating MYC stability. *Cell*, 153, 1552-1566.

Kitagawa, K., Kotake, Y., and Kitagawa, M. (2009). Ubiquitin-mediated control of oncogene and tumor suppressor gene products. *Cancer Sci*, 100, 1374-1381.

Kiyokawa, H., Kineman, R. D., Manova-Todorova, K. O., Soares, V. C., Hoffman, E. S., Ono, M., Khanam, D., Hayday, A. C., Frohman, L. A., and Koff, A. (1996). Enhanced growth of mice lacking the cyclin-dependent kinase inhibitor function of p27(Kip1). *Cell*, 85, 721-732.

Krek, W., Wirbelauer, C., Sutterluty, H., Blondel, M., Gstaiger, M., Peter, M., and Reymond, F. (2000). The F-box protein Skp2 is a ubiquitylation target of a Cul1-based core ubiquitin ligase complex: evidence for a role of Cul1 in the suppression of Skp2 expression in quiescent fibroblasts. *EMBO J*, 19, 5362-5375.

Kriegenburg, F., Seeger, M., Saeki, Y., Tanaka, K., Lauridsen, A.-M. B., Hartmann-Petersen, R., and Hendil, K. B. (2008). Mammalian 26S proteasomes remain intact during protein degradation. *Cell*, 135, 355-365.

Kuner, R., Falth, M., Pressinotti, N. C., Brase, J. C., Puig, S. B., Metzger, J., Gade, S., Schafer, G., Bartsch, G., Steiner, E., Klocker, H., and Sultmann, H. (2013). The maternal embryonic leucine zipper kinase (MELK) is upregulated in high-grade prostate cancer. *J Mol Med (Berl)*, 91, 237-248.

Kupelian, P. A., Mahadevan, A., Reddy, C. A., Reuther, A. M., and Klein, E. A. (2006). Use of different definitions of biochemical failure after external beam radiotherapy changes conclusions about relative treatment efficacy for localized prostate cancer. *Urology*, 68, 593-598.

LaTulippe, E., Satagopan, J., Smith, A., Scher, H., Scardino, P., Reuter, V., and Gerald, W. L. (2002). Comprehensive gene expression analysis of prostate cancer reveals distinct transcriptional programs associated with metastatic disease. *Cancer Res*, 62, 4499-4506.

Leitzmann, M. F., Stampfer, M. J., Michaud, D. S., Augustsson, K., Colditz, G. C., Willett, W. C., and Giovannucci, E. L. (2004). Dietary intake of n-3 and n-6 fatty acids and the risk of prostate cancer. *Am J Clin Nutr*, 80, 204-216.

Li, S. Z., Song, Y., Zhang, H. H., Jin, B. X., Liu, Y., Liu, W. B., Zhang, X. D., and Du, R. L. (2014). UbcH10 overexpression increases carcinogenesis and blocks ALLN susceptibility in colorectal cancer. *Sci Rep*, 4, 6910.

Lima, N. P., Silva, G. M., Park, M., and Pires-Neto, R. C. (2015). Mobility therapy and central or peripheral catheter-related adverse events in an ICU in Brazil. *J Bras Pneumol*, 41, 225-230.

Lin, H. P., Lin, C. Y., Hsiao, P. H., Wang, H. D., Jiang, S. S., Hsu, J. M., Jim, W. T., Chen, M., Kung, H. J., and Chuu, C. P. (2013). Difference in protein expression profile and chemotherapy drugs response of different progression stages of LNCaP sublines and other human prostate cancer cells. *PLoS One*, 8, e82625.

Lin, J., Raoof, D. A., Wang, Z., Lin, M. Y., Thomas, D. G., Greenson, J. K., Giordano, T. J., Orringer, M. B., Chang, A. C., Beer, D. G., and Lin, L. (2006). Expression and effect of inhibition of the ubiquitin-conjugating enzyme E2C on esophageal adenocarcinoma. *Neoplasia*, 8, 1062-1071.

Lin, Y., Hwang, W. C., and Basavappa, R. (2002). Structural and functional analysis of the human mitotic-specific ubiquitin-conjugating enzyme, UbcH10. *J Biol Chem*, 277, 21913-21921.

Liu, G., Sprenger, C., Wu, P. J., Sun, S., Uo, T., Haugk, K., Epilepsia, K. S., and Plymate, S. (2015). MED1 mediates androgen receptor splice variant induced gene expression in the absence of ligand. *Oncotarget*, 6, 288-304.

Loussouarn, D., Campion, L., Leclair, F., Campone, M., Charbonnel, C., Ricolleau, G., Gouraud, W., Bataille, R., and Jezequel, P. (2009). Validation of UBE2C protein as a prognostic marker in node-positive breast cancer. *Br J Cancer*, 101, 166-173.

Lu, J., Wen, M., Huang, Y., He, X., Wang, Y., Wu, Q., Li, Z., Castellanos-Martin, A., Abad, M., Cruz-Hernandez, J. J., Rodriguez, C. A., Perez-Losada, J., Mao, J. H., and Wei, G. (2013). C2ORF40 suppresses breast cancer cell proliferation and invasion through modulating expression of M phase cell cycle genes. *Epigenetics*, 8, 571-583.

Luoto, K. R., Meng, A. X., Wasylishen, A. R., Zhao, H., Coackley, C. L., Penn, L. Z., and Bristow, R. G. (2010). Tumor cell kill by c-MYC depletion: role of MYC-regulated genes that control DNA double-strand break repair. *Cancer Res*, 70, 8748-8759.

Ma, R., Kang, X., Zhang, G., Fang, F., Du, Y., and Lv, H. (2016). High expression of UBE2C is associated with the aggressive progression and poor outcome of malignant glioma. *Oncol Lett*, 11, 2300-2304.

Malumbres, M., and Barbacid, M. (2001). To cycle or not to cycle: a critical decision in cancer. *Nat Rev Cancer*, 1, 222-231.

Marti, A., Wirbelauer, C., Scheffner, M., and Krek, W. (1999). Interaction between ubiquitin-protein ligase SCFSKP2 and E2F-1 underlies the regulation of E2F-1 degradation. *Nat Cell Biol*, 1, 14-19.

Mateyak, M. K., Obaya, A. J., and Sedivy, J. M. (1999). c-Myc regulates cyclin D-Cdk4 and -Cdk6 activity but affects cell cycle progression at multiple independent points. *Mol Cell Biol*, 19, 4672-4683.

Matsuoka, S., Oike, Y., Onoyama, I., Iwama, A., Arai, F., Takubo, K., Mashimo, Y., Oguro, H., Nitta, E., Ito, K., Miyamoto, K., Yoshiwara, H., Hosokawa, K., Nakamura, Y., Gomei, Y., Iwasaki, H., Hayashi, Y., Matsuzaki, Y., Nakayama, K., Ikeda, Y., Hata, A., Chiba, S., Nakayama, K. I., and Suda, T. (2008). Fbxw7 acts as a critical fail-safe against premature loss of hematopoietic stem cells and development of T-ALL. *Genes Dev*, 22, 986-991.

Meyer, H. J., and Rape, M. (2011). Processive ubiquitin chain formation by the anaphase-promoting complex. *Semin cell dev biol*, 22, 544-550.

Mocciaro, A., and Rape, M. (2012). Emerging regulatory mechanisms in ubiquitin-dependent cell cycle control. *J Cell Sci*, 125, 255-263.

Mukhopadhyay, D., and Riezman, H. (2007). Proteasome-independent functions of ubiquitin in endocytosis and signaling. *Science*, 315, 201-205.

Muller, D., Bouchard, C., Rudolph, B., Steiner, P., Stuckmann, I., Saffrich, R., Ansorge, W., Huttner, W., and Eilers, M. (1997). Cdk2-dependent phosphorylation of p27 facilitates its Myc-induced release from cyclin E/cdk2 complexes. *Oncogene*, 15, 2561-2576.

Nagao, K., Yamamoto, Y., Hara, T., Komatsu, H., Inoue, R., Matsuda, K., Matsumoto, H., Hara, T., Sakano, S., Baba, Y., and Matsuyama, H. (2011). Ki67 and BUBR1 may discriminate clinically insignificant prostate cancer in the PSA range <4 ng/ml. *Jpn J Clin Oncol*, 41, 555-564.

Nagy, O., Pal, M., Udvardy, A., Shirras, C. A., Boros, I., Shirras, A. D., and Deak, P. (2012). lemmingA encodes the Apc11 subunit of the APC/C in Drosophila melanogaster that forms a ternary complex with the E2-C type ubiquitin conjugating enzyme, Vihar and Morula/Apc2. *Cell Div*, 7, 9.

Nakayama, K. I., and Nakayama, K. (2006). Ubiquitin ligases: cell-cycle control and cancer. *Nature Reviews. Cancer*, 6, 369-381.

Nameki, N., Yoneyama, M., Koshiba, S., Tochio, N., Inoue, M., Seki, E., Matsuda, T., Tomo, Y., Harada, T., Saito, K., Kobayashi, N., Yabuki, T., Aoki, M., Nunokawa, E., Matsuda, N., Sakagami, N., Terada, T., Shirouzu, M., Yoshida, M., Hirota, H., Osanai, T., Tanaka, A., Arakawa, T., Carninci, P., Kawai, J., Hayashizaki, Y., Kinoshita, K., Guntert, P., Kigawa, T., and Yokoyama, S. (2004). Solution structure of the RWD domain of the mouse GCN2 protein. *Protein Sci.*, 13, 2089-2100.

Nath, S., Banerjee, T., Sen, D., Das, T., and Roychoudhury, S. (2011). Spindle assembly checkpoint protein Cdc20 transcriptionally activates expression of ubiquitin carrier protein UbcH10. *J Biol Chem*, 286, 15666-15677.

NCI. (2002). *SEER Cancer Statistics Review, 1975-2002*. Bethesda, MD: National Cancer Institute. [Accessed September 2007].

O'Hagan, R. C., Ohh, M., David, G., de Alboran, I. M., Alt, F. W., Kaelin, W. G., Jr., and DePinho, R. A. (2000). Myc-enhanced expression of Cul1 promotes ubiquitin-dependent proteolysis and cell cycle progression. *Genes Dev*, 14, 2185-2191.

Okamoto, Y., Ozaki, T., Miyazaki, K., Aoyama, M., Miyazaki, M., and Nakagawara, A. (2003). UbcH10 is the cancer-related E2 ubiquitin-conjugating enzyme. *Cancer Res*, 63, 4167-4173.

Olsen, S. K., and Lima, C. D. (2013). Structure of a ubiquitin E1-E2 complex: insights to E1-E2 thioester transfer. *Mol Cell*, 49, 884-896.

Pallante, P., Berlingieri, M. T., Troncone, G., Kruhoffer, M., Orntoft, T. F., Viglietto, G., Caleo, A., Migliaccio, I., Decaussin-Petrucci, M., Santoro, M., Palombini, L., and Fusco, A. (2005). UbcH10 overexpression may represent a marker of anaplastic thyroid carcinomas. *Br J Cancer*, 93, 464-471.

Paller, C. J., and Antonarakis, E. S. (2013). Management of biochemically recurrent prostate cancer after local therapy: evolving standards of care and new directions. *Clin Adv Hematol Oncol*, 11, 14-23.

Pardee, A. B. (1974). A restriction point for control of normal animal cell proliferation. *Proc Natl Acad Sci U S A*, 71, 1286-1290.

PCFA. (2013). *Treatment: Treating localizsed prostate cancer*. NSW: Prostate Cancer Foundation of Australia.

Penney, K. L., Sinnott, J. A., Fall, K., Pawitan, Y., Hoshida, Y., Kraft, P., Stark, J. R., Fiorentino, M., Perner, S., Finn, S., Calza, S., Flavin, R., Freedman, M. L., Setlur, S., Sesso, H. D., Andersson, S. O., Martin, N., Kantoff, P. W., Johansson, J. E., Adami, H. O., Rubin, M. A., Loda, M., Golub, T. R., Andren, O., Stampfer, M. J., and Mucci, L. A. (2011). mRNA expression signature of Gleason grade predicts lethal prostate cancer. *J Clin Oncol*, 29, 2391-2396.

Pérez-Roger, I., Solomon, D., Sewing, A., and Land, H. (1997). Myc activation of cyclin E/Cdk2 kinase involves induction of cyclin E gene transcription and inhibition of p27 (Kip1) binding to newly formed complexes. *Oncogene*, 14, 2373-2381.

Perez de Castro, I., de Carcer, G., and Malumbres, M. (2007). A census of mitotic cancer genes: new insights into tumor cell biology and cancer therapy. *Carcinogenesis*, 28, 899-912.

Pietenpol, J. A., Bohlander, S. K., Sato, Y., Papadopoulos, N., Liu, B., Friedman, C., Trask, B. J., Roberts, J. M., Kinzler, K. W., Rowley, J. D., and et al. (1995). Assignment of the human p27Kip1 gene to 12p13 and its analysis in leukemias. *Cancer Res*, 55, 1206-1210.

Polyak, K., Kato, J. Y., Solomon, M. J., Sherr, C. J., Massague, J., Roberts, J. M., and Koff, A. (1994). p27Kip1, a cyclin-Cdk inhibitor, links transforming growth factor-beta and contact inhibition to cell cycle arrest. *Genes Dev*, 8, 9-22.

Rape, M. (2010). Assembly of k11-linked ubiquitin chains by the anaphase-promoting complex. *Subcell Biochem*, 54, 107-115.

Rape, M., and Kirschner, M. W. (2004). Autonomous regulation of the anaphase-promoting complex couples mitosis to S-phase entry. *Nature*, 432, 588-595.

Rape, M., Reddy, S. K., and Kirschner, M. W. (2006). The processivity of multiubiquitination by the APC determines the order of substrate degradation. *Cell*, 124, 89-103.

Ray, A., James, M. K., Larochelle, S., Fisher, R. P., and Blain, S. W. (2009). p27Kip1 inhibits cyclin D-cyclin-dependent kinase 4 by two independent modes. *Mol Cell Biol*, 29, 986-999.

Reddy, S. K., Rape, M., Margansky, W. A., and Kirschner, M. W. (2007). Ubiquitination by the anaphase-promoting complex drives spindle checkpoint inactivation. *Nature*, 446, 921-925.

Rivard, N., L'Allemain, G., Bartek, J., and Pouyssegur, J. (1996). Abrogation of p27Kip1 by cDNA antisense suppresses quiescence (G0 state) in fibroblasts. *J Biol Chem*, 271, 18337-18341.

Rodier, G., Montagnoli, A., Di Marcotullio, L., Coulombe, P., Draetta, G. F., Pagano, M., and Meloche, S. (2001). p27 cytoplasmic localization is regulated by phosphorylation on Ser10 and is not a prerequisite for its proteolysis. *EMBO J*, 20, 6672-6682.

Russo, A. A., Jeffrey, P. D., Patten, A. K., Massagué, J., and Pavletich, N. P. (1996). Crystal structure of the p27Kip1 cyclin-dependent-kinase inhibitor bound to the cyclin A-Cdk2 complex. *Nature*, 382, 325-331.

Santamaria, P. G., and Pagano, M. (2007). The pRb-Cdh1-p27 autoamplifying network. *Nat Cell Biol*, 9, 137-138.

Schmid, H. P., Riesen, W., and Prikler, L. (2004). Update on screening for prostate cancer with prostate-specific antigen. *Crit Rev Oncol Hematol*, 50, 71-78.

Schorl, C., and Sedivy, J. M. (2007). Analysis of cell cycle phases and progression in cultured mammalian cells. *Methods*, 41, 143-150.

Serrano, M., Hannon, G. J., and Beach, D. (1993). A new regulatory motif in cell-cycle control causing specific inhibition of cyclin D/CDK4. *Nature*, 366, 704-707.

Setlur, S. R., Mertz, K. D., Hoshida, Y., Demichelis, F., Lupien, M., Perner, S., Sboner, A., Pawitan, Y., Andren, O., Johnson, L. A., Tang, J., Adami, H. O., Calza, S., Chinnaiyan, A. M., Rhodes, D., Tomlins, S., Fall, K., Mucci, L. A., Kantoff, P. W., Stampfer, M. J., Andersson, S. O., Varenhorst, E., Johansson, J. E., Brown, M.,

Golub, T. R., and Rubin, M. A. (2008). Estrogen-dependent signaling in a molecularly distinct subclass of aggressive prostate cancer. *J Natl Cancer Inst*, 100, 815-825.

Sgambato, A., Cittadini, A., Faraglia, B., and Weinstein, I. B. (2000). Multiple functions of p27(Kip1) and its alterations in tumor cells: a review. *J. Cell. Physio*, 183, 18-27.

Shapiro, H. M. (1981). Flow cytometric estimation of DNA and RNA content in intact cells stained with Hoechst 33342 and pyronin Y. *Cytometry*, 2, 143-150.

Sheaff, R. J., Groudine, M., Gordon, M., Roberts, J. M., and Clurman, B. E. (1997). Cyclin E-CDK2 is a regulator of p27Kip1. *Genes Dev*, 11, 1464-1478.

Sherr, C. J., and Roberts, J. M. (1995). Inhibitors of mammalian G1 cyclin-dependent kinases. *Genes Dev*, 9, 1149-1163.

Shidaifat, F. (2009). Age-dependent expression of 5alpha-reductase and androgen receptors mRNA by the canine prostate. *Physiol Res*. 58,155-8.

Shimada, M., Kitagawa, K., Dobashi, Y., Isobe, T., Hattori, T., Uchida, C., Abe, K., Kotake, Y., Oda, T., Suzuki, H., Hashimoto, K., and Kitagawa, M. (2009). High expression of Pirh2, an E3 ligase for p27, is associated with low expression of p27 and poor prognosis in head and neck cancers. *Cancer Sci*, 100, 866-872.

Shuliang, S., Lei, C., Guangwu, J., and Changjie, L. (2013). Involvement of ubiquitin-conjugating enzyme E2C in proliferation and invasion of prostate carcinoma cells. *Oncol Res*, 21, 121-127.

Siegel, R., Ma, J., Zou, Z., and Jemal, A. (2014). Cancer statistics, 2014. *CA Cancer J Clin*, 64, 9-29.

Singh, J., Xie, C., Yao, M., Hua, S., Vignarajan, S., Jardine, G., Hambly, B. D., Sved, P., and Dong, Q. (2010). Food extracts consumed in Mediterranean countries and East Asia reduce protein concentrations of androgen receptor, phospho-protein kinase B, and phospho-cytosolic phospholipase A(2)alpha in human prostate cancer cells. *J Nutr*, 140, 786-791.

Song, L., and Rape, M. (2011). Substrate-specific regulation of ubiquitination by the anaphase-promoting complex. *Cell Cycle*, 10, 52-56.

Stanbrough, M., Bubley, G. J., Ross, K., Golub, T. R., Rubin, M. A., Penning, T. M., Febbo, P. G., and Balk, S. P. (2006). Increased expression of genes converting adrenal androgens to testosterone in androgen-independent prostate cancer. *Cancer Res*, 66, 2815-2825.

Stark, J. R., Perner, S., Stampfer, M. J., Sinnott, J. A., Finn, S., Eisenstein, A. S., Ma, J., Fiorentino, M., Kurth, T., Loda, M., Giovannucci, E. L., Rubin, M. A., and Mucci, L. A. (2009). Gleason score and lethal prostate cancer: does 3 + 4 = 4 + 3? *J Clin Oncol*, 27, 3459-3464.

Summers, M. K., Pan, B., Mukhyala, K., and Jackson, P. K. (2008). The unique N terminus of the UbcH10 E2 enzyme controls the threshold for APC activation and enhances checkpoint regulation of the APC. *Mol Cell*, 31, 544-556.

Sun, F., Indran, I. R., Zhang, Z. W., Tan, M. H., Li, Y., Lim, Z. L., Hua, R., Yang, C., Soon, F. F., Li, J., Xu, H. E., Cheung, E., and Yong, E. L. (2015). A novel prostate cancer therapeutic strategy using icaritin-activated arylhydrocarbon-receptor to co-target androgen receptor and its splice variants. *Carcinogenesis*, 36, 757-768.

Takahashi-Yanaga, F., and Sasaguri, T. (2008). GSK-3beta regulates cyclin D1 expression: a new target for chemotherapy. *Cellular signalling*, 20, 581-589.

Thalmann, G. N., Sikes, R. A., Wu, T. T., Degeorges, A., Chang, S. M., Ozen, M., Pathak, S., and Chung, L. W. (2000). LNCaP progression model of human prostate cancer: androgen-independence and osseous metastasis. *Prostate*, 44, 91-103 Jul 101;144(102).

Thompson, B. J., Buonamici, S., Sulis, M. L., Palomero, T., Vilimas, T., Basso, G., Ferrando, A., and Aifantis, I. (2007). The SCFFBW7 ubiquitin ligase complex as a tumor suppressor in T cell leukemia. *J Exp Med*, 204, 1825-1835.

Thompson, I. M., Pauler, D. K., Goodman, P. J., Tangen, C. M., Lucia, M. S., Parnes, H. L., Minasian, L. M., Ford, L. G., Lippman, S. M., Crawford, E. D., Crowley, J. J., and Coltman, C. A., Jr. (2004). Prevalence of prostate cancer among men with a prostate-specific antigen level < or =4.0 ng per milliliter. *N Engl J Med*, 350, 2239-2246.

Thrower, J. S., Hoffman, L., Rechsteiner, M., and Pickart, C. M. (2000). Recognition of the polyubiquitin proteolytic signal. *EMBO J*, 19, 94-102.

Townsley, F. M., Aristarkhov, A., Beck, S., Hershko, A., and Ruderman, J. V. (1997). Dominant-negative cyclin-selective ubiquitin carrier protein E2-C/UbcH10 blocks cells in metaphase. *Proc Natl Acad Sci U S A*, 94, 2362-2367.

Tracey, E., Ling, L., Baker, D., Dobrovic, A., and Bishop, J. (2009). *Cancer in New South Wales: Incidence and Mortality 2007* (1836-4551). Sydney, Cancer Institute NSW.

Tzelepi, V., Zhang, J., Lu, J. F., Kleb, B., Wu, G., Wan, X., Hoang, A., Efstathiou, E., Sircar, K., Navone, N. M., Troncoso, P., Liang, S., Logothetis, C. J., Maity, S. N., and

Aparicio, A. M. (2012). Modeling a lethal prostate cancer variant with small-cell carcinoma features. *Clin Cancer Res*, 18, 666-677.

Udagawa, T. (2008). Tumor dormancy of primary and secondary cancers. *APMIS*, 116, 615-628.

van Ree, J. H., Jeganathan, K. B., Malureanu, L., and van Deursen, J. M. (2010). Overexpression of the E2 ubiquitin-conjugating enzyme UbcH10 causes chromosome missegregation and tumor formation. *J Cell Biol*, 188, 83-100.

Vasiljevic, A., Champier, J., Figarella-Branger, D., Wierinckx, A., Jouvet, A., and Fevre-Montange, M. (2013). Molecular characterization of central neurocytomas: potential markers for tumor typing and progression. *Neuropathology*, 33, 149-161.

Visvader, J. E., and Clevers, H. (2016). Tissue-specific designs of stem cell hierarchies. *Nat Cell Biol*, 18, 349-355.

Wagner, K. W., Sapinoso, L. M., El-Rifai, W., Frierson, H. F., Butz, N., Mestan, J., Hofmann, F., Deveraux, Q. L., and Hampton, G. M. (2004). Overexpression, genomic amplification and therapeutic potential of inhibiting the UbcH10 ubiquitin conjugase in human carcinomas of diverse anatomic origin. *Oncogene*, 23, 6621-6629.

Walczak, C. E., Cai, S., and Khodjakov, A. (2010). Mechanisms of chromosome behaviour during mitosis. *Nat rev. Mol cell biol*, 11, 91-102.

Walker, A., Acquaviva, C., Matsusaka, T., Koop, L., and Pines, J. (2008). UbcH10 has a rate-limiting role in G1 phase but might not act in the spindle checkpoint or as part of an autonomous oscillator. *J Cell Sci*, 121, 2319-2326.

Wang, H., Zhang, C., Rorick, A., Wu, D., Chiu, M., Thomas-Ahner, J., Chen, Z., Chen, H., Clinton, S. K., Chan, K. K., and Wang, Q. (2011). CCI-779 inhibits cell-cycle G2-M progression and invasion of castration-resistant prostate cancer via attenuation of UBE2C transcription and mRNA stability. *Cancer Res*, 71, 4866-4876.

Wang, Q., Li, W., Zhang, Y., Yuan, X., Xu, K., Yu, J., Chen, Z., Beroukhim, R., Wang, H., Lupien, M., Wu, T., Regan, M. M., Meyer, C. A., Carroll, J. S., Manrai, A. K., Janne, O. A., Balk, S. P., Mehra, R., Han, B., Chinnaiyan, A. M., Rubin, M. A., True, L., Fiorentino, M., Fiore, C., Loda, M., Kantoff, P. W., Liu, X. S., and Brown, M. (2009). Androgen receptor regulates a distinct transcription program in androgen-independent prostate cancer. *Cell*, 138, 245-256.

Wang, Q., Tiffen, J., Bailey, C. G., Lehman, M. L., Ritchie, W., Fazli, L., Metierre, C., Feng, Y. J., Li, E., Gleave, M., Buchanan, G., Nelson, C. C., Rasko, J. E., and Holst, J. (2013). Targeting amino acid transport in metastatic castration-resistant prostate

cancer: effects on cell cycle, cell growth, and tumor development. *J Natl Cancer Inst*, 105, 1463-1473.

Wasylishen, A. R., and Penn, L. Z. (2010). Myc: the beauty and the beast. *Genes Cancer*, 1, 532-541.

Welcker, M., Orian, A., Grim, J. E., Eisenman, R. N., and Clurman, B. E. (2004). A nucleolar isoform of the Fbw7 ubiquitin ligase regulates c-Myc and cell size. *Curr Biol*, 14, 1852-1857.

Whitfield, J. R., and Soucek, L. (2012). Tumor microenvironment: becoming sick of Myc. *Cell Mol Life Sci*, 69, 931-934.

Wigle, D. T., Turner, M. C., Gomes, J., and Parent, M. E. (2008). Role of hormonal and other factors in human prostate cancer. *J Toxicol Environ Health B Crit Rev*, 11, 242-259.

Williams, C. D., Satia, J. A., Adair, L. S., Stevens, J., Galanko, J., Keku, T. O., and Sandler, R. S. (2010). Associations of red meat, fat, and protein intake with distal colorectal cancer risk. *Nutrition and cancer*, 62, 701-709.

Williamson, A., Banerjee, S., Zhu, X., Philipp, I., Iavarone, A. T., and Rape, M. (2011). Regulation of ubiquitin chain initiation to control the timing of substrate degradation. *Mol Cell*, 42, 744-757.

Wing, S. S., and Jain, P. (1995). Molecular cloning, expression and characterization of a ubiquitin conjugation enzyme (E2(17)kB) highly expressed in rat testis. *Biochem. J*, 305 ( Pt 1), 125-132.

Wu, D., Zhang, C., Shen, Y., Nephew, K. P., and Wang, Q. (2011). Androgen receptor-driven chromatin looping in prostate cancer. *Trends Endocrinol Metab*, 22, 474-480.

Wu, X. R., Sha, J. J., Liu, D. M., Chen, Y. H., Yang, G. L., Zhang, J., Chen, Y. Y., Bo, J. J., and Huang, Y. R. (2013). High expression of P53-induced Ring-h2 protein is associated with poor prognosis in clear cell renal cell carcinoma. *Eur J Surg Oncol*, 39, 100-106.

Xie, C., Powell, C., Yao, M., Wu, J., and Dong, Q. (2014). Ubiquitin-conjugating enzyme E2C: a potential cancer biomarker. *Int J Biochem Cell Biol*, 47, 113-117.

Yada, M., Hatakeyama, S., Kamura, T., Nishiyama, M., Tsunematsu, R., Imaki, H., Ishida, N., Okumura, F., Nakayama, K., and Nakayama, K. I. (2004). Phosphorylation-dependent degradation of c-Myc is mediated by the F-box protein Fbw7. *EMBO J*, 23, 2116-2125.

Yamanaka, A., Hatakeyama, S., Kominami, K., Kitagawa, M., Matsumoto, M., and Nakayama, K. (2000). Cell cycle-dependent expression of mammalian E2-C regulated by the anaphase-promoting complex/cyclosome. *Mol Biol Cell*, 11, 2821-2831.

Yao, M., Taylor, R. A., Richards, M. G., Sved, P., Wong, J., Eisinger, D., Xie, C., Salomon, R., Risbridger, G. P., and Dong, Q. (2010). Prostate-regenerating capacity of cultured human adult prostate epithelial cells. *Cells Tissues Organs*, 191, 203-212.

Yao, M., Xie, C., Kiang, M. Y., Teng, Y., Harman, D., Tiffen, J., Wang, Q., Sved, P., Bao, S., Witting, P., Holst, J., and Dong, Q. (2015). Targeting of cytosolic phospholipase $A_2$alpha impedes cell cycle re-entry of quiescent prostate cancer cells. *Oncotarget*, 6, 34458-34474.

Ye, Y., and Rape, M. (2009). Building ubiquitin chains: E2 enzymes at work. *Nat rev. Mol cell biol*, 10, 755-764.

Yin, X. Y., Grove, L., Datta, N. S., Long, M. W., and Prochownik, E. V. (1999). C-Myc overexpression and p53 loss cooperate to promote genomic instability. *Oncogene*, 18, 1177-1184.

Zbigniew Darzynkiewicz, Gloria Juan, and Srour, E. F. (2004). Current Protocols in Cytometry, John Wiley & Sons, Inc.

Zhao, L., Jiang, L., Wang, L., He, J., Yu, H., Sun, G., Chen, J., Xiu, Q., and Li, B. (2012). UbcH10 expression provides a useful tool for the prognosis and treatment of non-small cell lung cancer. *J Cancer Res Clin Oncol*, 138, 1951-1961.

Zhao, M., Zhang, N. Y., Zurawel, A., Hansen, K. C., and Liu, C. W. (2010). Degradation of some polyubiquitinated proteins requires an intrinsic proteasomal binding element in the substrates. *J Biol Chem*, 285, 4771-4780.